Influence of Climate Change on Pavement Design and Materials in Canada

by

©Surya Teja Swarna

A thesis submitted to the School of Graduate Studies

in partial fulfillment of the requirements for the degree of

Doctor of Philosophy (Ph.D.) in Civil Engineering

Faculty of Engineering & Applied Science,

Memorial University of Newfoundland,

October 2021

St. John's Newfoundland and Labrador Canada

Abstract

Anthropogenic climate change is having and will continue to have adverse effects on Canadian weather. Trends over the last 50 years elevate the rapid increase in number of the extreme event, the variations in temperature and precipitation, etc. The severe climatic variations in Canada are in line with global climate changes occurring due to increased greenhouse gas concentrations in the atmosphere. Under the current CO_2 emission scenarios, scientists predict that climate trends will further intensify in the near future. It is well known that asphalt pavements are highly sensitive to climate factors. Hence, reviewing both pavement design and materials while accounting climate change is a vital step that can help decelerate pavement deterioration. This study aims to quantify the impact of climate change on pavement performance, including revising pavement design and materials. To achieve this, the temperature and precipitation data were extracted from ten statistically downscaled climate change models, which were gathered from the pacific Canada Climate database. Also, the pavement materials, traffic, and structural data were collected from the Long-term Pavement Performance (LTPP) database. All these data were used in the Pavement Mechanistic-Empirical (ME) software to determine the pavement performance for both baseline and future climate.

Various adaptation strategies such as upgrading asphalt binder grade, increasing the thickness of asphalt concrete layer, increasing the base layer thickness, and using stabilized base layers were analyzed to mitigate the climate change impact and to extend the service life of the pavement. All of these adaptation strategies are based on climate change data and its effect on pavement performance. It is also evident that selecting a climate-appropriate asphalt binder is essential in ensuring the longevity of pavement surfaces. As the selection methodology depends on the pavement's temperature, several models can predict pavement temperatures based on recorded ambient air temperatures and other related factors. A commonality between the most predominant pavement temperature models is the geographical limitations to their application. As a result, widely used models such as the Long-Term Pavement Performance (LTPP) and Strategic Highway Research Program (SHRP) do not return accurate values for more Northern temperatures such as those observed in Canada. Thus, a new pavement temperature model was developed for Canadian climatic conditions to determine the appropriate asphalt binder grade for future climate. In addition, Life Cycle Assessment (LCA) and Life Cycle Cost Analysis (LCCA) were also carried out for all the alternatives to determine the CO_2 contributions to Canadian environment and changes in life cycle cost of Canadian pavement surfaces.

Acknowledgement

With an aspiration for a faster and better world and affinity for research and innovation in the field of Engineering and Technology, it was my unbound dream of studying in one of the top universities. Being a part of ARTEL pavement research group at the Memorial University of Newfoundland becomes my first step to achieve my dream. Throughout my journey to the doctorial program was excellent and I would like to acknowledge numerous individuals, without those contributions and support, my journey towards my goal might not be smooth.

I could not have accomplished this work as presented here had it not been for the expert support and constant encouragement from my supervisor Dr. Kamal Hossain. His enormous research experience and knowledge have brought me to think seriously on the problem I have taken up in this thesis. Also, his diverse interests helped me think over a problem with different perspectives. It has been a pleasure working under his supervision.

I would like to express my gratitude to my co-supervisor Dr. Ashutosh Sutra Dhar for his support, motivation, and engagement throughout my research program. Also, I would like to extend my deepest gratitude to Dr. Joseph Daraio for his continuous support in gathering and filtering the climate change data. His suggestions, advice, research ideas, and feedback helped me to enhance the quality of my thesis.

I extend my gratitude to Mr. Venkata Uday Bhaskar, R & D Engineer, SnowM Inc., for his support in handling climate data and his assistance in python and R Programming. I'm also grateful to Mr. Sri Harsha, web developer, City Tire & Auto Centre Ltd., for his support in developing the CABS tool using HTML and Java script. Also, I would like to extend my sincere thanks to Miss. Alyssa Bernier for her help in proofreading my manuscripts and thesis and giving a valuable input.

I heartily thank you so much for supporting me throughout my research. Your help has been invaluable to me.

I'd also like to extend my gratitude to Dr. Yusuf A. Mehta, Rowan University for giving access to AASHTOWare ME Pavement Design and his guidance and encouragement in writing journal articles. I gratefully acknowledge the support provided by Mr Ken Pike, Manager of Materials Engineering, Department of Transportation, Newfoundland and Labrador, Canada, for sharing valuable data such as material properties, traffic and structural design details of Trans-Canada Highway pavement section.

Thanks go to all my ARTEL research group members for their suggestions, and feedback. I am also expressing my gratitude to my friends Shivani Semwal, Kirti Vardhan, Dr. Sharath Chedella and Madavi Chedella for being the family members in St. John's and providing mental support during my stay. Besides that, I want to thank the Engineering Graduates' Students Society (EGSS), Telugu Association of Newfoundland (TAN), and Indian Youth Association (IYA) for giving me opportunity to work for them and helping me to improve my leadership skills.

In the last, I would like to extend my deepest and sincere thanks to my parents, my brother and his wife for their love and constant support throughout my program. I am forever indebted to my parents and my brother for giving me the opportunities and experiences that have made me who I am. They selflessly encouraged me to explore new directions in life and seek my own destiny. This journey would not have been possible without the dedicated support of my family, and I dedicate this milestone to them.

Table of contents

Abstract ii

Acknowledgement iv

Table of contents vi

Table of figures xviii

Table of tables xxiii

List of Abbreviations xxvii

List of Symbols and Notations xxxi

Chapter 1: Introduction 1

1.1 Background and motivation 1

1.1.1 Temperature 1

1.1.2 Precipitation 2

1.1.3 Other climate factors 2

1.2 Challenge: Quantification and mitigation of climate change impact 3

1.3 Current state of knowledge and gaps 3

1.4 Objectives 5

1.5 Thesis framework 5

1.6 Significant contributions 12

1.6.1 Journal articles 12

1.6.2 Conference papers 13

1.7 Co-Authorships 14

1.8 Reference 14

Chapter 2: Climate Change Impact and Adaptation for Highway Asphalt Pavements: A Literature Review 19

2.1 Abstract 19

2.2 Climate change and its impact 20

2.2.1 Climate change and its impact 20

2.2.2 Climate change models 21

2.2.3 Uncertainties in climate change models 23

2.2.4 Downscaling 24

2.2.5 Hourly data estimation 27

2.2.5.1 Chartered Institution of Building Services Engineers (CIBSE) Method 28

2.2.5.2 Sin(14R - 1) Method 29

2.2.5.3 Quarter-Sine (Q-sin) Method 30

2.2.5.4 Imposed Offset Morphing Method (IOMM) Method 32

2.3 Pavement materials perspective 33

2.3.1 SuperPave binder grade selection 33

2.3.2 Effect on surface HMA layer 36

2.3.3 Effect on subbase and subgrade layer 37

2.4 Performance and design perspective 38

2.4.1 Pavement performance 40
2.4.1.1 Structural performance 40
2.4.1.2 Functional performance 43
2.4.2 Pavement design and service life 44
2.5 Pavement maintenance and réhabilitation perspective 45
2.5.1 Pavement maintenance and rehabilitation 46
2.6 Economics and emissions perspective 49
2.6.1 Life Cycle Cost Analysis (LCCA) 49
2.6.2 Life Cycle Assessment (LCA) 51
2.7 Concluding remarks 52
2.8 Future work 54
2.9 References 55
Chapter 3: Impact of Climate Change on Pavement Performance in Canada's Newfoundland Island 65
3.1 Abstract 65
3.2 Introduction 66
3.3 Current knowledge on climate change effects 68
3.3.1 Climate prediction models 68
3.3.2 Pavement performance 71
3.4 Study objective and contribution 77

3.5 Methodology 77

3.5.1 First phase 78

3.5.2 Second phase 79

3.5.3 Third phase 80

3.6 Description of study sites 83

3.7 Results and discussion 86

3.7.1 Climate change models 86

3.7.2 AASHTOWare ME simulation and performance analysis 89

3.8 Conclusion 95

3.9 Pros and Cons 96

3.10 References 97

Chapter 4: Assessing Climate Change Impact on Asphalt Binder Grade: Selection and Its Implications 103

4.1 Abstract 103

4.2 Introduction 104

4.2.1 Temperature 104

4.2.2 Precipitation 105

4.2.3 Other climate factors 105

4.2.4 Change in asphalt binder grade due to Climate change 107

4.2.5 AASHTOWare Mechanistic-Empirical (ME) Pavement Design 108

4.3 Goal and objectives 109

4.4 Methodology 110

4.4.1 Phase 1: Collect climate change models 111

4.4.2 Phase 2: Extract climate change data 112

4.4.3 Phase 3: Determine asphalt binder grade for climate change data 113

4.4.4 Phase 4: Collect pavement materials, traffic, structural, and climate data 114

4.4.5 Phase 5: Assessing pavement performance for future climate 116

4.5 Results and discussion 117

4.6 Conclusion 126

4.7 Pros/cons 128

4.8 Reference 129

Chapter 5: Asphalt Binder Selection for Future Canadian Climatic Conditions Using Various Pavement Temperature Prediction Models 138

5.1 Abstract 138

5.2 Introduction 139

5.2.1 Change in asphalt binder selection 139

5.2.2 Pavement temperature prediction models 143

5.2.3 Summary of literature 147

5.3 Objective and scope 148

5.4 Locations and climate change models 148

5.5 Methodology 149
5.5.1 Phase 1: Gathering climate change models. 150
5.5.2 Phase 2: Climate change data extraction 150
5.5.3 Phase 3: Determining the average seven-day maximum and minimum pavement temperature 151
5.5.4 Phase 4: Assigning asphalt binder grade 152
5.5.5 Phase 5: Comparison between the pavement temperature models 152
5.6 Results and discussions 152
5.7 Conclusions 166
5.8 Contributions and limitations 167
5.8.1 Contributions: 167
5.8.2 Limitations 167
5.9 Reference: 167
Chapter 6: Pavement Temperature Model for Canadian Asphalt Binder Selection: Introduction to the CPT Model 173
6.1 Abstract 173
6.2 Introduction 174
6.2.1 Existing pavement temperature models, North America 174
6.2.2 Existing pavement temperature models outside of North America 179
6.2.3 Existing pavement temperature models in Canada 180

6.2.4 Relevance of pavement temperature models 183

6.2.5 Overall highlights of literature 184

6.3 Objective and scope 185

6.4 Methodology 186

6.4.1 Phase 1: Data collection 187

6.4.2 Phase 2: Clustering 188

6.4.3 Phase 3: Computing pavement temperatures using EICM 188

6.4.4 Phase 4: Pavement temperature model 188

6.4.5 Phase 5: Software tool 189

6.5 Results 190

6.6 Field verification 199

6.7 Cabs software 201

6.8 Conclusions 203

6.9 References 204

Chapter 7: Climate Change Adaptation Strategies for Canadian Asphalt Pavements 209

7.1 Abstract 209

7.2 Introduction 210

7.2.1 Climate change principles 210

7.2.2 Impact on pavement performance 211

7.2.3 Adaptation strategies 212

7.2.4 Pavement temperature models ... 215
7.3 Objective and scope ... 216
7.4 Methodology ... 217
7.4.1 Phase 1: Selecting climate change models ... 217
7.4.2 Phase 2: Extracting climate data ... 218
7.4.3 Phase 3: Obtaining pavement materials data ... 218
7.4.4 Phase 4: Evaluate pavement performance under future climate scenarios ... 220
7.4.5 Phase 5: Comparing climate change adaptation strategies ... 221
7.5 Results and discussion ... 223
7.6 Conclusions and recommendations ... 236
7.7 Contributions/limitations ... 238
7.7.1 Contributions: ... 238
7.7.2 Limitations: ... 239
7.8 Reference ... 239
Chapter 8: LCA and LCCA of Climate Change Adaptation Strategies for Canadian Pavements 246
8.1 Abstract ... 246
8.2 Introduction ... 247
8.2.1 Life-Cycle Assessment (LCA) ... 248
8.2.2 Climate change and LCA ... 249

8.2.3 Life-Cycle Cost Analysis (LCCA) ... 250
8.2.4 Climate change and LCCA ... 252
8.2.5 Climate change adaptation strategies ... 253
8.2.6 Highlights of literature ... 253
8.3 Objective and scope ... 254
8.4 Methodology ... 255
8.4.1 Site preparation and manufacturing ... 257
8.4.2 Construction ... 257
8.4.3 Maintenance ... 258
8.4.4 Use phase ... 258
8.5 Results and discussions ... 259
8.5.1 LCA and LCCA ... 260
8.5.2 Selecting best adaptation strategy ... 267
8.5.3 Correlations between LCA and LCCA factors ... 269
8.6 Conclusions ... 271
8.7 Contributions and limitations ... 273
8.7.1 Contributions ... 273
8.7.2 Limitations ... 273
8.8 References ... 274
Chapter 9: Conclusions and Discussions ... 279

9.1 Conclusions 279

9.1.1 Impact of climate change on pavement performance in Canada's Newfoundland Island 279

9.1.2 Assessing climate change impact on asphalt binder grade: selection and its implications 280

9.1.3 Asphalt binder selection for future Canadian climatic conditions using various pavement temperature prediction models 282

9.1.4 Pavement temperature model for Canadian asphalt binder selection: introduction to the CPT model 283

9.1.5 Climate change adaptation strategies for Canadian asphalt pavements 284

9.1.6 LCA and LCCA of climate change adaptation strategies for Canadian pavements 286

9.2 Recommendations 287

References 289

Appendix A. Data Extraction and Analysis 309

A.1. Python Coding 309

A.1.1. Extracting climate change data from climate change model 309

A.1.2. Hourly Temperature Code 313

A.1.3. Extracting Pavement Temperatures 317

A.1.4. Data Sorting for Cluster Analysis 322

A.1.5. Co-relation coefficients 324

A.1.6. Regression Model ... 325
A.2. R-Programming ... 327
A.2.1. K-Means Clustering ... 327
Appendix B. Climate Change Uncertainty ... 328
Appendix C. Mechanistic-Empirical Pavement Design ... 358
C.1 Design Inputs ... 358
C.2 Design Inputs ... 358
C.2.1 Hierarchical Approach ... 358
C.2.2 Climate ... 358
C.2.3 Traffic ... 361
C.2.4 Asphalt Mixes ... 364
C.2.5 Unbound materials ... 368
C.3 Methodology ... 372
C.4 Design Outputs ... 373
C.4.1 Rutting ... 373
C.4.2 Fatigue Cracking ... 375
C.4.3 Thermal Cracking ... 378
C.4.4 Smoothness ... 379
Appendix D. LCA and LCCA ... 382
D.1 Life Cycle Assessment (LCA) ... 382

D.1.1 Material Data 382

D.1.2 Summary of LCA output 383

D.2 Life Cycle Cost Analysis (LCCA) 386

Table of figures

Figure 1-1: Thesis framework; Part 1 ... 6

Figure 1-2: Thesis framework; Part 2 ... 7

Figure 1-3: Thesis framework; Part 3 ... 7

Figure 2-1: A sketch of the steps involved in developing a statistical downscaling model (Qiao et al., 2019) ... 27

Figure 2-2: Sinusoidal interpolation of daily temperature values (Chow & Levermore, 2007) ... 29

Figure 2-3: Sinusoidal curve fit using Q-sin method, (a) Quarter sine curve t in the region $\lambda > t_{min}$ and (b) Quarter sine curve t in the region $\lambda < t_{max}$ (Chow & Levermore, 2007) ... 31

Figure 2-4: Expected number of increments in high temperatures grade for: RCP 4.5 and for (a) 2010–2039, (b) 2040–2069 and (c) 2070–2099 and RCP 8.5 and for RCP 4.5 and for (d) 2010–2039, (e) 2040–2069 and (f) 2070–2099 (Underwood et al., 2017) ... 35

Figure 2-5: Estimated percent of roads requiring rehabilitation for various climatic conditions with adaptation strategies (Mallick et al., 2016) ... 47

Figure 2-6: Condition rating for various climate change scenarios: (a) RCP 2.6; (b) RCP 4.5; (c) RCP 6.0; (d) RCP 8.5 (Jeong et al., 2017) ... 48

Figure 2-7: Economic costs of a flexible pavement with the use of correct and incorrect asphalt grade, (a) Net present cost not including the initial construction cost and (b) Net present cost including the initial construction cost (Underwood et al., 2017) ... 51

Figure 3-1: Framework to evaluate the impact of climate change on pavement performance ... 78

Figure 3-2: Locations selected on Trans-Canada Highway to quantify the climate change impact. ... 79

Figure 3-3 Summary of climate factor for baseline and future climate in the Newfoundland ... 87

Figure 3-4 Average monthly temperature and precipitation for all scenarios 88

Figure 3-5 Hourly temperature data computed using M-IOMM and Sine(14R-1) compared to the existing LTPP data 89

Figure 3-6 Percentage change in pavement performance due to climate change 93

Figure 4-1: Methodology of the current study 111

Figure 4-2: Boxplot for seven-day average high and low pavement temperatures for Canadian cities 119

Figure 4-3: Performance (AC rutting) of Vancouver section for all climate change models (for the period of 2040-2070) 122

Figure 4-4: Change in performance parameters due to climate change compared to the baseline climate (1980-2010) 125

Figure 4-5: Percentage change in performance of Category II and III sections with upgraded asphalt grade compared to base asphalt grade. 126

Figure 5-1: A contour map for increase in average seven-day maximum temperature for 2010–2039 (a), 2040–2069 (b) and 2070–2099 (c) and average minimum temperature changes for 2010–2039 (d), 2040–2069 (e) and 2070–2099 (f) with respect to a baseline period of 1966 – 1995. (Underwood et al., 2017) 141

Figure 5-2: Economic costs of a flexible pavement with the use of correct and incorrect asphalt grade, (a) Net present cost not including the initial construction cost and (b) Net present cost including the initial construction cost (Underwood et al., 2017)... 142

Figure 5-3: Annual average air temperature for different climate change models in St. John's, NL, Ottawa, ON and Vancouver, BC, Canada 155

Figure 5-4: Boxplots for average seven-day high pavement temperatures estimated using different pavement temperature prediction models 156

Figure 5-5: Boxplots for low pavement temperatures estimated using different pavement temperature prediction models........ 157

Figure 5-6: Means of seven-day average high and low pavement temperatures estimated using different pavement temperature prediction models for 2040–2070-time period........ 158

Figure 5-7: Superpave binder grades produced from various crude oil blends........ 159

Figure 5-8: Expected number of increments in high temperature grade for future years........ 164

Figure 5-9: Expected number of increments in low temperature grade for future years........ 165

Figure 6-1: Pavement Temperature Model Methodology 187

Figure 6-2: K-Means Clustering Results for 254 Selected Data Points........ 190

Figure 6-3 : Geographical Location of Clusters Used in Pavement Temperature Model 191

Figure 6-4: Heat Plots for Canada Wide Analysis, (a) low pavement temperature and (b) high pavement temperature........ 192

Figure 6-5: Heat Plots for Cluster 1, (a) low pavement temperature and (b) high pavement temperature 192

Figure 6-6: Heat Plots for Cluster 2, (a) low pavement temperature and (b) high pavement temperature 193

Figure 6-7: Heat Plots for Cluster 3, (a) low pavement temperature and (b) high pavement temperature 193

Figure 6-8: Predicted vs Actual plot for validation data for Cluster 1 high-temperature model 199

Figure 6-9: CABS Software Tool Sample Output........ 202

Figure 6-10: Binder grades computed using CABS tool........ 203

Figure 7-1: Yearly percent of roads requiring rehabilitation under climate change and various

adaptation strategies (Mallick et al., 2016) 214
Figure 7-2: Methodology for the implementation of adaptation strategies 222
Figure 7-3: Percentage change in pavement performance parameters due to climate change compared to baseline climate (1980-2010) (Swarna et al., 2021) 225
Figure 7-4: Percentage change in pavement performance parameters for various climate change models compared to baseline climate (1980-2010) 226
Figure 7-5: Use of various adaptation strategies based on the cause of pavement distress........ 227
Figure 7-6: Adaptation strategies for various locations with distress parameters 232
Figure 7-7: Percentage change in pavement performance with various adaptation strategies compared to baseline climate 235
Figure 8-1: Life cycle considerations for roads (Meil & O'Connor, 2018)................................ 248
Figure 8-2: Study methodology flowchart 256
Figure 8-3: Percentage change in Emission (GWP) for climate change impact and adapted pavements compared to a baseline scenario for 2040-2070 time period 262
Figure 8-4: Percentage change in life cycle cost ($) for climate change impact and adapted pavement compared to a baseline pavement without climate change for 2040-2070 time period 263
Figure 8-5: Percent change in emission (GWP) for different time periods due to climate change impact and adapted pavement 265
Figure 8-6: Percent change in life cycle cost ($) for different periods due to climate change impact and adapted pavement 266
Figure 8-7: Impact of different climate change adaptation strategies in St. John's in 2040-2070 time period 268

Figure 8-8: Relationship between LCA and LCCA factors 270

Figure **C**-1: Monthly Rainfall Statistics 359

Figure **C**-2: Monthly Temperature Summary 359

Figure **C**-3: Monthly Precipitation and Windspeed 360

Figure **C**-4: Monthly Sunshine 360

Figure **C**-5: Hourly Air Temperature Distribution by Month (<-13 ºF to 50 ºF) 360

Figure **C**-6: Hourly Air Temperature Distribution by Month (50 ºF to >113 ºF) 361

Figure **C**-7: AADTT (Average Annual Daily Truck Traffic) growth over 30 years; (a)Classes 4-7, (b)Classes 8-10, (c) Classes 11-13, and (d) All Truck Classes 364

Figure **C**-8: Change in asphalt sub-layer modulus over 30 years 371

Figure **C**-9: Change in granular base sub-layer modulus over 30 years 372

Figure **C**-10: Mechanistic-Empirical Pavement Design methodology 372

Figure **C**-11: Permanent deformation over 30-year service life at 50% reliability 375

Figure **C**-12: AC Bottom-Up fatigue damage over 30-year service life at 50% reliability 377

Figure **C**-13: AC Bottom-Up fatigue cracking (Alligator) over 30-year service life at 50% reliability 377

Figure **C**-14: International Roughness Index (IRI) over 30-year service life 381

Figure **D**-1: Material input by percent mass 382

Figure **D**-2: Summary measures by life cycle stage chart 383

Figure **D**-3: Summary measures by life cycle stage clustered column chart 384

Figure **D**-4: Energy consumption absolute values by life cycle stage clustered column chart ... 385

Table of tables

Table 2-1: Impact of climate change on pavement performance reported in various studies 39

Table 2-2: Percentage change in pavement performance parameters due to increase in temperature and precipitation (Bizjak et al., 2014)... 41

Table 3-1: Carbon dioxide levels and temperature change from SRES Scenario (Nakicenovic, N., J. Alcamo, G. Davis, B. de Vries, J. Fenhann, S. Gaffin, K. Gregory, A. Grubler, T. Y. Jung et al., 2000) 69

Table 3-2: Various climate models used in past studies.. 74

Table 3-3: Input parameters for the study sites... 85

Table 3-4: Nomenclature for the climate change models used in the analysis............................. 86

Table 4-1: Major consequences to pavement infrastructure due to climate change (Dawson, 2014) 106

Table 4-2: Asphalt binder grade determined for the baseline and future climatic conditions.... 121

Table 5-1: Cliamte change models considered in the study 148

Table 5-2: Expected change in asphalt binder grade for 2040 – 2070....................................... 161

Table 6-1: Summary of Notable Pavement Temperature Models 182

Table 6-2: Various parameters for the pavement temperature model.. 197

Table 6-3: Verification data for developed pavement temperature model 200

Table 7-1: Change in asphalt binder grade for the selected location in Canada for future climate 229

Table 7-2: Appropriate adaptation strategies for selected locations.. 233

Table 8-1: 2021-2022 budget for highway maintenance and operations................................... 251

Table 8-2: Required adaptation strategies for selected Canadian locations 260

Table B-1: Uncertainty for Precipitation projections, climate change model: MRI- CGCM3... 328

Table B-2: Uncertainty for Precipitation projections, climate change model: CanESM2.......... 329

Table B-3: Uncertainty for Precipitation projections, climate change model: inmcm4 330

Table B-4: Uncertainty for Precipitation projections, climate change model: ACCESS1-0...... 331

Table B-5: Uncertainty for Precipitation projections, climate change model: MICROC5......... 332

Table B-6: Uncertainty for Precipitation projections, climate change model: CCSM4 333

Table B-7: Uncertainty for Precipitation projections, climate change model: MPI-ESM-LR ... 334

Table B-8: Uncertainty for Precipitation projections, climate change model: CSIRO-Mk3-6-0 335

Table B-9: Uncertainty for Precipitation projections, climate change model: GFDL-ESM2G . 336

Table B-10: Uncertainty for Precipitation projections, climate change model: CNRM-CM5... 337

Table B-11: Uncertainty for High Temperature projections, climate change model: MRI-CGCM3.. 338

Table B-12: Uncertainty for High Temperature projections, climate change model: CanESM2 339

Table B-13: Uncertainty for High Temperature projections, climate change model: inmcm4 .. 340

Table B-14: Uncertainty for High Temperature projections, climate change model: ACCESS1-0 341

Table B-15: Uncertainty for High Temperature projections, climate change model: MICROC5 342

Table B-16: Uncertainty for High Temperature projections, climate change model: CCSM4 .. 343

Table B-17: Uncertainty for High Temperature projections, climate change model: MPI-ESM-LR 344

Table B-18: Uncertainty for High Temperature projections, climate change model: CSIRO-Mk3-6-0 345

Table B-19: Uncertainty for High Temperature projections, climate change model: GFDL-ESM2G 346
Table B-20: Uncertainty for High Temperature projections, climate change model: CNRM-CM5 347
Table B-21: Uncertainty for Low Temperature projections, climate change model: MRI-CGCM3 348
Table B-22: Uncertainty for Low Temperature projections, climate change model: CanESM2 349
Table B-23: Uncertainty for Low Temperature projections, climate change model: inmcm4 ... 350
Table B-24: Uncertainty for Low Temperature projections, climate change model: ACCESS1-0 351
Table B-25: Uncertainty for Low Temperature projections, climate change model: MICROC5 352
Table B-26: Uncertainty for Low Temperature projections, climate change model: CCSM4 ... 353
Table B-27: Uncertainty for Low Temperature projections, climate change model: MPI-ESM-LR 354
Table B-28: Uncertainty for Low Temperature projections, climate change model: CSIRO-Mk3-6-0 355
Table B-29: Uncertainty for Low Temperature projections, climate change model: GFDL-ESM2G 356
Table B-30: Uncertainty for Low Temperature projections, climate change model: CNRM-CM5 357
Table **C**-1: Climate Data Source and Annual Statistics 359
Table **C**-2: Roadway specific input 361

Table **C**-3: Distributions by Vehicle Class 362

Table **C**-4: Volume Monthly Adjustment Factors 362

Table **C**-5: Number of Axles per Truck 362

Table **C**-6: Design structure details 365

Table **C**-7: Temperature Viscosity Relationship at (Short Term Aging and/or RTFO Condition) 365

Table **C**-8: Master curve data 366

Table **C**-9: Shift factors for the master curve 367

Table **C**-10: Creep compliance input 367

Table **C**-11: Thermal properties input 368

Table **C**-12: Non-stabilized Base: Crushed gravel properties 369

Table **C**-13: Crushed gravel gradation 369

Table **D**-1: Material report input 382

Table **D**-2: Life cycle cost by various categories over 30-year design life 386

List of Abbreviations

Abbreviation	Full form
AADT	Average Annual Daily Traffic
AADTT	Annual Average Daily Truck Traffic
AB	Alberta
AC	Asphalt Concrete
AOGCM	Atmosphere-Ocean General Circulation Models
BC	British Columbia
BCCA	Bias Correction/Constructed Analogues
BCCAQ	Bias Correction/Constructed Analogues with Quantile mapping reordering
BCSD	Bias-Correction Spatial Disaggregation
BHM	Hierarchical Bayesian Models
BOM	Bureau of Meteorology
BU	Bottom Up
CABS	Canadian Asphalt Binder Selection
CC	Climate Change
CCCma	Canadian Centre for Climate Modelling and Analysis
CCI	Climate change impact
CGCM2	Coupled Global Climate Model 2
CIBSE	Chartered Institution of Building Services Engineers
CMIP	Coupled Model Intercomparison Project
CMS	Climate Materials Structural

CORDEX	Coordinated Regional Downscaling Experiments
CPT	Canadian Pavement Temperature
CRREL	Cold Regions Research and Engineering Laboratory
CSIRO	Commonwealth Scientific and Industrial Research Organization
DTW	Department of Transportation and Works
EICM	Enhanced Integrated Climate Model
ESAL	Equivalent Single Axle Loads
ESM	Earth System Models
EVS	Explain Variance Score
GCM	General Circulation Model
GCM	Global Circulation Models
GHG	Green House Gases
HadCM3	Hadley Climate Model 3
HDM	Highway Development & Management
HMA	Hot Mix Asphalt
ID	Infiltration Drainage
IOMM	Imposed Offset Morphing Method
IPCC	Intergovernmental Panel on Climate Change
IRI	International Roughness Index
LCA	Life Cycle Assessment
LCC	Life Cycle Cost
LCCA	Life Cycle Cost Analysis
LTPP	Long-Term Pavement Performance

MAE	Mean Absolute Error
MAGICC	Model for the Assessment of Greenhouse-gas Induced Climate Change
MAPE	Mean Absolute Percentage Error
MB	Manitoba
ME	Mechanistic-Empirical
MEPDG	Mechanistic-Empirical Pavement Design Guide
MERRA	Modern Era Retrospective-Analysis for Research and Applications
M-IOMM	Modified Imposed Offset Morphing Method
NARCCAP	North American Regional Climate Change Assessment Program
NARR	North American Regional Reanalysis
NB	New Brunswick
NCHRP	National Cooperative Highway Research Program
NL	Newfoundland and Labrador
NLDTW	Newfoundland and Labrador Department of Transportation and Works
NS	Nova Scotia
OGFC	Open-Graded Friction Course
ON	Ontario
PCIC	Pacific Climate Impacts Consortium
PCM	Projected Climate Models
PEI	Prince Edward Island
PG	Performance Grade

QC	Quebec
QMAP	Quantile MAPping
RCM	Regional Climate Models
RCP	Representative Concentration Pathways
RD	Rut Depth
REMO	REgional MOdel
RMSE	Root Mean Square Error
SCENGEN	SCENario GENerator
SHRP	Strategic Highway Research Program
SK	Saskatchewan
SL	Service Life
SMA	Stone Matrix Asphalt
SP	SuperPave
SRES	Special Report on Emissions Scenarios
TCH	Trans-Canada Highway
TC	Transverse Cracking
PI	Plasticity Index
TD	Top Down
TMI	Thornthwaite Moisture Index
UKCP	United Kingdom Climate Projections
WCRP	World Climate Research Programme

List of Symbols and Notations

Symbol or Notation	Definition
T_{MAX}	Maximum temperature occurring at time t_{max}
T_{MIN}	Minimum temperature occurring at time t_{min}
f_1 and f_2	Factors of sinusoidal interpolation
$Temp_{(next)}$	Successive known temperature at time $t_{(next)}$
$Temp_{(prev)}$	Previous temperature at time $t_{(prev)}$
T_{ave}	Average air tempertaure
λ	Time of occurrence
T_{BMin}	Daily minimum temperatures extracted from the historic climate database
T_{BMax}	Daily maximum temperatures extracted from the historic climate database
T_{FMin}	Daily minimum temperatures extracted from the given projected climate data
T_{FMax}	Daily maximum temperatures extracted from the given projected climate data
R_{iF}	Hourly precipitation data for the future climate
R_{iB}	Hourly rainfall for historical climate data.
R_{BMAvg}	Average daily precipitation of each month extracted from the historic climate data base
R_{FMAvg}	Average daily precipitation of each month extracted from the given climate projection (climate change model)
T_{pM}	Daily maximum temperature
T_{pm}	Daily minimum temperature
T_{hr}	Hourly predicted temperature
T_{hM}	Historical daily maximum temperature

T_{hm}	Historical daily minimum temperature
P_{dapm}	Daily average of monthly precipitation calculated from the prediction model
P_{dahm}	Daily average of monthly precipitation calculated from historical data
P_{hhr}	Hourly precipitation from historical data
T_{min}	Time of minimum temperature
T_{max}	Time of maximum temperature
T_{next}	Next known minimum or maximum temperature
T_{pre}	Previous known minimum or maximum temperature
t	Time for which temperature is computed
t_{next}	Time for T_{next}
t_{pre}	Time for T_{pre}
FC_{total}	Corresponds to the area of fatigue cracking
TC	Length of transverse cracking in feet-mile
RD	Average rut depth measured in inches
PI	plasticity index of the subgrade soil
precip	Average annual rainfall in mm
FI	Average annual freezing index
Age	Age of pavement in years
$T_{P\ max}$	Average seven-day high pavement temperature
$T_{air\ max}$	Average seven-consecutive-day high air temperature
$\sigma_{air\ max}$	Standard deviation of seven-day high pavement temperature
$T_{P\ min}$	Low pavement temperature
$T_{air\ min}$	Low air temperature

$\sigma_{air\ min}$	Standard deviation of low pavement temperature
Lat	Latitude
H	Depth
Z	Standard normal distribution value
T_{surf}	High AC pavement temperature at the surface
T_{air}	High air temperature
Lat	Latitude of the section
T_d	High AC pavement temperature at a depth
d	Pavement depth
T_{pave}	High AC pavement temperature at 20 mm below the surface
R_S	Calculated daily solar radiation
T_{psmax}	Average monthly maximum pavement temperature
T_{psmin}	Average monthly minimum pavement temperature
T_{Amax}	Average monthly maximum air temperature
T_{Amin}	Average monthly minimum air temperature
DTRAD1	Sum of total daily radiation from 7:00 AM to 1:00 PM
DTRAD2	Sum of total daily radiation from 2:00PM to 6:00 PM
L_t	Latitude
M	Month
Y	Year
$T_{daily\text{-}minimum}$	Daily minimum HMA temperature
$T_{daily\text{-}maximum}$	Daily maximum HMA temperature
$T_{air\text{-}min}$	Daily minimum air temperature

$T_{air\text{-}max}$	Daily maximum air temperature
SR	Solar radiation
D	Depth
T_P	Surface pavement temperature
T_A	Air temperature
T_{A2}	Previous hour air temperature
W	Wind speed
T_{paveM}	Cumulative average seven-day high pavement temperature
T_{airM}	Cumulative average seven-day high ambient air temperature
T_{airS}	Air temperature standard deviation
T_{pavem}	Mean of low pavement temperature
T_{airm}	Mean of low ambient air temperature
T_{airs}	Standard deviation of low ambient air temperature
Lat^2	Square of latitude
H^2	Square of depth to surface.
T_{hD}	Historical distribution of hourly temperature
T_{hr}	Hourly predicted temperature
P_{hr}	hourly precipitation data
SL_1, SL_2, SL_3….	Service lives computed for each distress
$\|E^*\|_{eff}$	Effective dynamic modulus
E*	Dynamic Modulus
XX	High-temperature grade

YY	Low temperature grade
MG	Change in asphalt mixture gradation
BG	Change in asphalt binder grade
BT	Change in the base type
CO_2	Carbon Dioxide
CT	Change in asphalt layer thickness

Chapter 1: Introduction

1.1 Background and motivation

Environmental factors are one of the primary causes of pavement deterioration. The predominant climate-related pavement deterioration factors are temperature, precipitation, percent sunshine, wind speed, groundwater table, and humidity. All these factors are responsible for the deterioration of the pavement, and climate change has caused major shifts in all these factors.

The foremost effects of climate change are the rise in air temperature, changes in precipitation patterns and intensity, and changes in other minor climate factors, such as percent sunshine, wind speed, and humidity. Many studies have quantified the impact of these factors on the pavement. These studies reveal that temperature and precipitation are the most significant climate factors that cause pavement deterioration.

1.1.1 Temperature

Temperature is one of the primary factors that affect pavement deterioration. Several studies have reported temperature increase due to climate change in Canada (Vincent et al., 2018), United States (Paquin et al., 2014), South America (Marengo et al., 2012), Europe (Meleux et al., 2007), Africa (Jones & Thornton, 2009), Middle East (Evans, 2009), China (Zhai & Pan, 2003), India (Dash et al., 2007), Central Asia (Lioubimtseva & Henebry, 2009), Southeast Asia (Gasparrini et al., 2017) and Australia (Hughes, 2003). Pavement performance models show that increases in temperature will result in accelerated pavement deterioration.

Temperature affects pavement materials, which leads to pavement deterioration. Temperature increases can reduce the Dynamic Modulus (E*) of the surface Hot Mix Asphalt (HMA) layer, which leads to a reduction in the service life of pavement (Kumlai et al., 2016). The major advantages for temperature consideration are (1) the uncertainties in the climate change temperature prediction are less than that of the other climate factors (Kharin et al., 2007; Piras et al., 2015); (2) the impact of temperature is significantly higher than that of all the other factors (Gudipudi et al., 2017; Knott et al., 2019; Qiao et al., 2016; Qiao, Flintsch, et al., 2013; Rana et al., 2020; Underwood, 2019); and (3) temperature plays a vital role in selecting pavement surface materials (Fletcher et al., 2016; Mills et al., 2009; Viola & Celauro, 2015).

1.1.2 Precipitation

Precipitation is also a dynamic climate factor that affects pavement deterioration. An increase in precipitation might cause a moisture imbalance in the subgrade, which leads to a reduction of stiffness properties on the subgrade (Mallick et al., 2014, 2016). Also, rainfall is becoming more intense over shorter periods, which causes frequent flooding events. This change in the distribution of rainfall is the predominant factor affecting the base layers of pavement structure (Elshaer et al., 2018).

1.1.3 Other climate factors

Percent sunshine, wind speed, humidity, and groundwater level also signify the climate impact on pavement deterioration. As climate change projections are not available for these climate factors, Qiao et al. (2013) estimated the influence of a 5.0% change in percent sunshine, wind speed, and groundwater level on pavement performance. The results of this investigation did not suggest that these factors had a significant influence on pavement performance (Qiao, Dawson, et al., 2013; Qiao, Flintsch, et al., 2013). However, it is necessary to look at the climate change projections for these factors using a statistical approach and to observe the interaction of these factors with temperature and precipitation. A recent study stated that the increase in the percent sunshine is likely to affect the asphalt materials through asphalt aging, embrittlement, and cracking (Shao et al., 2017).

1.2 Challenge: Quantification and mitigation of climate change impact

The onset of climate change is a phenomenon expected to significantly impact infrastructure across the world (Qiao, Dawson, et al., 2013; Qiao, Flintsch, et al., 2013). Flexible pavements will strongly reflect these changes due to their temperature sensitive components and, as a result, they may begin to perform poorly. Currently, strict design methodology exists to uphold pavement conditions to a satisfactory level, promoting safety and comfort to drivers. With the expected future change in temperatures, these design methodologies must continue to evolve. Although there are appropriate design methodologies for today's climate, uncertainty remains regarding the best way to build the pavements for future climate. Exploring various design strategies while considering climate change is a challenging and necessary step to build resilient infrastructure.

1.3 Current state of knowledge and gaps

After a comprehensive review on the climate change impact on pavement performance and its mitigation, limitations and knowledge gaps are found in the existing literature. The limitations and knowledge gaps found in the reviewed literature are as follows:

- To date, the most of research studies in this domain relied on one or two climate models to quantify the impact of climate change. Considering only one or two climate change models could result in a high degree of uncertainty.
- Most of the studies in Canada are mainly based on GCM's with a grid of 300 km x 300 km. In addition, the climate change data used for the analysis is not corrected for bias, which leads to under/overestimation of pavement performance.

- Most of the current studies have relied on one pavement structure, one location or one climatic region. Therefore, conclusions drawn from these studies may not be generalizable to other pavement structures or climate regions.
- The influence of upgraded binder (considering climate change) on pavement performance or service life is not discussed in the current literature.
- Temperature models developed based on latitude are often accurate for only the regions in which they were developed. This drawback is felt particularly strongly in Northern Canada, where the extreme temperatures cannot be represented with one equation developed in the United States.
- The Long-Term Pavement Performance (LTPP) model, developed only for maximum latitudes of 52 degrees, has had limited testing in the Northern Canadian climate and does not fully represent the complex climate observed.
- The few existing pavement temperature models for Canadian climates have been developed for specific locations that are not applicable across the country. Therefore, it is inferred through the literature review that a national pavement temperature model is necessary for Canadian pavement designers.
- Most studies have used Long-Term Pavement Performance (LTPP) or Strategic Highway Research Program (SHRP) pavement temperature models to convert climate data to pavement temperatures. These models have limited geographical applications and may be less accurate for northern climates.
- Although several adaptation strategies have been investigated, there is limited research into the effects of combining them. Existing studies combined modified HMA and stabilized subgrades but none of the other possible adaptation strategies.

- Influence of climate change adaptation strategies on Canadian economy and the environment are not evaluated in the existing literature.

1.4 Objectives

The objectives of the research are as follows:

i. Quantifying climate change impact on pavement performance and pavement service life.
ii. Determining influence of temperature rise on asphalt binder grade selection using three different pavement temperature models such as Strategic Highway Research Program (SHRP) Pavement temperature model, the LTPP pavement temperature model, and the Enhanced Integrated Climate Model (EICM) software.
iii. Developing a pavement temperature model of Canadian climatic conditions.
iv. Developing a Canadian Asphalt Binder Selection (CABS) software tool to implement the pavement temperature model to determine the asphalt binder grade.
v. Evaluating the pavement performance of different climate change adaptation strategies for selected locations in Canada.
vi. Comparing the results of the different strategies to determine an appropriate adaptation strategy for each location.
vii. Quantifying the influence of climate change adaptation on Canadian environment and economy using life cycle assessment and life cycle cost analysis techniques.

1.5 Thesis framework

This thesis is prepared in manuscript format. The outcome of the study is presented in eight chapters. The thesis framework for Chapter 3 to Chapter 8 are illustrated in the Figure 1-1, Figure 1-2, and Figure 1-3

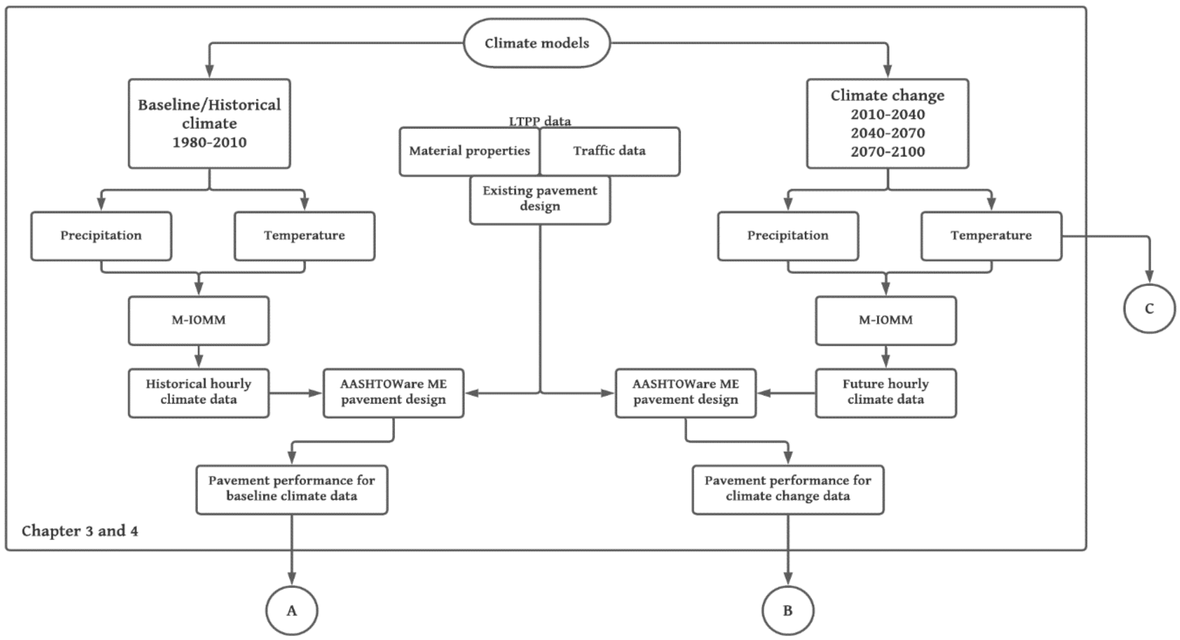

Figure 1-1: Thesis framework; Part 1

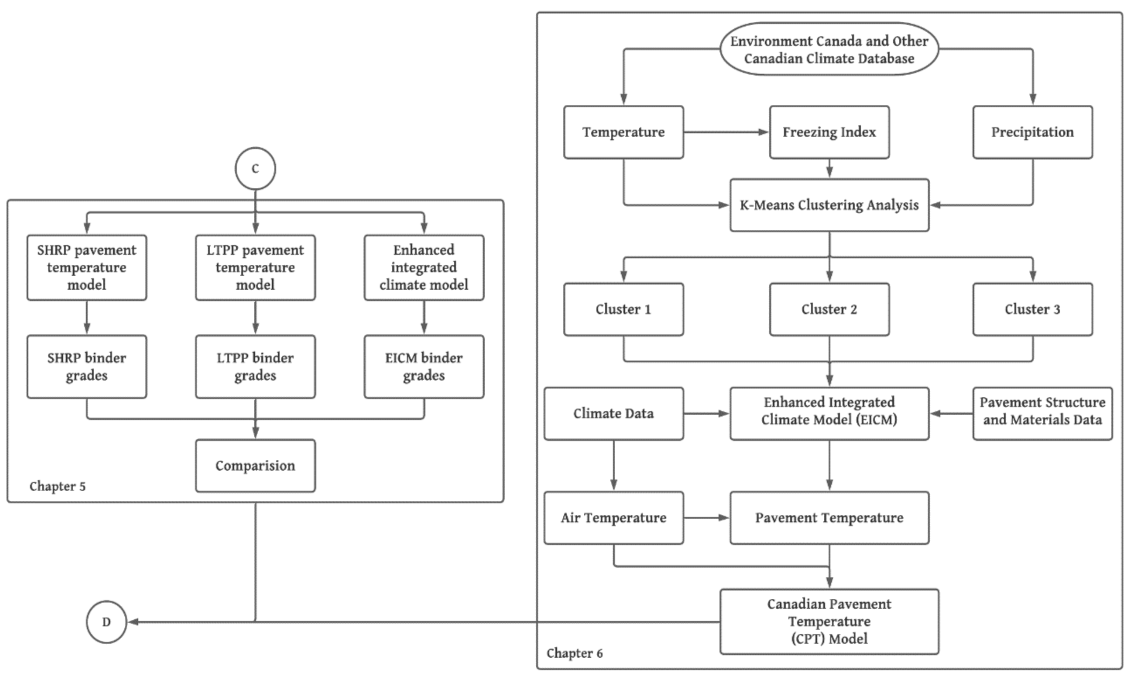

Figure 1-2: Thesis framework; Part 2

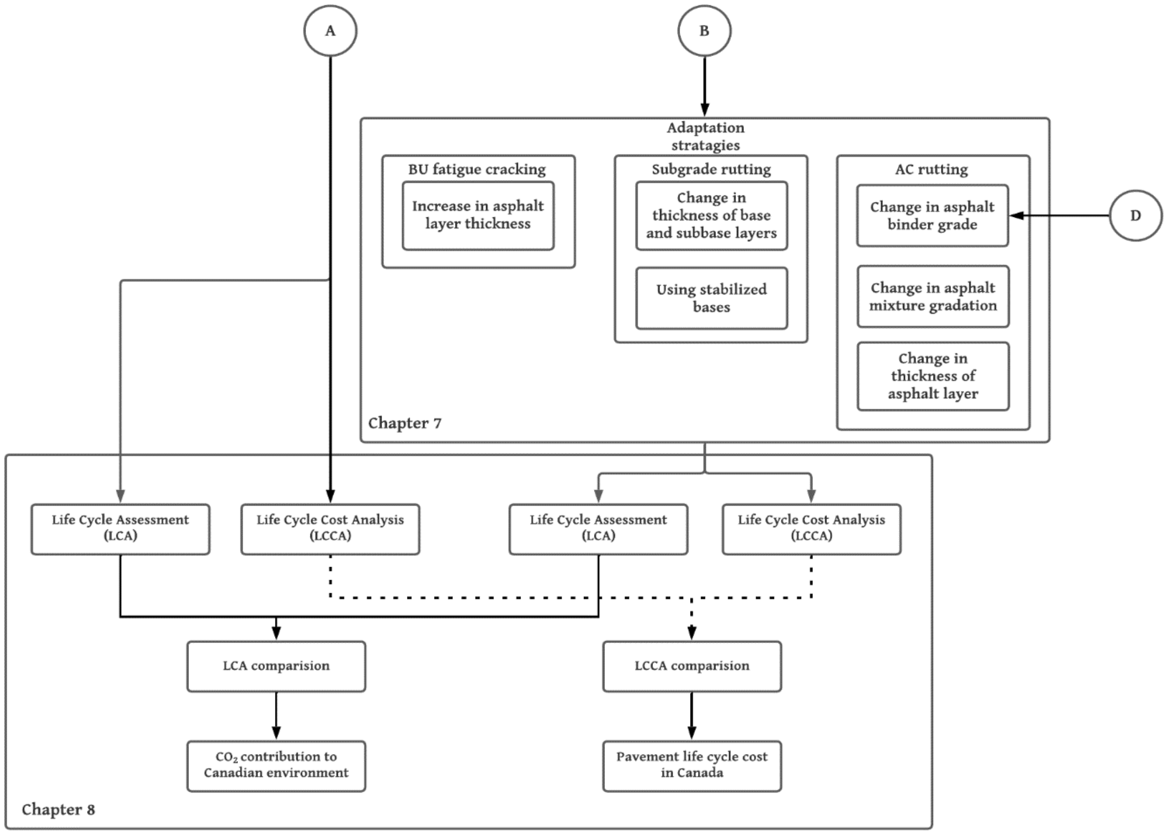

Figure 1-3: Thesis framework; Part 3

Chapter 1 presents the background, motivation, and the objectives of the present study.

Chapter 2 provides an extensive literature review on the influence of climate change on pavement design and materials, highlighting the quantification of climate change impact, and adaptation strategies to mitigate the impact. Also, the research gaps of the climate change impact on pavement infrastructure are shown and considered to finalize the research objectives and the works for Chapters 3-8. This chapter was submitted for publication to the Canadian Journal for Civil

Engineering (CJCE) as a review paper. “Swarna S T, Hossain K. (2021). Climate Change Impact and Adaptation for Pavement Infrastructure: A Literature Review. Canadian Journal of Civil Engineering. First Review Submitted.”

Chapter 3 investigates the impact of climate change on pavement design in the province of Newfoundland and Labrador, Canada. Mechanistic-Empirical Pavement Design Software, AASHTOWare was used to determine the pavement performance for both historical climate (referred as baseline climate) and the projected climate change. To predict the climate change model, a statistically downscaled climate change models were taken from Coordinated Regional Downscaling (CORDEX) Experiments. These models include daily maximum and minimum temperatures only. However, to estimate the hourly climate model, two relatively new hourly estimation procedures, such as Modified Imposed Offset Morphing Method (M-IOMM) and Sine (14R-1), are used. These climate change models were incorporated into the AASHTOWare ME Pavement software to predict the pavement performance and compared with the baseline climate. This study found that climate change causes the early deterioration of pavement compared to the baseline climate. This chapter was submitted for publication to the International Journal of Pavement Engineering and Technology (IJPRT) as a research article. “Swarna S T, Rana M, Hossain K. (2021). Impact of Climate Change on Pavement Performance in Canada’s Newfoundland Island. International Journal of Pavement Engineering and Technology. First Review Submitted.”

Chapter 4 quantifies impact of climate change on pavement performance in Canada. In addition, this chapter assesses the change in asphalt binder grade for the future climate to determine the influence of change in binder grade on the performance of pavements in Canada. To achieve this, the analysis was carried out in five phases. In the first phase, statistically downscaled climate change models were gathered from the pacific Canada Climate database. Then in the second phase, the temperature and precipitation data were extracted for the sixteen locations. In the third phase, the hourly temperature data are computed using M-IOMM. Then, in the fourth phase, the pavement materials, traffic, and structural data were collected from the Long-term Pavement Performance (LTPP) database. Lastly, the pavement performance was assessed using AASHTOWare Mechanistic-Empirical Pavement Design. This chapter was published in Transportation Research Record (TRR) Journal. "Swarna S T, Hossain K, Pandya H, Mehta Y A. (2021). Assessing Climate Change Impact on Asphalt Binder Grade: Selection and its Implications. Transportation Research Record: Journal of the Transportation Research Board. https://doi.org/10.1177/03611981211013026"

Chapter 5 aims to estimate the new asphalt binder grades for Canadian climatic conditions using the projected climate data. To achieve this, the study was organized in five phases. In the first phase, a total of ten statistically downscaled climate change models were accumulated from the Pacific Climate database. In the second phase, a python code was written and executed to extract the temperature data for the selected locations. Then, in the third phase, an average seven-day maximum pavement temperature and a minimum pavement temperature were determined using the three different pavement temperature prediction models: SHRP, LTPP, and EICM. Later in the fourth phase, the high-temperature grade (XX) and low temperature grade (YY) of an asphalt binder (PG XX – YY) were estimated using the average seven-day maximum and minimum pavement temperature respectively. Lastly, in the fifth phase, the asphalt binder grades are compared. This study presents a summary of revised asphalt binder grades for twenty-eight different locations across Canada. This chapter was published in Road Materials and Pavement Design (RMPD) Journal. "Swarna S T, Hossain K. (2021). Influence of Climate Change on

Asphalt Binder Selection for Canadian Climatic Conditions. Road Materials and Pavement Design. https://doi.org/10.1080/14680629.2021.2019093"

Chapter 6 focuses on developing a new pavement temperature model for Canadian climatic conditions. In this study, Canada has been geographically divided into three clusters with similar average annual air temperature, annual average precipitation, and freezing indexes to generate this new model. Independent pavement temperature equations have been developed to represent the locations found within each of the clusters by using a machine learning technique. Multiple linear regression models were generated using variables determined to be the most highly correlated. Across Canada, 9144 observation points were used for the model development, 10% of data was randomly separated for validation and from the remaining data, 80% of the data points were used to train the model and the remaining 20% were used to test the model. The resulting model returned satisfactory accuracy upon validation and represented a good alternative for Canadian pavement designers. Additionally, a software tool titled CABS has been developed to select asphalt binders based on the predicted pavement temperatures to implement the model. This chapter was submitted for publication to the Road Materials and Pavement Design (RMPD) Journal as a research article. "Swarna S T, Hossain K, Bernier A. (2022). Pavement Temperature Model for Canadian Asphalt Binder Selection: Introduction to The CPT Model. Road Materials and Pavement Design. Submitted on October 05, 2021. Under Review."

Chapter 7 describes a framework for selecting an appropriate adaptation strategy to mitigate climate change impact. To fulfill this, the influence of climate change on long-term pavement performance in Canada has been quantified over sixteen Canadian pavement sections located over various provinces in Canada. In addition, the fundamental causes of pavement deterioration due to climate change were determined using ten different climate change models. Various adaptation strategies such as upgrading asphalt binder grade, increasing the thickness of asphalt concrete layer, increasing the base layer thickness, and using stabilized base layers were analyzed to reduce pavement deterioration and to extend the service life of the pavement. Unlike the other studies, pavement temperatures were determined using EICM to determine the change in binder grade for the future climate in the adaptation process. A stone matrix asphalt mixture gradation is considered as another adaption strategy where the AC rutting is found to be very high. To reduce the subbase and subgrade rutting, an emulsion stabilized base is adapted for specific locations. This chapter was submitted for publication to the Journal of Cleaner Production (JCP) as a research article. "Swarna S T, Hossain K, Mehta Y, Bernier A. (2022). Climate Change Adaptation Strategies for Canadian Asphalt Pavements; Part 1: Adaptation Strategies. Journal of Cleaner Production. Submitted on November 15, 2021. Under Review."

Chapter 8 quantifies the influence of climate change impacts and its adaptation strategies on Canadian economy and the environment. It is evident that climate change accelerates pavement deterioration, which leads to the reduced service life of the pavement. To uphold the design service life, it is necessary to design and maintain the pavements considering the future climate. This adaptation results in preserving the pavements throughout the design service life, which might increase the life cycle cost of pavements; however, these will be beneficial in the long run. Besides, adapting to climate change might also increase greenhouse gases further in the atmosphere. So, there is a necessity to optimize the adaptation strategies to preserve the service life of pavement with less economic cost and less emissions. This chapter was submitted for publication to the Journal of Cleaner Production (JCP) as a research article. "Swarna S T, Hossain K, Bernier A. (2022). Climate Change Adaptation Strategies for Canadian Asphalt Pavements; Part 2: LCA and LCCA. Journal of Cleaner Production. Submitted on November 15, 2021. Under Review."

Chapter 9 summarizes the general conclusions of this study and recommendations and suggestions for future works.

At the end of all chapters, reference sections include the references cited in the chapters as parts of stand-alone papers.

1.6 Significant contributions

1.6.1 Journal articles

- **Swarna S T**, Hossain K, Bernier A. (2022). Climate Change Adaptation Strategies for Canadian Asphalt Pavements; Part 2: LCA and LCCA. Journal of Cleaner Production. Submitted on November 15, 2021. Under Review.
- **Swarna S T**, Hossain K, Bernier A. (2022). Climate Change Adaptation Strategies for Canadian Asphalt Pavements; Part 1: Adaptation Strategies. Journal of Cleaner Production. Submitted on November 15, 2021. Under Review.
- **Swarna S T**, Hossain K, Bernier A. (2022). Pavement Temperature Model for Canadian Asphalt Binder Selection: Introduction to The CPT Model. Road Materials and Pavement Design. Submitted on October 05, 2021. Under Review.
- **Swarna S T**, Hossain K. (2021). Influence of Climate Change on Asphalt Binder Selection for Canadian Climatic Conditions. Road Materials and Pavement Design. Submission No: RMPD-21-05-44. Accepted. In Press. https://doi.org/10.1080/14680629.2021.2019093
- **Swarna S T**, Hossain K. (2021). Climate Change Impact and Adaptation for Pavement Infrastructure: A Literature Review. Canadian Journal of Civil Engineering. First Review Submitted.
- **Swarna S T**, Rana M, Hossain K. (2021). Impact of Climate Change on Pavement

Performance in Canada’s Newfoundland Island. International Journal of Pavement Engineering and Technology. First Review Submitted.

- **Swarna S T**, Hossain K, Pandya H, Mehta Y A. (2021). Assessing Climate Change Impact on Asphalt Binder Grade: Selection and its Implications. Transportation Research Record: Journal of the Transportation Research Board. https://doi.org/10.1177/03611981211013026

1.6.2 Conference papers

- **Swarna S T**, Hossain K, Bernier A. (2022). Pavement Temperature Model for Canadian Asphalt Binder Selection: Introduction to The CPT Model. 101st Transportation Research Board (TRB) Conference. Washington DC, USA. **Accepted**.

- **Swarna S T**, Hossain K, Mehta Y, Bernier A. (2022). Climate Change Adaptation Strategies for Canadian Asphalt Pavements. 101st Transportation Research Board (TRB) Conference. Washington DC, USA. **Accepted**.

- **Swarna S T**, Hossain K, Bernier A. (2021). Selection of Appropriate Binder Grade for Changing Climate and Its Influence on Pavement Performance. 66th Annual Conference of Canadian Technical Asphalt Association (CTAA). Charlottetown, PE, Canada. **Presented**.

- **Swarna S T**, Hossain K, Pandya H, Mehta Y A. (2021). Assessing Climate Change Impact on Asphalt Binder Grade: Selection and its Implications. 100th Annual Meeting of the Transportation Research Board (TRB) of National Academies of Science and Engineering. Washington DC, USA. **Presented**.

- **Swarna S T**, Hossain K. (2020). Changes in Asphalt Binder Grade Due to Climate Change in Canada. Testing and Modeling of Road and Embankment Materials (PS) Session. Transportation Association of Canada (TAC) Annual Conference. Vancouver, BC, Canada. **Presented**.

- Rana M, **Swarna S T**, Hossain K. (2020). Climate Change Impact on Pavement Performance in Newfoundland, Canada. 99th Annual Meeting of the Transportation Research Board (TRB) of National Academies of Science and Engineering. Washington DC, USA. **Presented**.
- **Swarna S T**, Hossain K. (2019). Impact of Climate Change on Pavement Performance in Newfoundland, Canada. 64th Annual Conference of Canadian Technical Asphalt Association (CTAA). Montreal, Canada. **Presented**.

1.7 Co-Authorships

All the research presented in the journals and conference papers in chapters 2-8 has been conducted by the author of this thesis, Surya Teja Swarna, under the supervision of Dr. Kamal Hossain. Mr. Swarna also prepared the draft manuscript. The other co-authors supervised the research and reviewed the manuscript.

1.8 Reference

Chen, X., & Wang, H. (2020). Quantification of Warming Temperature Impact on Flexible Pavement Overlay Performance in New Jersey. *99th Annual Meeting of the Transportation Research Board (TRB) of National Academies of Science and Engineering, Washington DC*.

Dash, S. K., Jenamani, R. K., Kalsi, S. R., & Panda, S. K. (2007). Some evidence of climate change in twentieth-century India. *Climatic Change*, *85*(3–4), 299–321. https://doi.org/10.1007/s10584-007-9305-9

Elshaer, M., Ghayoomi, M., & Daniel, J. S. (2018). Bearing capacity analysis of pavement structures for short term flooding events. *Bearing Capacity of Roads, Railways and Airfields - Proceedings of the 10th International Conference on the Bearing Capacity of Roads, Railways and Airfields, BCRRA 2017*, *5*(October), 2127–2133. https://doi.org/10.1201/9781315100333-301

Evans, J. P. (2009). 21st century climate change in the Middle East. *Climatic Change*, *92*(3–4), 417–432. https://doi.org/10.1007/s10584-008-9438-5

Fletcher, C. G., Matthews, L., Matthews, L., Andrey, J., & Saunders, A. (2016). *Projected changes in mid-21st century extreme maximum pavement temperature in Canada Projected changes in mid-21 st century extreme maximum pavement temperature in Canada*. *April*. https://doi.org/10.1175/JAMC-D-15-0232.1

Gasparrini, A., Guo, Y., Sera, F., Vicedo-Cabrera, A. M., Huber, V., Tong, S., de Sousa Zanotti Stagliorio Coelho, M., Nascimento Saldiva, P. H., Lavigne, E., Matus Correa, P., Valdes Ortega, N., Kan, H., Osorio, S., Kyselý, J., Urban, A., Jaakkola, J. J. K., Ryti, N. R. I., Pascal, M., Goodman, P. G., … Armstrong, B. (2017). Projections of temperature-related excess mortality under climate change scenarios. *The Lancet Planetary Health*, *1*(9), e360–e367. https://doi.org/10.1016/S2542-5196(17)30156-0

Gudipudi, P. P., Underwood, B. S., & Zalghout, A. (2017). Impact of climate change on pavement structural performance in the United States. *Transportation Research Part D: Transport and Environment*, *57*(October), 172–184. https://doi.org/10.1016/j.trd.2017.09.022

Hughes, L. (2003). Climate change and Australia: Trends, projections and impacts. *Austral Ecology*, *28*(4), 423–443. https://doi.org/10.1046/j.1442-9993.2003.01300.x

Jones, P. G., & Thornton, P. K. (2009). Croppers to livestock keepers: livelihood transitions to

2050 in Africa due to climate change. *Environmental Science and Policy*, *12*(4), 427–437. https://doi.org/10.1016/j.envsci.2008.08.006

Kharin, V., Zwiers, F., Zhang, X., & Gabriele, H. (2007). *Changes in Temperature and Precipitation Extremes in the IPCC Ensemble of Global*. 1419–1444. https://doi.org/10.1175/JCLI4066.1

Knott, J. F., Sias, J. E., Dave, E. V, & Jacobs, J. M. (2019). *Seasonal and Long-Term Changes to Pavement Life Caused by Rising Temperatures from Climate Change*. *2673*(6), 267–278. https://doi.org/10.1177/0361198119844249

Kumlai, S., Jitsangiam, P., & Pichayapan, P. (2016). The implications of increasing temperature due to climate change for asphalt concrete performance and pavement design. *KSCE Journal of Civil Engineering*, *21*(4), 1222–1234. https://doi.org/10.1007/s12205-016-1080-6

Lioubimtseva, E., & Henebry, G. M. (2009). Climate and environmental change in arid Central Asia: Impacts, vulnerability, and adaptations. *Journal of Arid Environments*, *73*(11), 963–977. https://doi.org/10.1016/j.jaridenv.2009.04.022

Mallick, R., Jacobs, J. M., Miller, B. J., Daniel, J. S., Mallick, R. B., Jacobs, J. M., Miller, B. J., & Daniel, J. S. (2016). *Understanding the impact of climate change on pavements with CMIP5 , system dynamics and simulation*. *8436*(January 2017). https://doi.org/10.1080/10298436.2016.1199880

Mallick, R., Radzicki, M., Daniel, J., & Jacobs, J. (2014). Use of System Dynamics to Understand Long- Term Impact of Climate Change on Pavement Performance and Maintenance Cost. *Transportation Research Record Journal of the Transportation Research Board*, *5*(December 2014). https://doi.org/10.3141/2455-01

Marengo, J. A., Chou, S. C., Kay, G., Alves, L. M., Pesquero, J. F., Soares, W. R., Santos, D. C., Lyra, A. A., Sueiro, G., Betts, R., Chagas, D. J., Gomes, J. L., Bustamante, J. F., & Tavares, P. (2012). Development of regional future climate change scenarios in South America using the Eta CPTEC/HadCM3 climate change projections: Climatology and regional analyses for the Amazon, São Francisco and the Paraná River basins. *Climate Dynamics*, *38*(9–10), 1829–1848. https://doi.org/10.1007/s00382-011-1155-5

Meleux, F., Solmon, F., & Giorgi, F. (2007). Increase in summer European ozone amounts due to climate change. *Atmospheric Environment*, *41*(35), 7577–7587. https://doi.org/10.1016/j.atmosenv.2007.05.048

Mills, B., Tighe, S., Andrey, J., Smith, J., & Huen, K. (2009). Climate Change Implications for Flexible Pavement Design and Performance in Southern Canada. *Journal of Transportation Engineering*, *135*(10), 773–782. https://doi.org/10.1061/(asce)0733-947x(2009)135:10(773)

Paquin, D., De Elía, R., & Frigon, A. (2014). Change in North American atmospheric conditions associated with deep convection and severe weather using CRCM4 climate projections. *Atmosphere - Ocean*, *52*(3), 175–190. https://doi.org/10.1080/07055900.2013.877868

Piras, M., Mascaro, G., Deidda, R., & Vivoni, E. R. (2015). Science of the Total Environment Impacts of climate change on precipitation and discharge extremes through the use of statistical downscaling approaches in a Mediterranean basin. *Science of the Total Environment*. https://doi.org/10.1016/j.scitotenv.2015.06.088

Qiao, Y., Casey, D. B., Kuna, K. K., Kelly, K., & Macgregor, I. D. (2016). *Climate Resilience of Flexible Pavement Highways : Assessment of Current Practice*. *July 2017*, 1–14.

Qiao, Y., Dawson, A., Parry, T., & Flintsch, G. (2013). Quantifying the effect of climate change on the deterioration of a flexible pavement. *Proceedings of the International Conferences on the Bearing Capacity of Roads, Railways and Airfields, June 2013*.

Qiao, Y., Flintsch, G., Dawson, A., & Parry, T. (2013). Examining Effects of Climatic Factors on Flexible Pavement Performance and Service Life. *Transportation Research Record: Journal of the Transportation Research Board*, *2349*(1), 100–107. https://doi.org/10.3141/2349-12

Rana, M., Swarna, S., & Hossain, K. (2020). Climate Change Impact on Pavement Performance in Newfoundland , Canada. *99th Annual Meeting of the Transportation Research Board (TRB) of National Academies of Science and Engineering, Washington DC, USA*.

Shao, Z., Jenkins, G., & Oh, E. (2017). Assessing the impacts of climate change on road infrastructure. *International Journal of GEOMATE*, *13*(38), 120–128.

Underwood, S. (2019). A method to select general circulation models for pavement performance evaluation A method to select general circulation models for pavement performance evaluation. *International Journal of Pavement Engineering*, *0*(0), 1–13. https://doi.org/10.1080/10298436.2019.1580365

Vincent, L. A., Zhang, X., Mekis, Wan, H., & Bush, E. J. (2018). Changes in Canada’s Climate: Trends in Indices Based on Daily Temperature and Precipitation Data. *Atmosphere - Ocean*, *56*(5), 332–349. https://doi.org/10.1080/07055900.2018.1514579

Viola, F., & Celauro, C. (2015). Effect of climate change on asphalt binder selection for road construction in Italy. *Transportation Research Part D: Transport and Environment*, *37*, 40–47. https://doi.org/10.1016/j.trd.2015.04.012

Zhai, P., & Pan, X. (2003). Trends in temperature extremes during 1951-1999 in China. *Geophysical Research Letters*, *30*(17). https://doi.org/10.1029/2003GL018004

Chapter 2: Climate Change Impact and Adaptation for Highway Asphalt Pavements: A Literature Review

2.1 Abstract

For the past few decades, researchers all over the world have agreed that the service life of civil infrastructures is significantly affected by climate change. Pavement is one of these significant infrastructures that can be easily affected by climate change. However, it is well known that predicting climate change is highly complex and dynamic. Hence, a review has been done on available climate change models and the uncertainties involved in climate change prediction. In addition, a review of existing practices for downscaling and hourly data estimation is illustrated. This study mainly focuses on the existing climate change models and state-of-the-art literature relevant to climate change impact and adaption for pavement infrastructure. This review collates evidence of climate change effects in four predominant areas: (1) pavement materials, (2) pavement design and performance, (3) maintenance and rehabilitation, and (4) economics and emissions. This review disclosures that climate change is severely affecting pavement infrastructure in all aspects. Further, the service life of the pavement is significantly decreasing due to climate change, which ultimately increases the Life Cycle Cost (LCC) of pavements. A review has been done on the various adaptation and mitigation strategies to counterweigh the increase in LCC. The pro-active measures which might reduce LCC are changing the superpave binder grade, changing the design thicknesses and early triggered maintenance. These measures exhibit a significant reduction in increased LCC due to climate change. This review addresses various important question such as (1) what is climate change? (2) how to use climate change models? (3) how climate change impacts the pavement infrastructure? (4) what are the adaptation and mitigation strategies available? and (5) how economic costs and emissions change due to

climate change? This review is useful to understand the climate change and its implications on pavement infrastructure.

Keywords: Climate Change, Pavement Performance, Pavement Maintenance, Pavement Service Life, Life Cycle Cost Analysis, Temperature Rise

2.2 Climate change and its impact

2.2.1 Climate change and its impact

The last three decades have been riveting for scientists working on climate change. Monitoring, predicting, and communicating changes in weather patterns and their effects on human life has been a talking point amongst scientists, industrialists, and policymakers alike (IPCC, 2007). The changing environmental conditions have affected humans in a myriad of ways, directly and indirectly. It has become imperative to make changes in government policies and personal lifestyles to combat the adverse effects of the changing environmental conditions. An action plan on climate change has become one of the key agendas of political parties in recent national elections. Fueled by protests, awareness campaigns, and a sense of sustainable living, the consensus on this global issue has garnered enough attention that decisions on crucial activities in almost every sphere are being influenced, keeping their impact on the climate in mind. Transportation infrastructure is one of the sectors looking to adapt to the projections of the changing climate. In the past decade, a number of researchers have looked for ways to tweak pavement parameters to better combat the fluctuating climate conditions.

Temperature, precipitation, incoming percent of sunshine, humidity, wind speed, and groundwater levels are the climate factors that alter pavement performance, design, and service life (Knott, Jacobs, et al., 2019). In addition, the other factors such as permafrost thaw, freezing index and freeze and thaw cycles significantly influence the flexible pavement in the Northern part of Canada. An undesirable stress on these pavement parameters due to changes in the environmental variables leads to an increased cost for repairs and maintenance. Reviews on the impact of climate change on pavement performance have emphasized a change in design methodology in response to increasing costs. While some studies suggest implementing proactive measures, like increasing thickness (Knott et al., 2020) and upgrading superpave binder grades (Fletcher et al., 2016), others have recommended early triggered maintenance (Qiao et al., 2015). Each of these comes with elevated costs attached. In summary, change in environmental factors due to climate change is known to effect pavement infrastructure and reduction in service life. To maintain the design service life, various adaptation strategies are inevitable, and consequently, costs escalate.

2.2.2 Climate change models

Climate models are the most critical tools for understanding previous climate states and making predictions about the future. They account for natural and human-induced forcings on the climate system and simulate environmental conditions on a range of seasonal to decadal time scales. Physical laws governing the interactions between atmosphere, ocean, land, and sea ice are expressed in mathematical terms. These expressions of the Earth's systems are converted into computer languages, and parametrizations are then applied to build conceptual models (Flato et al., 2013). Models can be of varying complexities; the most complex ones require substantial supercomputing power. The Atmosphere-Ocean General Circulation Models (AOGCM) consider atmosphere, ocean, land, and sea ice in their parameterizations. Earth System Models (ESM) are the most complex and state of the art models currently available. They build upon AOGCMs by including biogeochemical cycles, carbon cycles, Sulphur cycles and ozone (Flato et al., 2013; Taylor et al., 2012).

Regional Climate Models (RCM) focus on a particular area (for example, North America) to simulate processes pertaining to the continent. Since climate models take in a range of natural and anthropogenic parameters as inputs, with assumptions about future scenarios, they are prone to uncertainties (Flato et al., 2013). This, coupled with a lack of efficient computing technologies, leads to approximations, further aggravating uncertainties. To minimize these uncertainties, climate models are often used in a collection of distinct models. The World Climate Research Programme (WCRP), the working group responsible for modeling for the Intergovernmental Panel on Climate Change (IPCC), uses the Coupled Model Intercomparison Project (CMIP) in their assessment reports. These intercomparisons deal with a large group of models from various modelling centers around the world, exploring the range of model behaviors and assessing the strengths and weaknesses of each through controlled experiments. These experiments help to capture errors that are specific to an individual model or that might require a universal theoretical adjustment. Experiments look at 'long-term' trends on a 100-year time scale and 'near-term' trends on a temporal scale of 10-30 years (Taylor et al., 2012).

The latest report released by IPCC uses the fifth phase of CMIP, the CMIP5, which is an ensemble of fifty-five distinct climate models. A notable development in the prediction methodology of the CMIP5 project is the categorization of future scenarios in terms of radiative forcings (Stocker et al., 2013). Known as the Representative Concentration Pathways (RCP), this concept defines four predicted greenhouse gas emission scenarios based on social and political aspects of the implementation of mitigation strategies. The RCP 2.6 criteria is the most optimistic one which assumes that the global annual Green House Gases (GHG) emissions will see a peak between 2010 –2020, after which the emissions will decline. In RCP 4.5, emissions would peak around 2040 and then decline. RCP 6.0 has a peak around 2080 and decline thereafter. On the pessimistic end, RCP 8.5 sees emissions continuing to rise until the end of 21st century (Stocker et al., 2013).

2.2.3 Uncertainties in climate change models

Natural processes are chaotic, and the effects of such processes generate some of the most intricate patterns in the Earth's environment. Evaluating and then interpreting such systems is a scientific challenge. If the effects of chaotic natural processes are climate systems, then evaluating them using climate models gives rise to uncertainties. Hence, the uncertainties in a climate system form the bulk of problems in a climate model. This section gives a brief investigation into the challenges that uncertainties pose in climate modelling and how scientists work to solve them.

Uncertainties in climate models arise from estimations that define initial conditions, calculated parameters – such as radiative forcing and future population projections – the equations binding them, and the model's design itself (Benjamin & Budescu, 2018). As Benjamin and Budescu revealed in their surveys, uncertainties play a massive role in how people perceive climate model results. The authors assessed test subjects' perceptions through their review of two different types of model outputs: one that used precise data but gave conflicting results and another that had imprecise inputs but gave complimentary results. They found that the public was more concerned about the consistency of results rather than the model itself and the physics behind it. Specifically, they had more confidence in imprecise but agreeing models than precise but conflicting ones, as these were prone to misinterpretation. Kudo et al. investigated how uncertainties from climate models impacted snow models (Kudo et al., 2017). In their projections of snow processes in Japan, the uncertainties amplified when they were coupled with derivatives from the Global Circulation Model (GCM) results. This resulted in a hugely uncertain prediction of the impact of climate change on snow processes. In a similar study by Kundzewicz et al., GCM projections were used to run hydrological models in order to predict future events (Kundzewicz et al., 2018). The authors mention that selecting an ensemble of several climate models, downscaling techniques to produce regional climate models (RCM), and scaling mismatch between RCMs and hydrological models are some sources of uncertainties. If these are corrected before running climate impact models, better estimations can be made.

Mauritzen et al. proposed a way to reduce uncertainties by considering climate sensitivity, which is defined as "a measure of how fast Earth responds to changes in atmospheric carbon dioxide (CO_2) concentration (Mauritzen et al., 2017). Their results emphasize that certain variables in the models have high sensitivity to CO_2 emissions and others have low sensitivity. Their analysis demonstrated that subsetting model runs based on sensitivities gave lower uncertainties than full set runs. In another research project, Wang et al. proposed a new method of handling uncertainties based on Hierarchical Bayesian Models (BHM), which only require one simulation run of a model (Wang et al., 2019). According to them, traditional methods using ensemble model runs are computationally expensive. Although BHM cannot provide the range of metrics traditional methods provide, some standard diagnostics can be extracted with comparatively less computational power and faster processing speed, while better managing uncertainties.

2.2.4 Downscaling

Global Circulation Models (GCM) cannot always be used in their crude form for climate-impact studies because of their resolution. Research in hydrology, transportation, agriculture crop modelling, etc. that involve small-scale estimations are hampered by the low-resolution GCM outputs. Although the scientific community has come a long way in producing finer resolution models since the advent of climate modelling (owing to increased computing power), they are still not good for some local and regional scale applications. Presently, GCMs produce outputs at horizontal resolutions of roughly between 1° - 2° latitude for atmospheric processes, i.e., ≈ 100-200 km (Flato et al., 2013). It is worth noting that some models can produce a finer resolution of 0.5 degrees for near-term model runs. On the other hand, Regional Circulation Models (RCM) are capable of running at 50 km to 25 km resolutions. Very few models also run at 10 km resolution (Flato et al., 2013). Climate-impact related studies often use finer resolutions to match the scale of their study site. Applications to transportation and pavement engineering require environment variables to be resolved to the scale of tens of kilometers, spatially, and every hour in a day, temporally.

Several downscaling techniques exist, ranging in mathematical complexity and ease of use. The simplest ones involve modifying parameters by a constant value, for example, increasing the mean temperature by 2°C. Some sophisticated techniques require nesting a high-resolution RCM into GCM outputs. This approach is known as "dynamical downscaling". A moderately complex approach, termed "statistical downscaling", is based on developing a statistical model built on historic data, which is then employed to resolve the coarse GCM future projection data (Qiao et al., 2019). A sketch of the steps involved is exhibited in Figure 2-1.

A review of different downscaling techniques by Camici et al. demonstrates that downscaling can be a significant source of uncertainty (Camici et al., 2014). Hence, it is essential to choose an appropriate technique suitable for a particular application. The authors suggest the use of multiple GCMs in such studies. Substantial research has been done to evaluate the efficiency of dynamical and statistical downscaling procedures suitable for different areas of study. Although both have their own strengths and weaknesses and produce similar results of the present climate, they deviate significantly in their future projections (Wood et al., 2004). The dynamical approach is more consistent physically as it uses complex RCM and GCMs. However, at the same time, nesting the models can magnify the uncertainties of their outputs (Finnis & Daraio, 2018). The statistical approach, on the other hand, heavily relies on the current and historical weather values as initial inputs (Finnis & Daraio, 2018). This can also be seen in Figure 2-1. The reliance on initial inputs can be a problem in regions where the distribution of weather stations is scarce. However, it is proven to be less complex and computationally less expensive (Murphy, 1998).

From the extensive literature review of recent years, it was found that most studies in the civil engineering sector use a statistical downscaling approach for their study. This can be attributed to the fact that statistical downscaling is less complex and requires lower computational power than the nesting method (Qiao et al., 2019; Stoner et al., 2019; Valle et al., 2017). Dynamical downscaling requires an understanding of complex physical theories and modelling construction to accurately perform the nesting of models. In contrast, with current climate data readily available, relatively simpler statistical downscaling techniques do not impede expertise in modelling.

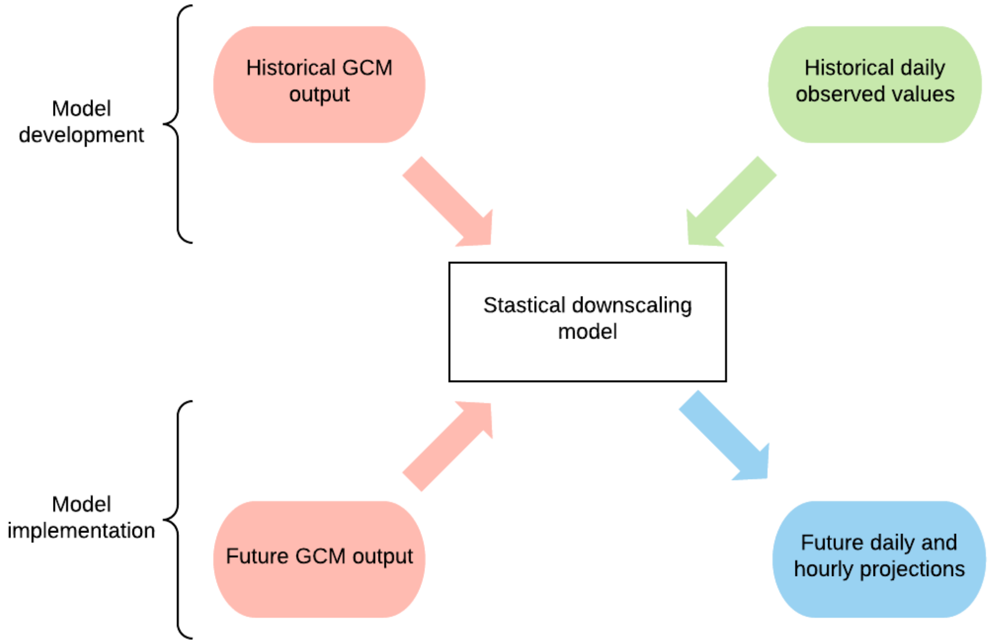

Figure 2-1: A sketch of the steps involved in developing a statistical downscaling model (Qiao et al., 2019)

2.2.5 *Hourly data estimation*

AASHTOWare Mechanistic-Empirical Pavement Design (MEPD) software, also named Mechanistic-Empirical Pavement Design Guide (MEPDG) software, is a robust pavement design system used to design both Asphalt Concrete (AC) and Portland Cement Concrete (PCC) pavements. This software considers four inputs: material properties for all the layers, traffic volume and distribution, climate, and structural design. The climate inputs in AASHTOWare software are hourly air temperature, wind speed, percent sunshine, precipitation, and relative humidity. Most of the studies used AASHTOWare to compute pavement performance and service life (ARA Inc, 2004). The MEPDG is sophisticated with the Enhanced Integrated Climate Model (EICM) to determine the pavement layer system's temperature and moisture distribution (Zapata et al., 2007). Therefore, AASHTOWare ME design uses hourly decomposed values of temperature, precipitation, percent sunshine, wind speed, and humidity as climate inputs to predict pavement performance. However, due to computational constraints, most climate change models only produce daily maximum and minimum air temperature, and average precipitation estimates of future climate in a changing climate scenario. Hence, it becomes imperative to convert daily climate model data to hourly values. Various algorithms for transforming the predicted climate data have been employed by researchers in the past. Some techniques used in the most recent studies are detailed below.

2.2.5.1 Chartered Institution of Building Services Engineers (CIBSE) Method

The Chartered Institution of Building Services Engineers (CIBSE) guide method (Chow & Levermore, 2007) fits daily maximum and minimum temperatures using sinusoidal curves at assigned times of occurrence of those temperatures in a day, as shown in Figure 2-2. The maximum and minimum temperature times are suggestions given by CIBSE Guide J and are constant for each month of the year. For example, the maximum temperature for a day in the month of January is assumed to occur at 1400 hours and minimum temperature at 0600 hours. Mathematically, hourly temperatures are calculated using:

$$T\ (t)\ =\ f_1\ \times T_{MIN}\ +\ f_2\ \times T_{MAX} \qquad \text{Equation 2-1}$$

where,

T_{MAX} is the maximum temperature occurring at time t_{max},

T_{MIN} is the minimum temperature occurring at time t_{min}.

Here, f_1 and f_2 are factors of sinusoidal interpolation, given by:

For $t < t_{min}$;

$$f_1 = \frac{\cos\left(\frac{\pi(t_{min}-t)}{24}+t_{min}-t_{max}\right)+1}{2}$$ Equation 2-2

For $t_{min} < t < t_{max}$;

$$f_1 = \frac{\cos\left(\pi(t - t_{min})+t_{min}-t_{max}\right)+1}{2}$$ Equation 2-3

For $t_{min} < t$;

$$f_1 = \frac{\cos\left(\frac{\pi(24+t_{min}-t)}{24}+t_{min}-t_{max}\right)+1}{2}$$ Equation 2-4

and $f_1 + f_2 = 1$

2.2.5.2 Sin(14R - 1) Method

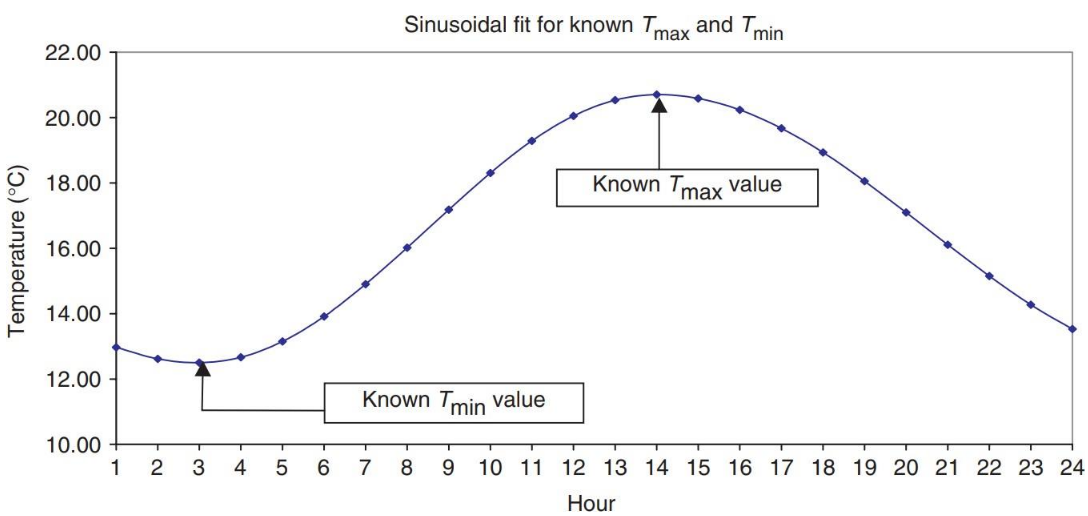

Figure 2-2: Sinusoidal interpolation of daily temperature values (Chow & Levermore, 2007)

This method also employs a *sine* curve fit to daily extremes, but the difference lies in the assumption of times of occurrence for these values. In contrast to the CIBSE method of assigning constant times for any day in a month, the sin(14R - 1) method takes into account the intensity of the incoming percent sunshine to define times of occurrence for extreme temperatures in a day. Knowing the latitude of the study location and the day of the year, sunrise time is first calculated using standard relations. The time of minimum temperature, tmin, is then taken as the hour before sunrise, whereas the time of maximum temperature, tmax, is assumed constant at 1400 hours, regardless of the time of the year. The sinusoidal curve is then fit and hourly values are extracted similar to the CIBSE method. A very similar technique, called the sin(14R) method, takes the time of occurrence for the minimum temperature to be the time of sunrise instead of the hour prior. The maximum temperature time is still taken at 1400 hours. Valle et al. demonstrated the utility of this modified technique in their assessment of pavement in changing climate conditions (Valle et al., 2017).

The above algorithms generate hourly temperatures for a single day. To calculate parameters for a number of consecutive days, a sinusoidal curve can be stretched to link a day's minimum with the immediate maximum of the next day. Knowing extreme temperatures and the times of their occurrence, hourly temperatures for each day can be extracted using:

$$T(t) = \frac{Temp_{(next)}+Temp_{(prev)}}{2} - \left[\frac{Temp_{(next)}-Temp_{(prev)}}{2} \times cos\left(\frac{\pi(t-t_{(prev)})}{t_{(next)}-t_{(prev)}}\right)\right] \qquad \text{Equation 2-5}$$

where $Temp_{(next)}$ is the successive known temperature at time $t_{(next)}$; $Temp_{(prev)}$ is the previous temperature at time $t_{(prev)}$

2.2.5.3 Quarter-Sine (Q-sin) Method

This method, developed by Chow and Levermore, is an adaptation of the sin(14R - 1) method (Chow & Levermore, 2007). Q-sin technique aims to achieve better accuracy in predicting hourly temperatures by including daily average temperature in its calculations in addition to daily extreme temperature data as in the previous algorithms. Consequently, a quarter sinusoidal curve is fitted with three points.

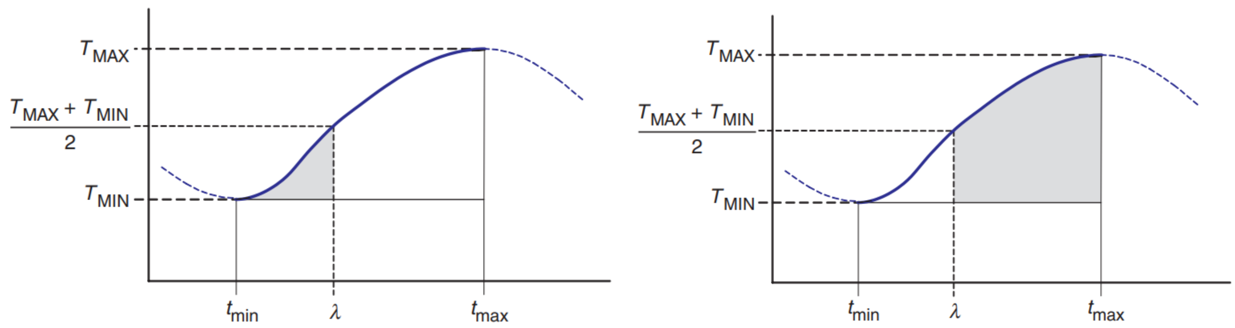

Figure 2-3: Sinusoidal curve fit using Q-sin method, (a) Quarter sine curve t in the region $\lambda > t_{min}$ and (b) Quarter sine curve t in the region $\lambda < t_{max}$ (Chow & Levermore, 2007)

Q-sin method also assigning the extremes occurrence times similar to the sin (14R -1) method. If the first point fits with Tmin and Tmax as endpoints. Then, Tave is estimated from this Q-sin curve and matched with the value acquired from the model outputs, as presented in Figure 2-3. Any difference in the values is accounted for with an adjustment in the curve fit. This process is devised to be a robust mechanism to minimize curve fitting errors by considering three points to fit an approximate curve. A quarter-sine curve is thus fit with T_{ave} as an interior point, and the time of its occurrence, λ, is derived. The difference between the two sine curves is used to eventually extract hourly temperature for a range of days. The equations involved are described below:

$$24 \times D = \left(\frac{T_{MAX}-T_{MIN}}{2}\right)(\lambda - t_{min})\left(1-\frac{2}{\pi}\right) + \left(\frac{T_{MAX}-T_{MIN}}{2}\right)(t_{max} - \lambda)\left(1+\frac{2}{\pi}\right) - \left(\frac{T_{MAX}-T_{MIN}}{2}\right)(t_{max} - t_{min}) \qquad \text{Equation 2-6}$$

$$\lambda = \frac{(t_{max}-t_{min})}{2} - \left(\frac{12 D_2 \pi}{(T_{MAX}-T_{MIN})}\right) \qquad \text{Equation 2-7}$$

Where,

T_{MAX} is the maximum temperature occurring at time t_{max},

T_{MIN} is the minimum temperature occurring at time t_{min}.

2.2.5.4 Imposed Offset Morphing Method (IOMM) Method

The Imposed Offset Morphing Method (IOMM) is based on reconstructing a past weather pattern to predict future daily climate variables with a finer temporal resolution and was used by Gudipudi et al, and many others (Belcher et al., 2005; Gudipudi et al., 2017). In principle, historic daily minimum and maximum temperature data are first acquired from climate model outputs, along with future projections of the daily extreme for equal ranges of years. Then, by applying a sequence of 'shifting', 'stretching', or a combination of both to the data, hourly values for a future period of time are obtained using historic hourly temperature distribution.

$$T_{iF} = \frac{T_{FMax} - T_{FMin}}{T_{BMax} - T_{BMin}} \times (T_{iB} - T_{BMin}) + T_{FMin} \qquad \text{Equation 2-8}$$

Where,

T_{BMin} and T_{BMax} : Daily minimum and maximum temperatures extracted from the historic climate database

T_{FMin} and T_{FMax} : Daily minimum and maximum temperatures extracted from the given projected climate data (climate change model)

T_{iB} : Hourly distribution of historic temperature

Similarly, using the historical hourly precipitation data, the future hourly precipitation data can be estimated from the daily average precipitation extracted from the climate change model. The following equation is used to compute the hourly precipitation data for the future climate:

$$R_{iF} = \left(\frac{(R_{FMAvg} - R_{BMAvg})}{R_{BMAvg}} \times R_{iB}\right) + R_{iB} \qquad \text{Equation 2-9}$$

Where,

Cumulative monthly rainfall for the baseline case was extracted and used to calculate an average daily precipitation rate for the respective month

R_{BMAvg} : Average daily precipitation of each month extracted from the historic climate data base

R_{FMAvg} : Average daily precipitation of each month extracted from the given climate projection (climate change model)

R_{iB} : The hourly rainfall for historical climate data.

The comparison between two hourly estimation models such as M-IOMM and Sine (14R-1) for St. John's location are presented in Chapter 3.

2.3 Pavement materials perspective

Other than traffic loads, climate factors are the primary causes of pavement material degradation. The predominant climate factors, such as temperature, precipitation, and percent sunshine are the causes of material disintegration. These changes in temperature and precipitation mean pavement materials are deteriorating earlier than expected, leading to the failure of the pavement structure. Upgrading the superpave binder grade according to the temperature rise may reduce the pavement deterioration and result in longer service life (Mills et al., 2009; Qiao, Dawson, et al., 2013; Underwood et al., 2017; Viola & Celauro, 2015).

2.3.1 SuperPave binder grade selection

Several studies noticed a temperature rise due to climate change in Canada (Vincent et al., 2018), United States (Paquin et al., 2014), South America (Marengo et al., 2012), Europe (Meleux et al., 2007), Africa (Jones & Thornton, 2009), Middle East (Evans, 2009), China (Zhai & Pan, 2003), India (Dash et al., 2007), Central Asia (Lioubimtseva & Henebry, 2009), Southeast Asia (Gasparrini et al., 2017) and Australia (Hughes, 2003). To account this temperature rise, Mills et al. estimated the change in superpave binder grade for seventeen sites in southern Canada, which revealed that low-temperature cracking would not be problematic in future years (Mills et al., 2009). It was also noticed that six out of 17 sites needed an upgrade to the high-temperature grade, and at eight out of 17 sites, there was a rise in low-temperature grade (Mills et al., 2009). Similar work has been done by Viola and Celauro in Italy to evaluate the asphalt binder upgrade at 71 different locations (Viola & Celauro, 2015). In this study, 2013 was considered as the baseline and upgrades in asphalt binder grades were estimated for 2033. It was noted that there was an increase of one grade in high-temperature grade over 27% of the Italian territory. On the other hand, there was no noticeable change in low-temperature grades in this territory (Viola & Celauro, 2015). A similar study was carried out for the binder selection in Chile (Delgadillo et al., 2018). A total of 94 weather stations were considered in the selection of asphalt binder grades throughout the country. This study identified a significant number of stations in need of a change in binder grade. Fletcher et al. estimated the change in pavement temperature for the selected superpave asphalt binder grade for the future climate in Canada. They concluded that nine out of 17 cities exhibited an increase in asphalt binder grade (Fletcher et al., 2016).

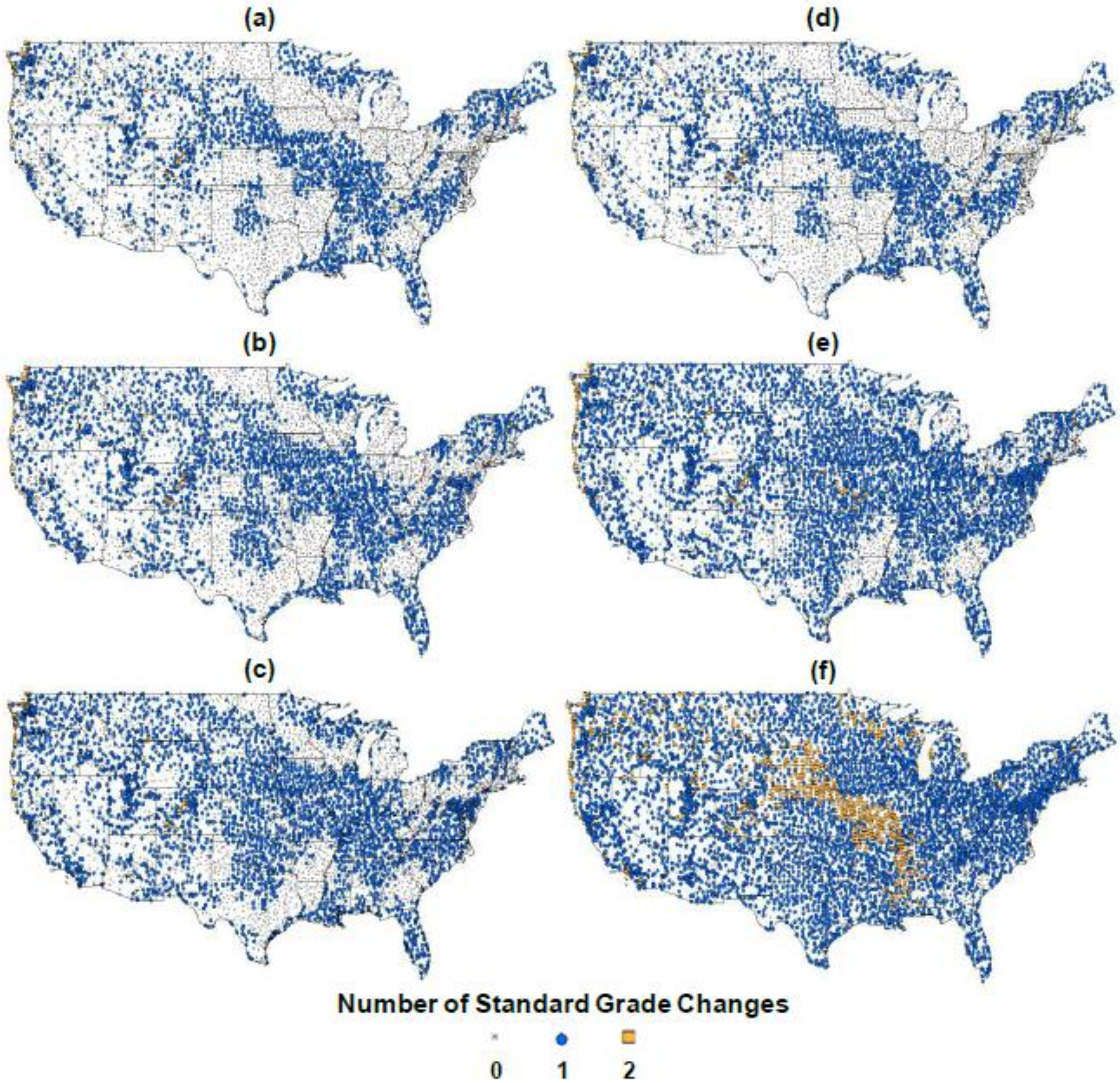

Figure 2-4: Expected number of increments in high temperatures grade for: RCP 4.5 and for (a) 2010–2039, (b) 2040–2069 and (c) 2070–2099 and RCP 8.5 and for RCP 4.5 and for (d) 2010–2039, (e) 2040–2069 and (f) 2070–2099 (Underwood et al., 2017)

In very recent years, a study was carried out to assess the upgrade of asphalt binder grade in the United States. The study noticed that, over the 799 observed weather stations, 35% of station's asphalt binder grade based on 1965-1996 is different from binder grade based on 1985-2014 weather data (Underwood et al., 2017). This study illustrated expected number of increments in high temperatures grade due to climate change for: RCP 4.5 and for (a) 2010–2039, (b) 2040–2069 and (c) 2070–2099 and RCP 8.5 and for RCP 4.5 and for (d) 2010–2039, (e) 2040–2069 and (f) 2070–2099 with respect to a baseline period of 1966 – 1995, as presented in Figure 2-4. This study also estimated the expected number of increments in high temperatures grade due to climate change for different RCP's and different periods, which concluded that the examined scenarios projected a maximum of two grade change for the future climate in the United States.

All of these studies used different climate change models and different methods for the estimation of pavement temperature from air temperature. Also, all the studies are spatiotemporally variable. However, the mutual conclusion of all of the studies is that the climate is becoming warmer, which requires adaption by upgrading the asphalt binder grade.

2.3.2 Effect on surface HMA layer

Mallick et al. discerned the impact of climate change on surface hot mix asphalt (HMA) layer modulus, which tends to reduce due to temperature rise (Mallick et al., 2014). Also, this study evaluated the adjusted modulus for the effect of water through inundation (flooding). However, Mallick et al. concluded that the inundation period was not significant. Therefore, the number of inundation cycles is assumed to have an influence on HMA modulus (Mallick et al., 2014). In another similar study, it was noted that the temperature rise due to climate change results in the reduction of stiffness properties of HMA layer (Mallick et al., 2016), which leads to an increase in pavement deformation.

Kumlai et al. studied the impact of increased temperature due to climate change on western Australian asphalt mixes. This study estimated the effective dynamic modulus ($|E^*|_{eff}$) for the increased effective pavement temperature. The results of this study revealed that the increase in effective temperature causes a significant reduction in the effective dynamic modulus, which tends to decrease the service life of pavement (Kumlai et al., 2016).

Shao et al. described the indirect impact of climate change on pavement materials and stated that the increase in temperature accelerates the aging of asphalt cement, resulting in an increase in brittle failure (cracking) of the surface layer (Shao et al., 2017). Further, this brittle failure allows surface water to enter pavement layers and causes pothole and loss of surface material. Qiao et al. also noticed a similar effect: an increase in precipitation causes ravelling and stripping of asphalt mix at the initial stage. Then, this stripping and ravelling allow surface water to infiltrate into the asphalt mixture, which affects the bonding between the asphalt binder and aggregate. Furthermore, the surface water infiltration leads to severe damage (potholes) to the pavements (Qiao et al., 2016). This surface water infiltration may lead to the cause of delamination if water enters between the two HMA layers (Swarna & Hossain, 2018).

2.3.3 Effect on subbase and subgrade layer

Qiao et al. noticed that the increase in precipitation is expected to increase the moisture content in unbound granular layers, leading to an increase in permanent deformation (Qiao et al., 2016). However, an increase in precipitation will lead to having greater runoff and is likely to result in small or negative net infiltration to the subgrade. Also, the warmer temperatures are expected to dry the aggregates sooner (Bizjak et al., 2014). Bizjak et al. concluded that uncracked pavement surfaces could handle the increase in precipitation. Nevertheless, extreme precipitation events are the key challenges for upgrading the drainage provision to account for these extreme events (Bizjak et al., 2014).

Mallick et al. estimated the duration of flooding needed for the cause of complete saturation of base layers ($T_{critical}$) (Mallick et al., 2017). In addition, the effect of pavement design factors on the $T_{critical}$ is also determined. This study found that the type of HMA gradation, voids in surface HMA layer, and thickness of surface HMA layer significantly impact the $T_{critical}$. It was also found that the thickness of base layer has a moderate effect on $T_{critical}$. In this study, Mallick et al. developed a simulation tool to determine the $T_{critical}$, which is useful to decide on the pavement's post-flood condition. In a similar study, Asadi et al. developed a computational algorithm to quantify life loss due to flooding and heavy rainfall (Asadi et al., 2020). The post-flooding structural response was determined based on ten different factors: gradation variables (D60, D10 and P200) of the base material, weighted plasticity (wPI) of subgrade material, Initial saturation of base and subgrade, thickness of base and HMA, infiltration rate, and infiltration time. Also, using the post-flood structural responses, loss of pavement life due to flooding was computed.

Mallick et al. evaluated the impact of average annual rainfall over the pavement structure and noticed that the increase in the number of inundations over time would result in the reduction of effective subgrade modulus. This reduction in effective modulus of subgrade will lead to an increase in permanent deformation. Here, in this study, the inundations are considered not only due to an increase in rainfall but also due to the increase in the number of category 3 hurricanes (Mallick et al., 2014). In continuation, another study noted that stabilized subgrades could enhance the pavement performance (Mallick et al., 2016). Also, strengthening the base layers of flexible pavement is another adaptation approach to counteract the increase in precipitation (Melvin et al., 2016).

2.4 Performance and design perspective

Many studies assess the impact of climate change on pavement performance using climate change models in various parts of the world, as presented in Table 2-1. Table 2-1 highlights that climate change predominantly causes permanent deformation and fatigue cracking. Also, it is evident that all of the studies considered temperature rise to assess the impact on pavement performance. Few studies considered all the climate factors to estimate the impact on pavement performance. In this chapter, the climate factors considered are temperature, precipitation, wind speed, percent sunshine or solar sunshine, humidity and groundwater table. Also, the pavement performance parameters considered are total rutting, asphalt concrete (AC) rutting, top-down (TD) cracking, bottom-up (BU) cracking, thermal/ traverse cracking and international roughness index.

Table 2-1: Impact of climate change on pavement performance reported in various studies

Author and Year	**Traffic**		**Climate Factors considered**						**Performance Parameters**					
		Temperature	**Precipitation**	**Wind Speed**	**Solar Sunshine**	**Humidity**	**Ground Water Table**	**TMI (Index)**	**Total Rutting**	**AC Rutting**	**TD Cracking**	**Thermal Cracking**	**BU Cracking**	**IRI**
(Tighe et al., 2008)	✓	✓	✓						↑	↑	↑	↓	↑	↑↓
(Mills et al., 2009)	✓	✓	✓						↑	↑	↑	↓	↑	↑↓
(Meagher et al., 2012)		✓	✓	✓	✓	✓			↑	↑			↑↓	
(Wistuba & Walther, 2013)		✓		✓	✓	✓							↑	
(Bizjak et al., 2014)		✓	✓						↑	↑	↑	↓	↑	↑↓
(Qiao, Flintsch, et al., 2013)		✓	✓	✓	✓		✓		↑	↑	↑		↑	↑
(Qiao, Dawson, et al., 2013)		✓	✓	✓	✓		✓		↑	↑	↑		↑	↑
(Zareie et al., 2016)	✓							✓						↑
(Gudipudi et al.,		✓	✓						↑	↑	↑		↑	

2017)														
(Shao et al., 2017)		✓	✓		✓			✓		↑			↑	↑
(Stoner et al., 2019)		✓	✓	✓	✓	✓			↑	↑	↑		↑↓	↑↓
(Underwood, 2019)		✓							↑	↑			↑	
(Rana et al., 2020)	✓	✓	✓						↑	↑	↑		↑	↓

✓ - *Considered in the study,* ↑ - *Increasing compared to the baseline climate,* ↓ - *Decreasing compared to the baseline climate,* ↑↓ - *Increasing and Decreasing compared to the baseline climate*

2.4.1 Pavement performance

2.4.1.1 Structural performance

The impacts of climate change on Canadian flexible pavements were investigated by University of Waterloo for a period of 20 years starting from 2050 using two climate change models, Coupled Global Climate Model 2 (CGCM2A2x) and Hadley Climate Model 3 (HadCM3B21). This study noticed that the change in temperature, rainfall and traffic growth are significant factors influencing pavement performance (Mills et al., 2009; Tighe et al., 2008). This study utilized AAHSTOWare ME Pavement Design to quantify the climate change impact on pavement performance. However, as there are no local calibration factors available for the Canadian provinces, author relied on global calibration factors to estimate the climate change impact on pavement performance, which might not be accurate prediction. Another study evaluated the consequences of climate change on the pavement deterioration process were assessed using the REgional MOdel (REMO), which was downscaled to a 10-km grid resolution and hourly time scale (Meagher et al., 2012). From this study, it was found that the impact of temperature rise on asphalt concrete permanent deformation is modest and negligible for fatigue cracking. In Europe, time variation curves of climate factors such as air temperature, global radiation, wind speed, and humidity are predicted to estimate these factors' effects on future pavement design. Surprisingly in central Europe, the impact of climate change was judged as negligible. Also, for Germany and Austria, adaption strategies as a consequence of climate change were not a necessity (Wistuba & Walther, 2013). In freezing zones, road transport relies on the frozen road during the winter season. However, the temperature rise in the northern regions will result in a shorter frozen period. In this kind of case, necessary upgrading of thin and unsealed pavements is necessary to provide reliable bearing capacity for the roads throughout winter (Bizjak et al., 2014). This research also determined the impact of an increase in temperature and precipitation individually on all the pavement distresses in Europe, as illustrated in Table 2-2. From this, it was noticed that, due to temperature rise, all the distresses are increasing except thermal cracking. Also, the same trends are observed for the increase in precipitation cases (Bizjak et al., 2014).

Table 2-2: Percentage change in pavement performance parameters due to increase in temperature and precipitation (Bizjak et al., 2014)

Location	**Warsaw**		**Trondheim**		**Rovaniemi**	
Percentage change in	**Precip**	**Temp**	**Precip**	**Temp**	**Precip**	**Temp**
Temperature (°C) / Precipitation (%) Increase	20	5	22	2	19	2
Terminal IRI (longitudinal roughness index) (%)	2.4	-2.7	2.5	0.2	2.1	-1.5
Asphalt top-down cracking (longitudinal cracking) (%)	38.4	51.4	3.6	43.9	8.9	45.1
Asphalt bottom-up cracking (alligator cracking) (%)	33.3	33.3	20	20	14.3	14.3
Asphalt thermal fracture (transverse cracking) (%)	0	-99.3	0	0	0	-87.6
Permanent deformation (asphalt) (%)	7.1	42.9	0	20	0	16.7

Permanent deformation (total pavement) (%)	14	16	16.2	2.7	12.8	5.1

*Precip = Precipitation & Temp = Temperature

The influence of climate factors such as temperature, precipitation, wind speed, percent sunshine, and groundwater table on pavement performance is assessed by Qiao et al. It was known that the climate change models are only available for temperature and precipitation, which were produced from MAGICC (Model for the Assessment of Greenhouse-gas Induced Climate Change) and SCENGEN (SCENario GENerator). Therefore, an increase of 5% was assumed for the other factors to estimate the impact on pavement performance. From this study, it was found that longitudinal cracking is affected by all the climate factors. Also, all the distresses are highly influenced by temperature rise (Qiao, Dawson, et al., 2013; Qiao, Flintsch, et al., 2013). Pavement performance is investigated using climate data from an assembly of 19 different climate change models from CMIP5 database for five different sites in the United States. Due to an increase in temperature, the percentage of AC rutting was expected to increase by 9 – 40% and the percentage of fatigue cracking was also expected to increase by 2 – 9%. Also, for the considered five-sections, there is no considerable difference in the pavement performance due to a change in precipitation (Gudipudi et al., 2017).

A recent study utilized Austroads Climate Tool to forecast climate change. This climate data was processed into proper form as input to HDM – IV so as to estimate the climate change impact on pavement performance. It was concluded that the increase in temperature is likely to affect the asphalt materials through asphalt aging, embrittlement and cracking. Further, rainfall alters moisture imbalance and leads to pavement deterioration (Shao et al., 2017). A very recent study assessed the impact of three climate change models on pavement performance in 24 different locations across the United States. The study exhibits different performance trends for 24 locations.

However, all the results were illustrating the decreasing trend for pavement performance under current design standards (Stoner et al., 2019). Also, it was noticed that the AC permanent deformation is mostly affected by the increase in temperature.

To select the appropriate GCM for the pavement performance evaluation, Underwood et al. verified the detailed pavement performance analyses using various models in four different provinces. This study illustrated a summary of model selection process based on pavement distress prediction and the type of region (Underwood, 2019). Also, this study noticed that there was an increase in rutting and fatigue cracking for the selected four sites due to an increase in air temperature alone (Underwood, 2019).

2.4.1.2 Functional performance

A study was carried out to estimate the impact of future temperature, precipitation and projected traffic on pavement roughness progression in Canada. From this study, it was found that the IRI is increasing in most of the Canadian provinces. Unexpectedly, a decreasing trend was noticed in Quebec and Newfoundland (Mills et al., 2009; Tighe et al., 2008). The same trend was noticed in a most recent study carried out by Rana et al. in the province of Newfoundland (Rana et al., 2020). Bizjak et al. also noticed a similar trend in Europe, as noticed in Table 2-2. Bizjak et al. estimated the pavement roughness due to an increase in temperature and precipitation individually, which revealed the approximate reason for the decreasing trend. It was noticed that the decrease in the IRI trend is predominantly occurred due to the rise in temperature. Meanwhile, an increasing IRI trend was noticed for the rise in precipitation (Bizjak et al., 2014).

Qiao et al. assessed the impact of all climate factors on the IRI of pavement in Virginia, USA. It was noted that the IRI is insensitive to the increase in temperature. However, the IRI is minorly affected by the change in precipitation (Qiao, Dawson, et al., 2013; Qiao, Flintsch, et al., 2013). The interaction effect of future traffic loads and Thornthwaite Moisture Index (TMI) on pavement deterioration was estimated for three thirty-year periods in the 21st century (Zareie et al., 2016). In this study, an increase in TMI can cause an 11-68% increase in roughness progress rate on pavement structure. In an another similar work, Stoner et al. noted that there was no significant difference in IRI between baseline and climate change (Stoner et al., 2019). However, Rana et al. noticed that in the province of Newfoundland, Canada, the distress such as total rutting, fatigue cracking and AC rutting are increasing and the IRI is decreasing, which is unusual case. Also, he noted that this might be because of the difference between the IRI model for freezing and non-freezing zone (Rana et al., 2020). From all the explained literature, many contradicting results have arisen. However, all these conflicting results might be because of using different climate change models in different locations. So, there is a necessity to find out the variables that affect the IRI of the pavement.

2.4.2 Pavement design and service life

Qiao et al. estimated change in the service life (SL) of the pavement due to climate change and found that there was a minimum of 20% reduction in pavement service life due to climate change (Qiao, Flintsch, et al., 2013). This service life is computed based on minimum acceptable service quality, defined as follows:

$SL = \text{minimum}(SL_1, SL_2, SL_3, \ldots\ldots)$

Where, SL_1, SL_2, SL_3…. are the service lives computed for each distress (such as longitudinal cracking, transverse cracking, fatigue cracking, IRI, AC rutting, and total rutting, which were the direct outputs of the MEPDG).

Jeong et al. assessed the impact of climate change on pavement service life for various climate change scenarios (Jeong et al., 2017), and, found that service life reduces drastically due to climate change. Also, it was noted that the service life for the RCP 2.6 scenario was higher than that of normal climate. However, the service life for the RCP 8.5 scenario was much lesser than the RCP 2.6 and normal climate. This conclude that there is a significant reduction in pavement service life due to climate change.

Knott et al. estimated the increase in hot mix asphalt (HMA) thickness to preserve the service life of pavement due to warming temperatures (Knott, Sias, et al., 2019). Factors such as seasonal average temperature, change in season length, and temperature-dependent resilient modulus were used to simulate the pavement response due to a rise in temperature. The results exhibit that the existing base layers are performing well with 85% reliability. However, HMA layer thickness needs to be increased by 7 to 32% based on the season. Further, Knott et al. extended the study to estimate the necessary increase in HMA and base layer thickness due to groundwater rise (Knott et al., 2020; Knott, Jacobs, et al., 2019). Here, the HMA thicknesses are estimated for 70 combinations of incremental temperature and groundwater rise. The results found that the temperature rise, and groundwater rise will reduce the pavement service life, especially in coastal regions. However, an increase in HMA layer thickness and base layer thickness will result in resilient pavements (Knott et al., 2020; Knott, Jacobs, et al., 2019).

2.5 Pavement maintenance and rehabilitation perspective

It is clearly described in the above sections that pavement deterioration is significantly increased due to climate change. This increase in pavement deterioration entails the early maintenance and rehabilitation to prevent pavement failure (Mills et al., 2006). Many studies estimated the need for early maintenance and rehabilitation due to climate change.

2.5.1 *Pavement maintenance and rehabilitation*

Tighe et al. estimated change in the timing of maintenance requirements occurring due to the both individual and combined influences of climate change and traffic growth in six regions of southern Canada (Mills et al., 2009; Tighe et al., 2008). This study noticed that the number of years to reach 2.7 m/km of IRI (maintenance threshold) significantly declined due to climate change and traffic growth in two provinces. However, in Quebec, the number of years to reach the maintenance threshold increased due to climate change alone. Then again, when traffic comes into the picture, the number of years to reach the maintenance threshold dropped. Chai et al. estimated the increase in annual maintenance costs due to climate change in Australia (Chai & Kelly, 2014). In this study, annual maintenance cost was expected to increase about 30% due to climate change conditions by 2060.

Qiao et al. also estimated the drastic reduction in the service life of pavement due to climate change (Qiao, Flintsch, et al., 2013). To conserve the pavement service life, pavement should undergo frequent and earlier maintenance than expected. In this regard, Qiao et al. noticed that the pavement maintenance was triggered 8-16% earlier due to climate change (Qiao et al., 2015). Another study used Monte Carlo analyses to estimate the percentage of roads that require rehabilitation at 50 and 100 years (Mallick et al., 2016). In this study, various conditions such as no climate change, climate change and climate change with different adaptation scenarios are evaluated, as illustrated in Figure 2-5. From this study, it was well noted that the modified HMA and stabilized subgrade would result in less percentage of roads need rehabilitation compared to climate change and no climate change conditions.

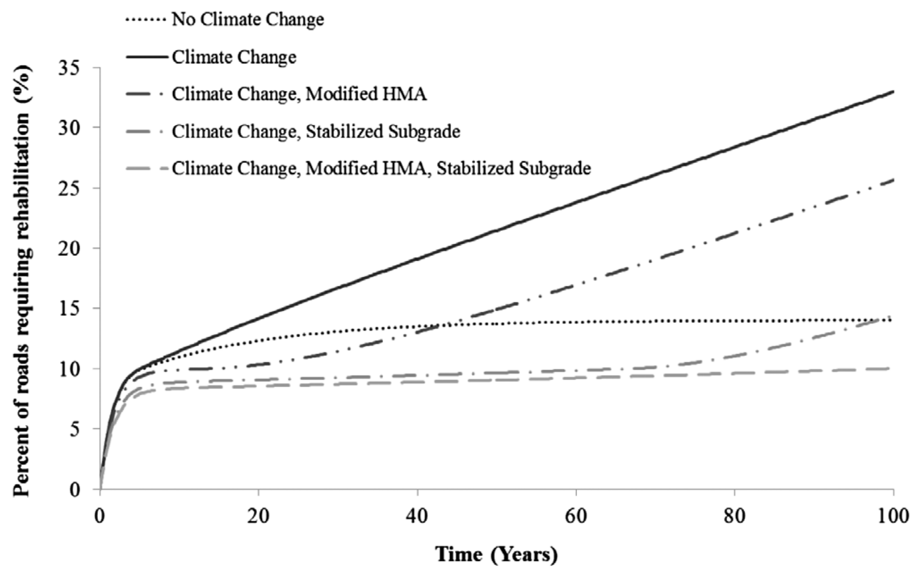

Figure 2-5: Estimated percent of roads requiring rehabilitation for various climatic conditions with adaptation strategies (Mallick et al., 2016)

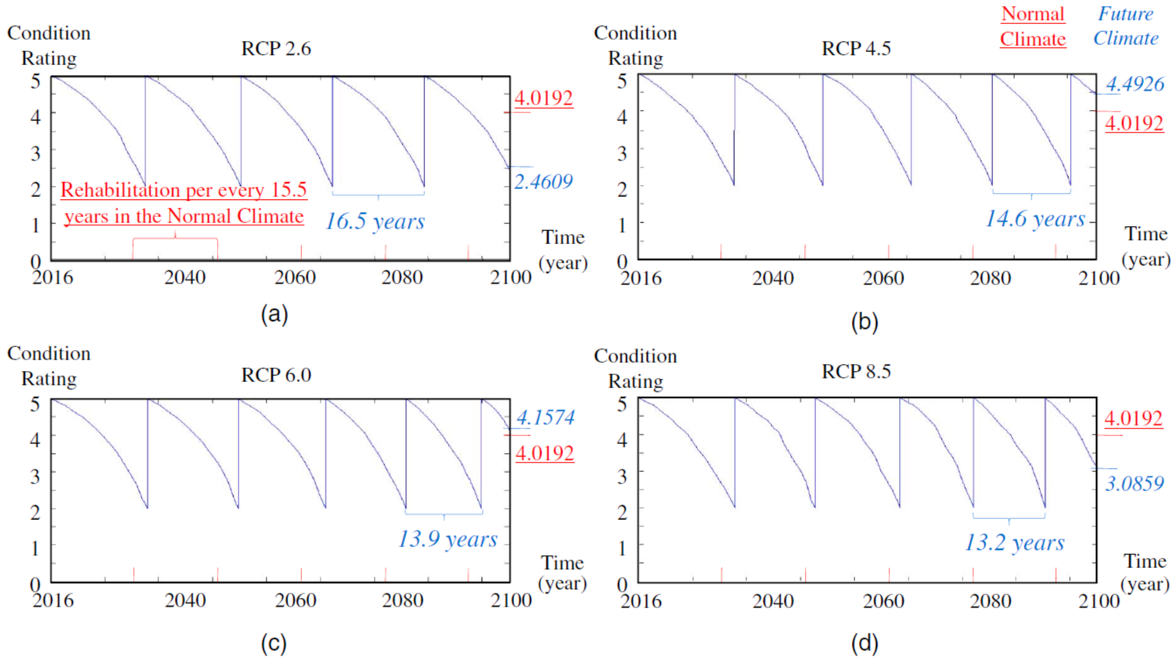

Figure 2-6: Condition rating for various climate change scenarios: (a) RCP 2.6; (b) RCP 4.5; (c) RCP 6.0; (d) RCP 8.5 (Jeong et al., 2017)

Jeong et al. assessed the impact of climate change on pavement service life for various climate change scenarios. Further, a climate change impact assessment system using fuzzy logic interface was proposed to predict the service life of infrastructure (Jeong et al., 2017). This method is predominantly developed to minimize the additional expenditure on pavement infrastructure by establishing proactive adaptation (rehabilitation) strategies. This study estimated the condition rating for pavement from 2016 to 2100 for various climate change scenarios, as illustrated in Figure 2-6. The rehabilitation cycle for RCP 2.6 is 16.5 years, which was much higher than RCP 8.5. Unexpectedly, the rehabilitation cycle for the normal climate was observed to be less than that of RCP 2.6, which might be because of the reduced CO_2 concentration level after 2020 for RCP 2.6. However, further analysis is needed to understand the effect of the RCP 2.6 climate change model compared to a normal climate.

Chen et al. estimated the impact of warming temperatures on flexible pavement overlay performance (Chen & Wang, 2020). To estimate this impact, a maintenance strategy of milling 3 inches and overlaying 3 inches was adopted when the pavement reaches a performance threshold of 10% lane area of total fatigue cracking. Similarly, a maintenance strategy of milling 3 inches and overlaying 6 inches was adopted when the pavement reaches a performance threshold of 20% lane area of total fatigue cracking. After the overlay, performance in terms of IRI, fatigue cracking and rut depth was monitored due to both normal and warming temperatures. Also, the service life of the overlay is estimated. And, it was concluded that the warming temperatures results in increased fatigue cracking, rutting, IRI and decreased service life for the pavement overlays (Chen & Wang, 2020).

2.6 Economics and emissions perspective

From the above review, it was evident that climate change accelerates pavement deterioration, which leads to the reduced service life of the pavement. To uphold the design service life, it is necessary to design and maintain the pavements considering the future climate. This adaptation results in preserving the pavements throughout the design service life, which might increase the life cycle cost of pavements; however, these will be beneficial in the long run. Besides, adapting to climate change might also increase greenhouse gases further in the atmosphere. So, there is a necessity to optimize the adaptation strategies to preserve the service life of pavement with less economic cost and less emissions.

2.6.1 Life Cycle Cost Analysis (LCCA)

Schweikert et al. estimated the impact of climate change on adaptation and opportunity costs for 10 countries, which were categorized based on income level (Schweikert et al., 2014).

These countries are divided into three categories: low, medium and high-income countries. Average annual costs and opportunity costs are estimated for both proactive (adaptation before impact) and reactive (adaptation after impact) adaptation measures. It was concluded that proactive measures could significantly reduce the economic costs and impacts of climate change when compared to the reactive measures. Also, developing countries will encounter relatively higher costs for road networks due to climate change impact through 2100, when compared to developed countries. Later, Schweikert et al. estimated the impact of climate change on road networks in South Africa (Schweikert et al., 2015). This study also came to a common conclusion that proactive adaptation measures can significantly reduce the annual average cost of road networks in South Africa. A similar study carried out by Melvin et al. to estimate the economics of proactive adaptation in Alaska (Melvin et al., 2016). This study noticed that the largest source of infrastructure damages in Alaska was road flooding. Proactive adaptation for the road flooding will reduce the adaptation cost from $2.3 billion to $340 million. Further to optimize the maintenance strategy, Qiao et al. estimated the impact of climate change on various maintenance strategies using MEPDG predictions, and corresponding life cycle cost was also computed (Qiao et al., 2015). The authors concluded that the maintenance might trigger much earlier than expected. Further, adapting to early maintenance will result in minimizing the total life cycle cost of pavements. Also, maintenance intervention optimization by reducing the total life cycle cost will improve the resilience of pavement infrastructure against climate change. However, ignoring the early triggered maintenance may increase the life cycle cost of pavement.

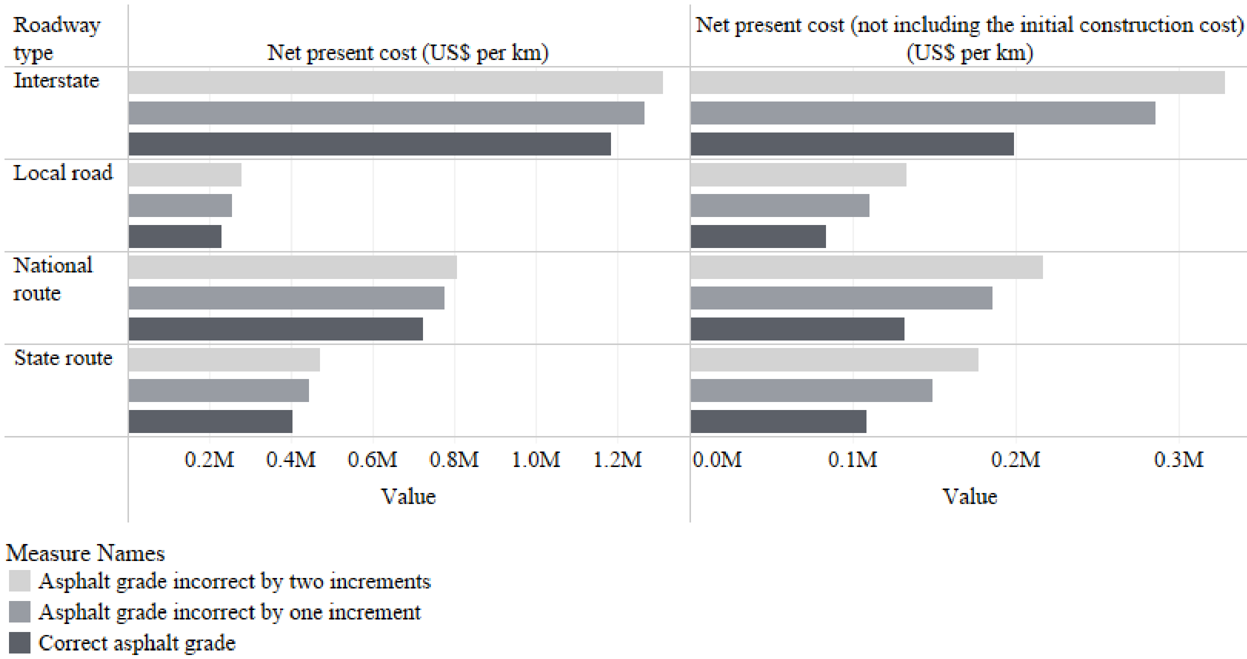

Figure 2-7: Economic costs of a flexible pavement with the use of correct and incorrect asphalt grade, (a) Net present cost not including the initial construction cost and (b) Net present cost including the initial construction cost (Underwood et al., 2017)

Underwood et al. estimated the economic costs of a flexible pavement with the use of correct and incorrect asphalt grade for all roadway types, as illustrated in Figure 2-7 (Underwood et al., 2017). For 2040, the estimated costs across the United States are US$19.0 and US$26.3 billion for RCP 4.5 and RCP 8.5 respectively. Similarly, for 2070, the estimated costs across the United States are US$21.8 and US$35.8 billion for RCP 4.5 and RCP 8.5 respectively. This clearly explains selecting the correct grade of asphalt binder plays an essential role in the economic costs of pavement.

2.6.2 Life Cycle Assessment (LCA)

Valle et al. carried out LCA for a segment of interstate pavements considering future climate data in pavement performance evaluation (Valle et al., 2017). Also, the authors calculated the GWP to compare various pavement structures, rehabilitation alternatives, and rehabilitation trigger thresholds for both historical climate and climate change data. From this study, it was concluded that LCA could provide a good decision process to select the appropriate pavement structure and rehabilitation alternative for the future climate. Sharma et al. estimated the early maintenance that was expected due to climate change (Sharma et al., 2020). Also, these frequent maintenance results in additional traffic delay emissions and costs. From this study, it was concluded that the need for early maintenance in Elpaso and Austin resulted in 70 tons of CO2 per day and $100,000 per maintenance day. Therefore, it is necessary to carry out the LAC for all the different adaptation strategies to select the optimal adaptation strategy. The road transportation sector is a major source of total human made GHG emissions. LCCA and LCA methodologies can be combined to optimize the construction and maintenance strategies to maximize serviceability and durability and also to reduce emissions (Qiao et al., 2020).

2.7 Concluding remarks

This review explores literature to quantify the impact of climate change on pavement infrastructure. Initially, a brief introduction to climate change models and uncertainties involved in them is given. Various downscaling techniques to resolve climate models into finer grid scales are discussed. To assess the impact of climate change on pavement performance, many studies utilized AASHTOWare ME design and HDM deterioration models. For this estimation, AASHTOWare takes in hourly climate data as input. Therefore, to convert the daily data from downscaled GCMs to hourly values, four hourly data estimation methods are described. Various evidence demonstrating that climate change accelerates pavement deterioration, leading to reduced service life, is illustrated in this study. To uphold the design service life, adaptation strategies such as upgrading asphalt binder grade, change in design thickness, and early triggered maintenance and rehabilitation techniques are discussed. Also, LCCA and LCA analyses of these adaptation strategies are exhibited. The conclusions drawn from this study are as follows:

1. From various studies, it has been noted that temperature is one of the predominant factors that affect pavement deterioration. An increase in temperature due to climate change will result in a shift in asphalt binder grade. In addition, temperature rise can alter the E* value of the surface HMA layer, which leads to a reduction in the service life of the pavement.

2. Precipitation is also a vital climate factor that affects pavement deterioration. An increase in precipitation causes moisture imbalance in the subgrade, which results in the reduction of subgrade stiffness properties. This reduction in properties leads to increased permanent deformation.

3. Other climate factors responsible for pavement deterioration are percent sunshine, wind speed, humidity and groundwater level. However, the effect of these climate factors may or may not be significant, depending on the climatic zone or location.

4. The increase in percent sunshine is likely to affect the asphalt materials through asphalt aging, embrittlement, and cracking, which results in increased thermal cracking and fatigue cracking. However, the temperature rise may reduce the thermal cracking in pavements.

5. The pavement roughness can be impacted by changing climate either negatively or positively, depending on the location, climatic zone, or environmental variables. However, the impact is noted to be not significant.

6. Rise in temperature and groundwater levels reduce the pavement service life, especially in coastal regions. Therefore, an increase in HMA layer thickness might be a good adaptation strategy for temperature rise. Besides, stabilizing base layers will result in a resilient

pavement against rising groundwater levels.

7. Changing climate will trigger the early maintenance of pavements, as is evident in most of the studies considered.

8. Adapting to future climate increases the economic cost of pavement. However, pro-active adaptation has been less burdensome on the life cycle cost than reactive adaptation strategies.

9. LCA can provide a good decision process to select the appropriate pavement structure and rehabilitation alternative for the future climate.

2.8 Future work

Although many studies quantify the impact of climate change on pavement materials, design, performance, maintenance, and rehabilitation, there is a necessity to enhance the accuracy of estimations. Similarly, the adaptation and mitigation strategies need to be optimized for climate change impact. Accordingly, some recommendations for future work are summarized below:

1. Most of the studies relied on a single climate model to estimate climate change effects on pavement infrastructure. This estimation can result lead to overestimation or underestimation. So, there is a necessity to consider a range of climate models and reporting the mean or median of the comprehensive set based on statistical distributions.

2. From the literature, it was noted that there is uncertainty involved with climate change models. Therefore, selecting a bias-corrected, statistically downscaled climate models will result in less uncertainty.

3. Temperature and precipitation are the two significant factors that affect pavement materials and design. Although the other climate factors are less significant, there is an indirect effect

on the pavement deterioration. Therefore, it is necessary to estimate the individual contributions of all other climate variables on pavement deterioration.

4. Future traffic is another factor that significantly affects pavement infrastructure. It is also necessary to estimate the impact of the interaction effect of climate factors and future traffic on the pavement service life.

5. Temperature rise due to climate change is the primary concern for asphalt concrete pavements. Many studies suggested adaptation and mitigation strategies such as asphalt binder upgrade, increasing HMA layer thickness and using modified HMA. However, it is necessary to examine the cost-effectiveness of these adaptation and mitigation strategies.

6. Several researchers suggested various adaptation strategies to counteract climate change impact. However, it is necessary to evaluate the LCCA and LCA of all the adaptation strategies to select the sustainable adaptation and mitigation strategy.

2.9 References

ARA Inc. (2004). *Guide for Mechanistic-Empirical Design of New and Rehabilitated Pavement Structures, Final Report. NCHRP Project 1-37A. National Cooperative Highway Research Program. Transportation Research Board, National Research Council, Washington, DC.*

Asadi, M., Nazarian, S., Mallick, R. B., & Tirado, C. (2020). Computational Process for Quantifying the Impact of Flooding on Remaining Life of Flexible Pavement Structures. *Journal of Transportation Engineering, Part B: Pavements*, *146*(4), 04020060. https://doi.org/10.1061/jpeodx.0000219

Belcher, S. E., Hacker, J. N., & Powell, D. S. (2005). Constructing design weather data for future climates. *Building Services Engineering Research and Technology*, *26*(1), 49–61.

https://doi.org/10.1191/0143624405bt112oa

Benjamin, D. M., & Budescu, D. V. (2018). The Role of Type and Source of Uncertainty on the Processing of Climate Models Projections. *Front Psychol*, *9*, 403.

Bizjak, K. F., Dawson, A., Hoff, I., Makkonen, L., Ylhaisi, J. S., & Carrera, A. (2014). The impact of climate change on the European road network The impact of climate change on the European road network. *Proceedings of the Institution of Civil Engineers*, *May 2014*. https://doi.org/10.1680/tran.11.00072

Camici, S., Brocca, L., Melone, F., & Moramarco, T. (2014). Impact of Climate Change on Flood Frequency Using Different Climate Models and Downscaling Approaches. *Journal of Hydrologic Engineering*, *19*(8), 1–15. https://doi.org/10.1061/(ASCE)HE.1943-5584.0000959

Chai, G., & Kelly, G. (2014). *The impacts of climate change on pavement maintenance in Queensland , Australia*. *May*.

Chen, X., & Wang, H. (2020). Quantification of Warming Temperature Impact on Flexible Pavement Overlay Performance in New Jersey. *99th Annual Meeting of the Transportation Research Board (TRB) of National Academies of Science and Engineering, Washington DC*.

Chow, D. H. C., & Levermore, G. J. (2007). New algorithm for generating hourly temperature values using daily maximum, minimum and average values from climate models. *Building Services Engineering Research and Technology*, *28*(3), 237–248. https://doi.org/10.1177/0143624407078642

Dash, S. K., Jenamani, R. K., Kalsi, S. R., & Panda, S. K. (2007). Some evidence of climate change in twentieth-century India. *Climatic Change*, *85*(3–4), 299–321.

https://doi.org/10.1007/s10584-007-9305-9

Delgadillo, R., Arteaga, L., Wahr, C., Alcafuz, R., Delgadillo, R., Arteaga, L., Wahr, C., & Alcafuz, R. (2018). The influence of climate change in Superpave binder selection for Chile. *Road Materials and Pavement Design*, *0*(0), 1–16. https://doi.org/10.1080/14680629.2018.1509803

Evans, J. P. (2009). 21st century climate change in the Middle East. *Climatic Change*, *92*(3–4), 417–432. https://doi.org/10.1007/s10584-008-9438-5

Finnis, J., & Daraio, J. (2018). *Projected Impacts of Climate Change for the Province of Newfoundland & Labrador: 2018 Update*.

Flato, G., Marotzke, J., Abiodun, B., Braconnot, P., Chou, S. C., Collins, W., Coz, P., Driouech, F., Emori, S., & Forest, C. (2013). *Evaluation of Climate Models 9*.

Fletcher, C. G., Matthews, L., Andrey, J., & Saunders, A. (2016). Projected changes in mid-twenty-first-century extreme maximum pavement temperature in Canada. *Journal of Applied Meteorology and Climatology*, *55*(4), 961–974. https://doi.org/10.1175/JAMC-D-15-0232.1

Gasparrini, A., Guo, Y., Sera, F., Vicedo-Cabrera, A. M., Huber, V., Tong, S., de Sousa Zanotti Stagliorio Coelho, M., Nascimento Saldiva, P. H., Lavigne, E., Matus Correa, P., Valdes Ortega, N., Kan, H., Osorio, S., Kyselý, J., Urban, A., Jaakkola, J. J. K., Ryti, N. R. I., Pascal, M., Goodman, P. G., … Armstrong, B. (2017). Projections of temperature-related excess mortality under climate change scenarios. *The Lancet Planetary Health*, *1*(9), e360–e367. https://doi.org/10.1016/S2542-5196(17)30156-0

Gudipudi, P. P., Underwood, B. S., & Zalghout, A. (2017). Impact of climate change on pavement structural performance in the United States. *Transportation Research Part D: Transport and*

Environment, *57*(October), 172–184. https://doi.org/10.1016/j.trd.2017.09.022

Hughes, L. (2003). Climate change and Australia: Trends, projections and impacts. *Austral Ecology*, *28*(4), 423–443. https://doi.org/10.1046/j.1442-9993.2003.01300.x

Jeong, H., Kim, H., Kim, K., & Kim, H. (2017). *Prediction of Flexible Pavement Deterioration in Relation to Climate Change Using Fuzzy Logic*. *23*(4). https://doi.org/10.1061/(ASCE)IS.1943-555X.0000363.

Jones, P. G., & Thornton, P. K. (2009). Croppers to livestock keepers: livelihood transitions to 2050 in Africa due to climate change. *Environmental Science and Policy*, *12*(4), 427–437. https://doi.org/10.1016/j.envsci.2008.08.006

Knott, J. F., Jacobs, J. M., Sias, J. E., Kirshen, P., & Dave, E. V. (2019). *A Framework for Introducing Climate-Change Adaptation in Pavement Management*.

Knott, J. F., Sias, J. E., Dave, E. V, & Jacobs, J. M. (2019). *Seasonal and Long-Term Changes to Pavement Life Caused by Rising Temperatures from Climate Change*. *2673*(6), 267–278. https://doi.org/10.1177/0361198119844249

Knott, J. F., Sias, J. E., Jacobs, J. M., Krishen, P., & Dave, E. V. (2020). Designing a Climate-Ready Coastal Road. *99th Annual Meeting of the Transportation Research Board (TRB) of National Academies of Science and Engineering, Washington DC*.

Kudo, R., Yoshida, T., & Masumoto, T. (2017). Uncertainty Analysis of Impacts of Climate Change on Snow Processes: Case Study of Interactions of GCM Uncertainty and an Impact Model. *Journal of Hydrology*, *548*, 196–207.

Kumlai, S., Jitsangiam, P., & Pichayapan, P. (2016). The implications of increasing temperature due to climate change for asphalt concrete performance and pavement design. *KSCE Journal* *of Civil Engineering*, *21*(4), 1222–1234. https://doi.org/10.1007/s12205-016-1080-6

Kundzewicz, Z. W., Krysanova, V., Benestad, R. E., Hov, Ø., Piniewski, M., & Otto, I. M. (2018). Uncertainty in Climate Change Impacts on Water Resources. *Environmental Science & Policy*, *79*, 1–8.

Lioubimtseva, E., & Henebry, G. M. (2009). Climate and environmental change in arid Central Asia: Impacts, vulnerability, and adaptations. *Journal of Arid Environments*, *73*(11), 963–977. https://doi.org/10.1016/j.jaridenv.2009.04.022

Mallick, R., Jacobs, J. M., Miller, B. J., Daniel, J. S., Mallick, R. B., Jacobs, J. M., Miller, B. J., & Daniel, J. S. (2016). *Understanding the impact of climate change on pavements with CMIP5 , system dynamics and simulation*. *8436*(January 2017). https://doi.org/10.1080/10298436.2016.1199880

Mallick, R., Radzicki, M., Daniel, J., & Jacobs, J. (2014). Use of System Dynamics to Understand Long- Term Impact of Climate Change on Pavement Performance and Maintenance Cost. *Transportation Research Record Journal of the Transportation Research Board*, *5*(December 2014). https://doi.org/10.3141/2455-01

Mallick, Tao, M., Daniel, J. S., Jacobs, J., & Veeraragavan, A. (2017). Development of a methodology and a tool for the assessment of vulnerability of roadways to flood-induced damage. *Journal of Flood Risk Management*, *10*(3), 301–313. https://doi.org/10.1111/jfr3.12135

Marengo, J. A., Chou, S. C., Kay, G., Alves, L. M., Pesquero, J. F., Soares, W. R., Santos, D. C., Lyra, A. A., Sueiro, G., Betts, R., Chagas, D. J., Gomes, J. L., Bustamante, J. F., & Tavares, P. (2012). Development of regional future climate change scenarios in South America using the Eta CPTEC/HadCM3 climate change projections: Climatology and regional analyses for the Amazon, São Francisco and the Paraná River basins. *Climate Dynamics*, *38*(9–10), 1829–1848. https://doi.org/10.1007/s00382-011-1155-5

Mauritzen, C., Zivkovic, T., & Veldore, V. (2017). On the Relationship Between Climate Sensitivity and Modelling Uncertainty. *Tellus A: Dynamic Meteorology and Oceanography*, *69*(1), 1–12.

Meagher, W., Daniel, J. S., Jacobs, J., & Linder, E. (2012). *Method for Evaluating Implications of Climate Change for Design and Performance of Flexible Pavements*. *2305*, 111–120. https://doi.org/10.3141/2305-12

Meleux, F., Solmon, F., & Giorgi, F. (2007). Increase in summer European ozone amounts due to climate change. *Atmospheric Environment*, *41*(35), 7577–7587. https://doi.org/10.1016/j.atmosenv.2007.05.048

Melvin, A. M., Larsen, P., Boehlert, B., Neumann, J. E., Chinowsky, P., & Espinet, X. (2016). *Climate change damages to Alaska public infrastructure and the economics of proactive adaptation*. https://doi.org/10.1073/pnas.1611056113

Mills, B., Tighe, S., Andrey, J., Smith, J., & Huen, K. (2009). Climate Change Implications for Flexible Pavement Design and Performance in Southern Canada. *Journal of Transportation Engineering*, *135*(10), 773–782. https://doi.org/10.1061/(asce)0733-947x(2009)135:10(773)

Mills, B., Tighe, S., Huen, K., & Parm, S. (2006). *Climate Change and the Performance of Pavement Infrastructure in Southern Canada : Context and Case Study Climate change and the performance of pavement infrastructure in southern Canada : Context and case study*. *June*. https://doi.org/10.1109/EICCCC.2006.277185

Murphy, J. (1998). An Evaluation of Statistical and Dynamical Techniques for Downscaling Local Climate. *Journal of Climate*, *12*, 2256–2284.

Paquin, D., De Elía, R., & Frigon, A. (2014). Change in North American atmospheric conditions associated with deep convection and severe weather using CRCM4 climate projections. *Atmosphere - Ocean*, *52*(3), 175–190. https://doi.org/10.1080/07055900.2013.877868

Qiao, Y., Casey, D. B., Kuna, K. K., Kelly, K., & Macgregor, I. D. (2016). *Climate Resilience of Flexible Pavement Highways : Assessment of Current Practice*. *July 2017*, 1–14.

Qiao, Y., Dawson, A., Parry, T., & Flintsch, G. (2013). Quantifying the effect of climate change on the deterioration of a flexible pavement. *Proceedings of the International Conferences on the Bearing Capacity of Roads, Railways and Airfields*, *June 2013*.

Qiao, Y., Dawson, A. R., Parry, T., & Flintsch, G. W. (2015). Evaluating the effects of climate change on road maintenance intervention strategies and Life-Cycle Costs. *Transportation Research Part D: Transport and Environment*, *41*(November 2015), 492–503. https://doi.org/10.1016/j.trd.2015.09.019

Qiao, Y., Dawson, A. R., Parry, T., Flintsch, G., & Wang, W. (2020). Flexible pavements and climate change: A comprehensive review and implicatio. *Sustainability (Switzerland)*, *12*(3), 1–21. https://doi.org/10.3390/su12031057

Qiao, Y., Flintsch, G., Dawson, A., & Parry, T. (2013). Examining Effects of Climatic Factors on Flexible Pavement Performance and Service Life. *Transportation Research Record: Journal of the Transportation Research Board*, *2349*(1), 100–107. https://doi.org/10.3141/2349-12

Qiao, Y., Santos, J., Stoner, A. M. K., & Flinstch, G. (2019). *Climate change impacts on asphalt road pavement construction and maintenance An economic life cycle assessment of* *adaptation measures in the State of. 2005*(Ipcc 2014), 1–14. https://doi.org/10.1111/jiec.12936

Rana, M., Swarna, S., & Hossain, K. (2020). Climate Change Impact on Pavement Performance in Newfoundland , Canada. *99th Annual Meeting of the Transportation Research Board (TRB) of National Academies of Science and Engineering, Washington DC, USA*.

Schweikert, A., Chinowsky, P., Espinet, X., & Tarbert, M. (2014). Climate change and infrastructure impacts: Comparing the impact on roads in ten countries through 2100. *Procedia Engineering*, *78*, 306–316. https://doi.org/10.1016/j.proeng.2014.07.072

Schweikert, A., Chinowsky, P., Kwiatkowski, K., Johnson, A., Shilling, E., Strzepek, K., & Strzepek, N. (2015). *Road Infrastructure and Climate Change : Impacts and Adaptations for South Africa*. *21*(3), 1–9. https://doi.org/10.1061/(ASCE)IS.1943-555X.0000235.

Shao, Z., Jenkins, G., & Oh, E. (2017). Assessing the impacts of climate change on road infrastructure. *International Journal of GEOMATE*, *13*(38), 120–128.

Sharma, M., Inti, S., Tandon, V., & Byreddy, H. (2020). Economical and Environmental Impact of Climate Change on Texas Pavements. *99th Annual Meeting of the Transportation Research Board (TRB) of National Academies of Science and Engineering, Washington DC*.

Stocker, T. F., Qin, D., Plattner, G.-K., Tignor, M., Allen, S. K., Boschung, J., Nauels, A., Xia, Y., Bex, V., & Midgley, P. M. (2013). Climate change 2013: The physical science basis. In *Contribution of working group I to the fifth assessment report of the intergovernmental panel on climate change*. https://doi.org/10.1017/CBO9781107415324.Summary

Stoner, A. M. K., Daniel, J. S., Jacobs, J. M., Hayhoe, K., & Scott-fleming, I. (2019). *Quantifying the Impact of Climate Change on Flexible Pavement Performance and Lifetime in the United*

States. https://doi.org/10.1177/0361198118821877

Swarna, S., & Hossain, K. (2018). Effect of Interface Bonds on Pavement Performance. *In TAC 2018: Innovation and Technology: Evolving Transportation-2018 Conference and Exhibition of the Transportation Association of Canada.*

Taylor, K. E., Stouffer, R. J., & Meehl, G. A. (2012). An overview of CMIP5 and the experiment design. *Bulletin of the American Meteorological Society*, *93*(4), 485–498. https://doi.org/10.1175/BAMS-D-11-00094.1

Tighe, S., Mills, B., Tighe, S. L., Smith, J., Mills, B., & Andrey, J. (2008). *Evaluating Climate Change Impact on Low- Volume Roads in Southern Canada on Low-Volume Roads in Southern Canada*. *October 2015*. https://doi.org/10.3141/2053-02

Underwood, S. (2019). A method to select general circulation models for pavement performance evaluation A method to select general circulation models for pavement performance evaluation. *International Journal of Pavement Engineering*, *0*(0), 1–13. https://doi.org/10.1080/10298436.2019.1580365

Underwood, S., Guido, Z., Gudipudi, P., & Feinberg, Y. (2017). *Increased costs to US pavement infrastructure from future temperature rise Increased costs to US pavement infrastructure from future temperature rise*. *September*. https://doi.org/10.1038/nclimate3390

Valle, O., Qiao, Y., Dave, E., & Mo, W. (2017). Life cycle assessment of pavements under a changing climate. *Pavement Life-Cycle Assessment*, *October*, 241–250. https://doi.org/10.1201/9781315159324-25

Vincent, L. A., Zhang, X., Mekis, Wan, H., & Bush, E. J. (2018). Changes in Canada’s Climate: Trends in Indices Based on Daily Temperature and Precipitation Data. *Atmosphere - Ocean*, *56*(5), 332–349. https://doi.org/10.1080/07055900.2018.1514579

Viola, F., & Celauro, C. (2015). Effect of climate change on asphalt binder selection for road construction in Italy. *Transportation Research Part D: Transport and Environment*, *37*, 40–47. https://doi.org/10.1016/j.trd.2015.04.012

Wang, J., Fonseca, R. M., Rutledge, K., Martín-Torres, J., & Yu, J. (2019). Weather Simulation Uncertainty Estimation Using Bayesian Hierarchical Models. *Journal of Applied Meteorology and Climatology*, *58*(3), 585–603.

Wistuba, M. P., & Walther, A. (2013). Consideration of climate change in the mechanistic pavement design. *Road Materials and Pavement Design*, *14*(SUPPL.1), 227–241. https://doi.org/10.1080/14680629.2013.774759

Wood, A. W., Leung, L. R., Sridhar, V., & Lettenmaier, D. P. (2004). *Hydrologic implications of dynamical and statistical approaches to downscaling climate model outputs*. 189–216.

Zapata, C. E., Andrei, D., Witczak, M. W., & Houston, W. N. (2007). Incorporation of environmental effects in pavement design. *Road Materials and Pavement Design*, *8*(4), 667–693. https://doi.org/10.3166/rmpd.8.667-693

Zareie, A., Amin, S. R., & Amador-jiménez, L. (2016). *Thornthwaite Moisture Index Modeling to Estimate the Implication of Climate Change on Pavement Deterioration*. *142*(4), 1–11. https://doi.org/10.1061/(ASCE)TE.1943-5436.0000840.

Zhai, P., & Pan, X. (2003). Trends in temperature extremes during 1951-1999 in China. *Geophysical Research Letters*, *30*(17). https://doi.org/10.1029/2003GL018004

Chapter 3: Impact of Climate Change on Pavement Performance in Canada's Newfoundland Island

3.1 Abstract

In recent years climate change has become a threat to both the existing and imminent pavement infrastructure. Therefore, there is a need for changing the design procedure of these pavements to overcome the challenges imposed by climate change. This study focuses on the projection of climate change using various models for Newfoundland climate regions, predominantly to investigate the impact of climate change on pavement design in the province of Newfoundland and Labrador, Canada. Mechanistic-Empirical Pavement Design Software, AASHTOWare was used to determine the pavement performance for both historical climate (referred as baseline climate) and the projected climate change. To predict the climate change model, a statistically downscaled climate change models were taken from Coordinated Regional Downscaling (CORDEX) Experiments. These models include daily maximum and minimum temperatures only. However, to estimate the hourly climate model, two relatively new hourly estimation procedures, such as Modified Imposed Offset Morphing Method (M-IOMM) and Sine (14R-1), are used. Similarly, an hourly model was implemented for precipitation using the M-IOMM method. These climate change models were incorporated into the AASHTOWare ME Pavement software to predict the pavement performance and compared with the baseline climate. This study found that climate change causes the early deterioration of pavement compared to the baseline climate.

Keywords: Climate Change, Pavement Performance, Temperature Rise, Projected Climate Models, Traffic Growth

3.2 Introduction

The earth's climate has been changing for the last 650,000 years, but since 1950 there has been a drastic change in climate due to increased emissions of greenhouse gases, such as carbon dioxide, methane, and nitrous oxide from anthropogenic actions. Many researchers agree that the current condition of climate change is significantly affecting pavement infrastructures (Gudipudi et al., 2017; Mills et al., 2007; Qiao et al., 2019). The foremost effects of climate change are a rise in global temperature, warming of the oceans, shrinking of the ice sheets, decreased snow cover, sea-level rise, and increased/decreased annual precipitation. Because of these effects, there is a long-term impact on pavement performance.

In recent years, with the use of newly available technology all over the world, prediction of climate change effects has become more convenient. Most of the studies related to climate change explain the increases in the frequency and severity of many types of extreme weather, such as changes in air temperature, rainfall, sea-level rise and hurricanes, all of which have direct effects on pavement performance. There is vast evidence that stresses how pavement infrastructure is sensitive to climate change, predominantly through thermal cracking, instability in pavement support layers, rutting, and freeze and thaw effects. Climate change can also have direct and indirect impacts on pavement performance. Change in the intensity of rainfall, for example, can alter moisture balances, which influences pavement performance. In addition, change in low temperatures can affect the aging of asphalt, resulting in an increase in cracking. Out of all these effects, change in temperature (Gudipudi et al., 2017) and change in precipitation (Lu et al., 2018) are the predominant factors that affect pavement performance. Gudipudi et al. concluded that the future change in temperature increases the asphalt concrete rutting by 9 – 40% in the United States (Gudipudi et al., 2017). In Canada, the increase in asphalt concrete rutting due to a change in temperature is 13 – 36% (Mills et al., 2009). Also, rainfall is becoming more intense in shorter periods, which causes frequent flooding. The wet day count has more impact on subgrade performance than the actual precipitation (Mndawe et al., 2016). Also, this results in reduced pavement life.

AASHTOWare Pavement Mechanistic-Empirical (ME) software, also referred as Mechanistic-Empirical Pavement Design Guide (MEPDG) software, is a robust pavement design system that considers the climate effect on pavement performance. The climate inputs in AASHTOWare software are hourly air temperature, wind speed, percent sunshine, precipitation, and relative humidity. Most of the studies used AASHTOWare to compute the impact of climate change on pavement performance and it's service life (Li et al., 2013; Mallick et al., 2014, 2016; Meagher et al., 2012; Mills et al., 2006, 2009; Qiao et al., 2013, 2015; Stoner et al., 2019; S. Tighe et al., 2008; Underwood, 2019; Valle et al., 2017). Fundamentally, this software is based on four key inputs that are material properties for all the layers, traffic volume and distribution, climate, and structural design.

The overall goal of this study is to evaluate the impact of climate change in several highway pavement sections in Canada's most easterly province, Newfoundland and Labrador. This study was organized as follows: Section 2 briefly summarizes the literature review on climate change prediction models and its effect on pavement performance. The objective and the contributions of this research are described in Section 3, while Section 4 provides an overview of methodology of this study. Section 5 provides the description of study sites and its climatic conditions. Section 6 describes the results and outcomes from this study, which includes the use of Sine(14R-1) and the performance predictions using AASHTOWare ME Pavement Design. The summary and the conclusions drawn from this study is illustrated in Section 7. Finally, the pro and cons of this research study are discussed in Section 8.

3.3 Current knowledge on climate change effects

3.3.1 Climate prediction models

There are many tools that can simulate climate change globally. Most of these climate change models consider the increase in Green House Gases (GHG) to predict the climate change. Some of the models consider climate change at a global average level. One of these models is the MAGICC model (Li et al., 2013; T. M.L. Wigley et al., 2009; Tom M L Wigley, 2008); this model estimates both changes in GHG concentrations and global temperature. The Intergovernmental Panel on Climate Change (IPCC) is the United Nations' body to evaluate the scientific view of climate change. In 2000, IPCC proposed a set of emission scenarios [also known as a special report on emission scenarios (SRES)] based on world population growth, industrial and agricultural development, and energy used (Nakicenovic, N., J. Alcamo, G. Davis, B. de Vries, J. Fenhann, S. Gaffin, K. Gregory, A. Grubler, T. Y. Jung et al., 2000). Carbon dioxide (CO_2) is one of the most predominant GHGs emitted by human anthropogenic activities. IPCC measured expected CO_2 concentration by 2050 and 2100 from developing the emission scenarios. In addition, IPCC also measured the increase in Global Mean Temperature (GMT) from 2010 to 2050 and 2100, as presented in Table 3-1.

Table 3-1: Carbon dioxide levels and temperature change from SRES Scenario (Nakicenovic, N., J. Alcamo, G. Davis, B. de Vries, J. Fenhann, S. Gaffin, K. Gregory, A. Grubler, T. Y. Jung et al., 2000)

SRES Scenario	Corresponding RCP Scenario	Key Assumptions	CO_2 Concentration 2050 (ppm)	Increase in GMT 2010 to 2050 (°C/°F)	CO_2 Concentration 2100 (ppm)	Increase in GMT 2010 to 2100 (°C/°F)
A1FI	RCP 8.5	Very high rates of growth in global income, moderate population growth, and very high fossil fuel use	570	1.5 (2.7)	993	4.1 (7.4)
A2	RCP 8.5	Moderate rates of economic growth, but very high rates of population growth	533	1.1 (2.0)	867	3.4 (6.1)
A1B	-	Same economic and population assumptions as of the A1FI scenario, but assumes more use of low-carbon- emitting power sources and clean technologies	533	1.2 (2.2)	717	2.6 (4.7)
B2	RCP 6	Population growth lower than A2; intermediate economic growth and more diverse technological change	476	1.1 (1.9)	620	2.2 (4.0)

B1	RCP 4.5	Same population growth as A1FI and A1B, but assumes a more service-oriented economy and much more use of low-carbon-emitting power sources and clean technologies	487	0.8 (1.5)	538	1.5 (2.7)

In 2014, IPCC started using a new set of emission scenarios called "Representative Concentration Pathways (RCP's)" (Moss et al., 2010). These new sets of emission scenarios are RCP 8.5, 6, 4.5 and RCP 2.6. The RCP scenarios are similar to the SRES scenarios; the only difference between the RCP and SRES scenarios is the CO_2 equivalent expected by 2100. The RCP 8.5 has a CO_2 equivalent value by 2100 between A1FI and A2. Also, RCP 6 and RCP 4.5 are almost equal to the B2 and B1 scenarios, respectively. RCP 2.6 is emitting less CO_2 equivalent compared to all SRES scenarios (Moss et al., 2010).

3.3.2 Pavement performance

Many researchers estimated the effect of climate change on pavement performance, as illustrated in Table 3-2. Mills et al. used Coupled Global Climate Model 2 (CGCM2A2x) and Hadley Climate Model 3 (HadCM3B21) models to quantify the effects of change in temperature, precipitation and freeze and thaw on deformation, cracking and IRI for pavement section in Canada (Mills et al., 2009). In addition, their study evaluated the impact of the rise in temperature and freeze and thaw on long-term maintenance of the Canadian road network (Mills et al., 2007). The same climate change model was used in another study to find out the combined influence of climate change and traffic growth on pavement performance. From this study, the authors concluded that climate change increases the severity of thermal cracking, rutting, frost heave, and thaw, which might lead to premature deterioration of pavement (S. L. Tighe et al., 2008). Li et al. analyzed the climate change data for temperature and precipitation using MAGICC/SCENGEN model and observed that climate change is increasing the severity of transverse cracking, which could lead to other distresses (Li et al., 2013). Another study used the same climate model in Virginia to determine the effect of temperature increase on the service life of the pavement and found that there may be a significant reduction in the service life of pavement due to temperature increase

(Qiao et al., 2013). In addition, this research also estimated life-cycle costs and concluded that the maintenance is triggered to be 8 - 16% earlier compared to the baseline climate (Qiao et al., 2015). Also, in 2017, another study used different climate models, such as the IPCC, SRES, and UKCP09 methods, and came to the same conclusion (Qiao et al., 2016).

Wistuba et al. used an IPCC SRES Scenario, such as A1B, A2 and B1, to study pavement damage in Germany and noticed that in the first six years of service, A1B and A2 performed similarly, but B1 exhibited an increased damage rate. After twenty-five years of service, A1B and B1 also performed similarly, but the A2 damage rate increased (Wistuba & Walther, 2013). However, the author claimed that the impact of climate on pavement infrastructure is found to be negligible for the central European countries. Schweikert et al. considered fifty-four distinct AR4 Global Circulation Model (GCM) scenarios to study the impact of climate on maintenance, repair, and construction. This study concluded that adaptation to climate change could reduce the life-cycle cost of the infrastructure (Schweikert et al., 2014). Viola et al. used a spatial interpolation method and projected the future rise in temperature. In addition, the authors studied the pavement temperature and recommended a change in the selection of superpave binder grade for various locations in Italy (Viola & Celauro, 2015). Similar work was done in Canada by another researcher who recommended the future pavement temperature grade (PG) for seventeen major Canadian cities using the ANUSPLIN model for climate change prediction (Fletcher et al., 2016).

Very recently, a study considered nineteen models with RCP 4.5 and 8.5 scenarios from various countries to assess the effect of change in temperature and precipitation pavement distresses such as AC rutting and fatigue cracking. In this research, the author noticed that there is an increase of 2–9% for fatigue cracking and 9–40% for AC rutting by the end of twenty years of service life (Gudipudi et al., 2017). Using the same models, Underwood et al. estimated the increased costs of pavement infrastructure from future temperature increase in the United States, which showed up to approximately US$19.0, and US$35.8 billion to pavement costs by 2040 for RCP 4.5 and 8.5 respectively (Underwood et al., 2017a). To select the appropriate GCM for the pavement performance evaluation, Underwood et al. verified the detailed pavement performance analyses with various models in four different states. This study illustrated a summary of model selection based on pavement distress prediction and the type of region (Underwood, 2019). Also, this study noticed that there is an increase in rutting and fatigue, cracking the selected four sites due to an increase in air temperature alone (Underwood, 2019). A very recent study assessed the impact of three climate change models on pavement performance in 24 different locations across the United States. The study exhibits different performance trends for 24 locations. However, all the results are illustrating the decreasing trend for pavement performance under current design standards (Stoner et al., 2019). Also, it was noticed that the AC permanent deformation is mostly affected by the increase in temperature.

Table 3-2: Various climate models used in past studies

Author	Year of study	Model used	Primary factors considered in the study	Key outcomes
Mills et al. (Mills et al., 2007)	2006	Coupled Global Climate Model 2 (CGCM2A2x) and Hadley Climate Model 3 (HadCM3B21)	Temperature, and freeze and thaw	Climate change may have important implications for the long-term maintenance of the Canadian road network.
Tighe et al. (S. L. Tighe et al., 2008)	2008		The combined influence of climate change and traffic growth	Climate change increases the severity of thermal cracking, rutting, frost heave, and thaw, which might lead to premature deterioration of the pavement.
Mills et al. (Mills et al., 2009)	2009		Temperature, precipitation, and freeze and thaw	There is a significant change in pavement performance in terms of deformation, cracking and IRI.
Meagher et al. (Meagher et al., 2012)	2012	NARCCAP climate change simulations	Temperature, precipitation, wind speed, percent sunshine and relative humidity	Pavement deterioration might be less sensitive to temperature compared to other climate factors, individually or in combination
Li et al. (Li et al., 2013)	2013	MAGICC/SCENGEN	Temperature and precipitation	Increase of transverse cracking due to temperature rise. This transverse cracking could lead to the cause of other distresses.
Qiao et al. (Qiao et al., 2013)	2013		Temperature rise	The service life of pavement in Virginia is reduced by greater than 20% due to a 5% rise in temperature.

Wistuba et al. (Wistuba & Walther, 2013)	2013	IPCC scenarios such as A1B, A2 and B1	Pavement temperature	In 6 years of service life, A1B and A2 are performing similarly, but the B1 damage rate is increased. In 25 years of service life, A1B and B1 are performing similarly, but the A2 damage rate is increased. For central European countries, the impact of climate on pavement infrastructure can be judged as negligible.
Schweikert et al. (Schweikert et al., 2014)	2014	Fifty-four distinct AR4 Global Circulation Model (GCM) scenarios	Impact of climate on maintenance, repair and construction	Adaptation to climate change can reduce the life-cycle cost of the infrastructure.
Mndawe et al. (Mndawe et al., 2016)	2015	Statistical projections	Precipitation	The wet day count has more impact on subgrade performance than the actual precipitation. Also, this results in reduced pavement life.
Viola et al. (Viola & Celauro, 2015)	2015	Spatial interpolation method (di Piazza et al., 2011)	Pavement temperature	Recommended a change in the selection of SUPERPAVE binder grade for various locations in Italy.
Qiao et al. (Qiao et al., 2015)	2015	MAGICC/SCENGEN	Life-Cycle Costs	Due to climate change, the maintenance are triggered to be 8 - 16% earlier when compared to the existing climate.
Fletcher et al. (Fletcher et al., 2016)	2016	ANUSPLIN	Pavement temperature	Found out the future pavement temperature grade (PG) for 17 major Canadian cities.
Qiao et al. (Qiao et al., 2016)	2016	IPCC several emission scenarios (SRES) and UKCP09 method	Temperature, precipitation, and sea-level rise	The influence of climate change may accelerate deterioration, reduce the service life, trigger maintenance earlier and eventually increases additional costs.

Gudipudi et al. (Gudipudi et al., 2017)	2017	Nineteen models with RCP 4.5 and 8.5 scenarios	Temperature and Precipitation	Leads to an increase of 2–9% for fatigue cracking and 9–40% for AC rutting by the end of 20 years' service life depending on the climate region of the pavement.
Underwood et al. (Underwood et al., 2017b)	2017		Temperature rise	With the rise in temperatures, the material selection process leads to an additional cost of approximately US$19.0 and US$35.8 billion to pavement costs by 2040 for RCP4.5 and 8.5, respectively.
Stoner et al. (Stoner et al., 2019)	2019	Coupled-Model Intercomparison Project Phase 5 (CMIP5) with RCP 8.5	Temperature rise	It was noticed that the AC permanent deformation is mostly affected by the increase in temperature
Underwood (Underwood, 2019)	2019	20 models from Coupled-Model Intercomparison Project Phase 5 (CMIP5), RCP 4.5 and 8.5	Temperature rise	Author gave a recommendation for climate change model selection based on a different region in the United States.

3.4 Study objective and contribution

The objective of this study is to evaluate the impact of climate change on asphalt pavement performance in Newfoundland while adopting a new method (Sine (14R-1)) for hourly temperature estimation. AASHTOWare ME Pavement Design Software is used to estimate the influence of climate on the pavement performance parameters. To achieve this, a statistically downscaled climate change model is utilized. This research also explored the climate data extraction and hourly data estimation methods such as Modified Imposed Offset Morphing Method (M-IOMM) and Sine (14R-1). In this study, these hourly data estimation methods were used to estimate the hourly temperature and hourly precipitation data from the extracted climate change daily data. As the AASHTOWare requires hourly climate data, this estimated climate data is used as a climate input in the pavement design. The contribution of the study is the employment of a new method “Sine(14R-1)” for the hourly data estimation, which is highly computational efficient and requires less data for the computation. In addition, the influence of climate change on asphalt pavements in Newfoundland is quantified and presented in this chapter.

3.5 Methodology

This study predominantly focuses on the effects of climate change on pavement performance for a Trans-Canada Highway (TCH) section in five different locations in the Newfoundland Province, Canada. To determine the performance of pavement using AASHTOWare ME pavement software, the necessary data needed are material properties, structural design of pavement, traffic details, and climate data. The methodology in this research mainly consists of five phases. In the first phase, the traffic, materials, and existing pavement design data on TCH are collected from the NL-Department of Transportation and Works (NLDTW) and LTPP database. In the second phase, both baseline and future climate data are collected from various sources. In the third phase, hourly data is computed using two advanced methods, such as the Modified Imposed Offset Morphing Method (M-IOMM) and the Sine (14R-1) method. In the fourth phase, the performance of the existing TCH pavement sections is estimated for both baseline and future climate using AASHTOWare ME pavement software. In the final phase, the pavement performance is compared between baseline and future climate. The framework of the current study is presented in Figure 3-1.

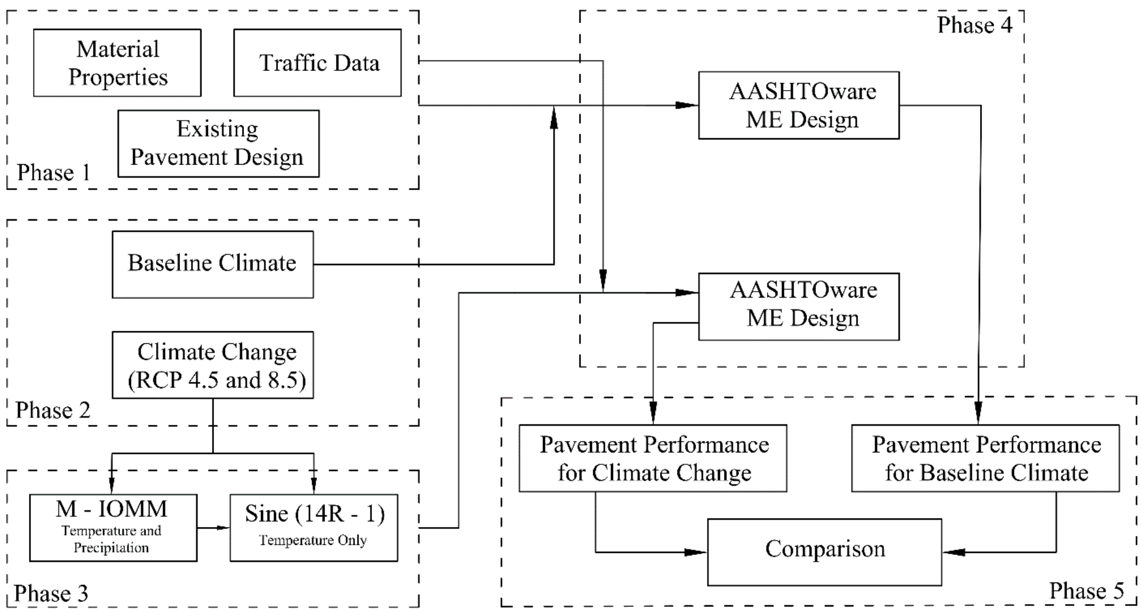

Figure 3-1: Framework to evaluate the impact of climate change on pavement performance

3.5.1 First phase

Five different locations on TCH were considered in the province of Newfoundland, Canada. These locations are located in five major cities such as St. John’s, Gander, Grand Falls, Deer Lake, and Corner Brook, illustrated in Figure 3-2. The traffic, materials, and existing pavement design data for these TCH pavement sections are collected from the NLDOT and LTPP Database.

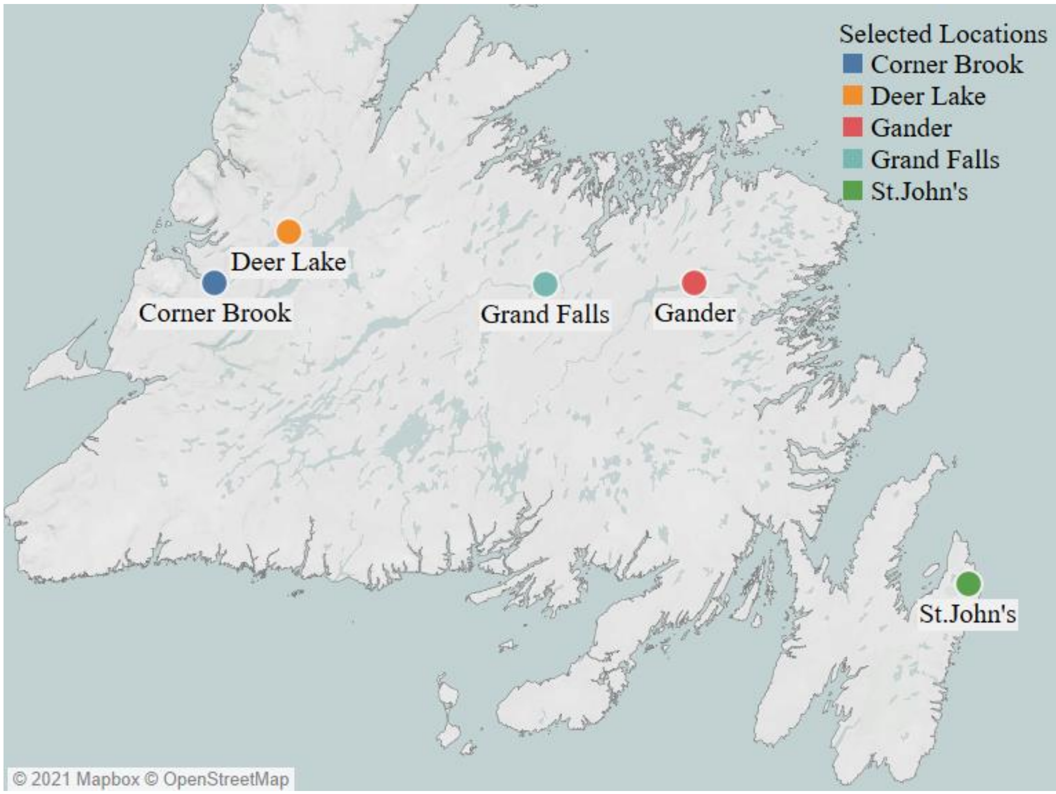

Figure 3-2: Locations selected on Trans-Canada Highway to quantify the climate change impact.

3.5.2 Second phase

AASHTOWare ME design software have a sophisticated climate dataset from Modern Era Retrospective-Analysis for Research and Applications (MERRA) and North American Regional Reanalysis (NARR). For the baseline climate, MERRA data was collected for a period of thirty years (ranging from 1988 to 2018) from LTPP infopave website. This collected MERRA data contains hourly temperature, wind speed, percentage of sunshine, precipitation, and relative humidity. In addition, climate change data was gathered from a statically downscaled Climate models using three different experiments developed by the Canadian Centre for Climate Modelling and Analysis (CCCma), Environment Canada. Data gathered from these models hold daily maximum and minimum temperatures and daily average precipitation ranging from 2006 to 2100. Since the climate change modeling is a challenging task with numerous factors, considering one climate change model could result in misleading performance predictions. Therefore, in this study, an average of three climate change models were determined to quantify the climate change impact.

3.5.3 Third phase

The climate inputs in AASHTOWare software are hourly air temperature, wind speed, percentage of sunshine, precipitation, and relative humidity. In this climate input, maximum air temperature and cumulative rainfall are evidently changing over time, while wind speed, percent sunshine and relative humidity are relatively constant (Kumlai et al., 2016). Therefore, only temperature and precipitation data are modified in case of the climate input. And, the wind speed, percent sunshine and relative humidity are kept constant in this study. The climate change factors quantified in this study are temperature increase and change in precipitation. The predicted daily maximum temperature (T_{pM}), daily minimum temperature (T_{pm}), and daily precipitation data are available in the collected model. However, AASHTOWare ME pavement design software accepts only hourly temperature and precipitation data. Therefore, two advanced methods are used to estimate the hourly data from the daily maximum and minimum temperature and also from daily precipitation data. Hourly temperature data is estimated using the Modified Imposed Offset Morphing Method (M-IOMM) and the Sine (14R-1) method. In addition, hourly precipitation is computed using the M-IOMM method alone because there is no continuity in the precipitation. In-brief, precipitation does not follow any pattern in a day. Therefore, we are using the historical hourly precipitation data to estimate future hourly precipitation data. These hourly estimation methods are explained in detail below.

The Modified Imposed Offset Morphing Method (M-IOMM): The Imposed Offset Morphing

Method (IOMM) is based on reconstructing a past weather pattern to predict future daily climate variables with a finer temporal resolution and was used by Gudipudi et al, and many other (Belcher et al., 2005; Gudipudi et al., 2017). In principle, historic daily minimum and maximum temperature data are first acquired from climate model outputs, along with future projections of the daily extreme for equal ranges of years. Then, by applying a sequence of 'shifting', 'stretching', or a combination of both to the data, hourly values for a future period of time are obtained. Daily maximum temperature (T_{pM}) and daily minimum temperature (T_{pm}) are extracted from the prediction model. Historical daily maximum temperature (T_{hM}) and daily minimum temperature (T_{hm}) are estimated using the available historical data. Hourly predicted temperature (T_{hr}) is computed using the historical distribution of hourly temperature (T_{hD}) from the following equation

$$T_{hr} = \frac{T_{pM} - T_{pm}}{T_{hM} - T_{hm}} \times (T_{hD} - T_{hm}) + T_{pm} \quad \text{Equation 3-1}$$

Hourly precipitation data (P_{hr}) are calculated using the following equation

$$P_{hr} = \left(\frac{(P_{dapm} - P_{dahm})}{P_{dahm}} \times p_{hhr}\right) + p_{hhr} \quad \text{Equation 3-2}$$

Where,

P_{dapm}= the daily average of monthly precipitation calculated from the prediction model

P_{dahm} = the daily average of monthly precipitation calculated from historical data

P_{hhr}= the hourly precipitation from historical data

Sine (14R-1) method: This method was first used by Chow and Levermore in 2007, to determine the hourly temperature data from high and low daily temperature. This method also employs a *sine* curve fit to daily extremes, but the difference lies in the assumption of times of occurrence for these values. In contrast to the Chartered Institution of Building Services Engineers (CIBSE) method of assigning constant times for any day in a month, the sine (14R-1) method takes into account the intensity of the incoming percent sunshine to define times of occurrence for extreme temperatures in a day. Knowing the latitude of the study location and the day of the year, sunrise time is first calculated using standard relations. The time of minimum temperature, T_{min}, is then taken as the hour before sunrise, whereas the time of maximum temperature, T_{max}, is assumed constant at 14.00 hour of any day, regardless of the time of the year. The sinusoidal curve is then fit, and hourly values are extracted similar to the CIBSE method. To produce hourly temperature data from daily maximum and minimum temperature, Chow and Levermore used the Sine (14R-1) method (Chow & Levermore, 2007). Sunrise/sunset time is gathered from the Environment Canada website to calculate the time for minimum temperature. Hourly temperature (T_{hr}) was calculated using the following equation

$$\mathrm{T_{hr}} = \left(\frac{\mathrm{T_{next}}+\mathrm{T_{pre}}}{2}\right) - \left[\left(\frac{\mathrm{T_{next}}-\mathrm{T_{pre}}}{2}\right) \times \cos\left(\frac{\pi(\mathrm{t}-\mathrm{t_{pre}})}{(\mathrm{t_{next}}-\mathrm{t_{pre}})}\right)\right] \quad \text{Equation 3-3}$$

Where,

T_{next} = next known minimum or maximum temperature (either T_{max} or T_{min})

T_{pre} = previous known minimum or maximum temperature (either T_{max} or T_{min})

t = time for which temperature is computed

t_{next} = time for T_{next}

t_{pre} = time for T_{pre}

Two sets of data are predicted to reveal climate change effects on pavement performance using AASHTOWare ME Pavement design. The two sets of estimations are as follows:

1st set: predicted temperature from M-IOMM method + wind speed and percentage of sunshine from historical data + precipitation from M-IOMM method + relative humidity from historical data

2nd set: predicted temperature from the Sine (14R-1) method + wind speed and percentage of sunshine from historical data + precipitation from M-IOMM method + relative humidity from historical data

Fourth phase: AASHTOWare ME Pavement software is used to determine the performance of the existing TCH pavement sections for both baseline and expected future climate change. The traffic, materials, climate and existing pavement design data collected from the Department of Transportation and Works, LTPP, MERRA, and CCCma are used as inputs in MEPDG to predict the performance. In total, five models, which include one baseline and four climate change models, are analyzed for a period of twenty years to estimate the effect of climate change on pavement infrastructure.

Fifth phase: The estimated pavement performance for both baseline and climate change are compared in terms of distress parameters such as asphalt rutting, fatigue cracking, overall rutting and thermal cracking. In addition, the predicted International Roughness Index (IRI) over twenty years of service life is also compared.

3.6 Description of study sites

Newfoundland is an eastern most Atlantic province in Canada, which has a very harsh climatic condition. A total of five pavement sections are considered in this study. These five pavement sections are located near to five major cities of Newfoundland, these locations are selected from all parts of Newfoundland Island (Avalon Peninsula, central and western Newfoundland). Here, two locations (Corner Brook and Deer Lake) are from western Newfoundland, two locations (Grand falls and Gander) are from central Newfoundland and one location (St. John's) is from Avalon Peninsula/eastern part of Newfoundland. As explained in the first phase, to estimate the TCH pavement performance, the necessary data such as traffic, material and structural pavement design are collected from the NLDOT and LTPP database, as described in Table 3-3. Annual Average Daily Truck Traffic (AADTT) data were collected from NLDOT for the period of 2017-2018. The traffic was kept constant to determine the impact of climate change alone.

Table 3-3: Input parameters for the study sites

Input	Variable	St. John's	Gander	Grand Falls	Deer Lake	Corner Brook
Layer-1 (AC)	Thickness (mm)	50	45.7	45.7	48.9	42.9
	Density(kg/m^3)	2466.84	2496.00	2496.00	2513.99	2548
	Air voids (Va, %)	4.42	4.99	4.99	4.71	3.97
	AC (%)	7.3	5.3	5.3	6.5	7.0
	Binder type (PG Grade)	58-28	58-28	58-28	58-28	58-28
Layer-2 (AC)	Thickness (mm)	60.0	35.6	35.6	37.8	33.7
	Density(kg/m^3)	2546.94	2576.89	2576.89	2598.54	2611.38
	Air voids (Va, %)	6.29	6.29	6.29	6.29	6.29
	AC (%)	6.2	5.0	5.0	6.5	6.1
	Binder type	58-28	58-28	58-28	58-28	58-28
Layer-3 (Crushed stone)	Thickness (mm)	250.0	251.5	251.5	157.5	114.3
	Resilient Modulus (MPa)	206.8	206.8	206.8	206.8	206.8
Layer-4 (Crushed stone)	Thickness (mm)	300.0	284.5	284.5	381	431.8
	Resilient Modulus (MPa)	206.8	206.8	206.8	206.8	206.8
Layer-5 (Subgrade)	Resilient Modulus (MPa)	125	110	110	95	90
Traffic	AADTT	947	663	663	780	550

3.7 Results and discussion

3.7.1 Climate change models

Table 3-4: Nomenclature for the climate change models used in the analysis

Nomenclature	RCPs	Data Source	Hourly Data Estimation Model	
			Temperature	Precipitation
PCM-01	4.5	CCCma	M-IOMM	M-IOMM
PCM-02			Sine (14R-1)	
PCM-03	8.5		M-IOMM	
PCM-04			Sine (14R-1)	

Hourly temperature and precipitation data for 2030-2050 were computed using M-IOMM and Sine (14R-1) methods to assess the climate change impact on pavement. These estimated climate data were considered as a climate input in MEPDG software for evaluating the performance of the TCH pavement sections. The performance was assessed for five TCH sections located in different cities in the province of Newfoundland, Canada. In this study, five climate models, such as one baseline model (also called historical climate data) and four Projected Climate Models (PCM) are considered. The collected climate change data (CCCma - RCP 4.5 and CCCma-RCP 8.5) were used to generate four PCMs. The PCMs are classified based on RCPs and temperature and precipitation prediction models, as illustrated in Table 3-4.

The comparison between the baseline and projected climate change for mean annual air temperature, mean annual precipitation, annual freezing index, average annual number of freeze and thaw cycles was illustrated in Figure 3-3, which shows a constant increase in temperature and precipitation for the climate change models in compared to the baseline climate. However, the annual freezing index and average annual number of freeze and thaw cycles are reducing for future climate. The average annual temperature in the western Newfoundland (Deer Lake and Corner Brook) is found to be around 4°C and for future climate, it is increasing to 5.5 - 6°C. However, in the central and eastern Newfoundland (St. John's, Gander and Grand Falls), the average annual temperature is around 5 - 6°C and it is increasing to 6.5 - 7°C for future climate.

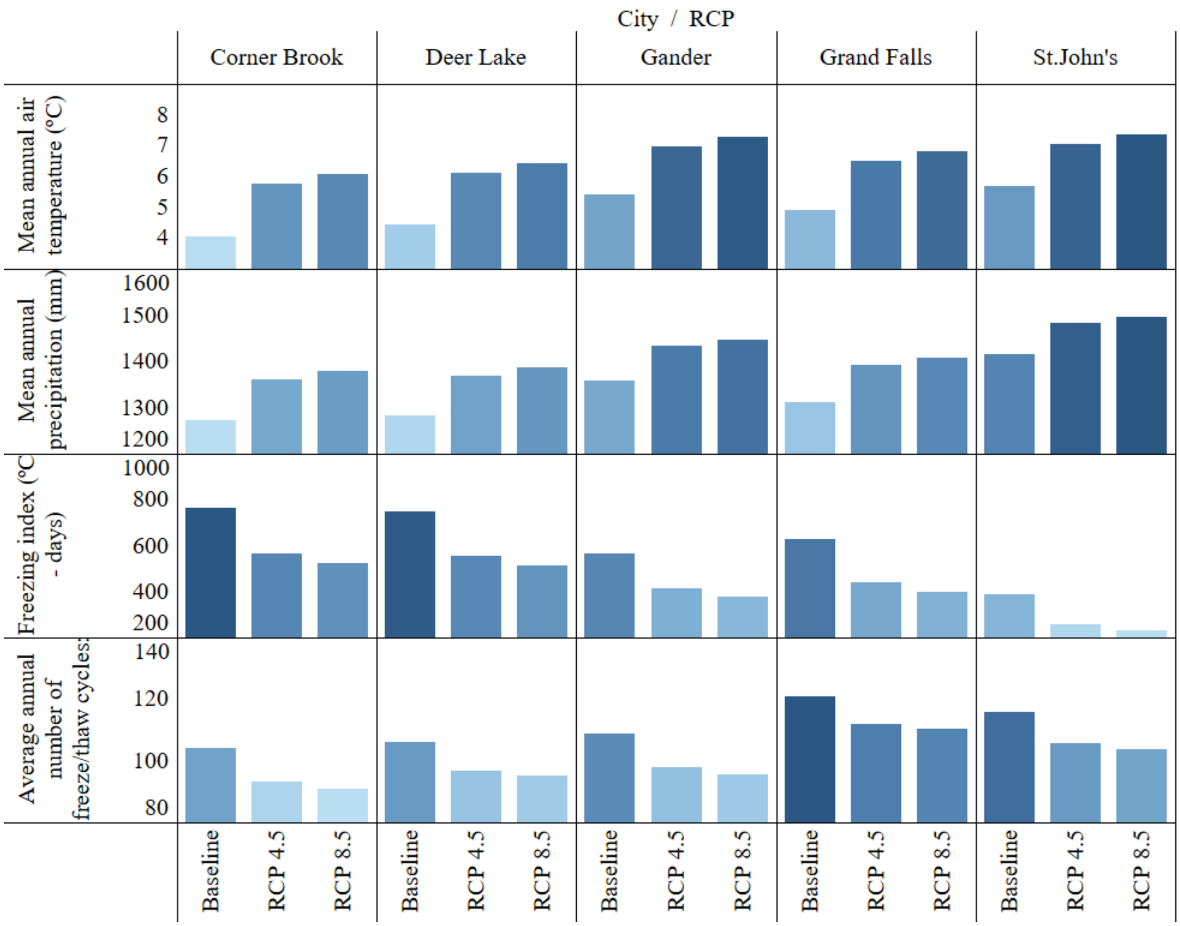

Figure 3-3 Summary of climate factor for baseline and future climate in the Newfoundland

In addition, a monthly distribution pattern for both baseline and future climate are illustrated in Figure 3-4. It is noticed that the temperature is constantly increasing throughout the year. However, the precipitation predicted from climate change model is increasing in the spring season (May to July) and then decreasing in the late summer season (September to October). The average precipitation remains constant in the winter season. Therefore, there might be a possibility of flooding in the spring season.

The hourly temperature distribution data are computed using M-IOMM and Sine(14R-1). These computed hourly data was compared with the existing LTPP temperature data and three days data from three different months are illustrated in Figure 3-5. Figure 3-5 shows that there is not much difference between these hourly distribution estimation methods and the existing data. Also, there is no significant difference between the M-IOMM and Sine(14R-1). Both the hourly distribution methods have assumptions, where M-IOMM mainly depends on the historic data and Sine(14R-1) depends on the fixed time for maximum and minimum temperature. The major advantage of Sine (14R-1) method is computational efficiency of using this method for hourly temperature estimation.

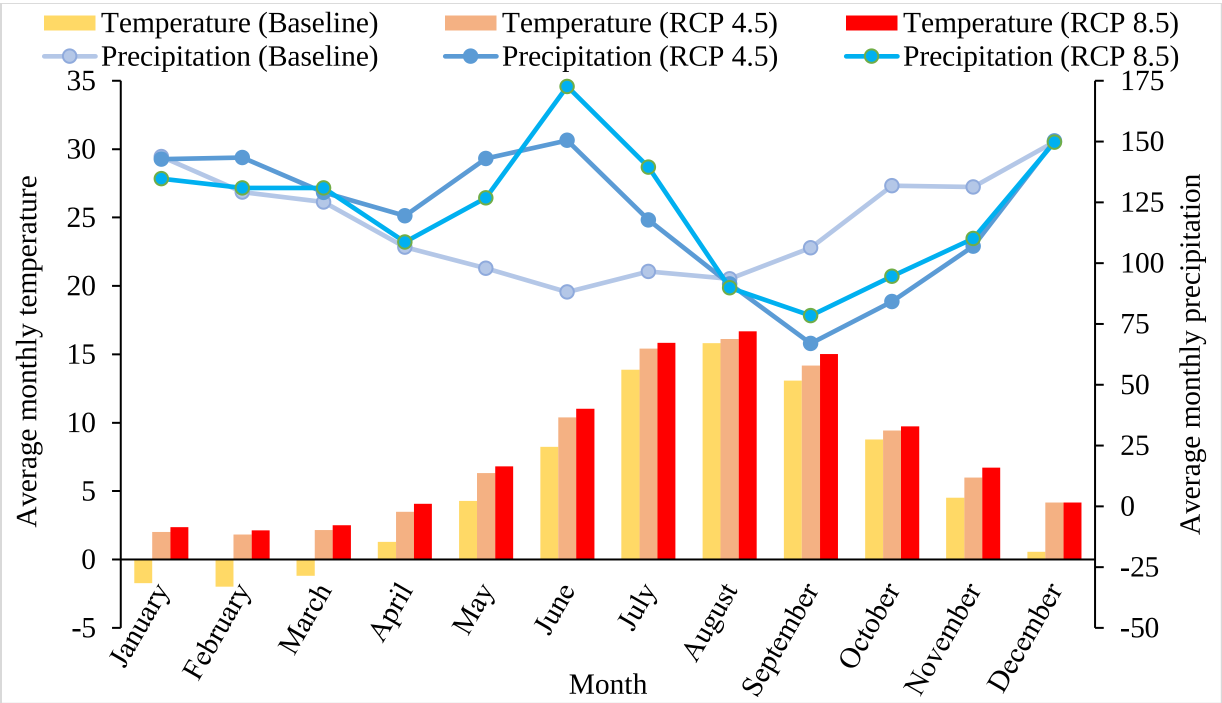

Figure 3-4 Average monthly temperature and precipitation for all scenarios

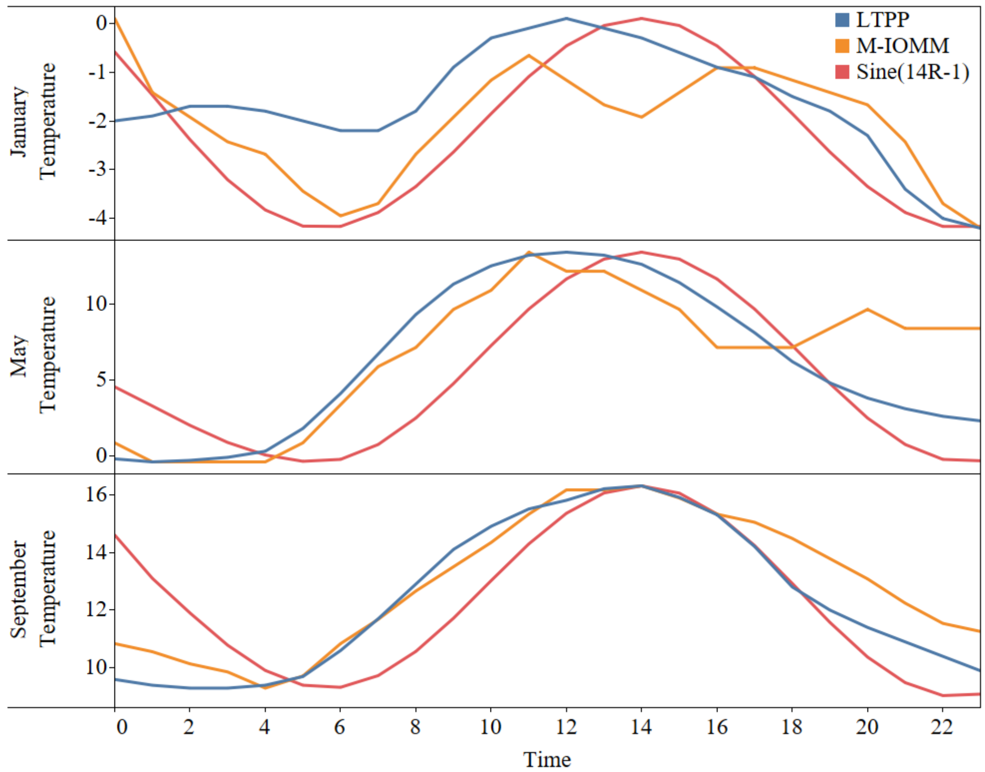

Figure 3-5 Hourly temperature data computed using M-IOMM and Sine(14R-1) compared to the existing LTPP data

3.7.2 AASHTOWare ME simulation and performance analysis

To evaluate the performance of the TCH pavement sections, the AASHTOWare ME Pavement Design software is used, which needs a fundamental input regarding the pavement section based on location. For the TCH sections, a design service life of twenty years is considered, including a construction period of six months, from July until December. The target limits for the distresses considered in this design are as follows: Terminal IRI (m/km) – 2.76, Permanent deformation for total pavement (Total rutting, mm) - 20, AC bottom-up fatigue cracking (BU fatigue cracking, % lane area) – 25, AC top-down fatigue cracking (TD fatigue cracking, m/km) – 375, Permanent deformation for AC only (AC rutting, mm) – 7. These are targeted with a reliability of 50%.

For estimating the effects of climate change alone, the climate change models with constant traffic were analyzed and compared with the baseline climate. The change in pavement distress predictions from Pavement ME between baseline and climate change are presented in Figure 3-6. Observations made from Figure 3-6 are as follows:

- IRI is decreasing for all the climate change models, which supports the conclusion made in past studies (Mills et al., 2009).
- Due to climate change, there is an average of 6-11% increase in total permanent deformation.
- In addition, there is an increase of 18 – 27% in AC rutting, which might be because of the constant increase in temperature throughout the year.
- AC bottom-up fatigue cracking is increasing by an average of 6% for all of the sections due to climate change.
- Permanent deformation in base layers is decreasing in all the location for future climate, which might be due to reduction in number of freeze and thaw cycles.
- Comparing the hourly temperature estimation methods, the Sine (14R-1) method exhibits slightly lower distress compared to M-IOMM method. However, the difference is not statistically significant.

The IRI for climate change models is less compared to the baseline climate. It is also noticed that, all the climate models are exhibiting the same performance over the entire design life. The unanticipated performance noticed in this study is that the IRI is improving while the pavement distresses (both rutting and cracking) are increasing, this may be due to an inaccurate calibration factor in the existing IRI model. To eliminate this, new calibration factors are required predominantly for the freezing zones.

The existing model included in MEPDG (AASHTO, 2008) was structurally simplified to account for site-specific properties. The model as presented in the Mechanistic-Empirical Pavement Design Guide Manual of Practice is as follows:

$$\mathrm{IRI} = \mathrm{IRI}_0 + 0.0150\ (\mathrm{SF}) + 0.400\ (\mathrm{FC}_{\mathrm{Total}}) + 0.0080\ (\mathrm{TC}) + 40.0\ (\mathrm{RD}) \qquad \text{Equation 3-4}$$

$$\mathrm{SF} = \mathrm{Age}\ [0.02003\ (\mathrm{PI} + 1) + 0.007947\ (\mathrm{Precip} + 1) + 0.000636\ (\mathrm{FI} + 1)] \qquad \text{Equation 3-5}$$

Where,

SF is a site factor that accounts for environmental, subgrade soil properties, and the age of the pavement structure

FC_{Total} corresponds to the area of fatigue cracking: combined alligator, longitudinal, and reflection cracking under the wheel path in feet^2

TC is the length of transverse cracking in feet-mile

RD is the average rut depth measured in inches

PI is the plasticity index of the subgrade soil

$Precip$ is the average annual rainfall in mm

FI is the average annual freezing index

Age is the age of pavement in years

These model parameters were calibrated based on LTPP data for the whole North America. However, this model does not directly include local calibration parameters. It is noticed that all the individual parameters in Equation 3-4 are increasing except SF. From Equation 3-5, the SF depends on the plasticity index, precipitation, and freezing index. In this case, the plasticity index is constant, and the precipitation is slightly increasing. However, the freezing index is drastically decreasing, which might be the main reason for improving IRI performance. The freezing indices for baseline climate and climate change are 401.75 °F and 0.43 °F, respectively. To correct this analytically, new calibration factors are needed for the province of Newfoundland and Labrador, Canada. Looking at the other side of this circumstance, the IRI model might not be capable of capturing the climate change effect.

Figure 3-6 also shows the predicted total permanent deformation over the design life of pavement for both baseline climate and climate change models. Here, the total permanent deformation for all the climate change models is higher, when compared to the baseline climate. Also, AC thermal cracking is reducing about 15-20% in the western part of Newfoundland. However, there is a very less reduction in the central and eastern newfoundland. This might be because of a significant change in freezing index, especially in western Newfoundland.

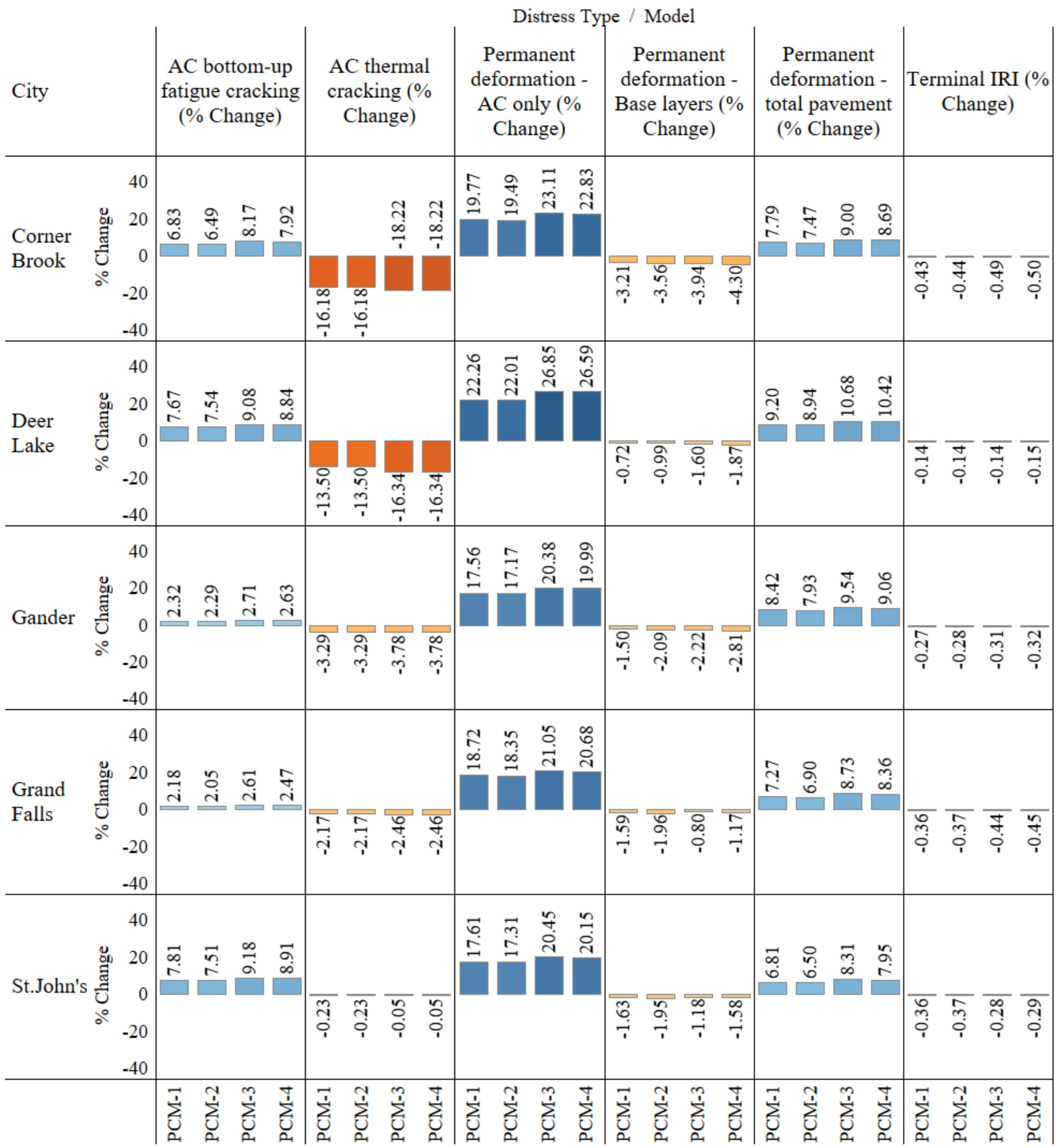

This plot represents the impact of climate change on pavement performance

The bars presented in this plot are the percentage change in performance parameters for future years with respect to baseline/historical climate. For example, in Corner brook, the AC BU fatigue cracking is increasing by 6.83% for PCM-1 future climate model when compared to baseline/historical climate. Similarly, the AC BU fatigue cracking rutting is increasing by 6.49%, 8.17% and 7.92% for PCM-2. PCM-3 and PCM-4 climate models, respectively wrt. baseline climate.

Figure 3-6 Percentage change in pavement performance due to climate change

Figure 3-6 also presents the predicted AC permanent deformation over the design life of pavement for both baseline climate and climate change models. Here, it is also noted that the AC permanent deformation is increasing about 7% for the eastern and central Newfoundland. However, there is only 2-3% increase in AC permanent deformation for the western part of Newfoundland, which might be because of lower temperature in the western Newfoundland compared to eastern and central Newfoundland. It is also noted that the permanent deformation in base layers is reducing with climate change, which might be occurring due to (1) reduction in freezing index or (2) reduction in freeze and thaw cycles or (3) warmer temperatures might dry the base layer aggregates sooner (Bizjak et al., 2014).

From Figure 3-6, it is clearly noticed that there is not much difference between the M-IOMM and Sine (14R-1) in terms of pavement performance. However, the major advantage of Sine (14R-1) method for computing the hourly temperature is the easiness of using Sine(14R-1) method for hourly prediction of temperature. M-IOMM requires historical hourly temperature to estimate the hourly temperature for future climate, while Sine (14R-1) method depends only on future daily maximum and minimum temperature.

In addition, a paired T-test was performed individually for all the distresses to determine the difference between the means of variable. The assumption of null hypothesis in this paired T-test is that there is a no significant difference between in performance predicted for RCP 4.5 and RCP 8.5. From this test, the p-value is found to be 0.1284, 0.3798, 0.982, 0.682, 0.425 for AC BU fatigue cracking, AC thermal cracking, base layer permanent deformation, total permanent deformation and IRI, respectively. It was found that p-values of all the distress were greater than $\alpha=0.05$ except AC permanent deformation, which fails to reject the null hypothesis. Therefore, it is concluded that there is no significant difference between the performance predicted for RCP 4.5 and RCP 8.5. However, in case of AC permanent deformation, the p-value is found to be 0.0311, which is less than significance level α=0.05. Therefore, it is concluded that it rejects the null hypothesis, which explains that there is a significant difference between the AC permanent deformation predicted for RCP 4.5 and RCP 8.5.

3.8 Conclusion

In the current study, the impact of climate change on pavement performance is evaluated using AASHTOWare software for both baseline climate and climate change models (PCM 01-04). Here, a new hourly temperature estimation procedure named Sine (14R-1) is considered for a reliable estimation of hourly data based on sunrise and is also continuous over the considered period. The performance of a pavement section on the Trans-Canada Highway in NL, Canada was assessed. The material, traffic, structural design, and climate data were collected from various sources such as NL Department of Transportation and Works, LTPP, MERRA climate database and Environment Canada. This pavement design was analyzed using AASHTOWare software for both baseline climate and climate change models. The predicted pavement distresses from the baseline and climate change models are compared and drawn conclusions as presented below.

- The climate change is significantly affecting the pavement performance over a design life of twenty years. Pavement distresses including total permanent deformation, BU fatigue cracking, AC layer rutting are highly affected by climate change.
- AC layer rutting is increased by 18-27%, which might be because of the constant increase in temperature throughout the design period. However, base layer and subgrade rutting is decreasing, which might be a resultant of decrease in freeze and thaw cycles.
- The proposed method 'Sine (14R-1)' exhibits approximately same distress compared to M-IOMM method. However, the major advantage of Sine (14R-1) method is computational efficiency of using this method for estimation of hourly temperature. M-IOMM requires

historical hourly temperature to estimate the hourly temperature for future climate, while Sine (14R-1) method depends only on future daily maximum and minimum temperature.

- There is no significant difference between the distress predicted for future climate using RCP 4.5 and RCP 8.5. However, in the case of AC permanent deformation, there is a significant difference in prediction for future climate using RCP 4.5 and RCP 8.5 models.
- The pavements might experience early failure in the province of Newfoundland, mainly due to climate change. Therefore, there is a necessity to look for adaptation strategies to avoid the early failure of pavement.
- The current IRI model might not be capable of capturing climate change impact. Further investigation is needed to better understand the performance of MEPDG-IRI model.

3.9 Pros and Cons

Pros:

- Selected five different locations in the province of Newfoundland to quantify the climate change impact.
- Considered three different climate models and average was found to reduce the biasness in the study.

Cons:

- Current study does not incorporate the local calibration factors for predicting pavement performance.
- Used M-IOMM hourly precipitation model along with Sine(14R-1) hourly temperature model, which might be an ideal case.

3.10 References

AASHTO. (2008). *Mechanistic-empirical pavement design guide. A manual of practice. Washington, DC: American Association of State Highway Officials, Highway Research Board.*

Belcher, S. E., Hacker, J. N., & Powell, D. S. (2005). Constructing design weather data for future climates. *Building Services Engineering Research and Technology*, *26*(1), 49–61. https://doi.org/10.1191/0143624405bt112oa

Bizjak, K. F., Dawson, A., Hoff, I., Makkonen, L., Ylhaisi, J. S., & Carrera, A. (2014). The impact of climate change on the European road network The impact of climate change on the European road network. *Proceedings of the Institution of Civil Engineers*, *May 2014*. https://doi.org/10.1680/tran.11.00072

Chow, D. H. C., & Levermore, G. J. (2007). New algorithm for generating hourly temperature values using daily maximum, minimum and average values from climate models. *Building Services Engineering Research and Technology*, *28*(3), 237–248. https://doi.org/10.1177/0143624407078642

di Piazza, A., Conti, F. Lo, Noto, L. V., Viola, F., & La Loggia, G. (2011). Comparative analysis of different techniques for spatial interpolation of rainfall data to create a serially complete monthly time series of precipitation for Sicily, Italy. *International Journal of Applied Earth Observation and Geoinformation*, *13*(3), 396–408. https://doi.org/10.1016/j.jag.2011.01.005

Fletcher, C. G., Matthews, L., Andrey, J., & Saunders, A. (2016). Projected changes in mid-twenty-first-century extreme maximum pavement temperature in Canada. *Journal of Applied Meteorology and Climatology*, *55*(4), 961–974. https://doi.org/10.1175/JAMC-D-15-0232.1

Gudipudi, P. P., Underwood, B. S., & Zalghout, A. (2017). Impact of climate change on pavement structural performance in the United States. *Transportation Research Part D: Transport and Environment*, *57*(October), 172–184. https://doi.org/10.1016/j.trd.2017.09.022

Kumlai, S., Jitsangiam, P., & Pichayapan, P. (2016). The implications of increasing temperature due to climate change for asphalt concrete performance and pavement design. *KSCE Journal of Civil Engineering*, *21*(4), 1222–1234. https://doi.org/10.1007/s12205-016-1080-6

Li, Q. J., Mills, L., McNeil, S., & Attoh-Okine, N. O. (2013). Integrating potential climate change into the mechanistic–empirical based pavement design. *Canadian Journal of Civil Engineering*, *40*(12), 1173–1183. https://doi.org/10.1139/cjce-2012-0465

Lu, D., Tighe, S. L., & Xie, W. (2018). Impact of flood hazards on pavement performance Impact of fl ood hazards on pavement performance. *International Journal of Pavement Engineering*, *0*(0), 1–7. https://doi.org/10.1080/10298436.2018.1508844

Mallick, R., Jacobs, J. M., Miller, B. J., Daniel, J. S., Mallick, R. B., Jacobs, J. M., Miller, B. J., & Daniel, J. S. (2016). *Understanding the impact of climate change on pavements with CMIP5 , system dynamics and simulation*. *8436*(January 2017). https://doi.org/10.1080/10298436.2016.1199880

Mallick, R., Radzicki, M., Daniel, J., & Jacobs, J. (2014). Use of System Dynamics to Understand Long- Term Impact of Climate Change on Pavement Performance and Maintenance Cost. *Transportation Research Record Journal of the Transportation Research Board*, *5*(December 2014). https://doi.org/10.3141/2455-01

Meagher, W., Daniel, J. S., Jacobs, J., & Linder, E. (2012). *Method for Evaluating Implications of Climate Change for Design and Performance of Flexible Pavements*. *2305*, 111–120.

https://doi.org/10.3141/2305-12

Mills, B., Tighe, S., Andrey, J., Huen, K., & Parm, S. (2007). Climate change and the performance of pavement infrastructure in southern Canada: Context and case study. *2006 IEEE EIC Climate Change Technology Conference, EICCCC 2006*, *June*. https://doi.org/10.1109/EICCCC.2006.277185

Mills, B., Tighe, S., Andrey, J., Smith, J., & Huen, K. (2009). Climate Change Implications for Flexible Pavement Design and Performance in Southern Canada. *Journal of Transportation Engineering*, *135*(10), 773–782. https://doi.org/10.1061/(asce)0733-947x(2009)135:10(773)

Mills, B., Tighe, S., Huen, K., & Parm, S. (2006). *Climate Change and the Performance of Pavement Infrastructure in Southern Canada : Context and Case Study Climate change and the performance of pavement infrastructure in southern Canada : Context and case study*. *June*. https://doi.org/10.1109/EICCCC.2006.277185

Mndawe, M. B., Ndambuki, J. M., Kupolati, W. K., Badejo, A. A., Dunbar, R., Ndambuki, J. M., Kupolati, W. K., Badejo, A. A., & Dunbar, R. (2016). *Assessment of the effects of climate change on the performance of pavement subgrade*. *1338*(March). https://doi.org/10.1080/20421338.2015.1023649

Moss, R. H., Edmonds, J. A., Hibbard, K. A., Manning, M. R., Rose, S. K., Van Vuuren, D. P., Carter, T. R., Emori, S., Kainuma, M., Kram, T., Meehl, G. A., Mitchell, J. F. B., Nakicenovic, N., Riahi, K., Smith, S. J., Stouffer, R. J., Thomson, A. M., Weyant, J. P., & Wilbanks, T. J. (2010). The next generation of scenarios for climate change research and assessment. *Nature*, *463*(7282), 747–756. https://doi.org/10.1038/nature08823

Nakicenovic, N., J. Alcamo, G. Davis, B. de Vries, J. Fenhann, S. Gaffin, K. Gregory, A. Grubler,

T. Y. Jung, T. K., E. L. La Rovere, L. Michaelis, S. Mori, T. Morita, W. Pepper, H. Pitcher, L. Price, K. Raihi, A. Roehrl, H.-H., & Rogner, A. Sankovski, M. Schlesinger, P. Shukla, S. Smith, R. Swart, S. van Rooijen, N. Victor, and Z. D. (2000). *Emissions Scenarios. A Special Report of Working Group III of the Intergovernmental Panel on Climate Change*.

Qiao, Y., Casey, D. B., Kuna, K. K., Kelly, K., & Macgregor, I. D. (2016). *Climate Resilience of Flexible Pavement Highways : Assessment of Current Practice*. *July 2017*, 1–14.

Qiao, Y., Dawson, A. R., Parry, T., & Flintsch, G. W. (2015). Evaluating the effects of climate change on road maintenance intervention strategies and Life-Cycle Costs. *Transportation Research Part D: Transport and Environment*, *41*(November 2015), 492–503. https://doi.org/10.1016/j.trd.2015.09.019

Qiao, Y., Flintsch, G., Dawson, A., & Parry, T. (2013). Examining Effects of Climatic Factors on Flexible Pavement Performance and Service Life. *Transportation Research Record: Journal of the Transportation Research Board*, *2349*(1), 100–107. https://doi.org/10.3141/2349-12

Qiao, Y., Santos, J., Stoner, A. M. K., & Flinstch, G. (2019). *Climate change impacts on asphalt road pavement construction and maintenance An economic life cycle assessment of adaptation measures in the State of*. *2005*(Ipcc 2014), 1–14. https://doi.org/10.1111/jiec.12936

Schweikert, A., Chinowsky, P., Espinet, X., & Tarbert, M. (2014). Climate change and infrastructure impacts: Comparing the impact on roads in ten countries through 2100. *Procedia Engineering*, *78*, 306–316. https://doi.org/10.1016/j.proeng.2014.07.072

Stoner, A. M. K., Daniel, J. S., Jacobs, J. M., Hayhoe, K., & Scott-fleming, I. (2019). *Quantifying the Impact of Climate Change on Flexible Pavement Performance and Lifetime in the United*

States. https://doi.org/10.1177/0361198118821877

Tighe, S. L., Smith, J., Mills, B., & Andrey, J. (2008). Evaluating Climate Change Impact on Low-Volume Roads in Southern Canada. *Transportation Research Record: Journal of the Transportation Research Board*, *2053*(1), 9–16. https://doi.org/10.3141/2053-02

Tighe, S., Mills, B., Tighe, S. L., Smith, J., Mills, B., & Andrey, J. (2008). *Evaluating Climate Change Impact on Low- Volume Roads in Southern Canada on Low-Volume Roads in Southern Canada*. *October 2015*. https://doi.org/10.3141/2053-02

Underwood, S. (2019). A method to select general circulation models for pavement performance evaluation A method to select general circulation models for pavement performance evaluation. *International Journal of Pavement Engineering*, *0*(0), 1–13. https://doi.org/10.1080/10298436.2019.1580365

Underwood, S., Guido, Z., Gudipudi, P., & Feinberg, Y. (2017a). Increased costs to US pavement infrastructure from future temperature rise. *Nature Climate Change*, *7*(10), 704–707. https://doi.org/10.1038/nclimate3390

Underwood, S., Guido, Z., Gudipudi, P., & Feinberg, Y. (2017b). *Increased costs to US pavement infrastructure from future temperature rise Increased costs to US pavement infrastructure from future temperature rise*. *September*. https://doi.org/10.1038/nclimate3390

Valle, O., Qiao, Y., Dave, E., & Mo, W. (2017). Life cycle assessment of pavements under a changing climate. *Pavement Life-Cycle Assessment*, *October*, 241–250. https://doi.org/10.1201/9781315159324-25

Viola, F., & Celauro, C. (2015). Effect of climate change on asphalt binder selection for road construction in Italy. *Transportation Research Part D: Transport and Environment*, *37*, 40–

47. https://doi.org/10.1016/j.trd.2015.04.012

Wigley, T. M.L., Clarke, L. E., Edmonds, J. A., Jacoby, H. D., Paltsev, S., Pitcher, H., Reilly, J. M., Richels, R., Sarofim, M. C., & Smith, S. J. (2009). Uncertainties in climate stabilization. *Climatic Change*, *97*(1), 85–121. https://doi.org/10.1007/s10584-009-9585-3

Wigley, Tom M L. (2008). *MAGICC / SCENGEN 5 . 3 : USER MANUAL (version 2)*. *version 2*.

Wistuba, M. P., & Walther, A. (2013). Consideration of climate change in the mechanistic pavement design. *Road Materials and Pavement Design*, *14*(SUPPL.1), 227–241. https://doi.org/10.1080/14680629.2013.774759

Chapter 4: Assessing Climate Change Impact on Asphalt Binder Grade: Selection and Its Implications

4.1 Abstract

Anthropogenic climate change is having and will continue to have unpredictable effects on Canadian weather. Trends in average annual temperatures have been rapidly increasing over the last 50 years. The severe climatic variations in Canada are in line with global changes in climate occurring due to increased greenhouse gas concentrations in the atmosphere. Under the current CO_2 emission scenarios, scientists predict the climate trends to further intensify in the near future. It is well known that asphalt binder is highly sensitive to climate factors. Hence, reviewing asphalt binder grade is a vital step, and that can help decelerate pavement deterioration. The objective of this study was to assess the change in asphalt binder grade for the future climate and to determine the influence of change in binder grade on the performance of pavements in Canada. To achieve this, the analysis was carried out in five phases. In the first phase, statistically downscaled climate change models were gathered from the pacific Canada Climate database. Then in the second phase, the temperature and precipitation data were extracted for the selected locations. Later in the third phase, the asphalt binder grade was determined for future climate data. In the fourth phase, the pavement materials, traffic, and structural data were collected from the Long-term Pavement Performance (LTPP) database. Lastly, the pavement performance with the base binder and the upgraded binder were assessed using AASHTOWare Mechanistic-Empirical Pavement Design. The results reemphasize the necessity of upgrading the asphalt binder grade in various provinces of Canada.

Keywords: Climate change, Asphalt binder, Pavement performance, AASHTOWare ME design, Pavement design

4.2 Introduction

Environmental factors are one of the primary causes of pavement deterioration. The predominant climate factors that affect pavement are temperature, precipitation, percent sunshine, wind speed, groundwater table, and humidity. All these factors are responsible for the deterioration of the pavement, and climate change has caused drastic shifts in all these factors.

The foremost effects of climate change are the rise in air temperature, change in precipitation patterns and intensity, and changes in other minor climate factors, such as percent sunshine, wind speed, and humidity. Many studies have quantified the impact of these factors on the pavement. These studies reveal that temperature and precipitation are the most significant climate factors that cause pavement deterioration. Dawson summarized the possible causes and effects on highways due to climate change, as illustrated in Table 4-1 (Dawson, 2014).

4.2.1 Temperature

Temperature is one of the predominant factors that affect pavement deterioration. Several studies have reported temperature increase due to climate change in Canada (Vincent et al., 2018), United States (Paquin et al., 2014), South America (Marengo et al., 2012), Europe (Meleux et al., 2007), Africa (Jones & Thornton, 2009), Middle East (Evans, 2009), China (Zhai & Pan, 2003), India (Dash et al., 2007), Central Asia (Lioubimtseva & Henebry, 2009), Southeast Asia (Gasparrini et al., 2017) and Australia (Hughes, 2003). Pavement performance models show that temperature increase will result in accelerated pavement deterioration.

Temperature affects pavement materials, which leads to pavement deterioration. Temperature rise can negatively affect the Dynamic Modulus (E*) of the surface HMA layer, which leads to reduction in the service life of pavement (Kumlai et al., 2016). The major advantages for temperature consideration are (1) the uncertainties in the climate change temperature prediction are less than that of the other climate factors (Kharin et al., 2007; Piras et al., 2015); (2) the impact of temperature is significantly higher than that of all the other factors (Gudipudi et al., 2017; Knott et al., 2019; Qiao et al., 2016; Qiao, Flintsch, et al., 2013; Rana et al., 2020; Underwood, 2019); and (3) temperature plays a vital role in selecting pavement surface materials (Fletcher, Matthews, Matthews, et al., 2016; Mills et al., 2009; Viola & Celauro, 2015).

4.2.2 Precipitation

Precipitation is also a dynamic climate factor that affects pavement deterioration. An increase in precipitation might cause a moisture imbalance in the subgrade, which leads to the reduction of stiffness properties on subgrade (Mallick et al., 2014, 2016). Also, rainfall is becoming more intense over shorter periods, which causes frequent flooding events. This change in the distribution of rainfall is the predominant factor affecting the base layers of pavement structure (Elshaer et al., 2018).

4.2.3 Other climate factors

Percent sunshine, wind speed, humidity, and groundwater level also signify the climate impact on pavement deterioration. As climate change projections are not available for these climate factors, Qiao et al. (2013) estimated the influence of a 5.0% change in percent sunshine, wind speed, and groundwater level on pavement performance. The results of this investigation did not suggest that these factors had a significant influence on pavement performance (Qiao, Dawson, et al., 2013; Qiao, Flintsch, et al., 2013). However, it is necessary to look at the climate change projections for these factors using a statistical approach. Moreover, it is necessary to observe the interaction of these factors with temperature and precipitation. A recent study stated that the increase in the percent sunshine is likely to affect the asphalt materials through asphalt aging, embrittlement, and cracking (Shao et al., 2017).

Table 4-1: Major consequences to pavement infrastructure due to climate change (Dawson, 2014)

Cause	Possible effects on highways	Effect
Increased mean temperatures in cold regions	Less pavement damage from frost heave	+
Increased mean temperatures in cold regions	More thawing periods with consequent loss of subgrade strength	–
Increased mean temperatures in cold regions	Ice roads unavailability	–
Increased mean temperatures in mild/warm climate zones	More evaporation leading to drier subgrades	+
Increased mean temperatures in mild/warm climate zones	More rapid ageing increases embrittlement, with a consequent loss of waterproofing of the surface seal. Surface water can enter the pavement causing potholing and loss of surface condition	–
Increased extreme hot temperatures	Rutting	–
Rising sea level	Coastal erosion degrading the road platform	–
Rising sea level	Higher risk of floods	–
Rising sea level	Higher salinity may lead to debonding of asphalt and cement-treated bases attack	–
Increased water availability during summer	Higher water table level, with the consequent risk of lower subgrade modulus	–
Increased frequency and intensity of heavy rainfalls	Increased water on the road during or immediately after massive rainfall events so pavement more susceptible to potholing and stripping	–
Increased frequency and intensity of heavy rainfalls	Increase in subgrade moisture content reduces its stiffness	–
Increased frequency and intensity of heavy rainfalls	Increased sedimentation/debris blocking the water drainage system	–
Increased frequency and intensity of heavy rainfalls	Inadequate culverts	–
Increased frequency and intensity of heavy rainfalls	Erosion of road platforms	–
Increased temperature and rainfall variability	More difficult to plan and execute construction	–
Increased temperature and rainfall variability	More difficult to plan and execute maintenance	–
Increased temperature and rainfall variability	For extreme events, either more contingency/ reserve staff and equipment needed on standby or must accept more losses because of contingencies/ reserves the sufficient	–

Decrease of small rainfalls	Dryer environment	+
Higher percent sunshine due to ozone hole	Reduction of asphalt stiffness, rutting	–
	Risk of oxidation = ageing	–
Increase in vegetation (in temperate zones)	Higher moisture content? in the near pavement zone	–
	Need for more maintenance	–
	More stability at the roadsides?	+
Higher wind intensity	Traffic safety problems	–

'+' - Positive effect, '–' - Negative effect

4.2.4 Change in asphalt binder grade due to Climate change

Mills et al. (2009) estimated the change in Superpave binder grade for seventeen sites in southern Canada using two climate change scenarios A2x and B21 from Coupled Global Climate Model 2 (CGCM2A2x) and the Hadley Climate Model 3 (HadCM3B21) experiments, respectively. This revealed that six out of 17 sites would need an upgrade to the high-temperature grade, and at eight out of 17 sites, there was a rise in low-temperature grade by 2050 compared to a baseline climate of 1961 - 1990 (Mills et al., 2009). Similar work has been done by Viola and Celauro (2015) in Italy to evaluate the asphalt binder upgrade requirements at 71 different locations (Viola & Celauro, 2015). In this study, a change in air temperatures were estimated for 2033 using spatial interpolation based on historical data (1984-2013), corresponding pavement temperatures were also computed. It was noted that there is a one-grade increase in high-temperature grade over 27% of the Italian territory. On the other hand, there was no potential change in low-temperature grades in this territory (Viola & Celauro, 2015).

A similar study (2018) estimated the asphalt binder grade in Chile using the MICRO5 climate change model for RCP 2.6 and RCP 8.5 emission scenarios (Delgadillo et al., 2018). A total of 94 weather stations were considered in the selection of asphalt binder grades throughout the country. This study identified a significant number of stations that require a change in binder grade. Fletcher et al. (2016) estimated the change in pavement temperature for selecting superpave asphalt binder grade for the future climate in Canada. The author considered 10 GCM simulations for the SRESA2 emissions scenario. The study concluded that nine out of 17 cities exhibited an increase in high-temperature asphalt binder grade (Fletcher, Matthews, Andrey, et al., 2016).

In very recent years, a study was carried out to assess the upgrade requirement for asphalt binder grade in the United States. Out of the 799 observed weather stations, 35% of the station’s asphalt binder grade for 1985-2014 climate is different from binder grade for 1965-1996 climate data (Underwood et al., 2017). Underwood et al. (2017) also estimated the economic costs of a flexible pavement with the use of correct and incorrect asphalt grade for all roadway types (Underwood et al., 2017). For 2040, the estimated costs across the United States are US$19.0 and US$26.3 billion for RCP 4.5 and RCP 8.5, respectively. Similarly, for 2070, the estimated costs across the United States are US$21.8 and US$35.8 billion for RCP 4.5 and RCP 8.5, respectively. This increased economic cost demonstrates that selecting the correct grade of asphalt binder plays an essential role in reducing the economic costs of pavement.

4.2.5 AASHTOWare Mechanistic-Empirical (ME) Pavement Design

AASHTOWare Pavement Mechanistic-Empirical (ME) software, also named as Mechanistic-Empirical Pavement Design Guide (MEPDG) software, is a robust pavement design system that considers the climate’s effect on pavement performance. Fundamentally, this software considers four inputs: material properties for all the layers, traffic volume and distribution, climate, and structural design. The climate inputs in AASHTOWare software are hourly air temperature, wind speed, percent sunshine, precipitation, and relative humidity. Most of the previous studies have used AASHTOWare to compute pavement performance and service life (Li et al., 2013;

Mallick et al., 2014, 2016; Meagher et al., 2012; Mills et al., 2006, 2009; Qiao et al., 2015; Qiao, Flintsch, et al., 2013; Stoner et al., 2019; Tighe et al., 2008; Underwood, 2019; Valle et al., 2017). Also, these performance parameters are the main functions required to calculate the need for maintenance and rehabilitation.

The overall summary of the literature highlights the impact of climate change and the influence of future climate on binder grade selection. However, there are few limitations and gaps in the existing literature:

- To date, the most of research studies in this domain relied on one or two climate models to quantify the impact of climate change. Considering only one or two climate change models could result in a high degree of uncertainty (Gudipudi et al., 2017).
- Most of the studies in Canada are mainly based on GCM's with a grid of 300 x 300 km. In addition, the climate change data used for the analysis is not corrected for bias, which leads to under/overestimation of pavement performance (Chen & Wang, 2020).
- Most of the current studies have relied on one pavement structure, one location or one climatic region. Therefore, conclusions drawn from these studies may not be generalizable to other pavement structures or climate regions (Gudipudi et al., 2017).
- The influence of upgraded binder (considering climate change) on pavement performance or service life is not discussed in the current literature.

4.3 Goal and objectives

The goals of this study include

a) Quantify the impact of increasing temperatures and changing precipitation patterns on pavement performance across various climatic regions in Canada.

b) Estimate the influence of temperature increase on asphalt binder grade selection. Then, using the upgraded binder grade, to quantify the influence of upgraded binder grade on pavement performance and service life.

The objective of this study includes five phases.

1. Collect statistically downscaled General Circulation Models (GCMs) from the pacific Canada climate database.
2. Extract the maximum and minimum temperature data for ten different climate change models.
3. Determine the binder grade using projected future maximum and minimum temperatures.
4. Collect pavement materials, traffic, and structural data from Long-Term Pavement Performance (LTPP) database and Newfoundland Department of Transportation and Works (NL-DTW).
5. Assess the pavement performance for both historical and future climate with the base and upgraded binder grade using AASHTOWare Mechanistic-Empirical (ME) Pavement Design.

4.4 Methodology

The methodology of this study (as presented in Figure 4-1) was divided into five phases. In the first phase, statistically downscaled climate change models were gathered from the pacific Canada climate database. Then in the second phase, the maximum and minimum temperature data were extracted for the selected locations using ten different climate change models. Later in the third phase, the asphalt binder grade was determined for the climate change data. Then in the fourth phase, the pavement materials, traffic, and structural data were collected from the LTPP database.

In addition, the hourly data was estimated using Modified Imposed Offset Morphing Method (M-IOMM) for the extracted climate change data. Lastly, the pavement performance with the base binder and the upgraded binder were assessed using AASHTOWare Mechanistic-Empirical (ME) Pavement Design.

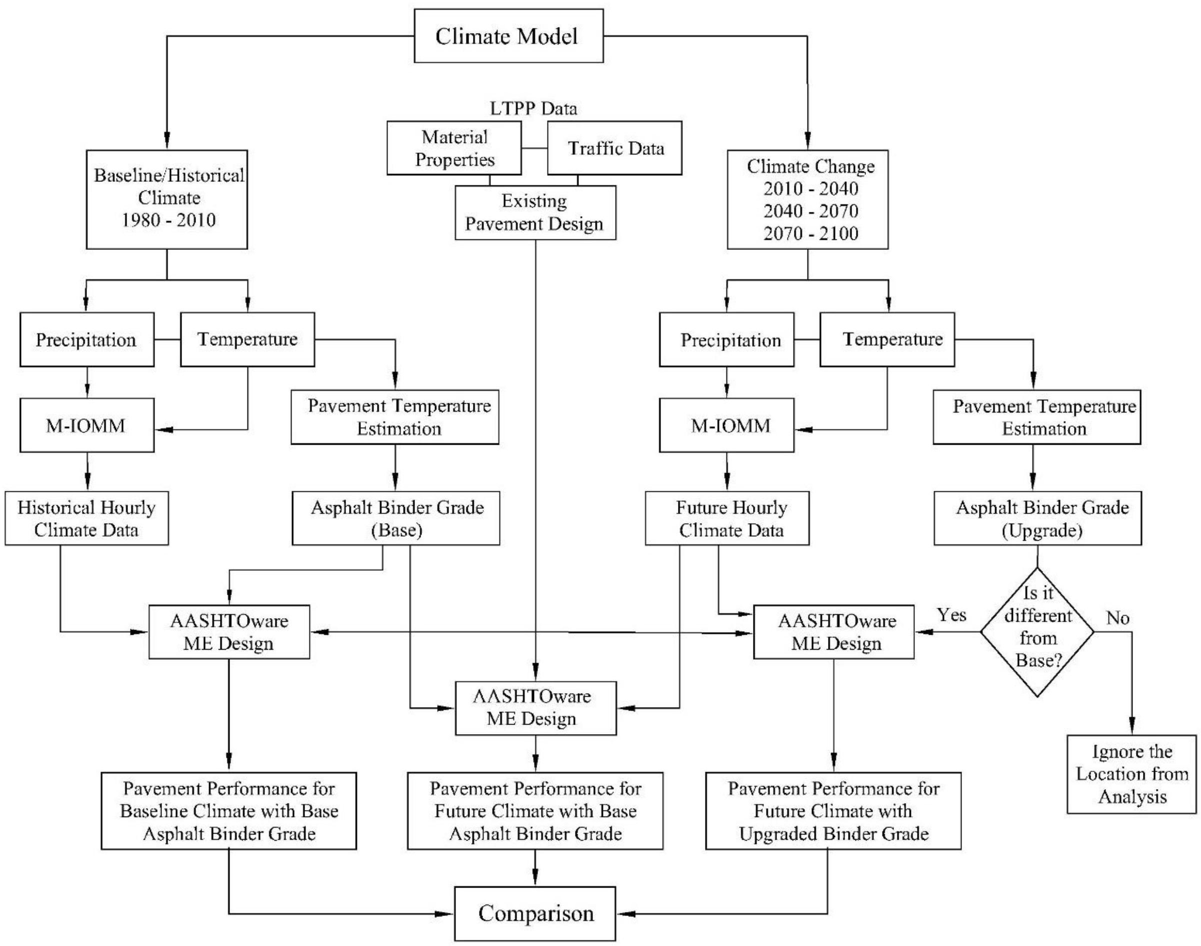

Figure 4-1: Methodology of the current study

4.4.1 Phase 1: Collect climate change models

Pacific Climate Impacts Consortium (PCIC) is a Canadian climate database, which offers statistically downscaled climate scenarios at a grid resolution of 1/8th degrees (300 arc-seconds or approximately 10 km) for a period of 1950 – 2100. The variables included in these climate scenarios are average daily precipitation, maximum and minimum daily temperature. These data are available for three different Representative Concentration Pathways (RCPs) (Meinshausen et al., 2011) such as RCP 2.6, RCP 4.5 and RCP 8.5. These climate scenarios are a combination of historical data and the downscaled climate change model. These downscaled models were constructed using Canadian historical daily data and General Circulation Models (GCM) projections from the Coupled Model Intercomparison Project Phase 5 (Taylor et al., 2012). From all the available climate models, ten climate models were selected based on data availability and method of statistical downscaling.

Data from the GCM sources available in the pacific climate database were downscaled to a very fine resolution using two different statistical downscaling methods such as Bias-Correction Spatial Disaggregation (BCSD) and Bias Correction/Constructed Analogues with Quantile mapping reordering (BCCAQ). BCCAQ is a hybrid method that associations with both Bias Correction/Constructed Analogues (BCCA) (Maurer et al., 2010) and quantile mapping (QMAP) (Gudmundsson et al., 2012). In this study, Models with BCCAQ statistical downscaling method were used. The climate change models used in this study were downloaded from the Pacific Climate data (https://www.pacificclimate.org/data/statistically-downscaled-climate-scenarios)(Pacificclimate, n.d.).

4.4.2 Phase 2: Extract climate change data

To extract the daily average precipitation, daily maximum, and minimum temperature from the climate change models for the selected sixteen locations, python codes were written and executed. As the downscaled model contain a square grid of size approximately 10 km x 10 km (1/8°), it was not possible to extract data for the exact location. Therefore, a short distance square method was used to select the nearest grid point. It was assumed that there was no temperature and precipitation difference between the actual location and the nearest grid point (within 10 km).

4.4.3 Phase 3: Determine asphalt binder grade for climate change data

From the extracted daily maximum and minimum air temperature, the average seven-day high and low air temperature were determined for every year from 2040 to 2070. Later, average seven-day high and low pavement temperatures were estimated for the 2040-2070 time period using the LTPP pavement temperature prediction model (Mohseni, 1998, 2005), as illustrated below.

$$T_{P\,max} = 54.325432 + 0.78\ T_{air\,max} - 0.0025\,Lat^2 - 15.41\ log_{10}(H + 25) + z(9 + 0.61\sigma^2_{Tair\,max})^{0.5} \quad \text{Equation 4-1}$$

$$T_{P\,min} = -1.56 + 0.72\ T_{air\,min} - 0.004\,Lat^2 + 6.26\ log_{10}(H + 25) + z(4.4\ + 0.52\ \sigma^2_{Tair\,min})^{0.5} \quad \text{Equation 4-2}$$

Where,

$T_{P\,max}$ = Average seven-day high pavement temperature (°C)

$T_{air\,max}$ = Average seven-consecutive-day high air temperature (°C)

$\sigma_{air\,max}$ = Standard deviation of seven-day high pavement temperature (°C)

$T_{P\,min}$ = Low pavement temperature (°C)

$T_{air\,min}$ = Low air temperature (°C)

$\sigma_{air\,min}$ = Standard deviation of low pavement temperature (°C)

Lat = Latitude (in degrees)

H = Depth (mm)

Z = Standard normal distribution value (depends on reliability) = 2.055 for 98% reliability

These seven-day high and low pavement temperatures were estimated at a depth of 20 mm and 0 mm, respectively. Where a seven-day high pavement temperature threshold about 20 mm (H = 20 mm) from the surface of the pavement and low pavement temperature threshold at the surface (H = 0 mm) of the asphalt pavement. Also, the reliability considered in this study as 98%, which has a standard normal distribution value (z) equals to 2.055. These pavement temperatures were computed for ten different climate change models.

From the estimated mean or median of the average seven-day high and low pavement temperatures, the high temperature and low temperature grades were assigned. As per Asphalt Institute Superpave Performance Graded Asphalt Binder Specifications (SP-1), the superpave grades were assigned in increments of 6°C for both high temperature and low temperature (SP-1, 1997). For example, in Vancouver, if the average seven-day high pavement temperature is 54.98°C, then the high-temperature grade assigned is 58°C. Similarly, if the low pavement temperature is -12.19°C, then the low temperature grade assigned is -16°C. Therefore, the performance asphalt grade is PG 58 – 16. The asphalt binder grades were assigned for all the selected locations following the same procedure explained in this methodology.

4.4.4 Phase 4: Collect pavement materials, traffic, structural, and climate data

Fifteen LTPP sections and one non-LTPP section were selected to estimate the pavement performance for both baseline and climate change data with base and upgraded asphalt binder grade. The selected locations for this study are illustrated in Table 4-2. The pavement materials, traffic, and structural data were collected from the LTPP database for the selected fifteen LTPP sections and St. John’s section data were collected from Newfoundland Department of Transportation and Works (NL-DTW).

The daily maximum temperature (T_{pM}), daily minimum temperature (T_{pm}), and daily precipitation data were extracted from the climate change models. However, AASHTOWare ME pavement design software accepts only hourly temperature and precipitation data. Therefore, Modified Imposed Offset Morphing Method (M-IOMM) was utilized to compute the hourly data from daily maximum and minimum temperature and daily average precipitation. Belcher et al. and Sailor et al. converted monthly mean temperature to hourly temperature by using the Imposed Offset Morphing method based on shifting and stretching the data (Belcher et al., 2005; Sailor, 2014). Gudipudi et al. modified this technique for hourly climate data preparation based on daily maximum temperature and daily minimum temperature (Gudipudi et al., 2017). Our past research evaluated the difference between the pavement distress predicted using different hourly data estimation methods such as Modified Imposed Offset Morphing Method (M-IOMM), Sine (14R-1), and other methods. From this study, it was noticed that there is no significant difference between these methods and the measured hourly data. The difference between the models is found to be ranging from -1.02% to 2.11%. This insignificant change elevates that the use of M-IOMM for computing the hourly data is significantly reliable. Daily maximum temperature (T_{pM}) and daily minimum temperature (T_{pm}) were extracted from the climate change models (as illuminated in Phase 2). Historical daily maximum temperature (T_{hM}) and daily minimum temperature (T_{hm}) were estimated using historical data available. Hourly predicted temperature (T_{hr}) was computed using the historical distribution of hourly temperature (T_{hD}) from the following equations 4-3 and 4-4.

$$T_{hr} = \frac{T_{pM}-T_{pm}}{T_{hM}-T_{hm}} \times (T_{hD} - T_{hm}) + T_{pm} \qquad \text{Equation 4-3}$$

Hourly precipitation data (P_{hr}) was calculated using the following equation

$$P_{hr} = \left(\frac{(P_{dapm} - P_{dahm})}{P_{dahm}} \times p_{hhr}\right) + p_{hhr} \qquad \text{Equation 4-4}$$

Where,

P_{dapm}= the daily average of monthly precipitation calculated by using excel program extracted from the prediction model

P_{dahm} = the daily average of monthly precipitation calculated by using excel program from historical data

P_{hhr} = the historical hourly precipitation data

4.4.5 Phase 5: Assessing pavement performance for future climate

The mechanistic-empirical pavement design tool, known as AASHTOWare Pavement ME Design, was considered a comprehensive pavement design tool developed based on a multitude of data inputs such as material properties, climatic data and traffic loading. Pavement ME can predict the performance of pavements over the design service life considering the change in the environmental factors and traffic loadings. For all sixteen sections, Level 1 inputs for the AC layers were used, such as layer thickness, percent air voids, percent effective binder, asphalt binder content, dynamic modulus, creep compliance, and indirect tensile strength. Level 1 and 2 inputs for subbase and subgrade were used. This data included Poisson's ratio, resilient modulus, gradation, and layer thickness for subbase, whereas subgrade was set as having a semi-finite thickness. The traffic data (Level 1) included two-way average annual daily truck traffic (AADTT), average annual daily traffic (AADT), percent traffic growth, type of growth function (i.e. linear or compound), percent vehicle class distribution, monthly adjustment factor, highway terrain, highway environment and a number of axles per truck (i.e. single, tandem and tridem). The climate inputs in AASHTOWare software are hourly air temperature, wind speed, percent sunshine, precipitation, and relative humidity. The period of 30 years from the section's construction date was used as the design life over which performance was predicted for sixteen sections. The reliability level considered in this ME analysis is 50%.

The performance of the selected pavement sections for both baseline, and future climate change expected were estimated. In addition, the performance was also estimated for both base asphalt binder grade and upgraded asphalt binder grade. In total, seven models, such as one baseline climate (1980-2010) with a base binder and three future climates (2010-2040, 2040-2070, and 2070-2100) with both base and upgraded binder, were analyzed for 30 years to estimate the effect of climate change on pavement infrastructure. The estimated pavement performance for both baseline and future climate were compared in terms of distress prediction. The distresses such as asphalt rutting, fatigue cracking, overall rutting and thermal cracking were compared. In addition, the International Roughness Index (IRI) was also predicted over 30 years of service life and compared.

4.5 Results and discussion

The annual average daily maximum and minimum temperatures were determined using climate change models. From the extracted data, it was noticed that the maximum and minimum temperatures were significantly increasing due to climate change. The climate change model predicts that the annual average daily maximum and minimum temperatures will increases drastically from 2040 to 2100 when compared to 1950 to 2040.

Average seven-day high and low pavement temperatures for all the ten models were estimated, and a boxplot of these temperatures is illustrated in Figure 4-2. The 7-day average pavement temperature data was statically tested for normality using Minitab and was found to be skewed data. Also, few outliers were noticed in the data, which confirms that the data was not normally distributed. It was confirmed also from the quartile distribution in the boxplot presented in Figure 4-2. Therefore, median of high pavement temperature might be a better representation compared the mean. However, both mean and median of high pavement temperatures are suggesting the same asphalt binder grade. On the other hand, in the case of low pavement temperature, the data were normally distributed. Therefore, the means of all the ten models were computed to estimate the asphalt binder grade. Using the calculated means of 7-day average high pavement temperature and the low pavement temperature, the binder grades were assigned for baseline (1980-2010) and future (2010-2040, 2040-2070, and 2070-2100) climate data, as illustrated in Table 4-2.

These sixteen sections were analyzed using AASHTOWare for four different periods with both base and upgraded binder. The four different periods consist of one baseline climate (1980-2010) and three future climates (2010-2040, 2040-2070 and 2070-2100). The pavement performance parameters such as IRI, total rutting, Asphalt Concrete (AC) only rutting, base and subgrade rutting, and bottom-up fatigue cracking were predicted for the thirty-year time periods. The target limits for the distresses considered in this design were as follows: Terminal IRI (m/km) - 172.00, Permanent deformation for total pavement (Total rutting, mm) - 0.75, AC bottom-up fatigue cracking (BU fatigue cracking, % lane area) – 25, AC top-down fatigue cracking (TD fatigue cracking, m/km) – 2000, Permanent deformation for AC only (AC rutting, mm) – 0.25. These were targeted with a reliability of 90%.

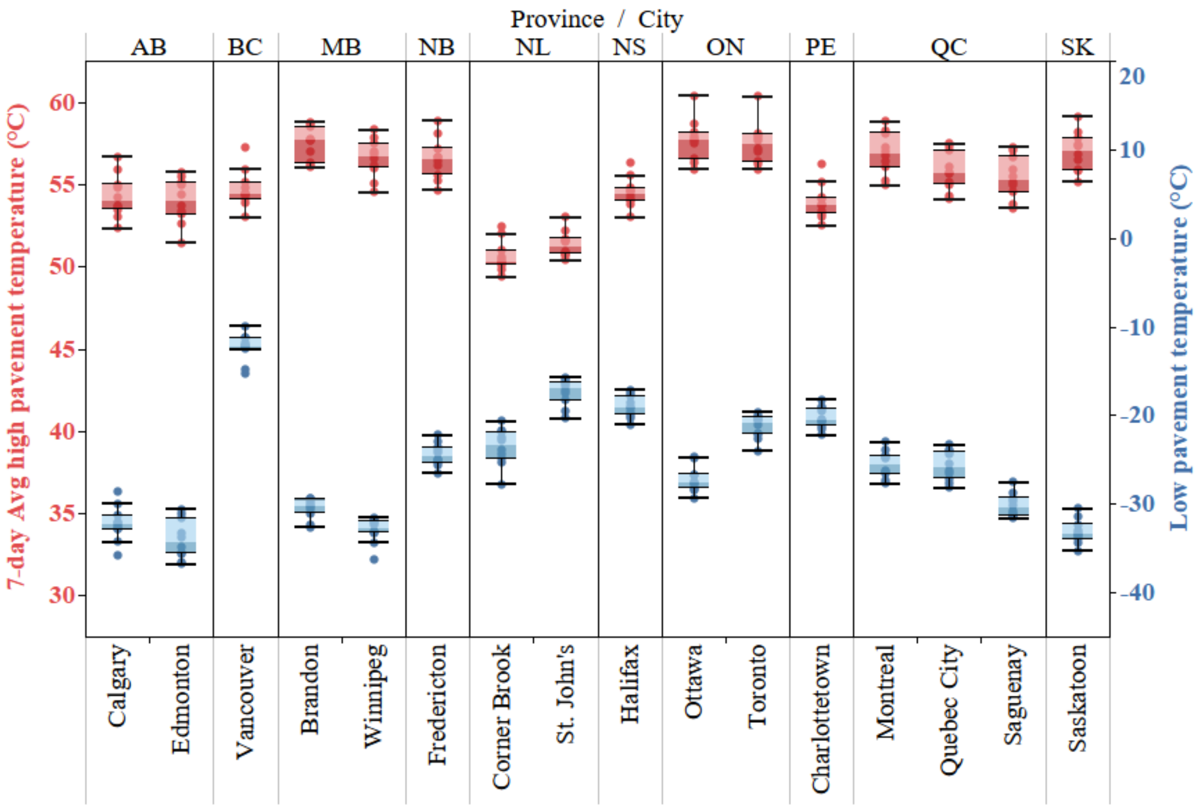

Figure 4-2: Boxplot for seven-day average high and low pavement temperatures for Canadian cities

From our analysis, it was found that most cities need a change in binder grade to adapt to the future climate. A further change in the binder, especially bumping up of high temperature, may be needed based on the traffic volume and speed characteristics of the pavement project.

All the locations selected in this study were divided into three categories based on a change in binder grade with respect to the base binder. The first category is with no change in binder grade for future climate, the second category is of locations with one high-temperature binder grade increment, and the last category is with two high-temperature binder grade increments. These categories are highlighted in Table 4-2. Only three locations does not need any change in binder grade for future climate. All other cities except Saskatoon and Brandon need one binder grade increment to adapt to future climate. Only Saskatoon and Brandon need two binder grade increments. The three locations which do not need any binder upgrade are Quebec City, Saguenay, and Corner Brook, falling under Category I. Therefore, these locations were ignored for the performance evaluation with an upgraded binder.

For the category II and III locations, the performance was evaluated for all periods and all the climate models. To date, there are hundreds of downscaled climate change models available. However, there is no specific climate change model, which can correctly simulate the future climate. Therefore, many recent studies suggested considering a group of models and the mean results of those models as a better representation (Gudipudi et al., 2017). An example is shown in Figure 4-3, a variation in AC rutting of the Vancouver section for all climate change models. From the results, it was found that the performance was different for all the climate change models. Here, the percentage change in the lowest and highest AC rutting due to the climate change models is approximately 25%. This variation explains that the climate change model selection plays a crucial role in quantifying climate change impact. Therefore, in this study, the mean of all the ten climate models was computed to witness the impact of climate change and the influence of change in asphalt binder grade on pavement performance. The change in pavement parameters sure to changing climate is illustrated in Figure 4-4.

Table 4-2: Asphalt binder grade determined for the baseline and future climatic conditions

Province	City	LTPP Section	Base Binder	Upgraded Binder		
			1980-2010	2010-2040	2040-2070	2070-2100
BC	Vancouver**	BC 82-6006	PG 52-16	PG 58-16	PG 58-16	PG 58-10
AB	Calgary**	AB 81-8529	PG 52-40	PG 58-40	PG 58-34	PG 58-28
AB	Edmonton**	AB 81-1804	PG 52-46	PG 58-40	PG 58-40	PG 58-34
SK	Saskatoon***	SK 90-6410	PG 52-52	PG 58-40	PG 58-34	PG 64-34
MB	Brandon***	MB 83-6454	PG 52-46	PG 58-34	PG 58-34	PG 64-28
MB	Winnipeg**	MB 83-6450	PG 58-40	PG 58-40	PG 58-34	PG 64-28
ON	Toronto**	ON 87-1806	PG 58-28	PG 58-28	PG 58-22	PG 64-22
ON	Ottawa**	ON 87-0901	PG 58-34	PG 58-34	PG 58-28	PG 64-28
QC	Montreal**	QC 89-3001	PG 58-34	PG 58-34	PG 58-28	PG 64-22
QC	Quebec City*	QC 89-1125	PG 58-34	PG 58-28	PG 58-28	PG 58-22
QC	Saguenay*	QC 89-0902	PG 58-34	PG 58-34	PG 58-34	PG 58-28
NB	Fredericton**	NB 84-1684	PG 58-34	PG 58-28	PG 58-28	PG 64-22
PEI	Charlottetown**	PEI 88-1646	PG 52-34	PG 58-28	PG 58-22	PG 58-16
NS	Halifax**	NS 86-6802	PG 52-28	PG 58-22	PG 58-22	PG 58-16
NL	Corner Brook*	NL 85-1803	PG 52-28	PG 52-28	PG 52-28	PG 52-22
NL	St. John's**	NL-DTW	PG 52-28	PG 52-22	PG 52-22	PG 58-16

** - Category I, ** - Category II, and *** - Category III*

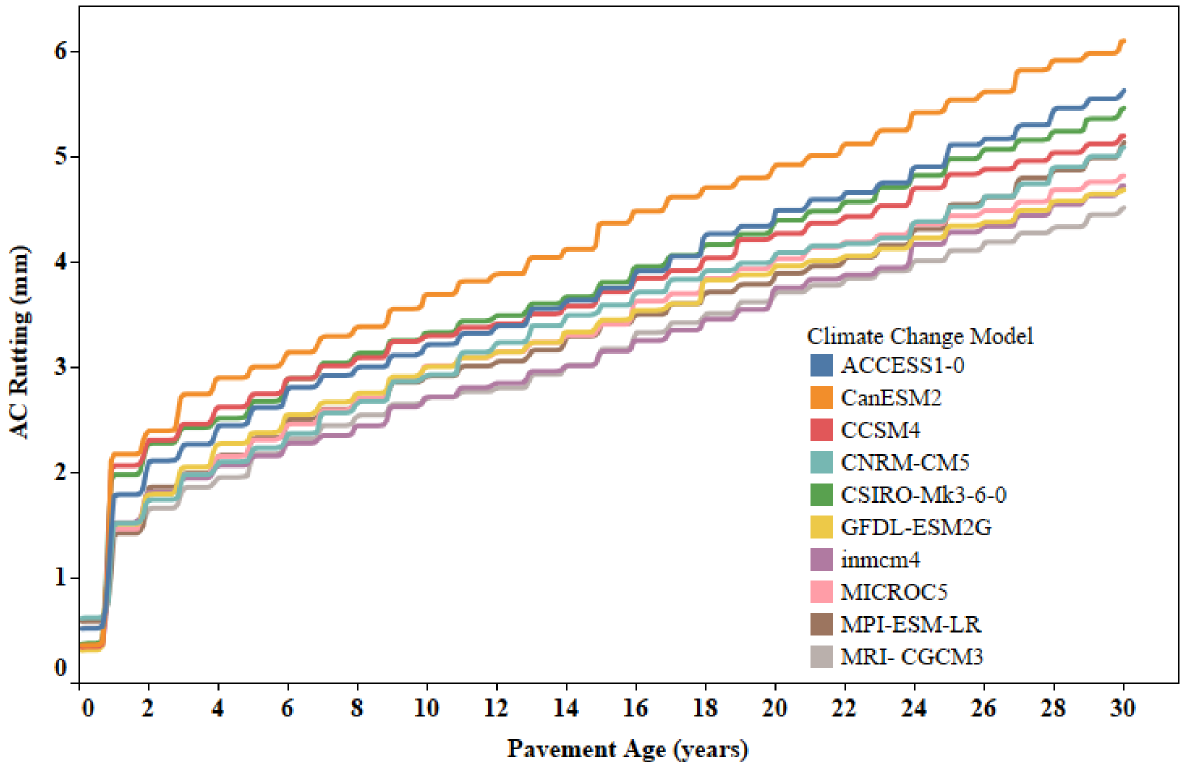

Figure 4-3: Performance (AC rutting) of Vancouver section for all climate change models (for the period of 2040-2070)

From Figure 4-4, several findings are extracted to determine the impact of climate change on pavement performance. The findings are as follows:

- IRI is slightly decreasing (< 2%) for 9 out of 16 sections. This might be occurring due to a reduction in freezing index or freeze and thaw cycles. In addition, there was about a 4.0% reduction in IRI for the Saskatoon section, which is mainly because of a substantial reduction in freezing index (900°C-days). For the remaining section, IRI is increasing due to an increase in all other distresses.

- Permanent deformation in subbase and subgrade is decreasing over 12 out of 16 locations, which might be occurring due to a reduction in freezing index or an increase in temperature. The increase in temperature might result in more evaporation of moisture in subbase, which leads to drier subbase and subgrade. However, as the Vancouver section is in high precipitation region, the subbase and subgrade rutting is increasing by about 10%.
- Asphalt concrete permanent deformation is increasing approximately by an average of 22.5% at all the locations, which is a resultant of increasing temperature.
- The total permanent deformation is also increasing for 11 out of 16 sections, where the AC rutting is leading compared to the base and subgrade rutting and vice versa. However, in Vancouver, both AC, subbase and subgrade rutting's are increasing, which results in a more considerable increase (~10%) in total rutting.
- AC bottom-up fatigue cracking is increasing by an average of 12% for all of the sections due to climate change except in Ottawa and Quebec City. For the Quebec City and Ottawa, the pavement design is overestimated concerning the traffic on those sections. Therefore, the reduction in freezing index and freeze and cycles results in less IRI, subbase and subgrade rutting and the AC BU fatigue cracking. Since the IRI and BU fatigue cracking are reducing, these sections don't need any further adaption due to climate change.

In addition, the impact of climate change on pavement performance with the base and upgraded binder is presented in Figure 4-5. The findings obtained from Figure 4-5 are as follows:

- With the change in asphalt binder grade, a permanent deformation in the AC layer is decreasing by 10% - 40%, which results in the extended service life of the pavement throughout Canada.

- Bottom-up fatigue cracking is also reducing over 10 out of 13 locations, with the upgrade in asphalt binder grade for the future climate. The reduction noticed in 6 out of 10 locations has less than a 10% decrease in fatigue cracking compared to the other three locations. However, the other four locations, BU fatigue cracking, reduces by about 20 – 60%. This reduces the porousness of rainfall water into the base layers, which results in less subbase and subgrade rutting.
- It was expected that the bottom-up fatigue cracking will increase with the use of stiffer binder. However, the bottom-up fatigue cracking is reducing with the use of stiff binders. This could be because of higher temperatures; the stiffer binder is no longer "stiff" at that temperature.
- Percentage change noticed in the subbase and subgrade permanent deformation is about 0.9 – 6.2%. However, there is no change over the Ontario province.
- As there is a decrease in all the distress, IRI is also reduced by about 2 – 8% for the future climate with the upgraded binder. However, for three locations (Brandon, Montreal and Saskatoon), the IRI is increasing by about 1 - 3%.
- From Figure 4-4, it was noticed that the IRI is reducing due to climate change. Besides, with the upgraded binder, the IRI is further reducing by 2 – 8%, which results in the extended service life of the pavement and reduced user cost.

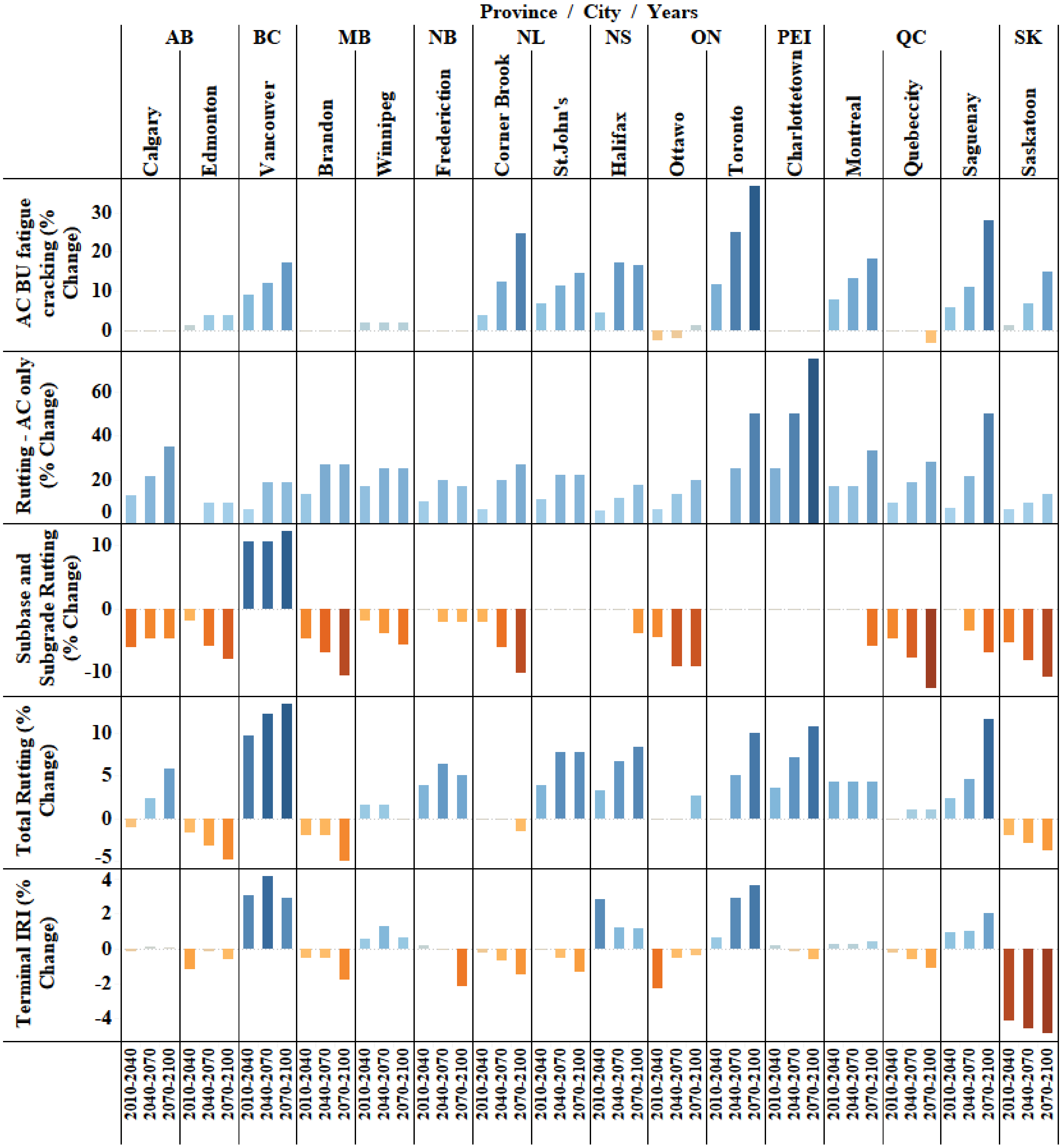

This plot represents the impact of climate change on pavement performance

The bars presented in this plot are the percentage change in performance parameters for future years with respect to baseline/historical climate. For example, in Calgary, the AC rutting is increasing by 13.04% for 2010-2040 when compared to 1980-2010. Similarly, the AC rutting is increasing by 21.74% and 34.78% for 2040-2070 and 2070-2100, respectively wrt. 1980-2010.

Figure 4-4: Change in performance parameters due to climate change compared to the baseline climate (1980-2010)

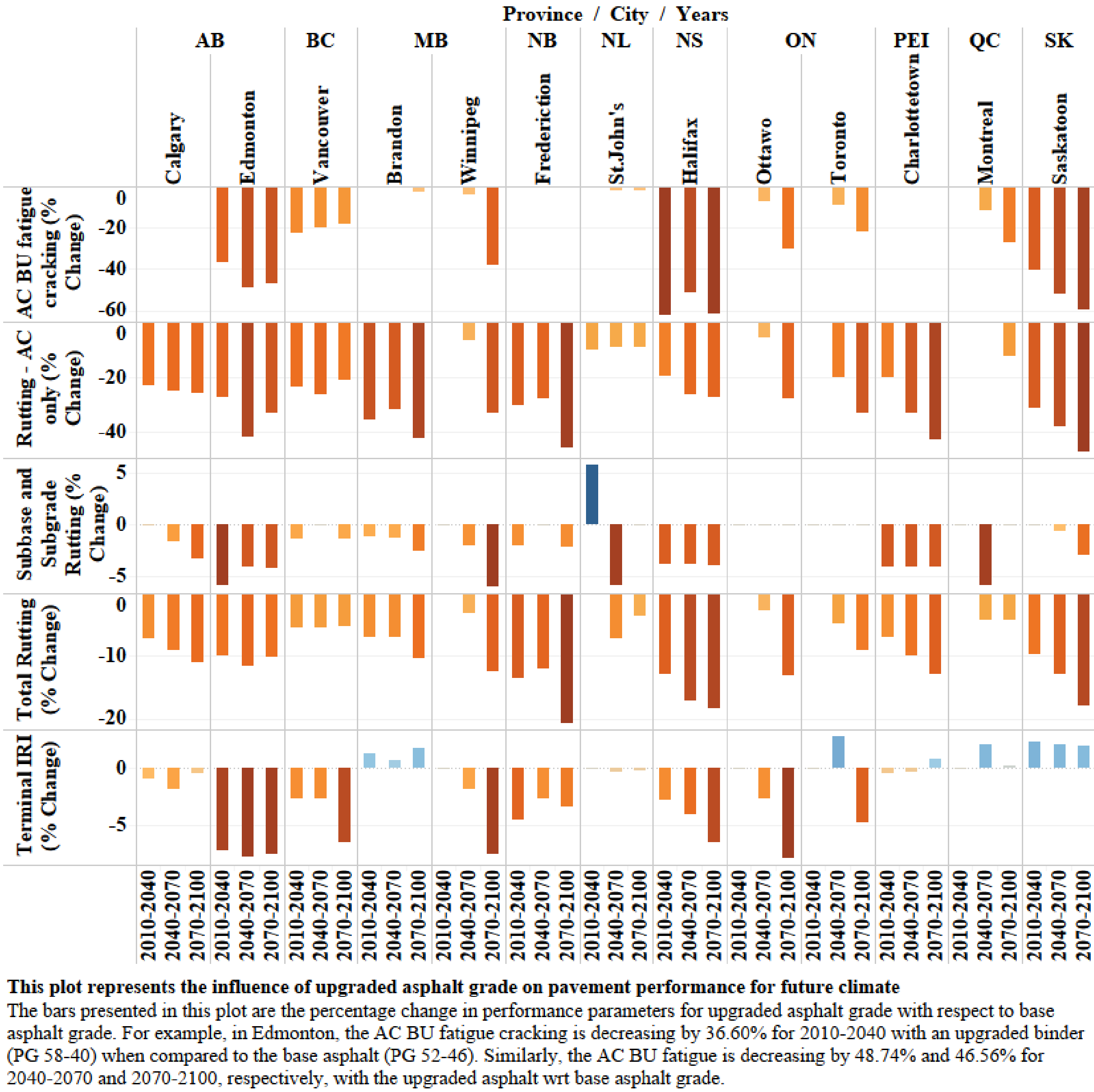

Figure 4-5: Percentage change in performance of Category II and III sections with upgraded asphalt grade compared to base asphalt grade.

4.6 Conclusion

In this study, the impact of climate change on pavement performance was quantified using ten different climate change models. Python codes were written and executed to extract the climate change data from the statistically downscaled climate models gathered from Pacific Canada. Using the extracted climate data, pavement temperatures were computed using the LTPP model and change in binder grade was determined for the future climatic conditions. In addition, the influence of this upgraded binder on pavement performance was estimated using AASHTOWare Pavement ME Design software and compared. This research resulted in drawing the following conclusions:

- All the locations, except Quebec City, Saguenay, and Corner Brook, need a change in binder grade to adapt to the future climate. All other cities, except Saskatoon and Brandon, need one binder grade increment to adapt to future climate. Only Saskatoon and Brandon need two binder grade increments.
- The pavement performance was susceptible to climate models. Therefore, the mean of all the ten climate models was utilized to witness the impact of climate change and the influence of change in asphalt binder grade on pavement performance.

Conclusions drawn from the impact of climate change on pavement performance are as follows:

- IRI is decreasing for 9 out of 13 sections and increasing for other sections. This decrease might be occurring due to a reduction in freezing index or freeze and thaw cycles.
- Permanent deformation in subbase and subgrade is decreasing in 12 out of 16 locations, which might be occurring due to a reduction in freezing index and an increase in temperature.
- Asphalt concrete permanent deformation is increasing at all the location, which might be a resultant of increasing temperature.
- The total permanent deformation is also increasing for 11 out of 16 locations. In these 11 sections, the increase in AC rutting is higher than the subbase and subgrade rutting.

- AC bottom-up fatigue cracking is increasing in all the pavement sections, except in the pavement sections located in Quebec City and St. John's, due to climate change.

Conclusions drawn from the influence of upgraded binder on pavement performance are as follows:

- With the upgrade of asphalt binder grade, a permanent deformation in the AC layer is significantly decreasing, which results in the extended service life of the pavement.
- The bottom-up fatigue cracking is also reduced due to change in asphalt binder grade for the future climate. This reduces the porousness of rainfall water into the base layers.
- There is no potential change in the subbase and subgrade permanent deformation in most of the pavement sections. However, there is an average of 2.2% reduction for other locations, which might be a result of the reduced BU fatigue cracking.
- There is a decrease in all the distress for the future climate with the upgraded binder.
- It was noticed that the IRI is reducing due to climate change. Besides, with the upgraded binder, the IRI is further reducing, which results in the extended service life of the pavement.
- Upgrading asphalt binder is a low cost and effective climate change adaptation strategy for Canadian pavements.

4.7 Pros/cons

Pros:

- Ten different climate change models were considered to quantify the influence of climate change on pavement performance.

- A bias-corrected statically downscaled models are utilized in this research to quantify the climate change impact on pavement performance.
- Different locations, different pavement structures, and various climatic regions were considered in this study.
- The influence of upgraded binder (considering climate change) on pavement performance or service life was discussed in the current study.

Cons:

- All the conclusions are drawn based on AASHTOWare analysis.
- The climate change models contain future climate data, which may be accurate or inaccurate, depending on the downscaling technique. Future data is not available to determine the reliability of these climate change models.
- Only one to two cities are considered from each of the province to determine the influence of upgraded binder on pavement performance.
- To determine the binder grade for future climate, LTPP pavement temperature prediction model is utilized to determine the 7-day average maximum pavement temperature and minimum temperature. Which may not be ideal case for the Canadian climate.
- AASHTOWare Pavement ME model local calibration factors are available only for 5 out of 13 locations. The performance predictions for remaining locations were computed using global calibration factors (not calibrating the models based on local materials and climate), which might affect the predicted results.

4.8 Reference

Belcher, S. E., Hacker, J. N., & Powell, D. S. (2005). Constructing design weather data for future climates. *Building Services Engineering Research and Technology*, *26*(1), 49–61. https://doi.org/10.1191/0143624405bt112oa

Chen, X., & Wang, H. (2020). Quantification of Warming Temperature Impact on Flexible Pavement Overlay Performance in New Jersey. *99th Annual Meeting of the Transportation Research Board (TRB) of National Academies of Science and Engineering, Washington DC*.

Dash, S. K., Jenamani, R. K., Kalsi, S. R., & Panda, S. K. (2007). Some evidence of climate change in twentieth-century India. *Climatic Change*, *85*(3–4), 299–321. https://doi.org/10.1007/s10584-007-9305-9

Dawson, A. (2014). *Anticipating and Responding to Pavement Performance as Climate Changes*. *December,* 4–5. https://doi.org/10.1007/978-3-662-44719-2

Delgadillo, R., Arteaga, L., Wahr, C., Alcafuz, R., Delgadillo, R., Arteaga, L., Wahr, C., & Alcafuz, R. (2018). The influence of climate change in Superpave binder selection for Chile. *Road Materials and Pavement Design, 0*(0), 1–16. https://doi.org/10.1080/14680629.2018.1509803

Elshaer, M., Ghayoomi, M., & Daniel, J. S. (2018). Bearing capacity analysis of pavement structures for short term flooding events. *Bearing Capacity of Roads, Railways and Airfields - Proceedings of the 10th International Conference on the Bearing Capacity of Roads, Railways and Airfields, BCRRA 2017*, *5*(October), 2127–2133. https://doi.org/10.1201/9781315100333-301

Evans, J. P. (2009). 21st century climate change in the Middle East. *Climatic Change*, *92*(3–4), 417–432. https://doi.org/10.1007/s10584-008-9438-5

Fletcher, C. G., Matthews, L., Andrey, J., & Saunders, A. (2016). Projected changes in mid-twenty-first-century extreme maximum pavement temperature in Canada. *Journal of Applied*

Meteorology and Climatology, *55*(4), 961–974. https://doi.org/10.1175/JAMC-D-15-0232.1

Fletcher, C. G., Matthews, L., Matthews, L., Andrey, J., & Saunders, A. (2016). *Projected changes in mid-21st century extreme maximum pavement temperature in Canada Projected changes in mid-21 st century extreme maximum pavement temperature in Canada*. *April*. https://doi.org/10.1175/JAMC-D-15-0232.1

Gasparrini, A., Guo, Y., Sera, F., Vicedo-Cabrera, A. M., Huber, V., Tong, S., de Sousa Zanotti Stagliorio Coelho, M., Nascimento Saldiva, P. H., Lavigne, E., Matus Correa, P., Valdes Ortega, N., Kan, H., Osorio, S., Kyselý, J., Urban, A., Jaakkola, J. J. K., Ryti, N. R. I., Pascal, M., Goodman, P. G., … Armstrong, B. (2017). Projections of temperature-related excess mortality under climate change scenarios. *The Lancet Planetary Health*, *1*(9), e360–e367. https://doi.org/10.1016/S2542-5196(17)30156-0

Gudipudi, P. P., Underwood, B. S., & Zalghout, A. (2017). Impact of climate change on pavement structural performance in the United States. *Transportation Research Part D: Transport and Environment*, *57*(October), 172–184. https://doi.org/10.1016/j.trd.2017.09.022

Gudmundsson, L., Bremnes, J. B., Haugen, J. E., & Engen-Skaugen, T. (2012). Technical Note: Downscaling RCM precipitation to the station scale using statistical transformations – A comparison of methods. *Hydrology and Earth System Sciences*, *16*(9), 3383–3390. https://doi.org/10.5194/hess-16-3383-2012

Hughes, L. (2003). Climate change and Australia: Trends, projections and impacts. *Austral Ecology*, *28*(4), 423–443. https://doi.org/10.1046/j.1442-9993.2003.01300.x

Jones, P. G., & Thornton, P. K. (2009). Croppers to livestock keepers: livelihood transitions to 2050 in Africa due to climate change. *Environmental Science and Policy*, *12*(4), 427–437. https://doi.org/10.1016/j.envsci.2008.08.006

Kharin, V., Zwiers, F., Zhang, X., & Gabriele, H. (2007). *Changes in Temperature and Precipitation Extremes in the IPCC Ensemble of Global*. 1419–1444. https://doi.org/10.1175/JCLI4066.1

Knott, J. F., Sias, J. E., Dave, E. V, & Jacobs, J. M. (2019). *Seasonal and Long-Term Changes to Pavement Life Caused by Rising Temperatures from Climate Change*. *2673*(6), 267–278. https://doi.org/10.1177/0361198119844249

Kumlai, S., Jitsangiam, P., & Pichayapan, P. (2016). The implications of increasing temperature due to climate change for asphalt concrete performance and pavement design. *KSCE Journal of Civil Engineering*, *21*(4), 1222–1234. https://doi.org/10.1007/s12205-016-1080-6

Li, Q. J., Mills, L., McNeil, S., & Attoh-Okine, N. O. (2013). Integrating potential climate change into the mechanistic–empirical based pavement design. *Canadian Journal of Civil Engineering*, *40*(12), 1173–1183. https://doi.org/10.1139/cjce-2012-0465

Lioubimtseva, E., & Henebry, G. M. (2009). Climate and environmental change in arid Central Asia: Impacts, vulnerability, and adaptations. *Journal of Arid Environments*, *73*(11), 963–977. https://doi.org/10.1016/j.jaridenv.2009.04.022

Mallick, R., Jacobs, J. M., Miller, B. J., Daniel, J. S., Mallick, R. B., Jacobs, J. M., Miller, B. J., & Daniel, J. S. (2016). *Understanding the impact of climate change on pavements with CMIP5 , system dynamics and simulation*. *8436*(January 2017). https://doi.org/10.1080/10298436.2016.1199880

Mallick, R., Radzicki, M., Daniel, J., & Jacobs, J. (2014). Use of System Dynamics to Understand Long- Term Impact of Climate Change on Pavement Performance and Maintenance Cost. *Transportation Research Record Journal of the Transportation Research Board*, *5*(December 2014). https://doi.org/10.3141/2455-01

Marengo, J. A., Chou, S. C., Kay, G., Alves, L. M., Pesquero, J. F., Soares, W. R., Santos, D. C., Lyra, A. A., Sueiro, G., Betts, R., Chagas, D. J., Gomes, J. L., Bustamante, J. F., & Tavares, P. (2012). Development of regional future climate change scenarios in South America using the Eta CPTEC/HadCM3 climate change projections: Climatology and regional analyses for the Amazon, São Francisco and the Paraná River basins. *Climate Dynamics*, *38*(9–10), 1829–1848. https://doi.org/10.1007/s00382-011-1155-5

Maurer, E. P., Hidalgo, H. G., Das, T., Dettinger, M. D., & Cayan, D. R. (2010). The utility of daily large-scale climate data in the assessment of climate change impacts on daily streamflow in California. *Hydrology and Earth System Sciences*, *14*(6), 1125–1138. https://doi.org/10.5194/hess-14-1125-2010

Meagher, W., Daniel, J. S., Jacobs, J., & Linder, E. (2012). *Method for Evaluating Implications of Climate Change for Design and Performance of Flexible Pavements*. *2305*, 111–120. https://doi.org/10.3141/2305-12

Meinshausen, M., Smith, S. J., Calvin, K., Daniel, J. S., Kainuma, M. L. T., Lamarque, J., Matsumoto, K., Montzka, S. A., Raper, S. C. B., Riahi, K., Thomson, A., Velders, G. J. M., & van Vuuren, D. P. P. (2011). The RCP greenhouse gas concentrations and their extensions from 1765 to 2300. *Climatic Change*, *109*(1), 213–241. https://doi.org/10.1007/s10584-011-0156-z

Meleux, F., Solmon, F., & Giorgi, F. (2007). Increase in summer European ozone amounts due to climate change. *Atmospheric Environment*, *41*(35), 7577–7587. https://doi.org/10.1016/j.atmosenv.2007.05.048

Mills, B., Tighe, S., Andrey, J., Smith, J., & Huen, K. (2009). Climate Change Implications for Flexible Pavement Design and Performance in Southern Canada. *Journal of Transportation*

Engineering, *135*(10), 773–782. https://doi.org/10.1061/(asce)0733-947x(2009)135:10(773)

Mills, B., Tighe, S., Huen, K., & Parm, S. (2006). *Climate Change and the Performance of Pavement Infrastructure in Southern Canada : Context and Case Study Climate change and the performance of pavement infrastructure in southern Canada : Context and case study*. *June*. https://doi.org/10.1109/EICCCC.2006.277185

Mohseni, A. (1998). *LTPP Seasonal Asphalt Concrete (AC) Pavement Temperature Models, FHWA-RD-97-103* (Vol. 7, Issue 2).

Mohseni, A. (2005). *LTPPBIND V3.1 A SUPERPAVE Binder Selection Program, Washington Pavement Systems LLC, Maiden, MD.*

Pacificclimate. (n.d.). *Statistically Downscaled Climate Scenarios*. Https://Www.Pacificclimate.Org/Data/Statistically-Downscaled-Climate-Scenarios.

Paquin, D., De Elía, R., & Frigon, A. (2014). Change in North American atmospheric conditions associated with deep convection and severe weather using CRCM4 climate projections. *Atmosphere - Ocean*, *52*(3), 175–190. https://doi.org/10.1080/07055900.2013.877868

Piras, M., Mascaro, G., Deidda, R., & Vivoni, E. R. (2015). Science of the Total Environment Impacts of climate change on precipitation and discharge extremes through the use of statistical downscaling approaches in a Mediterranean basin. *Science of the Total Environment*. https://doi.org/10.1016/j.scitotenv.2015.06.088

Qiao, Y., Casey, D. B., Kuna, K. K., Kelly, K., & Macgregor, I. D. (2016). *Climate Resilience of Flexible Pavement Highways : Assessment of Current Practice*. *July 2017*, 1–14.

Qiao, Y., Dawson, A., Parry, T., & Flintsch, G. (2013). Quantifying the effect of climate change on the deterioration of a flexible pavement. *Proceedings of the International Conferences on the Bearing Capacity of Roads, Railways and Airfields, June 2013*.

Qiao, Y., Dawson, A. R., Parry, T., & Flintsch, G. W. (2015). Evaluating the effects of climate change on road maintenance intervention strategies and Life-Cycle Costs. *Transportation Research Part D: Transport and Environment*, *41*(November 2015), 492–503. https://doi.org/10.1016/j.trd.2015.09.019

Qiao, Y., Flintsch, G., Dawson, A., & Parry, T. (2013). Examining Effects of Climatic Factors on Flexible Pavement Performance and Service Life. *Transportation Research Record: Journal of the Transportation Research Board*, *2349*(1), 100–107. https://doi.org/10.3141/2349-12

Rana, M., Swarna, S., & Hossain, K. (2020). Climate Change Impact on Pavement Performance in Newfoundland , Canada. *99th Annual Meeting of the Transportation Research Board (TRB) of National Academies of Science and Engineering, Washington DC, USA*.

Sailor, D. J. (2014). Risks of summertime extreme thermal conditions in buildings as a result of climate change and exacerbation of urban heat islands. *Building and Environment*, *78*, 81–88. https://doi.org/10.1016/j.buildenv.2014.04.012

Shao, Z., Jenkins, G., & Oh, E. (2017). Assessing the impacts of climate change on road infrastructure. *International Journal of GEOMATE*, *13*(38), 120–128.

SP-1. (1997). *Superpave: Performance Graded Asphalt Binder Specification and Testing. Asphalt Institute*.

Stoner, A. M. K., Daniel, J. S., Jacobs, J. M., Hayhoe, K., & Scott-fleming, I. (2019). *Quantifying the Impact of Climate Change on Flexible Pavement Performance and Lifetime in the United States*. https://doi.org/10.1177/0361198118821877

Taylor, K. E., Stouffer, R. J., & Meehl, G. A. (2012). An overview of CMIP5 and the experiment design. *Bulletin of the American Meteorological Society*, *93*(4), 485–498. https://doi.org/10.1175/BAMS-D-11-00094.1

Tighe, S., Mills, B., Tighe, S. L., Smith, J., Mills, B., & Andrey, J. (2008). *Evaluating Climate Change Impact on Low- Volume Roads in Southern Canada on Low-Volume Roads in Southern Canada*. *October 2015*. https://doi.org/10.3141/2053-02

Underwood, S. (2019). A method to select general circulation models for pavement performance evaluation A method to select general circulation models for pavement performance evaluation. *International Journal of Pavement Engineering*, *0*(0), 1–13. https://doi.org/10.1080/10298436.2019.1580365

Underwood, S., Guido, Z., Gudipudi, P., & Feinberg, Y. (2017). *Increased costs to US pavement infrastructure from future temperature rise Increased costs to US pavement infrastructure from future temperature rise*. *September*. https://doi.org/10.1038/nclimate3390

Valle, O., Qiao, Y., Dave, E., & Mo, W. (2017). Life cycle assessment of pavements under a changing climate. *Pavement Life-Cycle Assessment*, *October*, 241–250. https://doi.org/10.1201/9781315159324-25

Vincent, L. A., Zhang, X., Mekis, Wan, H., & Bush, E. J. (2018). Changes in Canada's Climate: Trends in Indices Based on Daily Temperature and Precipitation Data. *Atmosphere - Ocean*, *56*(5), 332–349. https://doi.org/10.1080/07055900.2018.1514579

Viola, F., & Celauro, C. (2015). Effect of climate change on asphalt binder selection for road construction in Italy. *Transportation Research Part D: Transport and Environment*, *37*, 40–47. https://doi.org/10.1016/j.trd.2015.04.012

Zhai, P., & Pan, X. (2003). Trends in temperature extremes during 1951-1999 in China. *Geophysical Research Letters*, *30*(17). https://doi.org/10.1029/2003GL018004

Chapter 5: Asphalt Binder Selection for Future Canadian Climatic Conditions Using Various Pavement Temperature Prediction Models

5.1 Abstract

Over the past twenty years, climate scientists have predicted that anthropogenic climate change would lead to an increase in global temperatures. In addition, the trends were predicted to further aggravate in the near future. Recent studies stated that this climate change has had a significant impact on pavement performance. As asphalt binder is susceptible to changes in temperature, it is necessary to understand the influence of climate change on asphalt binder grade selections. Therefore, the aim of this study is to estimate the new asphalt binder grades for Canada using the projected climate data. To achieve this, the study was organized in five phases. In the first phase, a total of ten statistically downscaled climate change models were accumulated from the Pacific Climate database. In the second phase, a python code was written and executed to extract the temperature data for the selected locations. Then, in the third phase, an average seven-day maximum pavement temperature and a minimum pavement temperature were determined using the three different pavement temperature prediction models: SHRP, LTPP, and EICM. Later in the fourth phase, the high-temperature grade (XX) and low temperature grade (YY) of an asphalt binder (PG XX – YY) were estimated using the average seven-day maximum and minimum pavement temperature respectively. Lastly, in the fifth phase, the asphalt binder grades are compared. This study presents a summary of revised asphalt binder grades for twenty-eight different locations across Canada.

5.2 Introduction

Canada is witnessing a rapid increase in annual average temperature since 1980. Scientists predict that these severities are in line with global changes in climate and occur due to increased concentrations of greenhouse gases in the atmosphere. In addition, climate scientists warned that the trends will further intensify in the near future. Also, several major studies have noticed a temperature rise due to climate change in Canada (Vincent et al., 2018), the United States (Paquin et al., 2014), South America (Marengo et al., 2012), Europe (Meleux et al., 2007), Africa (Jones & Thornton, 2009), the Middle East (Evans, 2009), China (Zhai & Pan, 2003), India (Dash et al., 2007), Southeast Asia (Gasparrini et al., 2017), Central Asia (Lioubimtseva & Henebry, 2009), and Australia (Hughes, 2003). This temperature rise may lead to a change in asphalt binder selection. If this change in asphalt binder grade is not considered in the account, this may increase pavement distresses and deterioration. Specifically, incorrect selection of high and low-temperature asphalt grades results in asphalt rutting and thermal cracking, respectively. Various studies predict that changing climates will result in accelerated pavement deterioration (Gudipudi et al., 2017; Qiao et al., 2019; Rana et al., 2020; Swarna et al., 2021). A recent study by Swarna et al. identified rising temperatures as a significant factor that affects the pavement performance in Canada (Swarna et al., 2021). In addition, it is also concluded that the upgrade in asphalt binder grade considering increased temperatures results in longer service life of pavement.

5.2.1 Change in asphalt binder selection

Mills et al. estimated the influence of climate change on asphalt binder grade selection for sixteen sections in Southern Canada using two different climate change scenarios from Coupled Global Climate Model 2 (CGCM2) and the Hadley Climate Model 3 (HadCM3) experiments. Author found that 6 out of 17 sections need an upgrade in both high and low temperature binder grade by 2050 (Mills et al., 2009). In Italy a similar study was conducted by Viola and Celauro to evaluate the change in asphalt binder for 71 different locations (Viola & Celauro, 2015). This study considered special interpolation to predict the air temperatures for 2033 using a historical temperature data (1984 - 2013). This study concluded that there was a significant increase in both high temperature and low temperature asphalt grade in Italian territory. However, it was also concluded that PG 64 - 22 can cover about 60% of the Italian territory. Also, PG 64 - 28 can cover about 10% of Italian territory, which might need a polymer modification to meet the Italian asphalt grade requirements (Viola & Celauro, 2015).

In Chile, a similar work was done to estimate the impact of climate change on asphalt Binder grade over 94 locations using MICRO 5 climate change model. In this study, boot low emission (RCP 2.6) and high emission scenarios (RCP 4.8) are considered (Delgadillo et al., 2018). The study reports a significant number of locations need a change in asphalt binder grade. Fletcher et al. also estimated the influence of climate change on high temperature binder grade selection in Canada. This study considers 10 different climate change models to determine the asphalt binder grade to reduce the uncertainty involved with climate change models. This study identified the change in high temperature asphalt binder grade for 9 out of 17 cities in Canada (Fletcher et al., 2016).

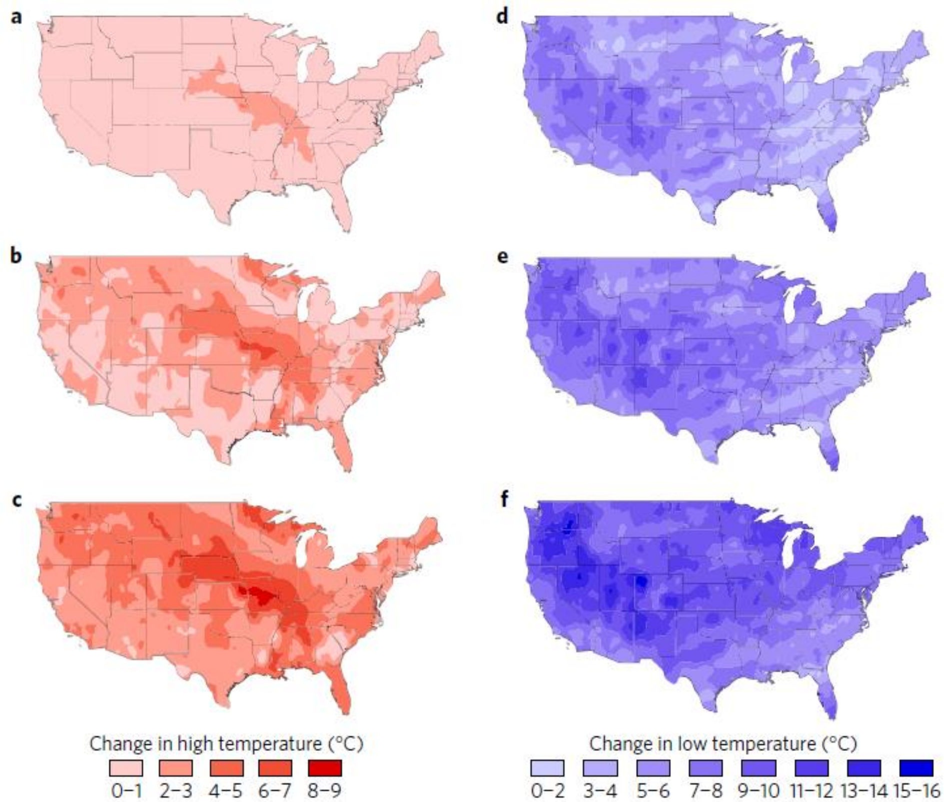

Figure 5-1: A contour map for increase in average seven-day maximum temperature for 2010–2039 (a), 2040–2069 (b) and 2070–2099 (c) and average minimum temperature changes for 2010–2039 (d), 2040–2069 (e) and 2070–2099 (f) with respect to a baseline period of 1966 – 1995. (Underwood et al., 2017)

In last five years, a study assessed the climate change influence on asphalt binder grade selection in the United States. The study identified that climate change will result in increased maintenance and rehabilitation cost (Underwood et al., 2017). This study illustrated a contour map to demonstrate the increase in average seven-day maximum temperature for 2010–2039 (a), 2040–2069 (b) and 2070–2099 (c) and average minimum temperature changes for 2010–2039 (d), 2040–2069 (e) and 2070–2099 (f) with respect to a baseline period of 1966 – 1995, as presented in Figure 5-1.

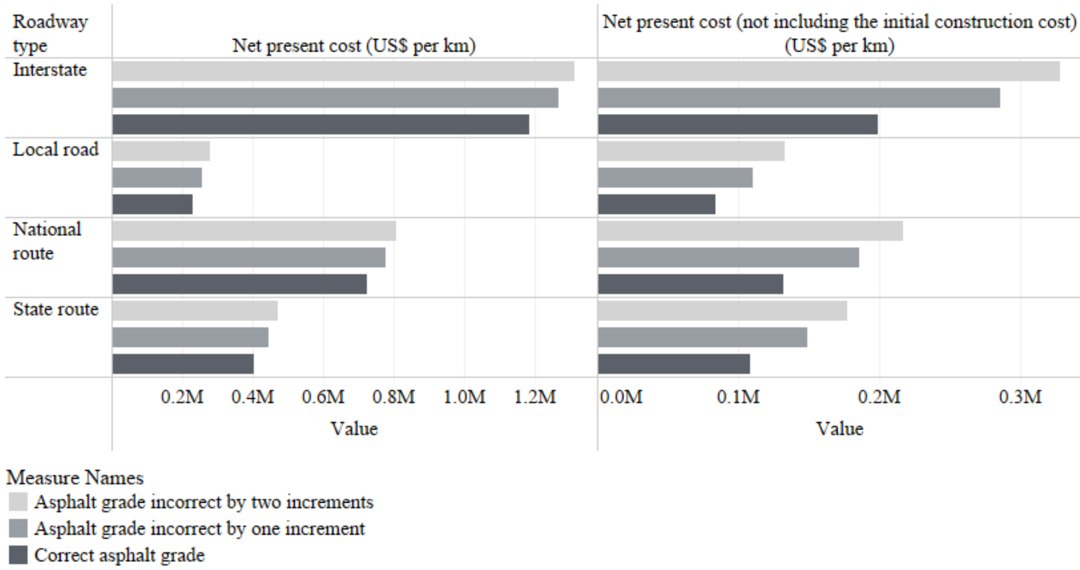

Figure 5-2: Economic costs of a flexible pavement with the use of correct and incorrect asphalt grade, (a) Net present cost not including the initial construction cost and (b) Net present cost including the initial construction cost (Underwood et al., 2017)

Recently, a study was done in the United States to determine the necessary upgrades for their asphalt binder grades because of climate change-related temperature increases. The study observed 799 locations, 35% of which were using incorrect asphalt binder grade for their temperatures (Underwood et al., 2017). Underwood et al. (2017) examined the impact of using incorrect asphalt binders on lifecycle costs of pavements across the United States as illustrated in Figure 5-2. Using incorrect binder, in 2040, results in a cost increase of US$19 billion for RCP4.5 and US$26.3 billion for RCP8.5 (Underwood et al., 2017). The significant increase in prices associated with the use of incorrect binder affirms the importance of the binder selection process and the consideration of future temperature rises to produce sustainable infrastructure.

Another study estimated the influence of climate change on binder grade selection in Canada using LTPP pavement temperature prediction model (Swarna et al., 2021). This study also estimated the influence of upgraded binder grade on the pavement performance for future climate. The predicted pavement distresses are significantly reducing with upgrade in asphalt binder grade, which leads to increase in service life of pavement (Swarna et al., 2021).

5.2.2 *Pavement temperature prediction models*

In 1990's, SHRP developed pavement temperature models using the yearly seven-day average maximum and the yearly one-day minimum temperature (Solaimanian & Bolzan, 1993). These pavement temperature models were developed only using several sites in United States. However, Robertson developed a C-SHRP low pavement temperature model using Canadian Data (Robertson, 1995).

(i) SHRP high pavement temperature prediction model for the surface

$$\mathrm{T_{surf}} = \mathrm{T_{air}} - 0.00618\ \mathrm{Lat}^2 + 0.2289\ \mathrm{Lat} + 24.4 \qquad \text{Equation 5-1}$$

Where,

T_{surf} = High AC pavement temperature at the surface, °C

T_{air} = High air temperature, °C

Lat = Latitude of the section, degrees.

(ii) SHRP high pavement temperature prediction model with a depth 'd'

$$\mathrm{T_d} = \mathrm{T_{surf}}(1 - 0.063\ \mathrm{d} + 0.007\ \mathrm{d}^2 - 0.0004\ \mathrm{d}^3) \qquad \text{Equation 5-2}$$

Where,

T_d = High AC pavement temperature at a depth 'd', °F

T_{surf} = High AC pavement temperature at the surface, °F

d = Pavement depth, inch

(iii) SHRP high pavement temperature prediction model for a depth of 20 mm

$$T_{pave} = (T_{air} - 0.00618\,Lat^2 + 0.2289\,Lat + 24.4)\,0.9545 - 17.78 \qquad \text{Equation 5-3}$$

Where,

T_{pave} = High AC pavement temperature at 20 mm below the surface, °C.

T_{air} = High air temperature, °C

Lat = Latitude of the section, degrees.

(iv) SHRP low pavement temperature prediction model with a depth ‘d’

$$T_d = T_{air} + 0.051\,d - 0.000063\,d^2 \qquad \text{Equation 5-4}$$

Where,

T_d = Low AC pavement temperature at a depth ‘d’, °C

T_{air} = High air temperature, °C

d = Pavement depth, mm

(v) C-SHRP Low Pavement Temperature Model with a depth ‘d’

$$T_{pave} = 0.859\,T_{air} + (0.002 - 0.0007\,T_{air})H + 0.17 \qquad \text{Equation 5-5}$$

Where,

T_{pave} = Low AC pavement temperature, °C.

T_{air} = High air temperature, °C

H = Pavement depth, mm

In the late 1990s, the LTPP Program used Seasonal Monitoring Program (SMP) data to develop a relationship between the air temperature and the pavement temperature, which resulted in the development of LTPP pavement temperature prediction model for selecting the Superpave asphalt binder grades (Mohseni, 1998, 2005). LTPP pavement temperature prediction models are developed based on both United States and Canadian data, the LTPP pavement temperature model can be used for estimating the pavement temperature in Canada. However, as the latitudes of sites considered in this study range between approximately 27 degrees (Texas) and approximately 52 degrees (Canada), this model may not be applicable for locations above 52 degrees latitude. The LTPP pavement temperature models for both high and low temperature are as follows:

$$T_{P\,max} = 54.32 + 0.78\ T_{air\,max} - 0.0025\,Lat^2 - 15.41\ log_{10}(H + 25) + z(9 + 0.61\sigma^2_{Tair\,max})^{0.5} \quad \text{Equation 5-6}$$

$$T_{P\,min} = -1.56 + 0.72\ T_{air\,min} - 0.004\,Lat^2 + 6.26\ log_{10}(H + 25) + z(4.4 + 0.52\ \sigma^2_{Tair\,min})^{0.5} \quad \text{Equation 5-7}$$

Where,

$T_{P\,max}$ = Average seven- consecutive-day high pavement temperature (°C)

$T_{air\,max}$ = Average seven-consecutive-day high air temperature (°C)

$\sigma_{air\,max}$ = Standard deviation of seven-day high pavement temperature (°C)

$T_{P\,min}$ = Low pavement temperature (°C)

$T_{air\,min}$ = Low air temperature (°C)

$\sigma_{air\,min}$ = Standard deviation of low pavement temperature (°C)

Lat = Latitude (in degrees)

H = Depth (mm)

Z = Standard normal distribution value (depends on reliability) = 2.055 for 98% reliability

In addition, a web-based LTPPBind online tool (LTPPBind, 2008) was developed to determine the suitable asphalt binder grade for a specific location. This tool considers two types of adjustments such as temperature adjustment and traffic adjustment. Temperature adjustment corresponds to depth of the layer, which can be used to determine the asphalt binder grade for the deeper layer. Traffic adjustment is based on design speed and traffic loadings in Equivalent Single Axle Loads (ESAL). However, this LTPPBind tool is not available for Canadian conditions.

In 2004, National Cooperative Highway Research Program (NCHRP) Project 1-37A (ARA Inc, 2004) introduced a Mechanistic Empirical Pavement Design Guide (MEPDG) for the design of new and rehabilitated pavement structures. MEPDG is capable of considering the temperature and moisture profile of the pavement structure using the Enhanced Integrated Climate Model (EICM). EICM considers a one-dimensional coupled heat and moisture flow program, which simulates the changes in temperature and moisture characteristics of pavement materials. EICM considers climate factors such as air temperature, precipitation, solar radiation, wind speed and humidity to determine the pavement temperature and moisture characteristics. EICM uses all the climate factors to determine the heat transfer between the pavement and the atmosphere (AASHTO, 2008). In addition, EICM is also capable of estimating the number of freeze and thaw cycles and its depth that pavement will experience in its service life.

EICM is developed based on three primary components, which includes (1) Climate Materials Structural (CMS) model developed by University of Illinois Urbana-Champaign (Dempsey et al., 1986). (2) frost-heave and settlement model (CRREL model) developed at the United States Army Cold Regions Research and Engineering Laboratory (Guymon et al., 1993), and (3) infiltration-drainage model (ID model) developed at the Texas A&M University Texas Transportation Institute (Lytton et al., 1993). The EICM is capable of predicting pavement temperature, resilient modulus adjustment factors, water content in base layers, pore water pressure, frost and thaw cycles, and frost heave throughout the pavement structure over the service life of pavement.

5.2.3 Summary of literature

All of these studies considered different climate change models, different locations and various pavement temperature prediction models. The common outcome of climate change studies reviewed is that climate change leads to an increase in temperature, which ultimately influences the asphalt binder grade selection.

The summary of the literature highlights the influence of future climate on binder grade selection. However, there are a few limitations and gaps in the existing literature:

- Most of the studies in this field used one or two climate change models to estimate the influence of climate change on asphalt binder grade selection. Considering only one or two climate change models could result in a high degree of uncertainty.
- Most of the studies and practical guidelines for asphalt binder specifications are based on either SHRP or LTPP pavement temperature prediction model for computing the pavement temperature throughout Canada. Considering these models for northern part of Canada and for Atlantic Provinces may not be accurate.
- No studies available for quantifying the climate change impact in the northern part of Canada.

5.3 Objective and scope

The key objective of this study is to estimate the changing asphalt binder grade for various geographic regions in Canada under the changed climate. To realize this objective, three different pavement temperature prediction models were utilized to estimate the pavement temperature from the air temperature. This study presents a summary of changes in asphalt binder grade for twenty-eight selected locations over Canada.

The scope of the study includes the extraction of daily maximum and minimum air temperature data from the ten climate models downloaded from the pacificclimate.org and estimates the pavement temperatures using three different models: SHRP, LTPP and EICM.

5.4 Locations and climate change models

A total of twenty-eight locations are selected throughout Canada. These locations are considered based on different climatic regions, geographical locations, and pavement structural designs. Also, to determine the influence of climate change on selection of asphalt binder grade, ten different climate change models are selected. These selected climate change models are developed by various institutions over the world as illustrated in the Table 5-1.

Table 5-1: Cliamte change models considered in the study

Developed Institution	Model Code
Centre National de Recherches Météorologiques	CNRM-CM5-r1
Canadian Centre for Climate Modeling and Analysis	CanESM2-r1
Commonwealth Scientific and Industrial Research Organization (CSIRO) and Bureau of Meteorology (BOM), Australia	ACCESS1-0-r1

Institute for Numerical Mathematics	Inmcm4-r1
Commonwealth Scientific and Industrial Research Organization in collaboration with Queensland Climate Change Centre of Excellence	CSIRO-Mk3-6-0-r1
National Centre for Atmospheric Research	CCSM4-r2
Japan Agency for Marine-Earth Science and Technology, Atmosphere and Ocean Research Institute, and National Institute for Environmental Studies	MIROC5-r3
Max Planck Institute for Meteorology	MPI-ESM-LR-r3
Meteorological Research Institute	MRI-CGCM3-r1
NOAA Geophysical Fluid Dynamics Laboratory	GFDL-ESM2G-r1

5.5 Methodology

The research was divided into five phases. In the first phase, ten different statistically downscaled climate change models were gathered from the Pacific Climate database. Then, in the second phase, a python code was written to extract the daily maximum and minimum air temperatures from the climate change models for the selected locations. In the third phase, from the extracted daily maximum and minimum temperature, average seven-day maximum pavement temperatures and minimum pavement temperatures were determined using three different pavement temperature prediction models. In the fourth phase, the high (XX) and low temperature grades (YY) of an asphalt binder (PG XX – YY) were estimated using the average seven-day high and low pavement temperature, respectively. Lastly, in the fifth phase, the asphalt binder grades were compared to select the optimum binder grade.

5.5.1 Phase 1: Gathering climate change models.

Pacific Climate Impacts Consortium (PCIC) is a Canadian climate database, which offers statistically downscaled climate scenarios at a grid resolution of 1/8th degrees (300 arc-seconds or approximately 10 km) for a period of 1950 – 2100. The variables included in this climate scenarios are the maximum and minimum daily temperatures. These data are available for three different Representative Concentration Pathways (RCPs) (Meinshausen et al., 2011) such as RCP 2.6, RCP 4.5 and RCP 8.5. These climate scenarios are a combination of historical data and the downscaled climate change models. These downscaled models were constructed using Canadian historical daily data and Global Climate Model (GCM) projections from the Coupled Model Intercomparison Project Phase 5 (Taylor et al., 2012). From all of the available climate models, ten climate models were selected based on data availability and methods of statistical downscaling.

Data from the GCM sources available in the pacific climate database were downscaled to a very fine resolution using two different statistical downscaling methods such as Bias-Correction Spatial Disaggregation (BCSD) and Bias Correction/Constructed Analogues with Quantile mapping reordering (BCCAQ). BCCAQ is a hybrid method that associations with both Bias Correction/Constructed Analogues (BCCA) (Maurer et al., 2010) and quantile mapping (QMAP) (Gudmundsson et al., 2012). In this study, models with BCCAQ statistical downscaling method were used. The RCP 8.5 scenario climate change models used in this study are downloaded from the Pacific Climate data (https://www.pacificclimate.org/data/statistically-downscaled-climate-scenarios).

5.5.2 Phase 2: Climate change data extraction

A python code is written and executed to extract the daily maximum and minimum air temperature from the ten different climate change models for the selected twenty-eight location.

As the downscaled model contains a square grid of 10 km x 10 km (1/12°) in size, it may not be possible to extract data for the precise location. Therefore, a short distance square method is used to select the nearest grid point. This method assumes that there is no temperature difference between the actual location and the nearest grid point. The python code writer extracted the daily maximum and minimum temperatures for the selected location.

5.5.3 Phase 3: Determining the average seven-day maximum and minimum pavement temperature

From the extracted daily maximum and minimum air temperatures, the average seven-day high and one-day low air temperatures are determined for three different time periods such as 2010-2040, 2040-2070, and 2070-2100. Later, average seven-day high and one-day low pavement temperatures are estimated for the considered time periods using three different pavement temperature prediction models. The pavement temperature prediction models considered in this study are the Strategic Highway Research Program (SHRP) Pavement temperature model, the LTPP pavement temperature model, and the Enhanced Integrated Climate Model (EICM) software.

These seven-day high pavement temperature and low pavement temperatures are estimated at a depth of 20 mm and 0 mm, respectively. Also, the reliability considered in this study for estimating pavement temperatures is 98%. In case of EICM, level 1 inputs of pavement design and materials data are used, which were taken from LTPP database. For Climate inputs, temperature and precipitation data were taken from climate change models. However, other factors such as wind speed, humidity and percent sunshine are kept constant for the specific location.

5.5.4 *Phase 4: Assigning asphalt binder grade*

From the estimated mean of average seven-day high and low pavement temperatures, the high temperature and low temperature grades are assigned. As per Asphalt Institute Superpave Performance Graded Asphalt Binder Specifications (SP-1), the Superpave grades were assigned in a 6°C increment format for both high temperatures and low temperatures (SP-1, 1997). For example (St. John's), if the average seven-day high pavement temperature is 51.12°C, then the high-temperature grade assigned is 52°C. Similarly, if the low pavement temperature is -23.87°C, then the low temperature grade assigned is -18°C. Therefore, the performance asphalt grade is PG 52 – 28. The asphalt binder grades were assigned for all the locations following the Asphalt Institute Superpave Performance Graded Asphalt Binder Specifications.

5.5.5 *Phase 5: Comparison between the pavement temperature models*

The pavement temperatures estimated using three different pavement temperature prediction models are compared, to understand the necessity and adaptability of a pavement temperature model for the Canadian climate. In addition, the asphalt binder grades assigned to the selected sites throughout Canada are also compared to determine the optimum asphalt binder grade to adopt for future climates.

5.6 Results and discussions

The annual average air temperatures projections for various climate change models in St. John's (east coast), Vancouver (west coast) and Ottawa (central Canada) were presented in Figure 5-3. From Figure 5-3, it is noted that the annual air temperatures are significantly increasing due to climate change. It is also observed that the climate change models predict that the annual average air temperatures will increase drastically between 2040 to 2100 when compared to 1950 to 2040. The annual average temperature patterns are found to more uncertain after 2040.

These climate change models are developed based on interaction between the atmosphere, the oceans, the land surface and the biosphere. Depending on the methodology of interaction and the downscaling techniques, different climate change models predict the climate change in different pattern. Considering one climate change model in a study may lead to high degree of uncertainty. Therefore, the average of projections from ten different climate change models are considered in this study to reduce the uncertainty in climate change.

Average cumulative seven-day high and low pavement temperatures for all the ten climate change models are estimated, and boxplots of estimated pavement temperatures were illustrated in Figure 5-4 and Figure 5-5. The pavement temperatures estimated using different climate change models are presented as points in the box plot. The difference between the pavement temperatures estimated for hottest and coldest model is about 2-3°C for 2010-2040 time period. However, for 2070-2100, the difference between the pavement temperatures estimated for hottest and coldest model is found to be 6-8°C. This explains the increase in climate model uncertainty over time. Low pavement temperature is also following the similar trend as the high pavement temperature. However, the difference between the pavement temperatures estimated for hottest and coldest model is less compared to the seven-day high pavement temperature for all the pavement sections.

From Figure 5-4 and Figure 5-5, it is also noticed that the pavement temperatures estimated using SHRP model are less compared to the pavement temperatures estimated using LTPP model and ECIM. This explains that the SHRP pavement temperature model underestimates the seven-day average high pavement temperature for Canadian climate. As the sites considered to develop the SHRP pavement temperature model are only from United States, the model may not be applicable for Canadian climates. In addition, it was also noticed that the range pavement temperatures estimated using LTPP model and EICM are approximately similar at most of the locations. However, for some of the locations, EICM pavement temperatures are estimated to be higher than both of the SHRP and LTPP models.

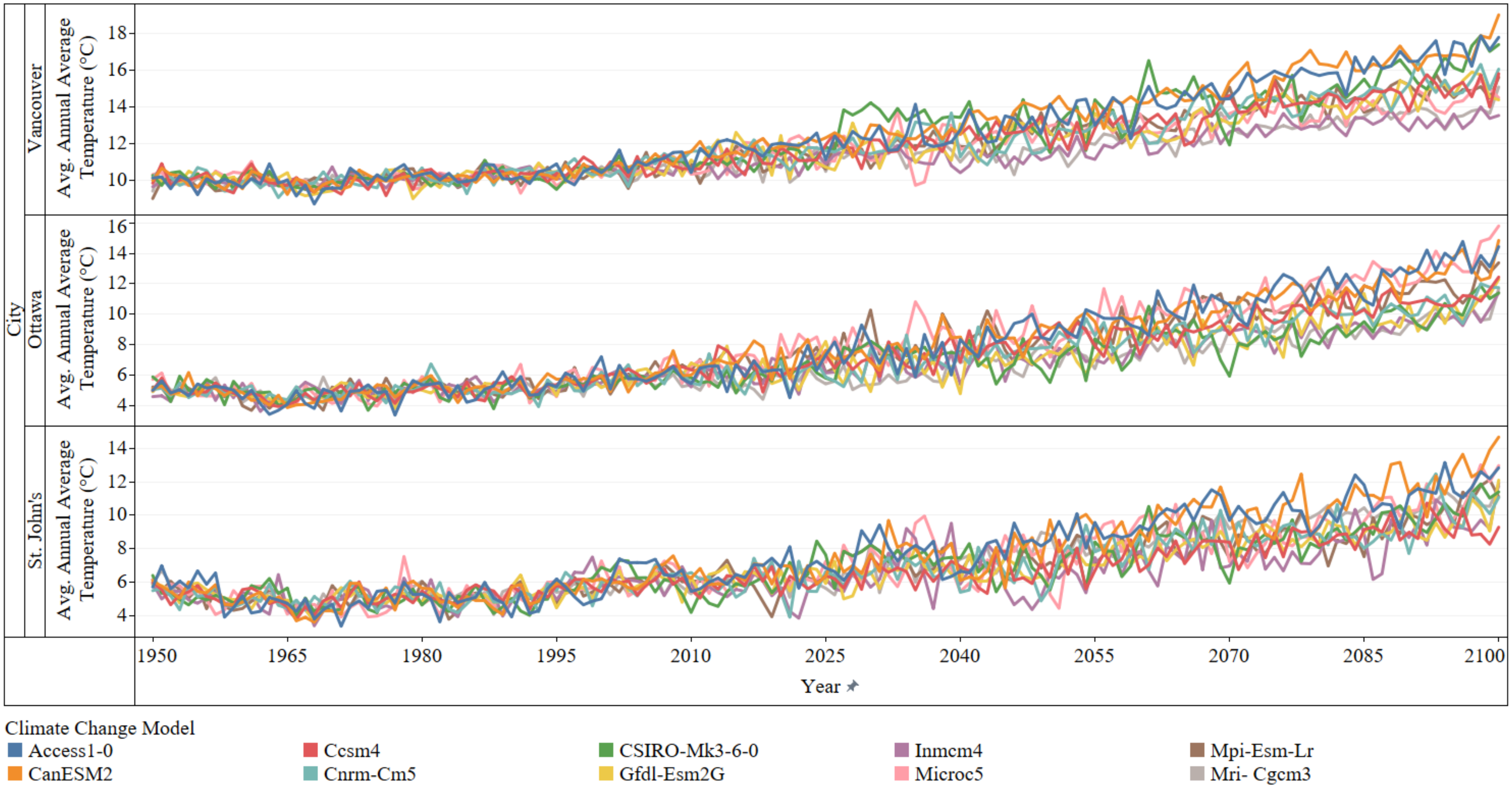

Figure 5-3: Annual average air temperature for different climate change models in St. John's, NL, Ottawa, ON and Vancouver, BC, Canada

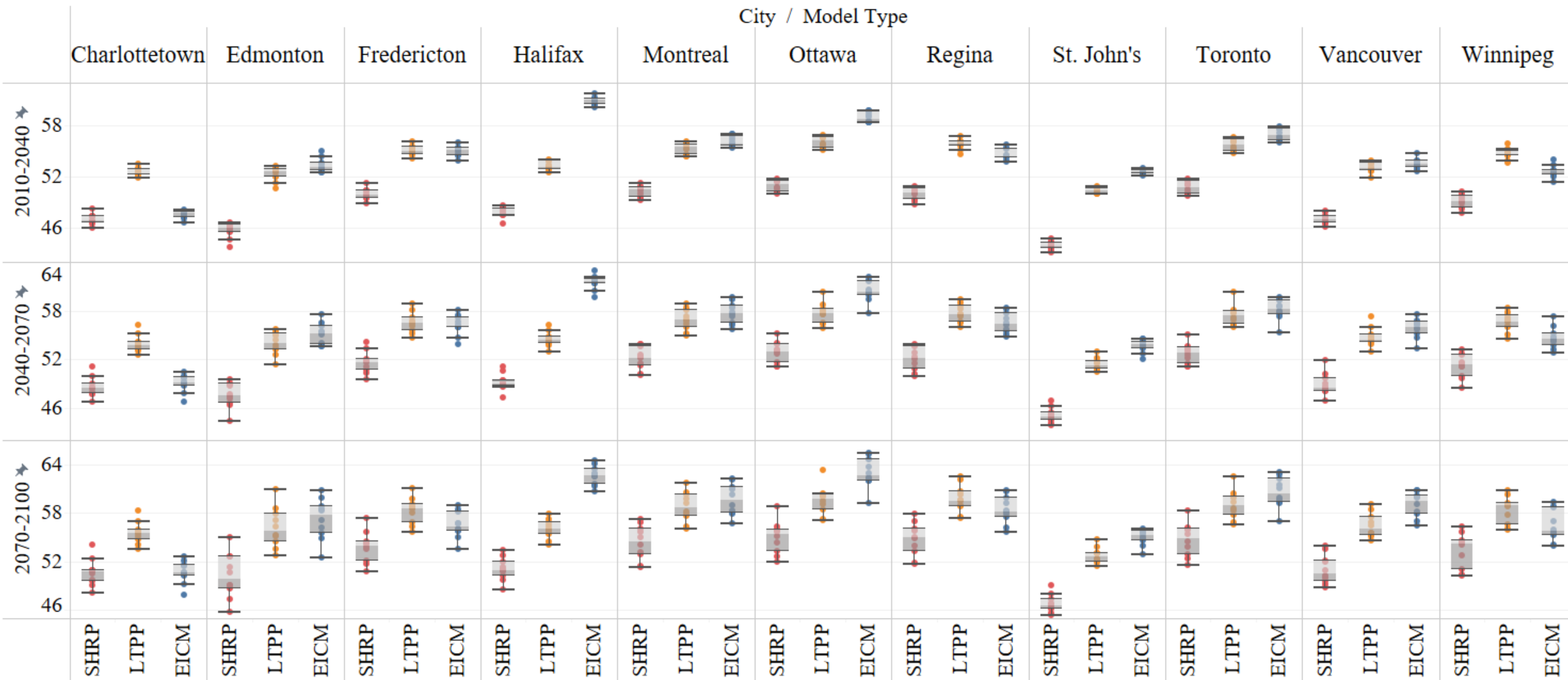

The plot represents the average seven-day high pavement temperature using different pavement temperature models and for different time periods
The box plots presented in this chart are darwn based on ten pavement temperature data points, which were estimated based on different climate change models. Also, the pavement temperature are ploted for differnet pavement temperature models and different time periods. For example, first three box plots at the top left under Charlottetown belong to a pavement section near to Charlottetown city and for 2010-2040 time period. In addition, first blox plot with red couloured data were computed using SHRP pavement temperature model. Similarly, orange coloured box plot is for LTPP and blue coloured box plot for EICM, respectively

Figure 5-4: Boxplots for average seven-day high pavement temperatures estimated using different pavement temperature prediction models

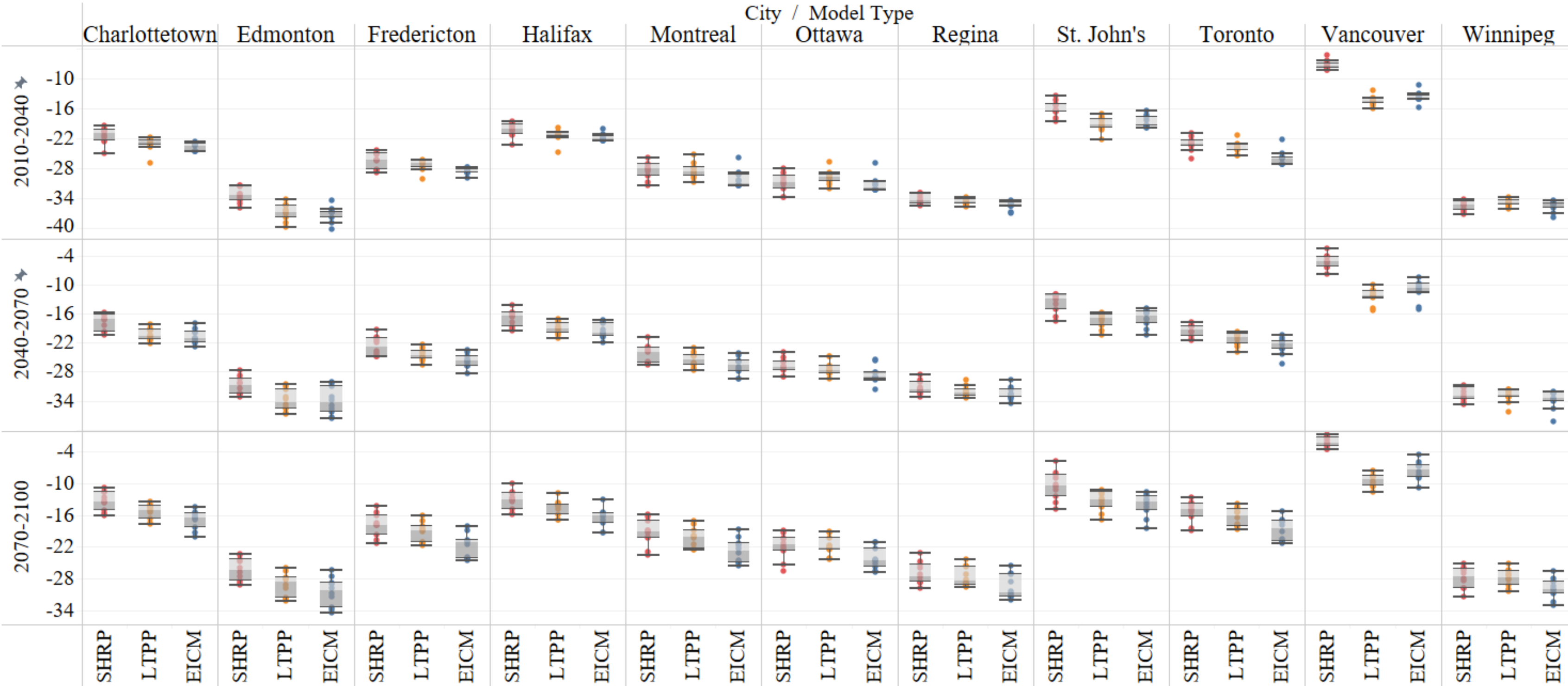

The plot represents the average low pavement temperature using different pavement temperature models and for different time periods
The box plots presented in this chart are darwn based on ten pavement temperature data points, which were estimated based on different climate change models. Also, the pavement temperature are ploted for different pavement temperature models and different time periods. For example, first three box plots at the top left under Charlottetown belong to a pavement section near to Charlottetown city and for 2010-2040 time period. In addition, first blox plot with red couloured data were computed using SHRP pavement temperature model. Similarly, orange coloured box plot is for LTPP and blue coloured box plot for EICM, respectively

Figure 5-5: Boxplots for low pavement temperatures estimated using different pavement temperature prediction models

The means of seven-day average high and low pavement temperatures for all climate changes are computed, to assign a binder grade. The means for 2040-2070 and various locations in Canada are presented in Figure 5-6. From Figure 5-6, it can be noted that the pavement temperatures estimated using the SHRP model are underestimated compared to pavement temperatures estimated using both LTPP model and EICM. On the other hand, the pavement temperatures estimated using LTPP model and EICM are approximately equal for most of the cities. However, for certain pavement sections, the pavement temperatures from EICM are much higher than the LTPP model.

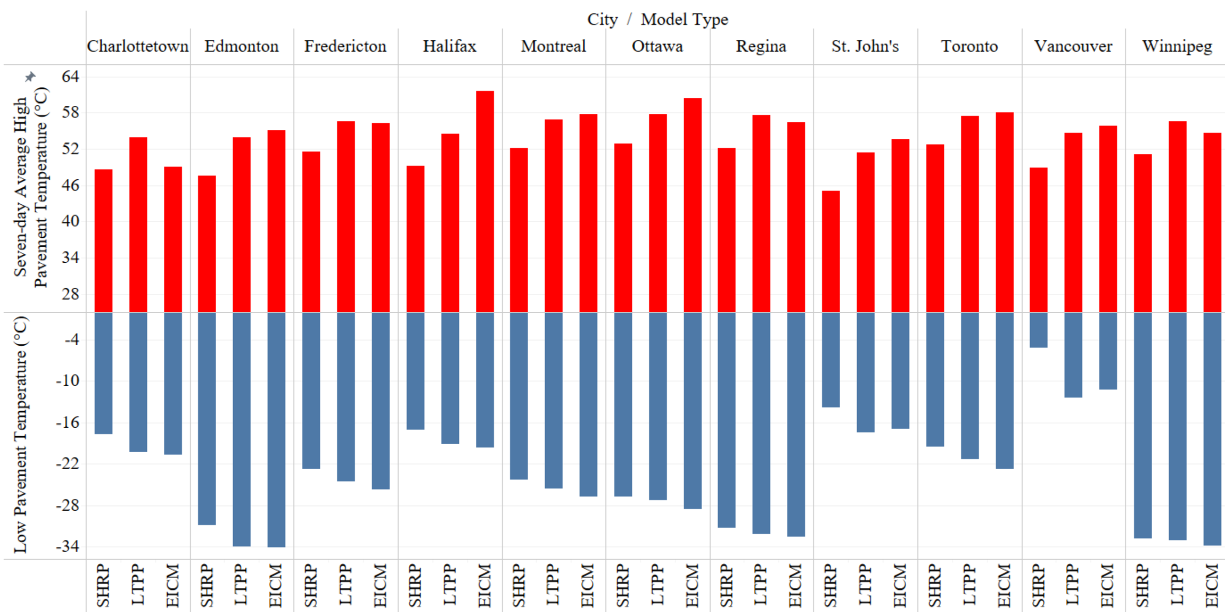

Figure 5-6: Means of seven-day average high and low pavement temperatures estimated using different pavement temperature prediction models for 2040–2070-time period

For the computed average cumulative seven-day high and low pavement temperatures, the asphalt binder grades are assigned following the Asphalt Institute Superpave Performance Graded Asphalt Binder Specifications. The predicted asphalt binder grades for future climate using the mean of pavement temperatures estimated for different climate change models are illustrated in Table 5-2.

From Table 5-2, it is noticed that most of locations requires a conventional binder grade produced from normal crude oil or high-quality crude oil. However, sites located in the northern part of Canada such as Prince George, Peace River, Prince Albert and Thompson expect a higher range binder grade (PG 58-40 and PG 64-34). As the difference between the high and low pavement temperature is greater than 90°C, a modification in the asphalt binder grade is needed for sites located in the northern part of Canada. It is also noticed that all the sites in Atlantic province need a conventional asphalt binder grade from ordinary crude oil, which is less expensive. Figure 5-7 presents the Superpave binder grades produced from various crude oils. The most expected binder grades for future climate from this study are highlighted in the Figure 5-7.

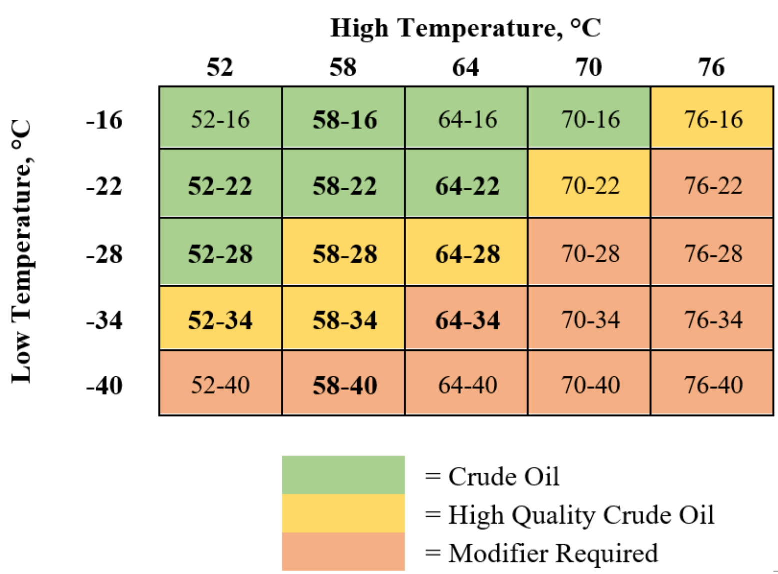

Figure 5-7: Superpave binder grades produced from various crude oil blends

From Table 5-2, it can also be noted that the predicted asphalt grades using different methods are found to be same for most of the locations. However, for some of the locations such as Calgary, Toronto, Ottawa, Halifax and St. John’s, the SHRP and LTPP pavement temperature models are under-estimating compared to the EICM. In addition, for some of the locations in Atlantic Provinces, the SHRP and LTPP pavement temperature models are over-estimating compared to the EICM.

Transport Canada and all provincial Department of Transportation and Works (DTWs) in Canada are relaying on SHRP and LTPP pavement temperature models for determining the asphalt binder grade. This may lead to selecting an incorrect asphalt binder grade in Canada, especially in the northern part of Canada. Therefore, it is necessary to develop a new robust pavement temperature prediction model for Canadian climate.

Table 5-2: Expected change in asphalt binder grade for 2040 – 2070

Province	City	Base Binder	Binder grade for 2010 - 2040			Binder grade for 2040 - 2070			Binder grade for 2070 - 2100		
			SHRP	LTPP	EICM	SHRP	LTPP	EICM	SHRP	LTPP	EICM
BC	Vancouver	PG 52-16	PG 58-16	PG 58-16	PG 58-16	PG 58-10	PG 58-16	PG 58-16	PG 58-10	PG 58-10	PG 64-10
BC	Prince George	PG 52-46	PG 52-40	PG 58-40	PG 58-40	PG 58-34	PG 58-40	PG 58-40	PG 58-34	PG 58-34	PG 58-34
BC	Kelowna	PG 58-28	PG 58-28	PG 58-28	PG 58-28	PG 64-22	PG 64-28	PG 58-28	PG 64-22	PG 64-22	PG 64-22
AB	Peace River	PG 52-58	PG 52-40	PG 52-40	PG 58-40	PG 58-40	PG 58-40	PG 58-40	PG 58-34	PG 58-34	PG 64-34
AB	Calgary	PG 52-40	PG 52-40	PG 58-40	PG 58-40	PG 58-34	PG 58-34	PG 64-34	PG 58-28	PG 58-28	PG 64-34
AB	Edmonton	PG 52-46	PG 52-40	PG 58-40	PG 58-40	PG 58-34	PG 58-34	PG 58-40	PG 58-34	PG 58-34	PG 58-34
SK	Saskatoon	PG 52-52	PG 58-40	PG 58-40	PG 58-40	PG 58-34	PG 58-34	PG 58-34	PG 64-34	PG 64-34	PG 64-34
SK	Prince Albert	PG 52-52	PG 58-40	PG 58-40	PG 58-40	PG 58-40	PG 58-40	PG 58-40	PG 58-34	PG 58-34	PG 64-34
SK	Regina	PG 52-52	PG 58-40	PG 58-40	PG 58-40	PG 58-34	PG 58-34	PG 58-34	PG 64-28	PG 64-28	PG 64-34
MB	Brandon	PG 52-46	PG 58-34	PG 58-34	PG 58-34	PG 58-34	PG 58-34	PG 58-34	PG 64-28	PG 64-28	PG 58-28
MB	Thompson	PG 52-52	PG 52-46	PG 52-46	PG 58-40	PG 58-40	PG 58-40	PG 58-40	PG 58-34	PG 58-34	PG 58-34
MB	Winnipeg	PG 58-40	PG 58-40	PG 58-40	PG 58-40	PG 58-34	PG 58-34	PG 58-34	PG 64-28	PG 64-28	PG 58-34
ON	Dryden	PG 52-46	PG 58-40	PG 58-40	PG 52-40	PG 58-34	PG 58-34	PG 58-34	PG 58-28	PG 58-28	PG 58-34
ON	Toronto	PG 58-28	PG 58-28	PG 58-28	PG 58-28	PG 58-22	PG 58-22	PG 64-28	PG 64-22	PG 64-22	PG 64-22

ON	Ottawa	PG 58-34	PG 58-34	PG 58-34	PG 64-34	PG 58-28	PG 58-28	PG 64-34	PG 64-22	PG 64-22	PG 64-28
QC	Montreal	PG 58-34	PG 58-34	PG 58-34	PG 58-34	PG 58-28	PG 58-28	PG 58-28	PG 64-22	PG 64-22	PG 64-28
QC	Quebec City	PG 58-34	PG 58-34	PG 58-34	PG 58-34	PG 58-28	PG 58-28	PG 58-28	PG 58-22	PG 58-22	PG 64-28
QC	Saguenay	PG 58-34	PG 58-34	PG 58-34	PG 52-34	PG 58-34	PG 58-34	PG 58-34	PG 58-28	PG 58-28	PG 58-28
NB	Fredericton	PG 58-34	PG 58-28	PG 58-28	PG 58-34	PG 58-28	PG 58-28	PG 58-28	PG 64-22	PG 64-22	PG 58-22
NB	Saint John	PG 52-40	PG 52-28	PG 58-28	PG 52-28	PG 58-22	PG 58-22	PG 52-22	PG 58-16	PG 58-16	PG 52-22
NB	Moncton	PG 52-40	PG 58-28	PG 58-28	PG 52-28	PG 58-22	PG 58-22	PG 52-22	PG 58-22	PG 58-22	PG 52-22
PEI	Charlottetown	PG 52-34	PG 52-28	PG 58-28	PG 52-28	PG 58-22	PG 58-22	PG 52-22	PG 58-16	PG 58-16	PG 52-22
NS	Halifax	PG 52-28	PG 58-22	PG 58-22	PG 64-22	PG 58-22	PG 58-22	PG 64-22	PG 58-16	PG 58-16	PG 64-22
NS	Truro	PG 52-40	PG 58-28	PG 58-28	PG 52-28	PG 58-22	PG 58-28	PG 52-28	PG 58-22	PG 58-22	PG 52-22
NS	Antigonish	PG 52-40	PG 58-28	PG 58-28	PG 52-28	PG 58-22	PG 58-22	PG 52-22	PG 58-16	PG 58-16	PG 52-22
NL	Corner Brook	PG 52-28	PG 52-28	PG 52-28	PG 52-28	PG 52-22	PG 52-28	PG 52-28	PG 58-22	PG 58-22	PG 52-22
NL	Grand Falls	PG 52-28	PG 58-28	PG 58-28	PG 52-28	PG 58-28	PG 58-28	PG 52-28	PG 58-22	PG 58-22	PG 58-22
NL	St. John's	PG 52-28	PG 52-22	PG 52-22	PG 58-22	PG 52-16	PG 52-22	PG 58-22	PG 58-16	PG 58-16	PG 58-16

Comparing with the base asphalt grade, it is noted that all the locations expect a change in asphalt binder grade either in the high temperature or low temperature grade for future climate. It is also found that at certain cold locations, the base asphalt grade itself need a modification to sustain at for more 90°C temperature range. However, as the temperatures are getting warmer with the climate change, the low pavement temperature are expected to increase. This could result in a conventional asphalt binder grade for those locations, which reduces the cost of construction.

Compared to the base binder grade computed for 1980-2010, the expected number of increments are determined for both high and low temperature grades and plotted in Figure 5-8 and Figure 5-9. From Figure 5-8, it can be noticed that the EICM suggests that the western and central provinces of Canada need an increment in high temperature asphalt grade for 2010-2040. However, SHRP procedures do not suggest any increment, and in the case of LTPP, there are mixed results. For 2040-2070, the three pavement temperature models suggest equal increments for all of the locations except seven locations. Out of these seven locations, six locations need an increment in case of EICM, where the LTPP and SHRP follows the same pattern. For the last time period (2070-2100), all the locations need an increment in a high temperature grade for all three cases. However, EICM exhibits two increments in most of the locations in British Columbia, Alberta and Saskatchewan. The other models only suggest two increments for Saskatchewan.

Similarly, in the case of low temperature grade from Figure 5-9, the three models suggest a similar result for all of the locations except two. These two locations are located in Northern Alberta and Northern Manitoba. For 2040-2070 and 2070-2100, all the three models present the same result at most of the locations. However, there were higher increments as per SHRP and LTPP where, EICM presents less increments. In 2070-2100, SHRP and LTPP results in a maximum of four increments, while EICM results in a maximum of three increments.

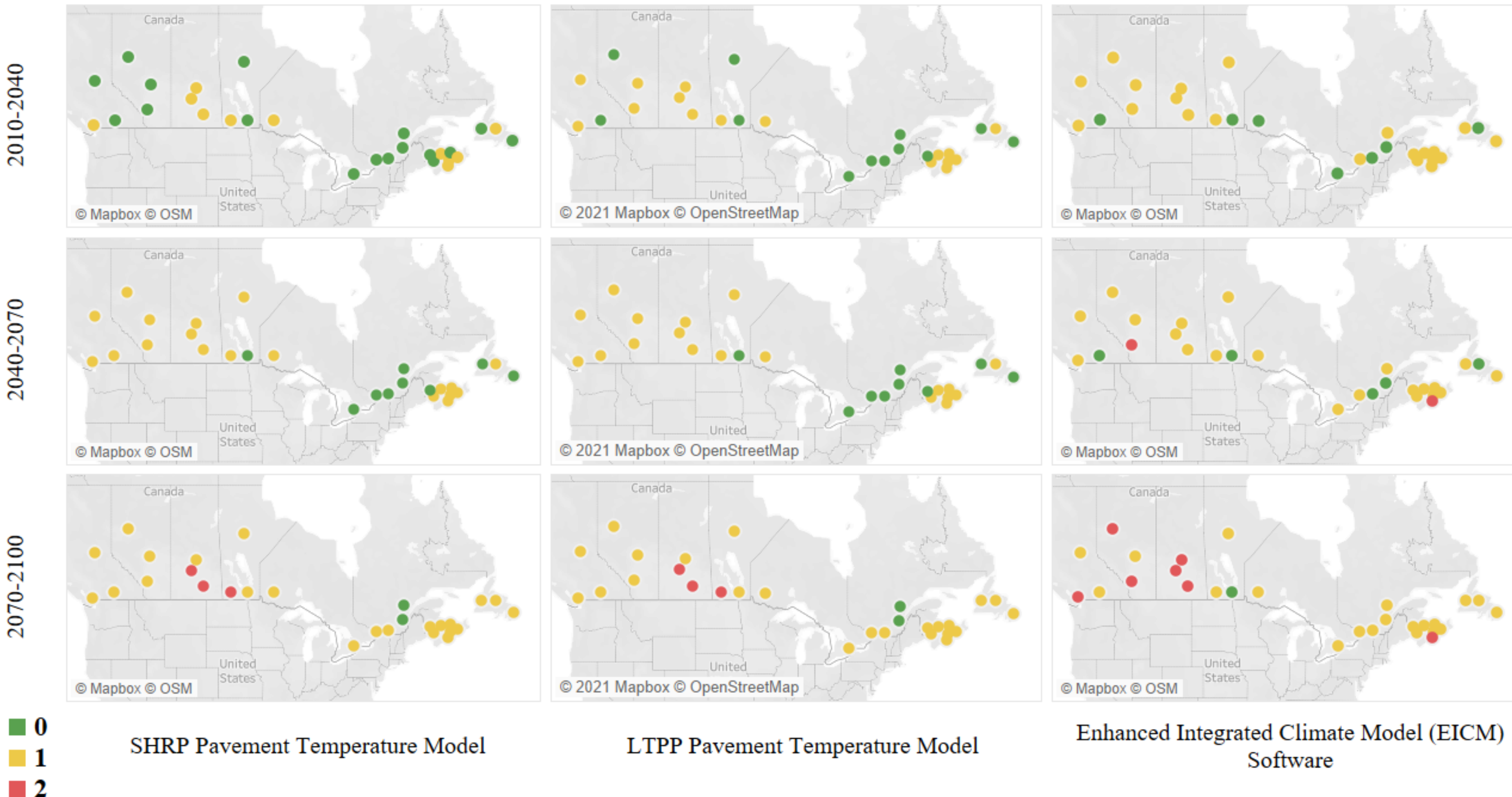

The plot represents the expected number of increments in high temperature grade
The points presented in this plot are the expected number of increments in high temperature grade for future climate compared to the baseline climate (1980-2010). For example, in the first plot (2010-2040 with SHRP Pavement temperature model), the blue colour points in the western part of Canada denotes no increment in hign temperature grade, the orange colour points in the south east part of canada denotes one increment in low temperature grade. One increment in high temperature grade represent increase of binder grade from PG 58-28 to PG 64-28.

Figure 5-8: Expected number of increments in high temperature grade for future years

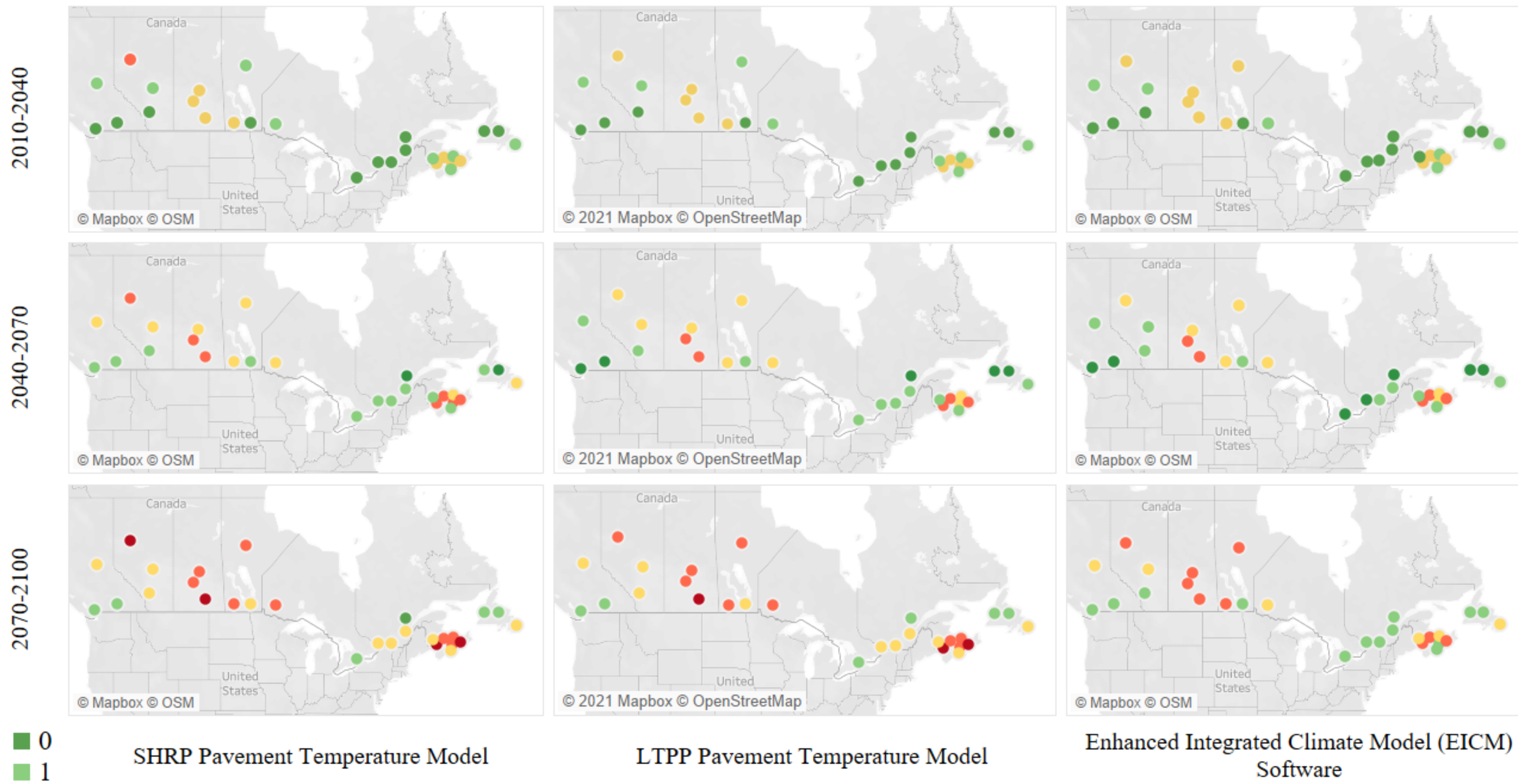

The plot represents the expected number of increments in low temperature grade

The points presented in this plot are the expected number of increments in low temperature grade for future climate compared to the baseline climate (1980-2010). For example, in the first plot (2010-2040 with SHRP Pavement temperature model), the blue colour points in the south west part of Canada denotes no increment in low temperature grade, the orange colour points in the south east part of canada denotes one increment in low temperature grade. One increment in low temperature grade represent increase of binder grade from PG 58-28 to PG 58-22.

Figure 5-9: Expected number of increments in low temperature grade for future years

5.7 Conclusions

This study presents an analysis to determine the change in asphalt binder grade over 28 different locations in Canada. This analysis aimed to understand the influence of climate change and pavement temperature prediction model on the asphalt binder grade selection process. This study considered an average of 10 different bias-corrected statistically downscaled climate change models to reduce the uncertainty involved with the climate change models. The pavement temperatures models considered in this study are: the SHRP pavement temperature model, the LTPP pavement temperature prediction model, and the EICM at 98% reliability. The outcomes from this study enable us to make following conclusions:

- The SHRP pavement temperature model is under-predicting the pavement temperatures when compared to LTPP and EICM models.
- Pavement temperatures estimated using LTPP model and EICM are approximately similar at most of the locations. However, for some of the locations, EICM pavement temperatures are estimated to be higher than both SHRP and LTPP models.
- Most of the location in Canada need a conventional asphalt binder grade. However, the northern part of Canada needs a modification in asphalt binder grade.
- By 2070, Canada needs about two increments in high temperature grade and four increments in low temperature grade as per SHRP and LTPP models. Meanwhile, EICM estimates a maximum of two and three increments for high and low temperatures respectively.
- Canada might need a new pavement temperature prediction model considering all geographic regions.

- Canadian future climate expects a change in asphalt binder grade either in the high temperature or low temperature grade. Therefore, it is necessary to consider future climate in finding out the asphalt binder grade.

5.8 Contributions and limitations

5.8.1 Contributions:

- Ten different climate change models were considered to estimate the influence of climate change on binder grid selection in Canada.
- A total of 28 locations were selected throughout Canada, which includes locations in northern part of Canada.
- Three different pavement temperature prediction models were considered to determine the future asphalt grade.

5.8.2 Limitations

- In case of EICM, only air temperature and precipitation data were taken from climate change models. the other climate factors such as wind speed, humidity and percent sunshine were kept constant.

5.9 Reference:

AASHTO. (2008). *Mechanistic-Empirical Pavement Design Guide: A Manual of Practice: Interim Edition. American Association of State Highway and Transportation Officials.*

ARA Inc. (2004). *Guide for Mechanistic-Empirical Design of New and Rehabilitated Pavement Structures, Final Report. NCHRP Project 1-37A. National Cooperative Highway Research Program. Transportation Research Board, National Research Council, Washington, DC.*

Dash, S. K., Jenamani, R. K., Kalsi, S. R., & Panda, S. K. (2007). Some evidence of climate change in twentieth-century India. *Climatic Change*, *85*(3–4), 299–321. https://doi.org/10.1007/s10584-007-9305-9

Delgadillo, R., Arteaga, L., Wahr, C., Alcafuz, R., Delgadillo, R., Arteaga, L., Wahr, C., & Alcafuz, R. (2018). The influence of climate change in Superpave binder selection for Chile. *Road Materials and Pavement Design*, *0*(0), 1–16. https://doi.org/10.1080/14680629.2018.1509803

Dempsey, B. J., Herlache, W. A., & Patel, A. J. (1986). Climatic-Materials-Structural Pavement Analysis Program. *Transportation Research Record*, *1095*, 111–123.

Evans, J. P. (2009). 21st century climate change in the Middle East. *Climatic Change*, *92*(3–4), 417–432. https://doi.org/10.1007/s10584-008-9438-5

Fletcher, C. G., Matthews, L., Andrey, J., & Saunders, A. (2016). Projected changes in mid-twenty-first-century extreme maximum pavement temperature in Canada. *Journal of Applied Meteorology and Climatology*, *55*(4), 961–974. https://doi.org/10.1175/JAMC-D-15-0232.1

Gasparrini, A., Guo, Y., Sera, F., Vicedo-Cabrera, A. M., Huber, V., Tong, S., de Sousa Zanotti Stagliorio Coelho, M., Nascimento Saldiva, P. H., Lavigne, E., Matus Correa, P., Valdes Ortega, N., Kan, H., Osorio, S., Kyselý, J., Urban, A., Jaakkola, J. J. K., Ryti, N. R. I., Pascal, M., Goodman, P. G., … Armstrong, B. (2017). Projections of temperature-related excess mortality under climate change scenarios. *The Lancet Planetary Health*, *1*(9), e360–e367. https://doi.org/10.1016/S2542-5196(17)30156-0

Gudipudi, P. P., Underwood, B. S., & Zalghout, A. (2017). Impact of climate change on pavement structural performance in the United States. *Transportation Research Part D: Transport and Environment*, *57*(October), 172–184. https://doi.org/10.1016/j.trd.2017.09.022

Gudmundsson, L., Bremnes, J. B., Haugen, J. E., & Engen-Skaugen, T. (2012). Technical Note:

Downscaling RCM precipitation to the station scale using statistical transformations – A comparison of methods. *Hydrology and Earth System Sciences*, *16*(9), 3383–3390. https://doi.org/10.5194/hess-16-3383-2012

Guymon, G. L., Berg, R. L., & Hromadka, T. V. (1993). *Mathematical Model of Frost Heave and Thaw Settlement in Pavements. CRREL Report 93-2.* (Issue April).

Hughes, L. (2003). Climate change and Australia: Trends, projections and impacts. *Austral Ecology*, *28*(4), 423–443. https://doi.org/10.1046/j.1442-9993.2003.01300.x

Jones, P. G., & Thornton, P. K. (2009). Croppers to livestock keepers: livelihood transitions to 2050 in Africa due to climate change. *Environmental Science and Policy*, *12*(4), 427–437. https://doi.org/10.1016/j.envsci.2008.08.006

Lioubimtseva, E., & Henebry, G. M. (2009). Climate and environmental change in arid Central Asia: Impacts, vulnerability, and adaptations. *Journal of Arid Environments*, *73*(11), 963–977. https://doi.org/10.1016/j.jaridenv.2009.04.022

Lytton, R. L., Pufahl, D. E., Michalak, C. H., Liang, H. S., & Dempsey., B. J. (1993). *An Integrated Model of the Climatic Effects on Pavements. FHWA-RD-90-033.*

Marengo, J. A., Chou, S. C., Kay, G., Alves, L. M., Pesquero, J. F., Soares, W. R., Santos, D. C., Lyra, A. A., Sueiro, G., Betts, R., Chagas, D. J., Gomes, J. L., Bustamante, J. F., & Tavares, P. (2012). Development of regional future climate change scenarios in South America using the Eta CPTEC/HadCM3 climate change projections: Climatology and regional analyses for the Amazon, São Francisco and the Paraná River basins. *Climate Dynamics*, *38*(9–10), 1829–1848. https://doi.org/10.1007/s00382-011-1155-5

Maurer, E. P., Hidalgo, H. G., Das, T., Dettinger, M. D., & Cayan, D. R. (2010). The utility of daily large-scale climate data in the assessment of climate change impacts on daily streamflow in California. *Hydrology and Earth System Sciences*, *14*(6), 1125–1138. https://doi.org/10.5194/hess-14-1125-2010

Meinshausen, M., Smith, S. J., Calvin, K., Daniel, J. S., Kainuma, M. L. T., Lamarque, J., Matsumoto, K., Montzka, S. A., Raper, S. C. B., Riahi, K., Thomson, A., Velders, G. J. M., & van Vuuren, D. P. P. (2011). The RCP greenhouse gas concentrations and their extensions from 1765 to 2300. *Climatic Change*, *109*(1), 213–241. https://doi.org/10.1007/s10584-011-0156-z

Meleux, F., Solmon, F., & Giorgi, F. (2007). Increase in summer European ozone amounts due to climate change. *Atmospheric Environment*, *41*(35), 7577–7587. https://doi.org/10.1016/j.atmosenv.2007.05.048

Mills, B., Tighe, S., Andrey, J., Smith, J., & Huen, K. (2009). Climate Change Implications for Flexible Pavement Design and Performance in Southern Canada. *Journal of Transportation Engineering*, *135*(10), 773–782. https://doi.org/10.1061/(asce)0733-947x(2009)135:10(773)

Mohseni, A. (1998). *LTPP Seasonal Asphalt Concrete (AC) Pavement Temperature Models, FHWA-RD-97-103* (Vol. 7, Issue 2).

Mohseni, A. (2005). *LTPPBIND V3.1 A SUPERPAVE Binder Selection Program, Washington Pavement Systems LLC, Maiden, MD.*

Paquin, D., De Elía, R., & Frigon, A. (2014). Change in North American atmospheric conditions associated with deep convection and severe weather using CRCM4 climate projections. *Atmosphere - Ocean*, *52*(3), 175–190. https://doi.org/10.1080/07055900.2013.877868

Qiao, Y., Santos, J., Stoner, A. M. K., & Flinstch, G. (2019). *Climate change impacts on asphalt road pavement construction and maintenance An economic life cycle assessment of adaptation measures in the State of*. *2005*(Ipcc 2014), 1–14.

https://doi.org/10.1111/jiec.12936

Rana, M., Swarna, S., & Hossain, K. (2020). Climate Change Impact on Pavement Performance in Newfoundland , Canada. *99th Annual Meeting of the Transportation Research Board (TRB) of National Academies of Science and Engineering, Washington DC, USA*.

Robertson, W. . (1995). Using the SHRP Specification to Select Asphalt Binders for LowTemperature Service (Unpublished). *14th Annual Canadian Technical Asphalt Association Conference, Charlottetown, PEI*.

Solaimanian, M., & Bolzan, P. (1993). Analysis of the I ntegrated Model of Climatic Effects on Pavements. In *SHRP-A-637*.

SP-1. (1997). *Superpave: Performance Graded Asphalt Binder Specification and Testing. Asphalt Institute*.

Swarna, S. T., Hossain, K., Pandya, H., & Mehta, Y. A. (2021). Assessing Climate Change Impact on Asphalt Binder Grade Selection and its Implications. *Transportation Research Record*. https://doi.org/https://doi.org/10.1177/03611981211013026

Taylor, K. E., Stouffer, R. J., & Meehl, G. A. (2012). An overview of CMIP5 and the experiment design. *Bulletin of the American Meteorological Society*, *93*(4), 485–498. https://doi.org/10.1175/BAMS-D-11-00094.1

Underwood, S., Guido, Z., Gudipudi, P., & Feinberg, Y. (2017). Increased costs to US pavement infrastructure from future temperature rise. *Nature Climate Change*, *7*(10), 704–707. https://doi.org/10.1038/nclimate3390

Vincent, L. A., Zhang, X., Mekis, Wan, H., & Bush, E. J. (2018). Changes in Canada’s Climate: Trends in Indices Based on Daily Temperature and Precipitation Data. *Atmosphere - Ocean*, *56*(5), 332–349. https://doi.org/10.1080/07055900.2018.1514579

Viola, F., & Celauro, C. (2015). Effect of climate change on asphalt binder selection for road construction in Italy. *Transportation Research Part D: Transport and Environment*, *37*, 40–47. https://doi.org/10.1016/j.trd.2015.04.012

Zhai, P., & Pan, X. (2003). Trends in temperature extremes during 1951-1999 in China. *Geophysical Research Letters*, *30*(17). https://doi.org/10.1029/2003GL018004

Chapter 6: Pavement Temperature Model for Canadian Asphalt Binder Selection: Introduction to the CPT Model

6.1 Abstract

The selection of a climate-appropriate asphalt binder is essential in ensuring the longevity of pavement surfaces. As the selection methodology depends on the pavement's temperature, several models predict pavement temperatures based on recorded ambient air temperatures and other related factors. A commonality between the most predominant pavement temperature models is the geographical limitations to their application. As a result, widely used models such as LTPP and SHRP do not return accurate values for more Northern temperatures, as observed in Canada. Thus, a new pavement temperature model has been developed for use across Canadian pavements. Canada has been geographically divided into three clusters with similar average annual air temperature, annual average precipitation, and freezing indexes to generate this new model. Independent pavement temperature equations have been developed to represent the locations found within each of the clusters by using a machine learning technique. Multiple linear regression models were generated using variables determined to be the most highly correlated. Across Canada, 9144 observation points were used for the model development, 10% of data was randomly separated for validation and from the remaining data, 80% of the data points were used to train the model and the remaining 20% were used to test the model. The resulting model returned satisfactory accuracy upon validation and represented a good alternative for Canadian pavement designers. Additionally, a software tool title CABS has been developed to select asphalt binders based on the predicted pavement temperatures to implement the model.

Keywords: Pavement temperature, Pavement temperature prediction models, Canadian climate, Asphalt binder.

6.2 Introduction

To promote longevity in asphalt pavements, it is necessary to consider the temperatures experienced throughout the pavement surface layer during the asphalt binder grade selection process (Chen et al., 2019). Although local ambient air temperature data is readily available for most geographical locations, it does not accurately represent the temperatures experienced by the pavement (Sreejith, 2021). Daily maximum pavement temperatures are known to significantly exceed the maximum air temperatures, which heavily impacts the selection of an asphalt binder (Bobes-Jesus et al., 2013; Herb et al., 2009). As a result, various pavement temperature prediction models are available to estimate temperatures throughout the surface layer (Chen et al., 2019). Existing pavement temperature models primarily belong to three categories: finite element models, analytical models, or statistical models (Adwan et al., 2021). However, the most predominant models used and accepted in the industry are geographically restrictive and do not accurately estimate temperatures for all locations, especially more Northern regions (Solaimanian & Bolzan, 1993). In Canada, there is a lack of appropriate pavement temperature models. Although some models have been developed for specific locations in the country, no model can be applied to its entirety.

6.2.1 Existing pavement temperature models, North America

A predominant pavement temperature model used primarily in the United States has been developed by the Strategic Highway Research Program (SHRP) (Solaimanian & Bolzan, 1993), (Mohseni, 1998). The low pavement temperature was taken as the low air temperature to produce an extremely conservative approximation. However, the high pavement temperature can be estimated using the developed model. Two forms of the model are presented, the first (Equation 6-1) being for surface temperature and the second (Equation 6-2) for a depth of 20 millimetres

(Mohseni, 1998).

$$T_{P\,max} = T_{air\,max} - 0.00618Lat^2 + 0.2289\,Lat + 24.4 \qquad \text{Equation 6-1}$$

$$T_{pav} = (T_{air\,max} - 0.00618Lat^2 + 0.2289\,Lat + 42.4)0.9545 - 17.78 \qquad \text{Equation 6-2}$$

Where,

$T_{P\,max}$ = High pavement temperature at surface (°C)

T_{pav} = High pavement temperature for a depth of 20 mm

$T_{air\,max}$ = Average seven-consecutive-day high air temperature (°C)

Lat = Latitude (in degrees)

In 1993, an analysis of the SHRP pavement temperature model was performed to determine the accuracy of the predicted temperatures (Solaimanian & Bolzan, 1993). Only one of the four test locations used to compare actual data with predicted data was in Canada. In the province of Saskatchewan, the test location showed a maximum pavement surface temperature underprediction of 2.8 °C and a maximum overprediction of 5.0 °C when using the SHRP model (Solaimanian & Kennedy, 1993). The other locations within the United States generally performed better than the Canadian location. Given the immensely varied nature of the climate in Saskatchewan, it can be assumed that these discrepancies will only be more significant as the test location moves further north (Solaimanian & Bolzan, 1993). This observation suggests that SHRP is unable to predict the pavement temperatures across all Canadian climatic conditions.

C-SHRP is a low pavement temperature model that was specifically developed using Canadian data. As the standard procedure of assuming the low air temperature is equivalent to the low pavement temperature was less accurate in Canada, a model was developed to fill the gap (Mohseni, 1998). To determine maximum pavement temperatures in Canada, the SHRP equation remains unchanged in this methodology. The equation is as follows.

$$T_{pav} = 0.859T_{air} + (0.002 - 0.0007T_{air})H + 0.17 \qquad \text{Equation 6-3}$$

Where,

T_{pav}= Low pavement temperature (°C)

T_{air} = Low air temperature (°C)

H = Depth, mm

A common alternative to the SHRP model is the Long-Term Pavement Performance (LTPP) pavement temperature model. LTPP relies on latitude to determine temperature and was developed under similar conditions as SHRP (Solaimanian & Bolzan, 1993). However, it considered pavement sections from latitudes of 27 degrees (Texas) to 52 degrees (Southern Canada) in its development. The data used to generate the LTPP model was from the Seasonal Monitoring Program (SMP) (Bosscher et al., 1998; Salem et al., 2004). The LTPP pavement temperature prediction models are presented below.

$$T_{P\,max} = 54.325432 + 0.78\ T_{air\,max} - 0.0025\,Lat^2 - 15.41\ log_{10}(H + 25) + z(9 + 0.61\sigma^2_{Tair\,max})^{0.5} \qquad \text{Equation 6-4}$$

$$T_{P\,min} = -1.56 + 0.72\ T_{air\,min} - 0.004\,Lat^2 + 6.26\ log_{10}(H + 25) - z(4.4\ + 0.52\ \sigma^2_{Tair\,min})^{0.5} \qquad \text{Equation 6-5}$$

Where,

$T_{P\,max}$ = Average seven-day high pavement temperature (°C)

$T_{air\,max}$ = Average seven-consecutive-day high air temperature (°C)

$\sigma_{air\,max}$ = Standard deviation of seven-day high pavement temperature (°C)

$T_{P\,min}$ = Low pavement temperature (°C)

$T_{air\ min}$ = Low air temperature (°C)

$\sigma_{air\ min}$ = Standard deviation of low pavement temperature (°C)

Lat = Latitude (in degrees)

H = Depth (mm)

Z = Standard normal distribution value (depends on reliability) = 2.055 for 98% reliability

Discrepancies have been identified between actual pavement temperatures and predicted pavement temperatures for locations in Northern Canada, resulting in selecting an incorrect asphalt binder (Solaimanian & Bolzan, 1993). LTPP and SHRP alike are known to underpredict maximum pavement temperatures and overpredict minimum pavement temperatures (Islam et al., 2015). This may be due to the limited environmental factors considered in the models (Milad et al., 2021).

In 2006, the University of Minnesota created a pavement temperature model using a one-dimensional finite difference approach. This approach allowed them to simulate temperature gradients within the pavement profile. The resulting model performed well in the summer months but performed slightly worse during winter temperatures (Herb et al., 2009). This effect would be exaggerated in a climate such as in Canada, where the freeze-thaw cycles are much more intense.

The Alaskan region presents similar challenges to pavement designers as is experienced in Canada. In their recent study, Raad et al. focused mainly on the minimum pavement temperature. The authors developed a minimum pavement temperature model based solely on air temperature and geographical region. Additionally, an equation was presented to apply to each of the three regions (Raad et al., 1998). The concept of addressing varied climates with a zoning approach proved effective in this study and may help develop pavement temperature models in Canada.

Maritime Zone:

$$T_{min} = 0.853T_{air} - 1.735 \qquad \text{Equation 6-6}$$

Transitional Zone

$$T_{min} = 0.779T_{air} - 3.129 \qquad \text{Equation 6-7}$$

Continental Zone:

$$T_{min} = 0.677T_{air} - 7.561 \qquad \text{Equation 6-8}$$

All Zones:

$$T_{min} = 0.809T_{air} - 3.150 \qquad \text{Equation 6-9}$$

Where,

T_{min} = Predicted minimum pavement temperature (°C)

T_{air} = Measured ambient air temperature (°C)

In 2006, Diefenderfer et al. developed a pavement temperature model for use in Virginia. The model was generated with data obtained from the Virginia Smart Road facility and was later verified using the LTPP model. The equations resulting from the study follow. Although proving satisfactory for the pavement temperatures within Virginia, the model is geographically limited in its applications (Diefenderfer et al., 2006).

$$T_{pmax} = 2.78752 + 0.6861T_{amax} + 5.6736 \times 10^{-4}R_S - 27.8739P_d \qquad \text{Equation 6-10}$$

$$T_{pmin} = -1.2097 + 0.6754T_{amin} + 3.7642 \times 10^{-4}R_S + 7.2.043P_d \qquad \text{Equation 6-11}$$

Where,

T_{pmax} = Predicted maximum pavement temperature (°C)

T_{pmin} = Predicted minimum pavement temperature (°C)

T_{amax} = Maximum daily air temperature (°C)

T_{amin} = Minimum daily air temperature (°C)

R_S = Calculated daily solar radiation (kJ/m^2)

P_d = Depth from the surface (m)

A viable alternative to these popular pavement temperature models generated in the United States is the Enhanced Integrated Climate Model (EICM), which has proved to predict Canadian trends more accurately (Zapata & Houston, 2008).

6.2.2 *Existing pavement temperature models outside of North America*

Outside of North America, some countries have developed their own pavement temperature models to determine the appropriate asphalt binder grade for their climatic conditions.

To address gaps in available models for the climate of India, Chandrappa and Biligiri developed a pavement temperature model. The authors collected maximum and minimum average monthly air temperatures and average monthly global radiation from seven climate stations. This study generated a model to predict average monthly minimum and maximum pavement temperatures (Chandrappa & Biligiri, 2016). Before this model, India struggled with pavement temperature models due to the lack of available data (Nivitha & Krishnan, 2014).

$$T_{psmax} = 0.14 \times DTRAD1 - 0.075 \times DTRAD2 + 2.241 \times log(e^{TAmax}) + 20.736 \times log(L_t) + 0.001 \times M^2 + 0.03 \times Y \qquad \text{Equation 6-12}$$

$$T_{psmin} = 0.003 \times (DTRAD1)^2 + 2.233 \times log\left(e^{TAmin}\right) - 157.421 \times \left(\frac{1}{L_t}\right) + 0.002 \times M^2 + 0.02 \times Y \qquad \text{Equation 6-13}$$

Where,

T_{psmax} = Average monthly maximum pavement temperature (°C)

T_{psmin} = Average monthly minimum pavement temperature (°C)

T_{Amax} = Average monthly maximum air temperature (°C)

T_{Amin} = Average monthly minimum air temperature (°C)

DTRAD1 = Sum of total daily radiation from 7:00 AM to 1:00 PM

DTRAD2 = Sum of total daily radiation from 2:00PM to 6:00 PM

L_t = Latitude

M = Month (January 1, February 2, etc.)

Y = Year

In 2005, Minhoto et al. developed a finite element model to determine pavement temperatures in Northeast Portugal. Using hourly solar radiation, temperature data, and average daily wind speed, the resulting model predicted pavement temperatures (Minhoto et al., 2005).

6.2.3 Existing pavement temperature models in Canada

A recent study attempted to generate a pavement temperature model for use in Edmonton, Alberta. Asefzadeh et al. generated a pavement temperature model that considered the unique weather extremes experienced in Canadian climates. Unlike other models, this one does not rely on latitude, given that it is solely used for one location in Canada. For this reason, it has few applications for use outside of Edmonton. Daily maximum and minimum pavement temperatures are computed with the following equations (Asefzadeh et al., 2017).

$$T_{daily-minimum} = -2.8704 + 0.8900 \times T_{air-min} + 1.26 \times 10^{-4} \times SR + 0.1759 \times (SR \times T^2{}_{air-min})^{0.25} + 15.2324 \times D$$ Equation 6-14

$$T_{daily-maximum} = 2.0237 + 0.8709 \times T_{air-max} + 7.6 \times 10^{-4} \times SR - 16.1886 \times D$$ Equation 6-15

Where,

$T_{daily-minimum}$= daily minimum HMA temperature (°C)

$T_{daily-maximum}$= daily maximum HMA temperature (°C)

$T_{air-min}$= daily minimum air temperature (°C)

$T_{air-max}$= daily maximum air temperature (°C)

SR = solar radiation (kJ/m^2)

D = depth (m).

Another recent study generated a low pavement temperature model based on pavement temperature data collected at the University of Waterloo. Two models were created, the first for hourly surface temperature and the second for daily average pavement temperature. The variables found to be of interest in this study were air temperature, wind speed and sunshine (Hosseini et al., 2015). The resulting hourly pavement surface equation follows.

$$T_P = -1.5008 + 0.2140T_A + 0.2646(T_{A2}) + 0.7471S + 0.0022W$$ Equation 6-16

Where,

T_P= Surface pavement temperature (°C)

T_A= Air temperature (°C)

T_{A2}= Previous hour air temperature (°C)

S = 1 if Sunny, 0 otherwise

W = Wind Speed (Km/h)

Similar to the work conducted in Edmonton, a pavement temperature model has been developed for Ottawa, Ontario. In 2011, Hassan et al. used air temperature, dew point, relative humidity, wind speed, wind gust, and wind direction to predict pavement temperatures. Several weather stations within the city were considered, and a model representing all of the locations was developed. The purpose was to aid the city in its winter maintenance regimes (Sherif & Hassan, 2004). Although this was achieved, this model does not function for locations outside of Ottawa and requires large amounts of data that may not always be available in other circumstances and locations. However, many of these factors have been found to influence the air temperature directly above pavements and should be considered in models when possible (Bogren et al., 2001).

A summary of some notable pavement temperature models is included in Table 6-1.

Table 6-1: Summary of Notable Pavement Temperature Models

Authors	Year	Location	Parameters	Type of model
SHRP (Solaimanian & Bolzan, 1993)	1993	USA	• Air temperature • Depth • Latitude	Quadratic model
LTPP (Mohseni, 1998)	1998	USA and Southern Canada	• Air temperature • Depth • Latitude • Reliability	Non-linear regression model
Liu and Yuan (Liu & Yuan, 2000)	2000	USA	• Air temperature • Pavement temperature • Depth • Time	Analytical model
Hermansson (A. Hermansson, 2000;	2004	Sweden	• Solar radiation • Air temperature	Simulation model

Å. Hermansson, 2004)			• Wind velocity	
Minhoto et al. (Minhoto et al., 2005)	2005	Northeast Portugal	• Solar radiation • Air temperature • Wind speed	Finite element model
Hassan et al. (Hassan et al., 2008)	2008	Oman	• Air temperature	Regression model
Matić et al. (Matić et al., 2014)	2012	Serbia	• Air temperature • Depth	Neural network
Hoseini et al. (Hosseini et al., 2015)	2015	Canada	• Air temperature • Sunshine • Wind velocity	Linear regression model
Mammeri et al. (Mammeri et al., 2015)	2015	France	• Air temperature • Depth • Solar radiation • Humidity	Finite element model
Ariawan et al. (Ariawan et al., 2015)	2015	Indonesia	• Air temperature • Humidity	Linear regression model
Chandrappa and Biligiri (Chandrappa & Biligiri, 2016)	2016	India	• Air temperature • Daily solar radiation • Latitude • Month	Linear regression model
Asefzadeh et al. (Asefzadeh et al., 2017)	2017	Canada	• Air temperature • Solar radiation	Regression model

6.2.4 Relevance of pavement temperature models

The consequence of inaccurate pavement temperature models is the increased risk of selecting an incorrect asphalt binder. It has recently been determined that the use of an incorrect asphalt binder will not only contribute to poor pavement performance but also result in increased costs. A recent study investigating 799 locations in the United States reported that 35% of these locations used an incorrect binder based on their local temperatures. It is estimated that by 2040, an incorrect binder will result in a cost increase of US$19 billion under Representative

Concentration Pathway (RCP) 4.5 and US$26.3 billion under RCP 8.5 (Underwood et al., 2017).

A new concern raised in the asphalt binder industry is not only the current selection of an appropriate binder but also this selection under future climate change situations. Permanent deformation in future pavements is expected to decrease by 10-40% when using an appropriately selected upgraded binder. The reduced frequency and severity of pavement distresses reduces the International Roughness Index (IRI) by 2-8% in future climates. Although the onset of climate change will decrease the IRI due to the reduced freezing index and number of freeze and thaw cycles, using an upgraded binder can help to reduce the IRI further (Swarna et al., 2021). Overall, it is understood that climate change will significantly impact the asphalt binder selection process in North America and across the globe (Delgadillo et al., 2020; Swarna et al., 2021; Viola & Celauro, 2015). Therefore, using accurate pavement temperature models will only become more critical with the onset of climate change, and it is imperative to implement such models as early as possible.

6.2.5 Overall highlights of literature

In general, the literature review revealed that the search for accurate pavement temperature models is an ongoing process in several locations. The highlights of the literature are as follows.

- An important parameter that significantly impacts pavement temperatures is solar radiation, which is difficult to estimate without years of historical data. Most current pavement temperature models rely on the use of latitude as an approximation for solar radiation, sunshine time, and sunset (Solaimanian & Bolzan, 1993).
- Temperature models developed based on latitude are often accurate for only the regions in which they were developed. This drawback is felt particularly strongly in Northern Canada,

where the extreme temperatures cannot be represented with one equation developed in the United States.

- The LTPP model, developed only for maximum latitudes of 52 degrees, has had limited testing in the Northern Canadian climate and does not fully represent the complex climate observed.
- The few existing pavement temperature models for Canadian climates have been developed for specific locations that are not applicable across the country. Further, several of them are targetter for winter maintenance applications. Therefore, it is understood through the literature review that a national pavement temperature model is necessary for Canadian pavement designers.

6.3 Objective and scope

The objectives of this study are:

1. Develop a pavement temperature model for Canadian climatic conditions.
2. Develop a software tool (CABS) to implement the pavement temperature model to determine the asphalt binder grade.

The scope of this study is to:

1. Obtain historical climate data from online databases.
2. Assess Canadian historical climate trends to create clusters of locations represented by similar temperature, precipitation, and freezing patterns.
3. Using the Enhanced Integrated Climatic Model (EICM), calculate the pavement temperatures based on historically obtained data.
4. Verify the Pearson Correlation Coefficients between potential variables.

5. Generate equations using multiple linear regression to predict the pavement temperature within each cluster based on air temperature and latitude.
6. Validate the model with manually collected data from within each of the cluster regions.
7. Render the model available through means of a software tool.

6.4 Methodology

This study was executed through five phases. The first phase involved climate data collection for 254 locations across Canada. Temperature and precipitation data were gathered from the Environment Canada open-sourced database. From this data, the freezing index could be computed for each of the selected locations by taking the difference between the mean daily temperature and zero degrees Celsius. In the second phase, a python code was written and executed to group the locations into three clusters of similar climate trends. In the third phase, pavement temperatures were obtained using EICM for each of the locations. Then, in the fourth phase, potential variables were evaluated by determining the Pearson correlation coefficient between the pavement temperature and the other variables that were considered to develop a model. Using a multiple linear regression analysis, maximum and minimum pavement temperature equations were developed for each of the three clusters. The clustering allowed the model to accurately represent the entirety of Canada, despite its immensely varied climate trends. The fourth phase included the generation of a software tool titled CABS, which allows users to quickly use the developed model to determine which asphalt binder grade they require. A summary of the methodology is included in Figure 6-1.

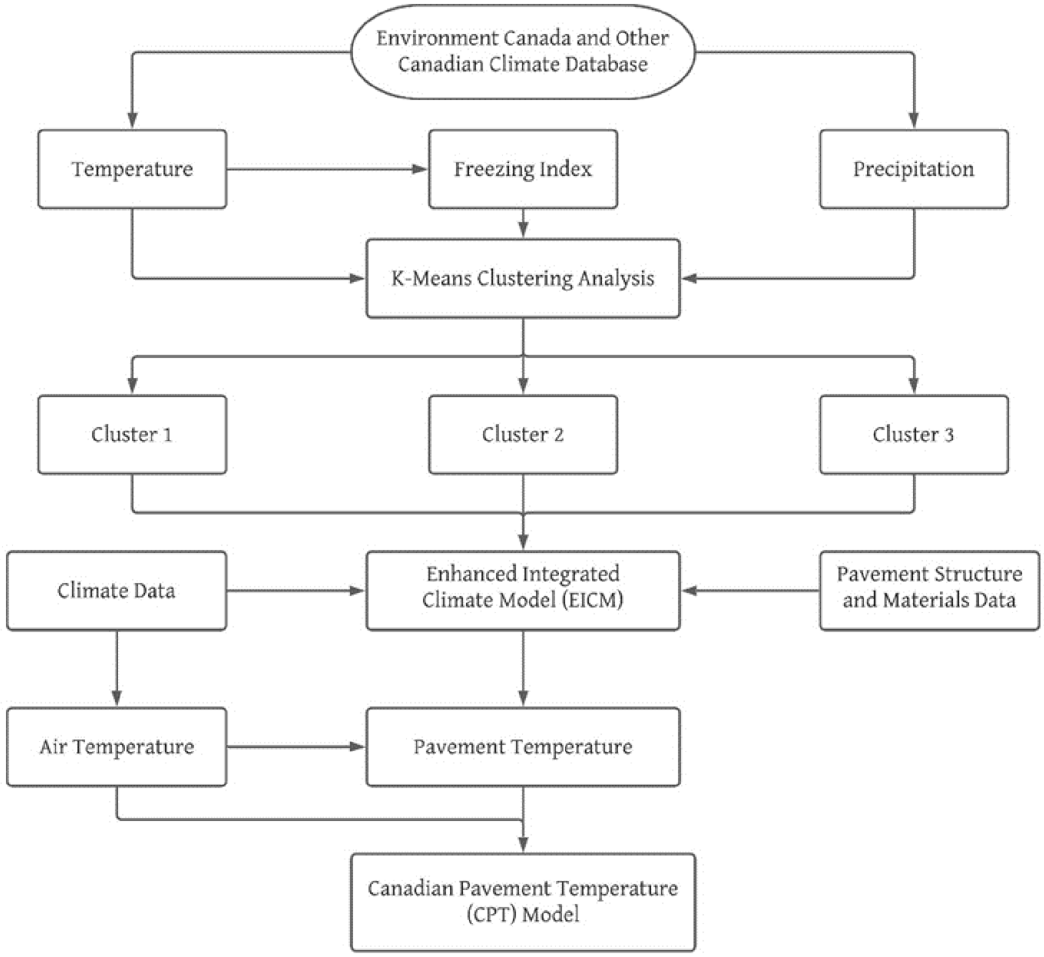

Figure 6-1: Pavement Temperature Model Methodology

6.4.1 Phase 1: Data collection

Environment and Climate Change Canada maintain online open-access databases providing historical temperatures and precipitation data for download. For this study, hourly recorded temperatures and daily precipitation were obtained from the database for 254 selected locations across Canada. The data was collected for 45 years from 1970 to 2015. The daily freezing index was calculated from the historical data as the difference between the mean daily temperature and zero degrees Celsius.

6.4.2 Phase 2: Clustering

To accurately represent the complex climate trends within Canada, a set of three clusters were generated using the K-means clustering methodology. A python code was written and executed to identify which among the 254 selected locations had the most similar temperature and precipitation data collected during Phase 1. The code performed an iterative process where clusters were randomly generated and tested until the slightest variation between cluster data was obtained. It was determined that for this situation, the data could accurately be represented with a K value of three and thus by generating three clusters.

6.4.3 Phase 3: Computing pavement temperatures using EICM

EICM Software is used to determine the pavement temperature profile in the asphalt concrete layer. A total of 64 pavement sections are considered from the LTPP Database. In addition, the necessary information, such as pavement materials and structure details, are gathered from the LTPP Database and analyzed in EICM software to determine the pavement temperature profile. In terms of climate input, air temperature and precipitation data are considered from the Environment Canada Database. The other climate factors such as wind speed, percent sunshine and humidity are taken from the Modern-Era Retrospective analysis for Research and Applications (MERRA) database. Pavement temperatures at the 254 locations were determined and used for the Canadian Pavement Temperature model development.

6.4.4 Phase 4: Pavement temperature model

Although the EICM output data was used to generate the new pavement temperature model, it was first necessary to determine the appropriate factors that significantly affect the pavement temperature. Therefore, the Pearson correlation coefficients were determined between pavement temperature and various interest factors. Heat plots were generated for both the maximum and minimum pavement temperature models for each of the three clusters, showing the correlation between the examined factors. For each developed equation, the heat plots were carefully analyzed to select the most highly correlated variables.

A machine learning technique was used to develop a multiple linear pavement temperature model considering the highly correlated factors. In this technique, 10% of the data were extracted randomly from the existing data for validation purposes. The remaining 90% data was divided into train data and test data for developing the model. After developing the model, various parameters such as Root Mean Square Error (RMSE), Mean Absolute Error (MAE), Explain Variance Score (EVS) and Mean Absolute Percentage Error (MAPE) were computed to determine the accuracy of the model. Then, the randomly extracted 10% validation data was used to validate the model. In this process, a predicted vs actual graph was plotted to check whether the developed model was working or not. Further verification was performed by comparing collected pavement temperatures within each of the clusters to predicted temperatures.

6.4.5 Phase 5: Software tool

With the pavement model validated, a software tool was developed to aid in using and implementing the proposed model. Inputs are daily maximum and minimum ambient air temperatures, latitude, and location. It is necessary to input the location and not just the latitude so that the software can identify under which cluster the location falls and thus which temperature model to apply. Available within the software are the 254 locations initially clustered in Phase 2, but it can also determine which cluster the city falls in based on coordinates if the desired location is not available. The software tool can then predict the pavement temperature at the requested location and return the corresponding asphalt binder grade to the user.

6.5 Results

As previously mentioned, the K-means clustering process generated three regional clusters. Each cluster represents a specific climate zoning, these being wet-freeze zones, dry-freeze zones, and Western wet non-freezing zones. The K-means grouping results are represented in Figure 6-2. The resulting clusters are geographically represented in Figure 6-3.

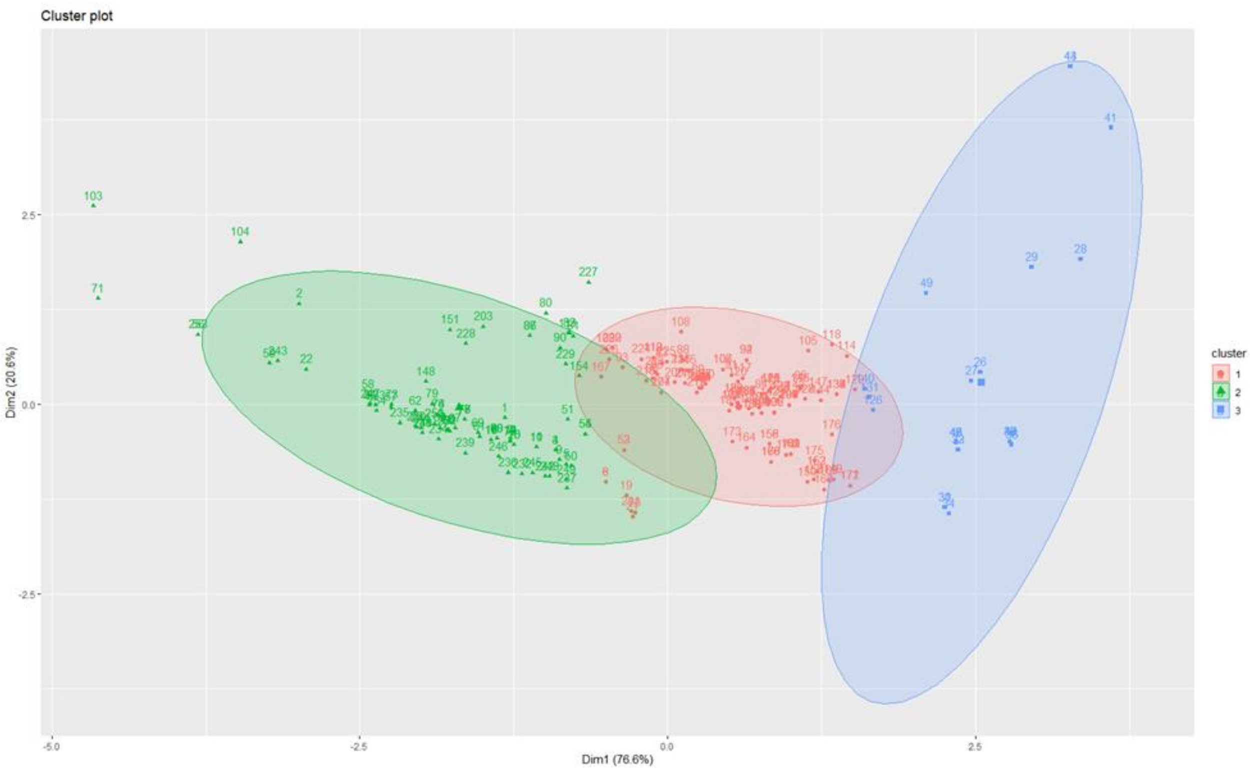

Figure 6-2: K-Means Clustering Results for 254 Selected Data Points

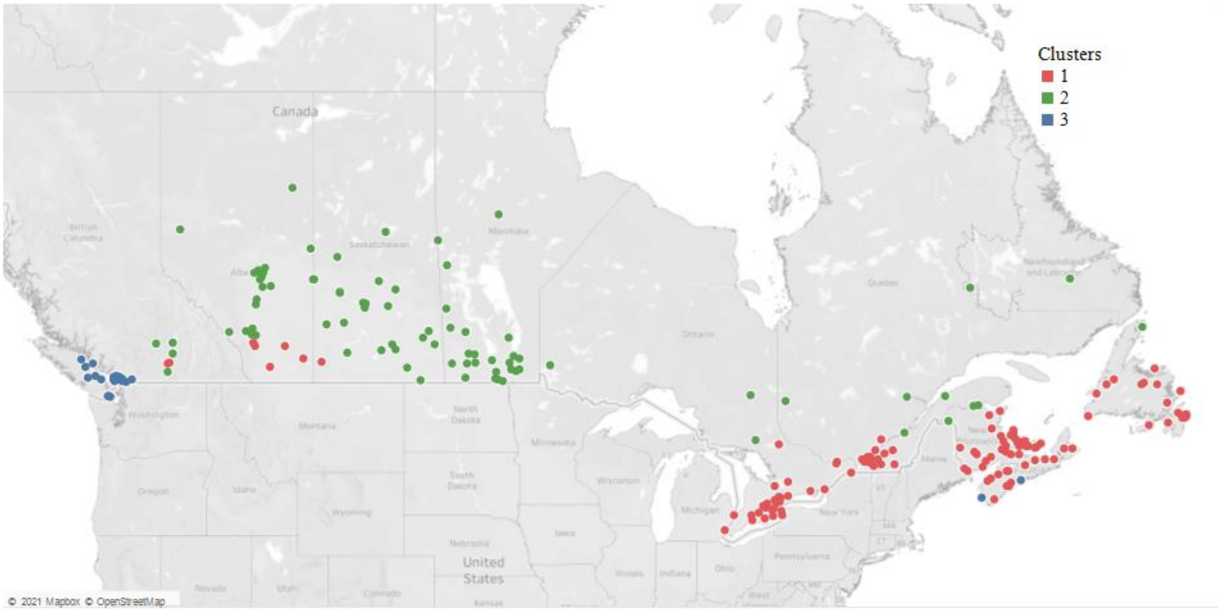

Figure 6-3 : Geographical Location of Clusters Used in Pavement Temperature Model

The cluster represented in red is Cluster 1 and encompasses most of the Atlantic provinces and southern regions of Quebec and Ontario. The cluster is characterized by freezing temperatures and high annual precipitation and is thus referred to as the wet-freeze zone. Represented in green is Cluster 2, encompassing Manitoba, Saskatchewan, Central and Northern Alberta, Eastern and Northern British Columbia, Northern Ontario, Quebec, New Brunswick, and Labrador. These regions also experience freezing but significantly less rain, making it a dry-freeze zone. The final cluster represented in blue is Cluster 3, Western British Columbia. The region is unique for its lack of freezing temperatures and extended periods of rain, thus known as a wet-non-freezing zone.

The development of the model was heavily dependent on the Pearson's correlation coefficients generated to validate the correlation between climate factors and pavement temperatures. Therefore, each correlation coefficient's heat plot was analyzed to determine the most significant variables. The heat plots are included in Figure 6-4 through Figure 6-7. The blue plots represent the minimum temperature analysis, and the red plots represent the maximum temperature analysis. The minimum temperature heat plot for Cluster 1 is discussed in detail, but the process was repeated for each developed equation.

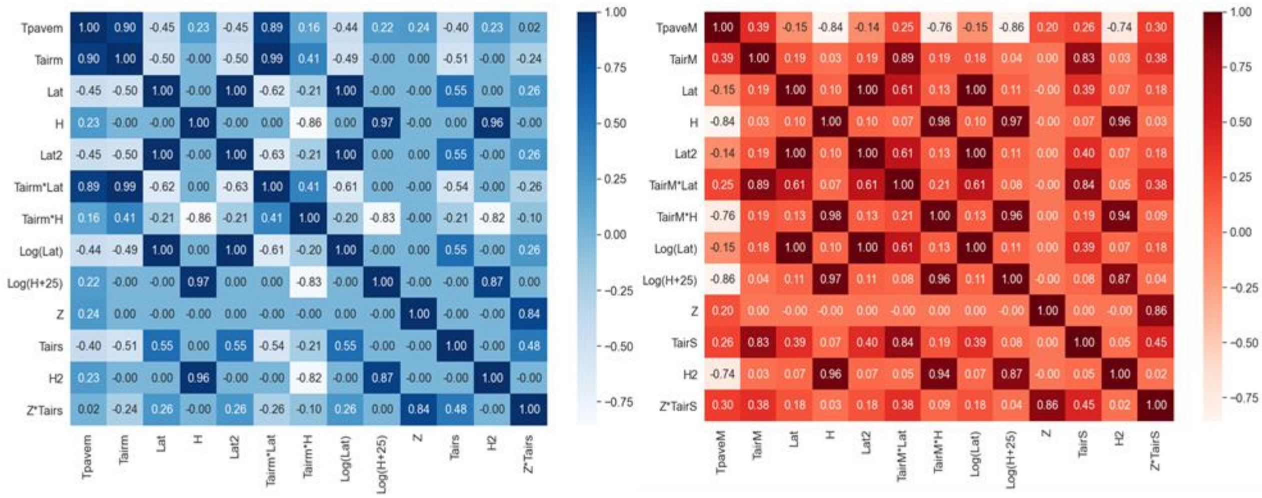

Figure 6-4: Heat Plots for Canada Wide Analysis, (a) low pavement temperature and (b) high pavement temperature

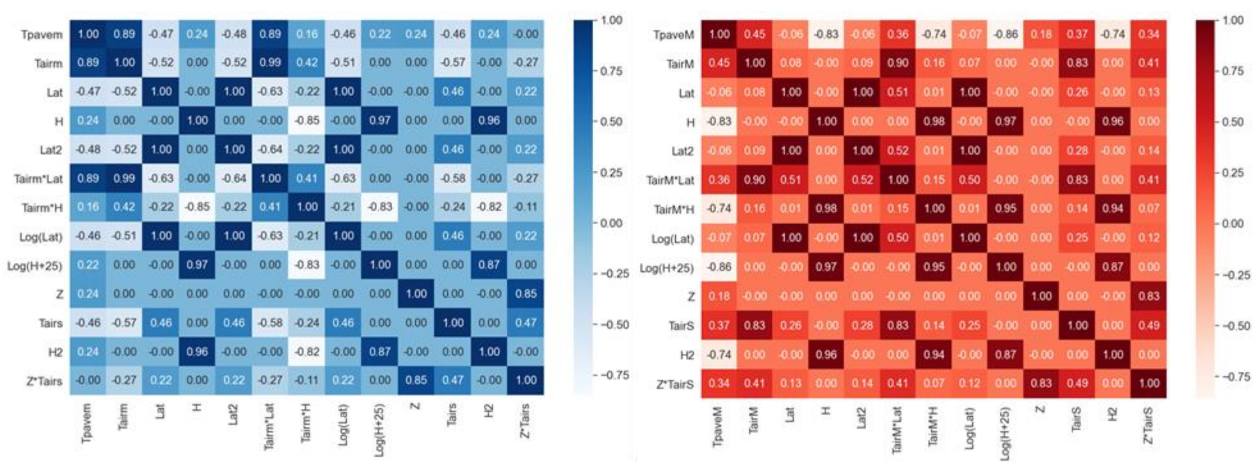

Figure 6-5: Heat Plots for Cluster 1, (a) low pavement temperature and (b) high pavement temperature

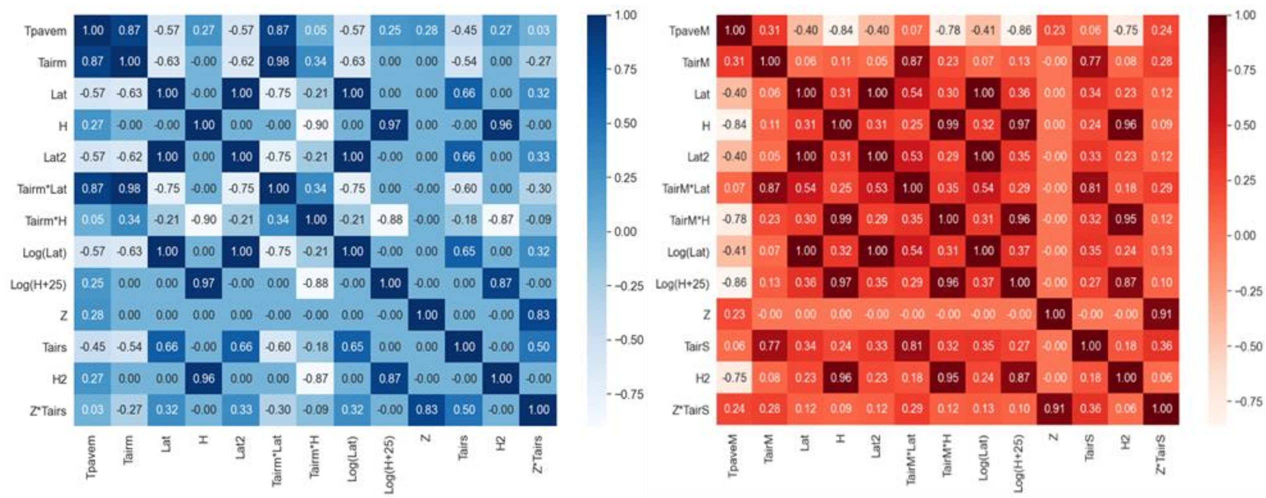

Figure 6-6: Heat Plots for Cluster 2, (a) low pavement temperature and (b) high pavement temperature

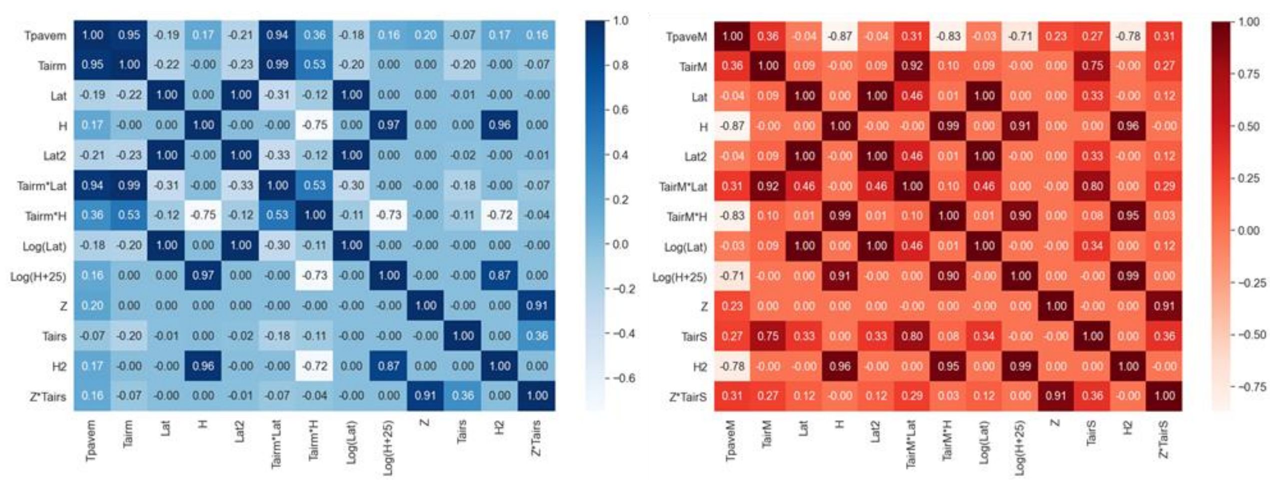

Figure 6-7: Heat Plots for Cluster 3, (a) low pavement temperature and (b) high pavement temperature

Where, Tpavem = Annual low pavement temperature, Tairm = Annual low ambient air temperature, TpaveM = Culumative average seven-day high pavement temperature, TairM = Culumative average seven-day high ambient air temperature, Lat = latitude, H = depth to surface, Lat2 = Square of latitude, Z = Standard normal value, Tairs = temperature standard deviation, H2 = Square of Depth to Surface.

For Cluster 1, as expected, the strongest independent correlation within all of the heat plots was observed between the pavement temperature and the ambient air temperature. It was known that latitude would need to be considered when determining an approximation for solar radiation, but this heat plot revealed that the latitude squared was more significantly correlated with the pavement temperature. The pavement depth was more highly correlated to the pavement temperature than any of its modified forms and was thus taken as is. Standard deviation and reliability were also included in this model.

It was found that not all of the clusters had the same highly correlated variables. Similarly, the highly correlated variables changed between maximum and minimum pavement temperature models. In each scenario, the more highly correlated variables were used in their respective model.

The observations were split into two groups first to train and then to test the data to develop the model. Initially, the train and test data were assumed as 70% and 30%, respectively. Then, the train and test data were increased to 75% and 25%, then to 80% and 20%, respectively. Out of these three models, it was found that the 80% train and 20% test data resulted in a better model. Therefore, the models developed with 80% train data and 20% test data are considered the final models. Two different models were developed for both maximum and minimum pavement temperatures within each of the three clusters. For each developed equation, the selected variables were verified to be statistically significant, returning a p-value of less than 0.05.

The following equations summarize the model developed for each of the clusters and one for the entirety of Canada.

Entire Canada:

$$T_{paveM} = 75.8695 + 0.6662 \times T_{airM} - 0.2854 \times Lat - 18.5231 \times \log_{10}(H + 25) + 0.9916 \times Z \times T_{airS} \quad \text{Equation 6-17}$$

$$T_{pavem} = 3.5095 + 0.7890 \times T_{airm} - 0.1316 \times Lat + 0.0564 \times H - 0.8427 \times Z \times T_{airs} \quad \text{Equation 6-18}$$

Cluster 1:

$$T_{paveM} = 78.6582 + 0.7334 \times T_{airM} \times (1 + 0.0011 \times H) - 0.2156 \times Lat - 22.5812 \times \log_{10}(H + 25) + 1.0969 \times Z \times (1 + 0.375 \times T_{airS}) \quad \text{Equation 6-19}$$

$$T_{pavem} = 2.9185 + 0.769 \times T_{airm} - 0.0015 \times Lat^2 + 0.0542 \times H - 2.7853 \times Z - 0.8852 \times T_{airs} \quad \text{Equation 6-20}$$

Cluster 2:

$$T_{paveM} = 99.1268 + 0.7749 \times T_{airM} \times (1 + 0.0004 \times H) - 24.4383 \times \log_{10} Lat - 18.26 \times \log_{10}(H + 25) + 1.2387 \times Z \times (1 + 0.269 \times T_{airS}) \quad \text{Equation 6-21}$$

$$T_{pavem} = 10.3279 + 0.7670 \times T_{airm} - 0.1923 \times Lat + 0.0592 \times H - 3.075 \times Z - 1.2607 \times T_{airs} \quad \text{Equation 6-22}$$

Cluster 3:

$$T_{paveM} = 36.9982 + 0.7052 \times T_{airM} - 0.002 \times Lat^2 - 0.1133 \times H - 0.4096 \times T_{airS} \times (1 - 2.4487 \times Z) \quad \text{Equation 6-23}$$

$$T_{pavem} = -3.3067 + 0.8467 \times T_{airm} + 0.0007 \times Lat^2 + 0.0589 \times H - 3.1769 \times Z + 0.0902 \times T_{airs} \quad \text{Equation 6-24}$$

Where,

T_{paveM} = Cumulative average seven-day high pavement temperature

T_{airM} = Cumulative average seven-day high ambient air temperature

T_{pavem} = Low pavement temperature

T_{airm} = Low ambient air temperature

Lat = Latitude

T_{airS} = Air temperature standard deviation

Z = Reliability

For the developed model, various parameters such as Root Mean Square Error (RMSE), Mean Absolute Error (MAE), Explain Variance Score (EVS) and Mean Absolute Percentage Error (MAPE) were computed to determine the accuracy of the model. Here, RMSE determines the standard deviation of the residuals, and MAE determines the average magnitude of the residuals. Lower values of RMSE and MAE signifies a higher accuracy model. Similarly, MAPE is a measure that determines the prediction accuracy of the regression. If the MAPE is less than 10%, the model signifies excellent performance, and if it is less than 20%, the model signifies good performance. EVS is another factor that defines the dispersion of errors in a given dataset. The EVS factor ranges from 0 to 1. The higher the EVS values, the better the regression model. The developed models are included in Table 6-2.

Table 6-2: Various parameters for the pavement temperature model

Model type	Model	No. of observations	Test data	Train data	Validation data	R^2	RMSE	MAE	EVS	MAPE
High Pavement Temperature	Entire Canada	9144	914	6584	1646	0.93	0.71	0.54	0.98	0.01
	Cluster 1	5004	500	3603	901	0.96	0.37	0.27	0.99	0.01
	Cluster 2	3168	317	2281	570	0.95	0.37	0.24	0.99	0.01
	Cluster 3	972	97	700	175	0.97	1.05	0.96	0.95	0.02
Low Pavement Temperature	Entire Canada	9144	914	6584	1646	0.93	2.42	1.52	0.93	0.07
	Cluster 1	5004	500	3603	901	0.92	2.27	1.44	0.93	0.07
	Cluster 2	3168	317	2281	570	0.98	2.46	1.66	0.92	0.07
	Cluster 3	972	97	700	175	0.98	1.61	1.13	0.98	0.08

It is observed that each clustered model apart from one returned an R^2-value greater than 0.950, with a maximum achieved of 0.982. Of the three clusters, Cluster 1 proves to have the lowest R^2, likely due to the geographical vastness of the cluster. However, all three clusters proved to perform better than the Canada-wide model, confirming the importance of a clustered approach in representing the Canadian climate.

The validation of the pavement temperature models revealed that the developed equations would accurately predict pavement temperatures. Using 80% of the observations to train the models and the remaining 20% to test the models, the performance could be evaluated. The MAPE returned for all of the models was well below the threshold of 10%, with a maximum of 8%. The MAPE values calculated for the high pavement temperature model were particularly strong, with the highest value being 2%. Similarly, the EVS values returned all approach 1, indicating the regression model is performing well.

There is a two-step validation component for this model. In the first step, the training data is used to validate the model in five iterations by selecting the test data as 20% of the entire data. As this data includes the train data, the second validation step is done using the initial 10% of randomly extracted data. Then the actual vs predicted graph was plotted to check the accuracy of the model. An example of predicted vs actual plot for Cluster 1 high temperature was plotted as presented in Figure 6-8. From Figure 6-8, it was noted that the predicted vs. actual data were falling exactly on the 45° line, which passes through the centre. To further determine the accuracy, a trend line was plotted for the data. The equation for the trend line was found to have an intercept of 1.10503 and a slope of 0.97805. The slope defines the accuracy of the model and the intercept defines the mean error of the model. Similarly, all the models were validated and found to be accurate.

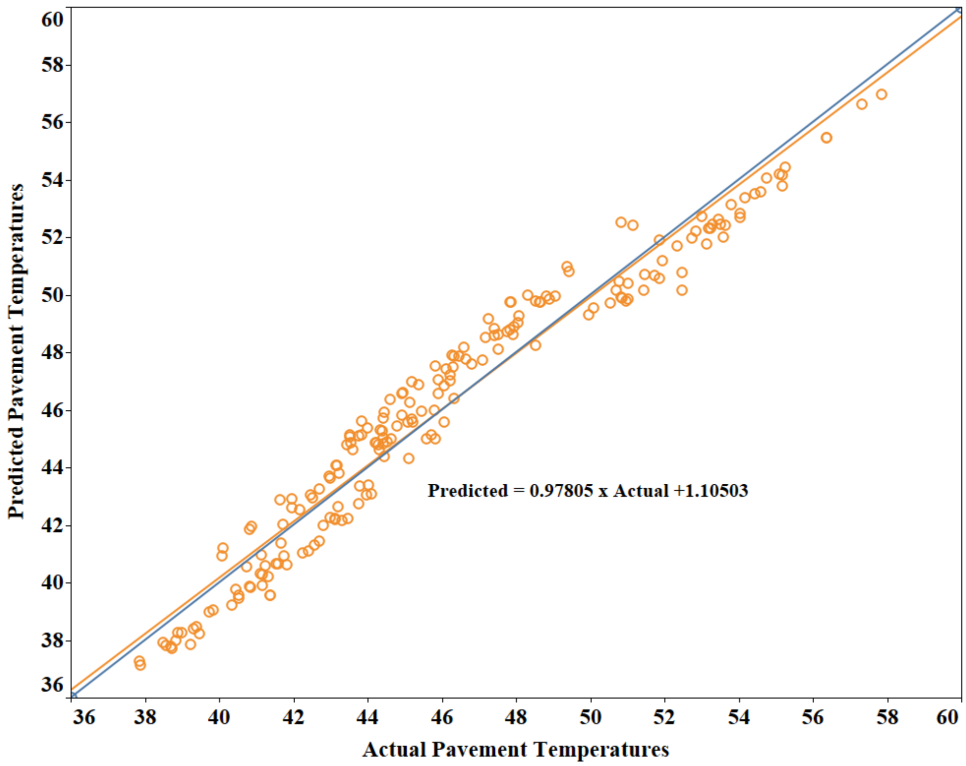

Figure 6-8: Predicted vs Actual plot for validation data for Cluster 1 high-temperature model

6.6 Field verification

To verify the models developed, field measurements were collected from three different locations (St. John's, NL., Waterloo, ON, and Surrey, BC). In addition, the measured pavements temperature were gathered from various published papers to verify the model (Hosseini et al., 2015; Huber et al., 1989; Sherif & Hassan, 2004). These pavement temperatures and the corresponding air temperatures are used to verify the developed Canadian pavement temperature models, as illustrated in Table 6-3.

The locations investigated include Surrey, Mc Lean, Waterloo, Ottawa, and St. John's. All these measurements are based on one-year data and are measured at the surface of the pavement except McLean high temperature, which was measured at a depth of 20 mm from the surface of the pavement. From Table 6-3, it was noted that the difference between the measured and the predicted is ranging from -1.33 to 0.60 °C. In High temperatures, two measurements were taken from Surry, BC, one was measure during summer, and the second one was measured during the heatwave time. In the second measurement, it was noticed that the measured pavement temperature is 1.33 °C higher than the predicted pavement temperature; this might be because of the unexpected high temperature that occurred in June 2021 due to the heatwave (increased solar radiation and hot winds).

Table 6-3: Verification data for developed pavement temperature model

Model	**Location**	**Latitude**	**Air Temperature (°C)**	**Pavement Temperature (°C)**		**Difference**
				Measured	**Predicted**	
High Temperature	St. John's, NL	47.574398	29.41	57.80	58.41	0.61
	McLean, SK	50.514373	21.21	44.90	43.88	-1.02
	Surrey (1), BC	49.167033	32.08	55.10	54.79	-0.31
	Surrey (2), BC	49.167033	45.10	65.30	63.97	-1.33
Low temperature	St. John's, NL	47.574398	-21.90	-19.90	-20.27	-0.37
	Ottawa, ON	45.410961	-27.90	-21.50	-21.65	-0.15
	Waterloo, ON	43.473217	-16.50	-11.90	-12.60	-0.70
	McLean, SK	50.514373	-18.30	-12.20	-13.42	-1.22
	Surrey, BC	49.167033	-10.30	-10.70	-10.34	0.36

In cluster 1 (St. John's, Ottawa, and Waterloo), the difference between the observed and the predicted temperatures were noticed to be less than 0.65 °C. In cluster 2 (McLean, SK), the difference was noticed to be just above 1°C. However, in cluster 3 (Surrey, BC), the difference was found to be less than 0.5 °C. This concludes that the developed pavement temperatures are reasonably accurate, considering the existing pavement temperature models.

6.7 CABS software

The final step in the model generation was the development of an online binder selection application. The Canadian Asphalt Binder Selection (CABS) software tool allows users to quickly obtain the suggested base binder grade based on pavement temperatures using SHRP, LTPP, and the newly developed Canadian Pavement Temperature (CPT) model, which was discussed above. The SHRP and LTPP equations employed in the software are as discussed in equations 6-1 to 6-5.

The CABS web-based software tool can be accessed by anyone through the following link: https://artel.engr.mun.ca/software/MUN-CABS.html. Upon initial entry to CABS, the software will prompt the user to input a project name and a project engineer. Next, the user should select the province and location of interest for their purposes through the available drop-down lists. Once the province is selected, the location drop-down list will be customized to display all the locations investigated within this province through the study. If the desired location is not available in this list, the user can select the part of province, where the project is located. The final drop-down menu allows the user to select which pavement temperature model is to be used; CPT, SHRP, or LTPP. Based on the selected model, CABS will prompt the user to input the required relevant variables. In the case of the CPT model for example, air temperatures, standard deviations, depth to surface, latitude, and reliability are the required inputs. Furthermore, for the CPT model, CABS automatically determines which cluster the location of interest falls within based on the inputted location information. When all of the required data is entered, the “calculate” button may be clicked and the pavement temperature will be computed and displayed. In addition to providing the high and low pavement surface temperatures, CABS also returns the recommended base asphalt binder grade. It should be noted that the suggested binder is not corrected for traffic and is only recommended based on the computed temperatures. A snapshot of the CABS software interface is shown in Figure 6-9. In addition, using the CABS tool the binder grades are determined for some cities in Canada and the reported binders are presented in Figure 6-10.

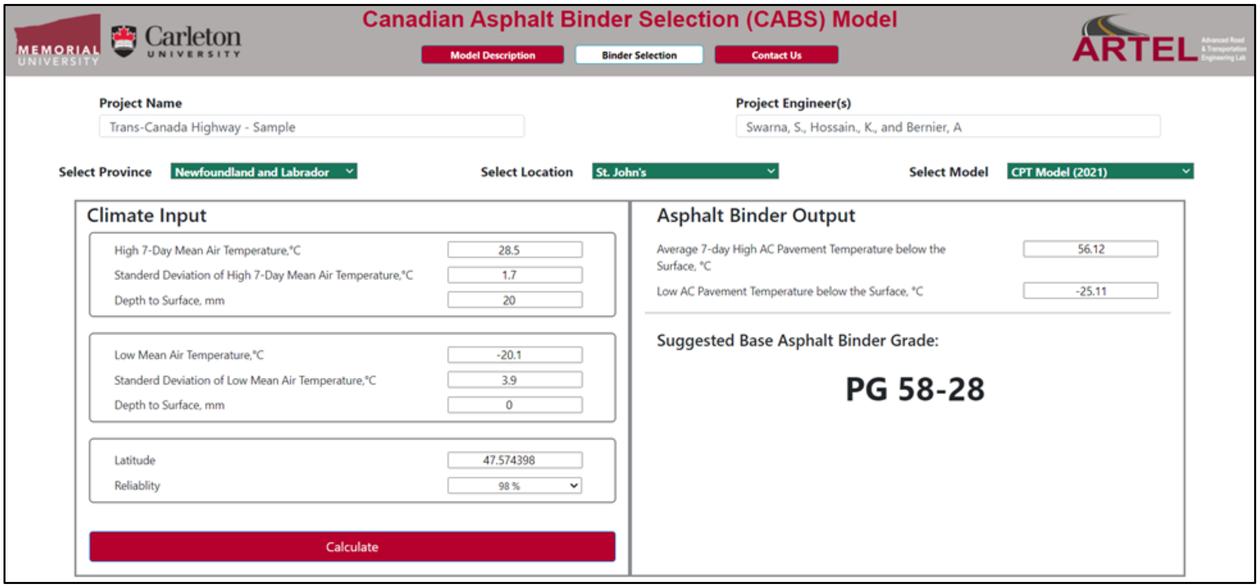

Figure 6-9: CABS Software Tool Sample Output

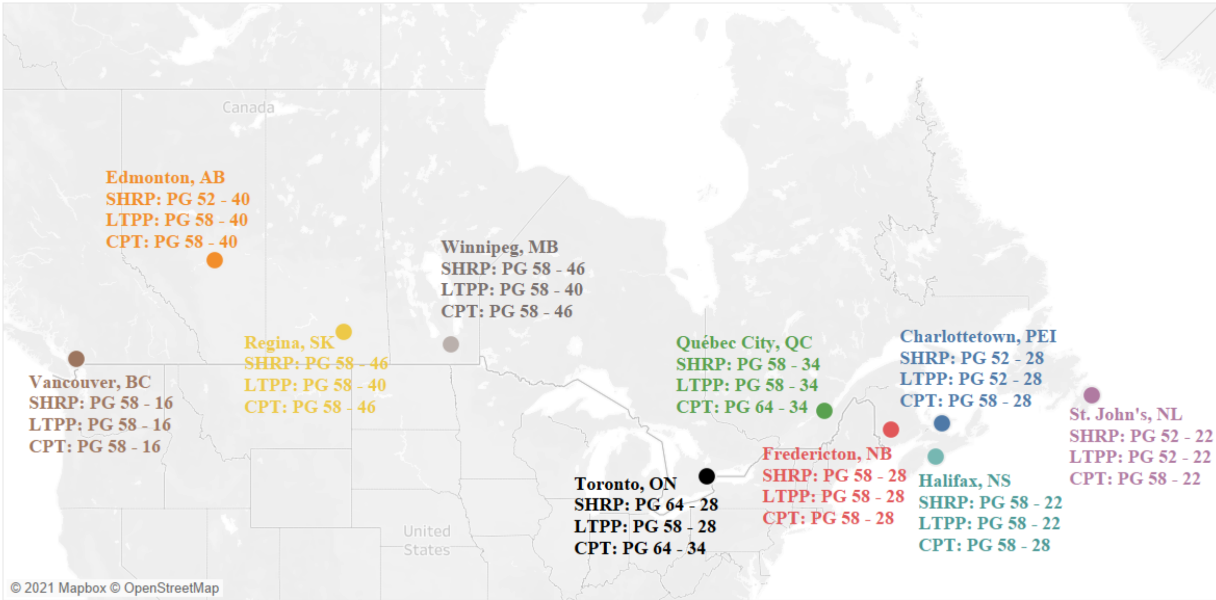

Figure 6-10: Binder grades computed using CABS tool

6.8 Conclusions

A pavement temperature model has been developed to more accurately represent pavement temperatures experienced in the Canadian climate. The country was divided into three clusters, each with a model, to address the problem caused by the varied climate. Upon completion of the research, the following conclusions could be drawn:

- Canada's climate can be divided into three clusters; wet-freeze, dry-freeze, and Western wet-non-freezing, to better represent the geographical variances in temperature and precipitation.
- Pearson correlation coefficients have been used to identify which parameters are most correlated to pavement temperature. Correlated parameters varied between clusters and model types.

- The R^2-values obtained for the clusters are generally better than that of the Canada-wide model. It is thus confirmed that representing Canadian climate with the clustered approach is a more accurate way of predicting pavement temperatures.
- The developed pavement temperature models are found to be accurate for the Canadian climatic conditions.
- The models are validated using an unused data set, randomly picked from the entire data before developing the model. And these were further verified with the field measurements.
- CABS software was developed to allow users to quickly obtain the suggested base binder grade based on pavement temperatures using SHRP, LTPP, and the newly developed CPT models.

6.9 References

Adwan, I., Milad, A., Memon, Z. A., Widyatmoko, I., Zanuri, N. A., Memon, N. A., & Yusoff, N. I. M. (2021). Asphalt pavement temperature prediction models: A review. In *Applied Sciences* (Vol. 11, Issue 9). https://doi.org/10.3390/app11093794

Ariawan, I. M. A., Subagio, B. S., & Setiadji, B. H. (2015). Development of asphalt pavement temperature model for tropical climate conditions in West Bali region. *Procedia Engineering*, *125*. https://doi.org/10.1016/j.proeng.2015.11.126

Asefzadeh, A., Hashemian, L., & Bayat, A. (2017). Development of statistical temperature prediction models for a test road in Edmonton, Alberta, Canada. *International Journal of Pavement Research and Technology*, *10*(5), 369–382. https://doi.org/10.1016/j.ijprt.2017.05.004

Bobes-Jesus, V., Pascual-Muñoz, P., Castro-Fresno, D., & Rodriguez-Hernandez, J. (2013). Asphalt solar collectors: A literature review. *Applied Energy*, *102,* 962–970.

https://doi.org/10.1016/j.apenergy.2012.08.050

Bogren, J., Gustavsson, T., & Karlsson, M. (2001). Temperature differences in the air layer close to a road surface. *Meteorological Applications*, *8*(4), 385–395. https://doi.org/10.1017/S1350482701004017

Bosscher, P. J., Bahia, H. U., Thomas, S., & Russell, J. S. (1998). Relationship between pavement temperature and weather data: Wisconsin field study to verify superpave algorithm. *Transportation Research Record*, *1609*(1), 1–11. https://doi.org/10.3141/1609-01

Chandrappa, A. K., & Biligiri, K. P. (2016). Development of Pavement-Surface Temperature Predictive Models: Parametric Approach. *Journal of Materials in Civil Engineering*, *28*(3). https://doi.org/10.1061/(asce)mt.1943-5533.0001415

Chen, J., Wang, H., & Xie, P. (2019). Pavement temperature prediction: Theoretical models and critical affecting factors. *Applied Thermal Engineering*, *158*, 113755. https://doi.org/10.1016/j.applthermaleng.2019.113755

Delgadillo, R., Arteaga, L., Wahr, C., & Alcafuz, R. (2020). The influence of climate change in Superpave binder selection for Chile. *Road Materials and Pavement Design*, *21*(3), 607–622. https://doi.org/10.1080/14680629.2018.1509803

Diefenderfer, B. K., Al-Qadi, I. L., & Diefenderfer, S. D. (2006). Model to predict pavement temperature profile: Development and validation. *Journal of Transportation Engineering*, *132*(2), 162–167. https://doi.org/10.1061/(ASCE)0733-947X(2006)132:2(162)

Hassan, H. F., Al-Nuaimi, A., Al-Oraimi, S., & Jafar, T. M. A. (2008). Development of asphalt binder performance grades for Omani climate. *Construction and Building Materials*, *22*(8), 1684–1690. https://doi.org/10.1016/j.conbuildmat.2007.06.016

Herb, W., Velasquez, R., Stefan, H., Marasteanu, M. O., & Clyne, T. (2009). Simulation and characterization of asphalt pavement temperatures. *Road Materials and Pavement Design*, *10*(1), 233–247. https://doi.org/10.1080/14680629.2009.9690190

Hermansson, A. (2000). Simulation model for calculating pavement temperatures including maximum temperature. *Transportation Research Record*, *1699*(1), 134–141. https://doi.org/10.3141/1699-19

Hermansson, Å. (2004). Mathematical model for paved surface summer and winter temperature: Comparison of calculated and measured temperatures. *Cold Regions Science and Technology*, *40*(1–2), 1–17. https://doi.org/10.1016/j.coldregions.2004.03.001

Hosseini, F., Hossain, S. M. K., Fu, L., Johnson, M., & Fei, Y. (2015). Prediction of Pavement Surface Temperature Using Meteorological Data for Optimal Winter Operations in Parking Lots. *Proceedings of the International Conference on Cold Regions Engineering*, *January*, 440–451. https://doi.org/10.1061/9780784479315.039

Huber, G. A., Heiman, G. H., & Chursinoff, R. W. (1989). Prediction of Pavement Layer Temperature During Winter Months Using a Computer Model. *Canadian Technical Asphalt Association*.

Islam, M. R., Ahsan, S., & Tarefder, R. A. (2015). Modeling temperature profile of hot-mix asphalt in flexible pavement. *International Journal of Pavement Research and Technology*, *8*(1), 47–52. https://doi.org/10.6135/ijprt.org.tw/2015.8(1).47

Liu, C., & Yuan, D. (2000). Temperature distribution in layered road structures. *Journal of Transportation Engineering*, *126*(1). https://doi.org/10.1061/(ASCE)0733-947X(2000)126:1(93)

Mammeri, A., Ulmet, L., Peti, C., & Mokhtari, A. M. (2015). Temperature modelling in pavements: The effect of long-and short-wave radiation. *International Journal of Pavement*

Engineering, *16*(3), 198–213. https://doi.org/10.1080/10298436.2014.937809

Matić, B., Matić, D., Sremac, S., Radović, N., & Vidikant, P. (2014). A model for the pavement temperature prediction at specified depth using neural networks. *Metalurgija*, *53*(4).

Milad, A., Adwan, I., Majeed, S. A., Yusoff, N. I. M., Al-Ansari, N., & Yaseen, Z. M. (2021). Emerging Technologies of Deep Learning Models Development for Pavement Temperature Prediction. *IEEE Access*, *9*(1), 23840–23849. https://doi.org/10.1109/ACCESS.2021.3056568

Minhoto, M. J. C., Pais, J. C., Pereira, P. A. A., & Picado-Santos, L. G. (2005). Predicting asphalt pavement temperature with a three-dimensional finite element method. *Transportation Research Record*, *1919*(1), 96–110. https://doi.org/10.3141/1919-11

Mohseni, A. (1998). *LTPP Seasonal Asphalt Concrete Pavement Temperature Models*.

Nivitha, M. R., & Krishnan, J. M. (2014). Development of Pavement Temperature Contours for India. *Journal of The Institution of Engineers (India): Series A*, *95*(2), 83–90. https://doi.org/10.1007/s40030-014-0074-y

Raad, L., Saboundjian, S., Sebaaly, P., & Epps, J. (1998). Minimum pavement temperature modeling and mapping for alaskan conditions. *Transportation Research Record*, *1643*, 86–94. https://doi.org/10.3141/1643-12

Salem, H. M., Bayomy, F. M., Al-Taher, M. G., & Genc, I. H. (2004). Using long-term pavement performance data to predict seasonal variation in asphalt concrete modulus. *Transportation Research Record*, *1896*(1), 119–128. https://doi.org/10.3141/1896-12

Sherif, A., & Hassan, Y. (2004). Modelling pavement temperature for winter maintenance operations. *Canadian Journal of Civil Engineering*, *31*(2), 369–378. https://doi.org/10.1139/l03-107

Solaimanian, M., & Bolzan, P. (1993). Analysis of the Integrated Model of Climatic Effects on Pavements. *Strategic Highway Research Program, National Research Council*, *A001*.

Solaimanian, M., & Kennedy, T. W. (1993). Predicting Maximum Pavement Surface Temperature Using Maximum Air Temperature and Hourly Solar Radiation. *Transportation Research Record*, *1417*.

Sreejith, G. H. (2021). Pavement Temperature Data Maps for Worldwide Locations. *International Journal of Pavement Research and Technology*. https://doi.org/10.1007/s42947-021-00064-8

Swarna, S. T., Hossain, K., Pandya, H., & Mehta, Y. A. (2021). Assessing Climate Change Impact on Asphalt Binder Grade Selection and its Implications. *Transportation Research Record*. https://doi.org/https://doi.org/10.1177/03611981211013026

Underwood, S., Guido, Z., Gudipudi, P., & Feinberg, Y. (2017). Increased costs to US pavement infrastructure from future temperature rise. *Nature Climate Change*, *7*(10), 704–707. https://doi.org/10.1038/nclimate3390

Viola, F., & Celauro, C. (2015). Effect of climate change on asphalt binder selection for road construction in Italy. *Transportation Research Part D: Transport and Environment*, *37*, 40–47. https://doi.org/10.1016/j.trd.2015.04.012

Zapata, C. E., & Houston, W. N. (2008). *Calibration and Validation of the Enhanced Integrated Climatic Model for Pavement Design*. Transportation Research Board. https://doi.org/10.17226/23098

Chapter 7: Climate Change Adaptation Strategies for Canadian Asphalt Pavements

7.1 Abstract

There is strong evidence for climate change leading to a rise in temperatures and a change in precipitation trends. These environmental changes pose a threat to pavement infrastructure worldwide. Therefore, it is necessary to modify pavement design procedures to consider climate change. In addition, it is necessary to consider suitable pavement materials for future climate. The objective of this study is to develop a framework for selecting an appropriate adaptation strategy to mitigate climate change impact. To fulfill this, the influence of climate change on long-term pavement performance in Canada has been quantified over sixteen Canadian pavement sections located over various provinces in Canada. In addition, the fundamental causes of pavement deterioration due to climate change were determined using ten different climate change models. Various adaptation strategies such as upgrading asphalt binder grade, increasing the thickness of asphalt concrete layer, increasing the base layer thickness, and using stabilized base layers were analyzed to reduce pavement deterioration and to extend the service life of the pavement. Unlike the other studies, pavement temperatures were determined using EICM to determine the change in binder grade for the future climate in the adaptation process. A stone matrix asphalt mixture gradation is considered as another adaption strategy where the AC rutting is found to be very high. To reduce the subbase and subgrade rutting, an emulsion stabilized base is adapted for specific locations. This study emphasizes the necessity of climate change adaptation strategies for Canadian asphalt concrete pavements.

Keywords: Climate change, Adaptation Strategies, Pavement performance, AASHTOWare ME design, Pavement design

7.2 Introduction

The onset of climate change is a phenomenon expected to significantly impact infrastructure across the world. Flexible pavements will strongly reflect these changes due to their temperature sensitive components and as a result, they may begin to perform poorly. Currently, strict design methodology exists to uphold pavement conditions to a satisfactory level, promoting safety and comfort to drivers. With the expected change in future temperatures, these design methodologies will need to continue to evolve. Although appropriate design methodologies for today's climate have been developed, uncertainty remains regarding the best way to build climate change enduring pavements. Exploring various design strategies considering climate change is an essential step to build resilient infrastructure.

7.2.1 Climate change principles

Climate change is the direct result of a phenomenon known as the greenhouse gas effect. A small amount of greenhouse gasses (GHGs) has always been found in the Earth’s atmosphere and have served to keep solar radiation reflecting off Earth into the atmosphere (Meinshausen et al., 2011; Stocker et al., 2013). The gasses trap heat into the atmosphere and thus increase the temperatures of the global climate system. However, with the onset of industrialization, an increase in GHG emissions has been observed. A surplus of GHG’s is being trapped in the atmosphere and increasing the temperatures more than is necessary. For example, the concentration of carbon dioxide in the atmosphere has increased by 35% since 1750, whereas it had remained relatively constant before (Humphrey, 2008). Several models exist to estimate weather changes to predict the impacts of climate change (Moss et al., 2010; Wigley et al., 2009).

7.2.2 *Impact on pavement performance*

Recent study has confirmed that climate change will harm pavement performance in the future (Fletcher et al., 2016). In Canada, the impacts on flexible pavements were first investigated for 2050 to 2070 using two climate change models, Hadley Climate Model 3 (HadCM3B21) and Coupled Global Climate Model 2 (CGCM2A2x). This study revealed that the future variation in temperature, rainfall and traffic growth are essential factors that will influence pavement performance (Mills et al., 2009; Tighe et al., 2008). Another study investigated the consequences of climate change on pavement deterioration processes using the REgional MOdel (REMO), downscaled to an hourly time scale and a 10-km grid resolution. The study found that the effects of temperature rise on permanent deformation are significant (Meagher et al., 2012). In Europe, time variation curves of various climate factors, including air temperature, wind speed, global radiation, and humidity, are predicted to approximate the effects of the climate factors on pavement performance. In central Europe, the effect of climate change on pavement performance is estimated to be significant (Wistuba & Walther, 2013).

Similarly, adaptation strategies resulting from climate change are deemed unnecessary for Germany and Austria (Wistuba & Walther, 2013). Road transport during winter seasons relies on frozen roads in freezing zones. However, climate change-related temperature rises in northern regions will cause shorter freezing periods. In these situations, upgrading thin and unsealed pavements is necessary to maintain reliable bearing capacity for the roads throughout the winter seasons (Bizjak et al., 2014).

A recent study utilized the Austroads Climate Tool to forecast climate change. The resulting climate data was processed, and input into the Highway Development & Management (HDM)-4 road maintenance software and the impact on pavement performance was estimated.

Asphalt aging, embrittlement and cracking were the effects forecasted as a result of the increased temperatures. Furthermore, it was determined that increased rainfall would alter moisture conditions and lead to further pavement deterioration (Shao et al., 2017). A recent study assessed the impact of climate change on pavement performance in 24 different locations across the United States by using three different models. The study revealed varying performance trends across the 24 locations. However, all locations agreed that pavement performance would decrease under current design standards and climate change (Stoner et al., 2019).

These studies reveal that pavements around the world will experience the impact of climate change (Schweikert et al., 2014; Wistuba & Walther, 2013). Additionally, a very recent study investigated the impacts of climate change on airport pavements, finding that adaptation strategies will be necessary in the future (Barbi et al., 2021). These studies all reinforce the importance of considering climate change effects in pavement design and including stakeholders in discussions early in the process (Haslett et al., 2021).

7.2.3 Adaptation strategies

A possible adaptation measure to ensure resiliency in asphalt pavements is the appropriate upgrading of the asphalt binder. A recent study has reinforced the importance of selecting appropriate binders by revealing the pavement distresses occurring under future climates with no upgraded binder. Permanent deformation in the asphalt concrete (AC) was found to increase by an average of approximately 24.7% in all observed sections under future climates. Similarly, bottom-up (BU) fatigue cracking in AC was found to increase by an average of 11.46% for all sections due to climate change (Swarna et al., 2021). These trends suggest that inappropriate binder selection may become a significant problem in future climates, and the practice of upgrading binders should be investigated as a potential maintenance technique. It should also be noted that many locations around the globe are currently using incorrect binders (Delgadillo et al., 2018; Mills et al., 2009; Underwood et al., 2017; Viola & Celauro, 2015).

Alternatively, the increasing the hot mix asphalt (HMA) thickness may be a viable climate change adaptation measure (Knott, Sias, et al., 2019). A study investigated factors such as seasonal average temperature, change in season length, and temperature-dependent resilient modulus to simulate the pavement response in the face of climate change. The results showed that existing base layers are performing suitably with 85% reliability. However, HMA layer thickness needs to be increased by 7 to 32% to adapt to climate change. Furthermore, Knott et al. extended the study to estimate the necessary increase in the base layer and HMA thickness due to groundwater rise, another climate change-related phenomenon (Knott et al., 2020; Knott, Jacobs, et al., 2019). The study found that temperature and groundwater rise will reduce the pavement service life, particularly in coastal regions. To prevent this, an increase in HMA and base layer thicknesses may result in more resilient pavements (Knott et al., 2020; Knott, Jacobs, et al., 2019).

Another adaptation strategy to consider is the use of stabilized subgrades. Mallick et al. have used a Monte Carlo simulation to predict the percentage of roads that will require rehabilitation 50 and 100 years into the future. Various conditions were investigated, such as no climate change, climate change and climate change with different mitigation scenarios. Among the mitigation scenarios investigated was the use of a stabilized subgrade. Overall, the study found that stabilized subgrades would result in a smaller percentage of roads needing rehabilitation than some other options under climate change conditions (Mallick et al., 2016). The study results affirm the potential behind the use of stabilized subgrades as a climate change adaptation measure, which should be further investigated. Mallick et al. also investigated the effects of employing a stabilized subgrade in combination with a modified HMA. Combining the adaptation strategies reduced the percentage of roads requiring rehabilitation both 50 and 100 years into a future of climate change. The results of the study are included in Figure 7-1 (Mallick et al., 2016).

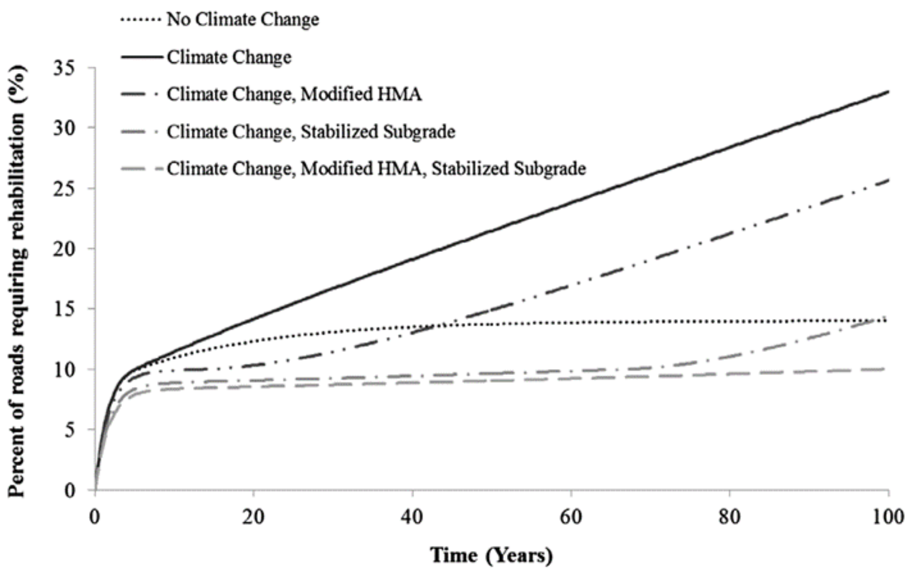

Figure 7-1: Yearly percent of roads requiring rehabilitation under climate change and various adaptation strategies (Mallick et al., 2016)

Some studies have been conducted to identify necessary maintenance and rehabilitation in future pavements. A southern Canada investigation attempted to estimate changes in the timing of maintenance requirements due to both the individual and combined influences of climate change and traffic growth (Mills et al., 2009; Tighe et al., 2008). The study found that the number of years needed to reach the 2.7 m/km IRI maintenance threshold significantly decreased due to climate change and traffic growth in two provinces. However, in Quebec, the number of years to reach the maintenance threshold increased due to climate change alone, but the number decreased when traffic growth was considered. Similarly, Qiao et al. estimated the change in pavement service life due to climate change and found that it drastically reduced (Qiao et al., 2013). Under climate change conditions, pavement should undergo frequent and earlier maintenance than what is expected today. It was observed that pavement maintenance was triggered 8-16% earlier due to climate change (Qiao et al., 2015).

7.2.4 Pavement temperature models

Pavement temperature models were used in combination with climate change predicted data to conduct the research proposed in many of the aforementioned studies. In this regard, selecting an accurate pavement temperature model is crucial for the study's success. It has been determined that some predominant pavement temperature models are restrictive in their geographic applications and do not accurately predict pavement temperatures in Canada. LTPP was developed for areas falling between the latitudes of Texas and Southern Canada and thus is not viable for Northern Canadian locations (Swarna et al., 2021). Similarly, SHRP was developed primarily with data reigning from the United States and may return errors for applications in Canada (Mohseni, 1998). A viable alternative to these popular pavement temperature models is Enhanced Integrated Climate Model (EICM), proving to predict Canadian trends more accurately (Zapata & Houston, 2008).

Highlights of Literature

Climate change is known to affect pavements around the world. A few studies have investigated the effectiveness of climate change adaptation techniques, including stabilized base layers, asphalt binder grade upgrades, and increased asphalt concrete thicknesses. All of these techniques are effective in minimizing pavement distresses related to climate change. However, there are some gaps and limitations in the previous studies:

- Previous studies have used only one or two climate change models to extract their data and determine their pavement performance. The limited use of climate change models may result in a higher degree of uncertainty, which previous studies have concluded (Gudipudi et al., 2017).

- Most studies have used LTPP or SHRP pavement temperature models to convert climate data to pavement temperatures. Previous studies found that these models have limited geographical applications and may be less accurate for northern climates (Swarna et al., 2021).
- Although several adaptation strategies have been investigated, there is limited research into the effects of combining them. Existing studies combined modified HMA and stabilized subgrades but none of the other possible adaptation strategies (Mallick et al., 2016).
- When adaptation strategies have been explored in the past, they were limited in their scope. Examining only one pavement temperature, one climatic region, or one location may prevent the conclusions from being generalized to wider applications (Gudipudi et al., 2017).

7.3 Objective and scope

The goals of this study include

a) Evaluate the pavement performance of different climate change adaptation strategies for selected locations in Canada.

b) Compare the results of the different strategies to determine an appropriate adaptation strategy for each location.

c) Develop a framework for selecting an appropriate adaptation strategy to mitigate climate change impact.

The objective of this study includes five phases

1. Select appropriate climate change models to forecast future temperatures and precipitation.
2. Extract the climate change data from the selected models for specific locations of interest within Canada.
3. Obtain relevant pavement material data from available databases. And convert daily climate data into hourly data using Modified Imposed Offset Morphing Method (M-IOMM).
4. Evaluate the pavement performance for the climate change scenarios.
5. Identify the relevant adaptation measures for each of the investigated locations within Canada.

7.4 Methodology

The methodology of this study can be described in five different phases. The first phase included collecting statistically downscaled climate change models from the online Pacific Climate database (Pacific Climate, n.d.). The second phase involved extracting the relevant daily maximum and minimum temperatures from the selected climate change models. The third phase required remaining pavement material data to be obtained and to convert the daily data into useable hourly data. The fourth phase included the analysis of the pavement performance using AASHTOWare Mechanistic-Empirical (ME) Pavement Design tool. The fifth phase incorporated the adaptation strategies to determine which ones are necessary at each investigated location.

7.4.1 Phase 1: Selecting climate change models

Pacific Climate Impacts Consortium is a climate database offering statistically downscaled climate change scenarios at grid resolutions of 1/12th degrees (300 arc-seconds or approximately 10 km) for 1950–2100. Included in these climate scenarios are variables for maximum and minimum daily temperature and average daily precipitation. These variables are available for three representative concentration pathways (RCPs) (Meinshausen et al., 2011): RCP 2.6, 4.5, and 8.5. These statistically downscaled climate models were developed using daily historical Canadian data and GCM projections (Taylor et al., 2012). The RCP level considered in this study is RCP 8.5. Among all available climate models, 10 were selected based on data availability.

The Pacific Climate database GCM sources were accessed, and the data was downscaled to a finer resolution using two statistical downscaling methods: bias correction/constructed analogs with quantile mapping reordering (BCCAQ) and bias correction spatial disaggregation. BCCAQ is a method combining quantile mapping (QMAP) (Gudmundsson et al., 2012) and bias correction/constructed analogs (BCCA) (Maurer et al., 2010). This study used models with the BCCAQ method. All climate change models used for this study were obtained and downloaded from the Pacific Climate database (Pacific Climate, n.d.).

7.4.2 Phase 2: Extracting climate data

The data requiring extraction from the climate change prediction models was daily average precipitation, daily maximum, and minimum temperatures. To extract this data, python codes were written and executed. As previously mentioned, the downscaled model is based on a square grid of 10 km by 10 km, and it was not always possible to extract data for the exact desired location. As a result, a short-distance square method was used to identify the closest grid point to the location. It was necessary to assume no differences in climate data between the exact location and the approximated nearest grid point (maximum of 7.07 km away).

7.4.3 Phase 3: Obtaining pavement materials data

Sixteen total sections were selected to estimate the pavement performance, the first fifteen being LTPP sections and the remaining one non-LTPP section. The current pavement materials, structural data, and traffic data were obtained from the LTPP database for the 15 LTPP sections. The one non-LTPP section was located in St. John's, NL and the data were collected from the Newfoundland Department of Transportation and Works (NL-DTW).

As previously mentioned, the daily maximum and minimum temperatures and daily precipitation data were determined through the climate change models. However, only hourly temperature and precipitation data are accepted as inputs in the AASHTOWare ME Pavement Design software. Therefore, the modified imposed offset morphing method (M-IOMM) was used to convert the daily maximum and minimum temperature and daily average precipitation into useable hourly data. Sailor (Sailor, 2014) and Belcher et al. (Belcher et al., 2005) used the modified imposed offset morphing method to convert monthly mean temperature to hourly temperature by shifting and stretching the data. Furthermore, Gudipudi et al. revised the methodology to obtain hourly climate data from daily maximum and daily minimum temperatures (Gudipudi et al., 2017). When evaluating the difference between the predicted pavement distress using different hourly data estimation methods, including M-IOMM, sine (14R-1), and others, it was noticed that there is no significant difference between them. The measured difference between the models ranges from -1.02% to 2.11%. The insignificant changes that were measured indicate that using M-IOMM to convert the daily data into hourly data should be sufficiently reliable.

Daily maximum temperature (T_{pM}) and daily minimum temperature (T_{pm}) were determined through the climate change models described in Phase 2. The historical daily maximum temperature (T_{hM}) and historical daily minimum temperature (T_{hm}) were determined using available historical data. Hourly predicted temperature (T_{hr}) was then computed using the historical distribution of hourly temperature (T_{hd}) from Equation 7-1.

$$T_{hr} = \frac{T_{pM} - T_{pm}}{T_{hM} - T_{hm}} \times (T_{hD} - T_{hm}) + T_{pm} \qquad \text{Equation 7-1}$$

Similarly, hourly precipitation data (P_{hr}) was derived from the daily average monthly precipitation (P_{dapm}), the historical daily average monthly precipitation (P_{dahm}), and the historical hourly precipitation (P_{hhr}) using Equation 7-2.

$$P_{hr} = \left(\frac{(P_{dapm} - P_{dahm})}{P_{dahm}} \times P_{hhr}\right) + P_{hhr} \qquad \text{Equation 7-2}$$

7.4.4 Phase 4: Evaluate pavement performance under future climate scenarios

The AASHTOWare mechanistic-empirical pavement design tool is a comprehensive software developed based on many data inputs, including material properties, traffic loading, and climate data. Employing these inputs allows the software to predict the pavement performance over the design service life while considering changes in the environmental factors and traffic loading demands. Both Level 1 and 2 inputs for all asphalt concrete (AC) layers were used in this study: layer thickness, percent effective binder, dynamic modulus, percent air voids, asphalt binder content, creep compliance, and indirect tensile strength. Similarly, both Level 1 and 2 inputs were used for subbase and subgrade layers. In this situation, Level 1 and 2 inputs include mixture gradation, Poisson’s ratio, resilient modulus, and layer thickness for the subbase. The subgrade used all the same inputs but considered the thickness as being semi-finite. The Level 1 traffic data included average annual daily traffic, two-way average annual daily truck traffic, percent traffic growth, type of growth function (i.e., linear or compound), percent vehicle class distribution, highway terrain, highway environment, monthly adjustment factor, and the number of axles per truck (i.e., single, tandem, or tridem). The climate inputs required in AASHTOWare software are hourly air temperature, percent sunshine, precipitation, wind speed, and relative humidity. A period of 30 years starting from each respective section's construction date was taken as the design life for which the performance was predicted. For this study, the reliability level was taken as 50%.

Finally, the performance of the pavement sections was computed using AASHTOWare ME Design. In total, four models— one baseline climate (1980–2010) and three future climates (2010–2040, 2040–2070, and 2070–2100)—were analyzed over 30 years to estimate the effect of climate change on pavement performance and distresses. The distresses of interest were asphalt rutting, fatigue cracking, total rutting and International Roughness Index (IRI).

7.4.5 Phase 5: Comparing climate change adaptation strategies

The first adaptation strategy investigated was to address AC rutting. Rutting was computed using AASHTOWare for both the baseline and the climate change data. If the rutting was worse under the climate change scenario, it was determined that an adaptation strategy was necessary. The upgrading of the asphalt binder was first attempted to address the rutting problems. If the rutting under climate change using the upgraded binder was less than the baseline scenario, the suggested adaptation measure was identified as upgrading the binder. If not, further measures were investigated.

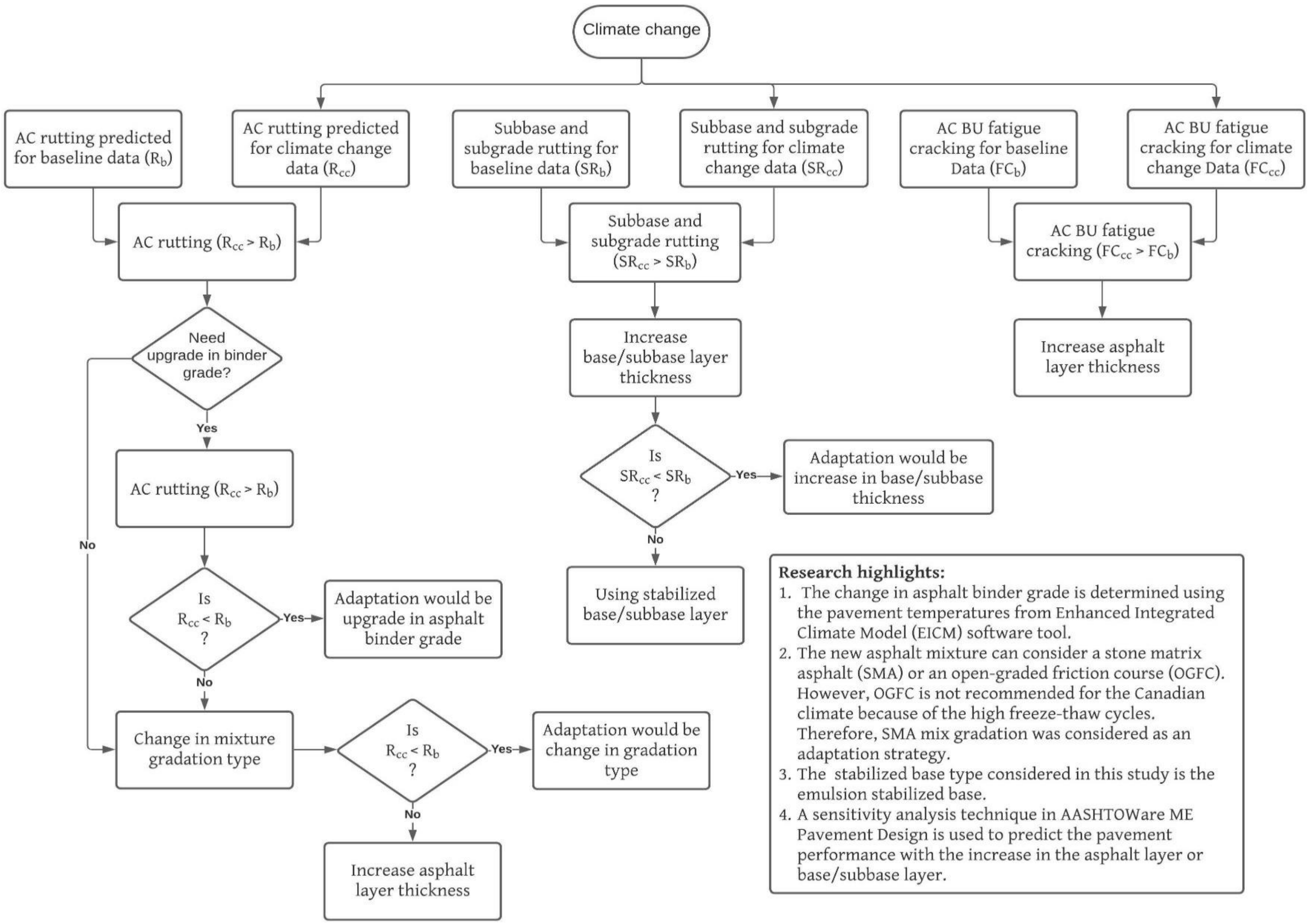

Figure 7-2: Methodology for the implementation of adaptation strategies

Where the upgraded binder failed to ameliorate the rutting, the different mixture gradation (SMA) was considered. The asphalt mixture used for baseline climate is dense-graded mix for all the pavement sections. The mixture gradation can be a stone matrix asphalt (SMA), or an open-graded friction course (OGFC). However, OGFC is not recommended for the Canadian climate because of the high freeze-thaw cycles (Uzarowski et al., 2008). Therefore, SMA mixture gradation was considered as an adaptation strategy. Again, the rutting with the changed mixture gradation was compared to the baseline scenario to determine if the strategy was suitable. If it was found that rutting was still a problem, the final strategy was to increase the layer of asphalt thickness. The order in which these adaptation strategies were explored was selected to provide the most economical solution, exploring the more minor measures first.

The following adaptation strategy was targeted at improving subgrade and subbase rutting. The same initial process was followed to determine if an adaptation strategy was necessary, and if it was, the thickness of the base layers was increased. The base layers' performance with increased thickness was evaluated, and if rutting was still occurring, a stabilized base/subbase layer was suggested instead. The final adaptation strategy investigated was to address AC bottom-up fatigue cracking. When present, fatigue cracking was mitigated using an increased asphalt layer thickness. The outline of these adaptation strategies is presented in Figure 7-2.

7.5 Results and discussion

Figure 7-3 illustrates the percentage change in pavement performance under climate change for 16 locations across Canada. In addition, Figure 7-4 illustrates the percentage change in pavement performance for different climate change models. From Figure 7-3 and Figure 7-4, following conclusions can be made:

- IRI decreases slightly across nine of the 16 sections and significantly for one. Although the frequency and severity of distresses are increasing, the reduced freezing index and freeze-thaw cycles might improve roughness for over half of the locations. The significant decrease in IRI in Saskatoon is likely related to a much more significant decrease in the freezing index at this location.
- Higher temperatures across all of the locations resulted in an increase in AC rutting throughout Canada.
- Subgrade and subbase rutting are decreasing across all selected locations apart from Vancouver. As Vancouver is known for severe precipitation, which is also further increasing under climate change, there will be an increase in subgrade rutting. The other parts of Canada will see more dry weather resulting in less deterioration of base layers.
- Bottom-up fatigue cracking increases by an average of 12% for all sections except Ottawa and Quebec City. These locations overestimate traffic in their pavement design and have thus already adapted to climate change in this regard.
- Despite reducing base layer rutting at many locations, total rutting increases for 12 of the 16 locations. This is due to the severity of AC rutting throughout all locations, increasing by up to 60% in the worst-case situations.
- The increase in uncertainty over time in a climate change model reflects to the predicted pavement performance, which is quite evident in Figure 7-4. Therefore, average of pavement performance predicted for ten climate models is considered to quantify the climate change impact.

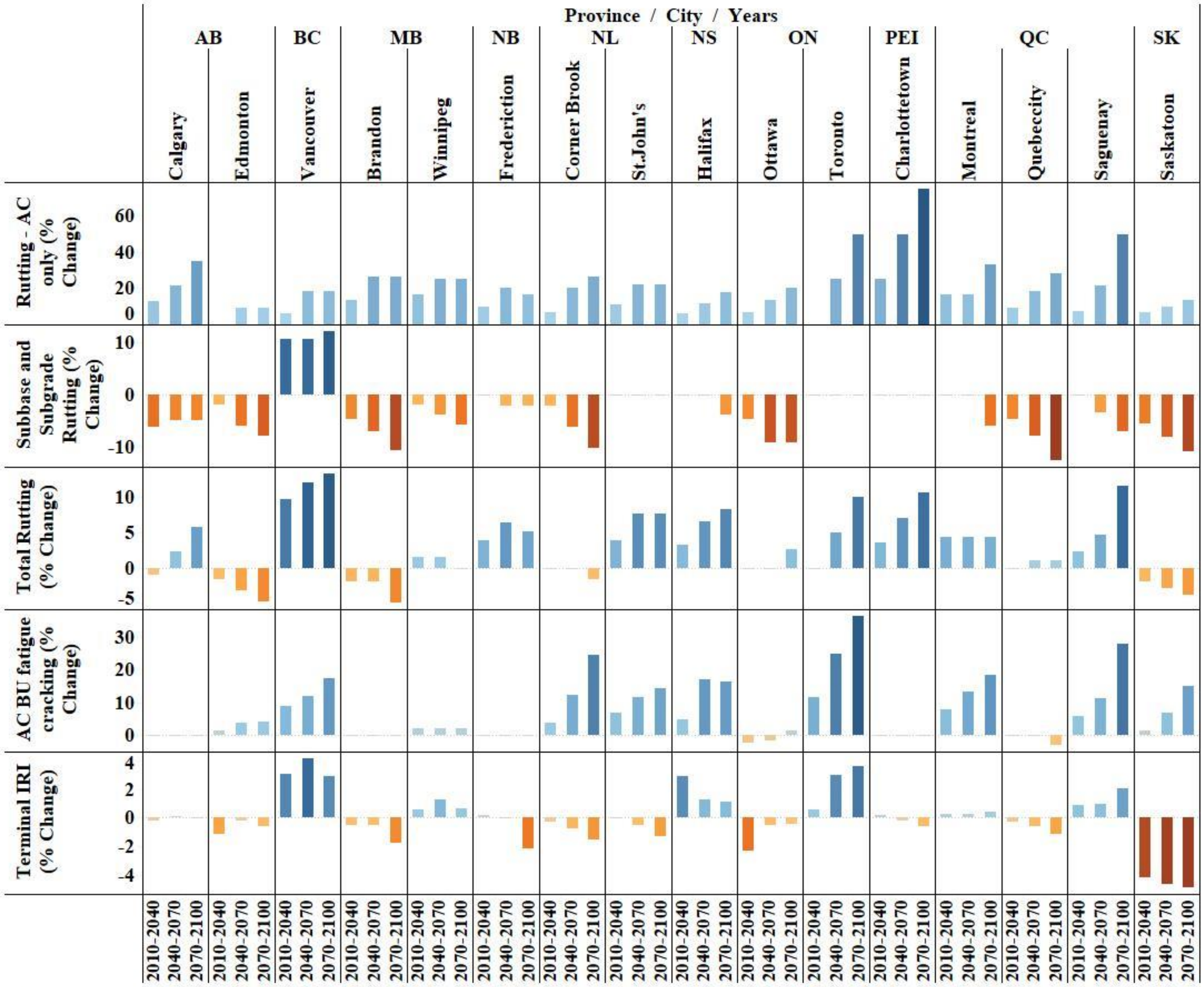

This plot represents the impact of climate change on pavement performance

The bars presented in this plot are the percentage change in performance parameters for future years with respect to baseline/historical climate. For example, in Calgary, the AC rutting is increasing by 13.04% for 2010-2040 when compared to 1980-2010. Similarly, the AC rutting is increasing by 21.74% and 34.78% for 2040-2070 and 2070-2100, respectively wrt. 1980-2010.

Figure 7-3: Percentage change in pavement performance parameters due to climate change compared to baseline climate (1980-2010) (Swarna et al., 2021)

Note: AC = Asphalt Concrete, BU = Bottom-Up, IRI = International Roughness Index

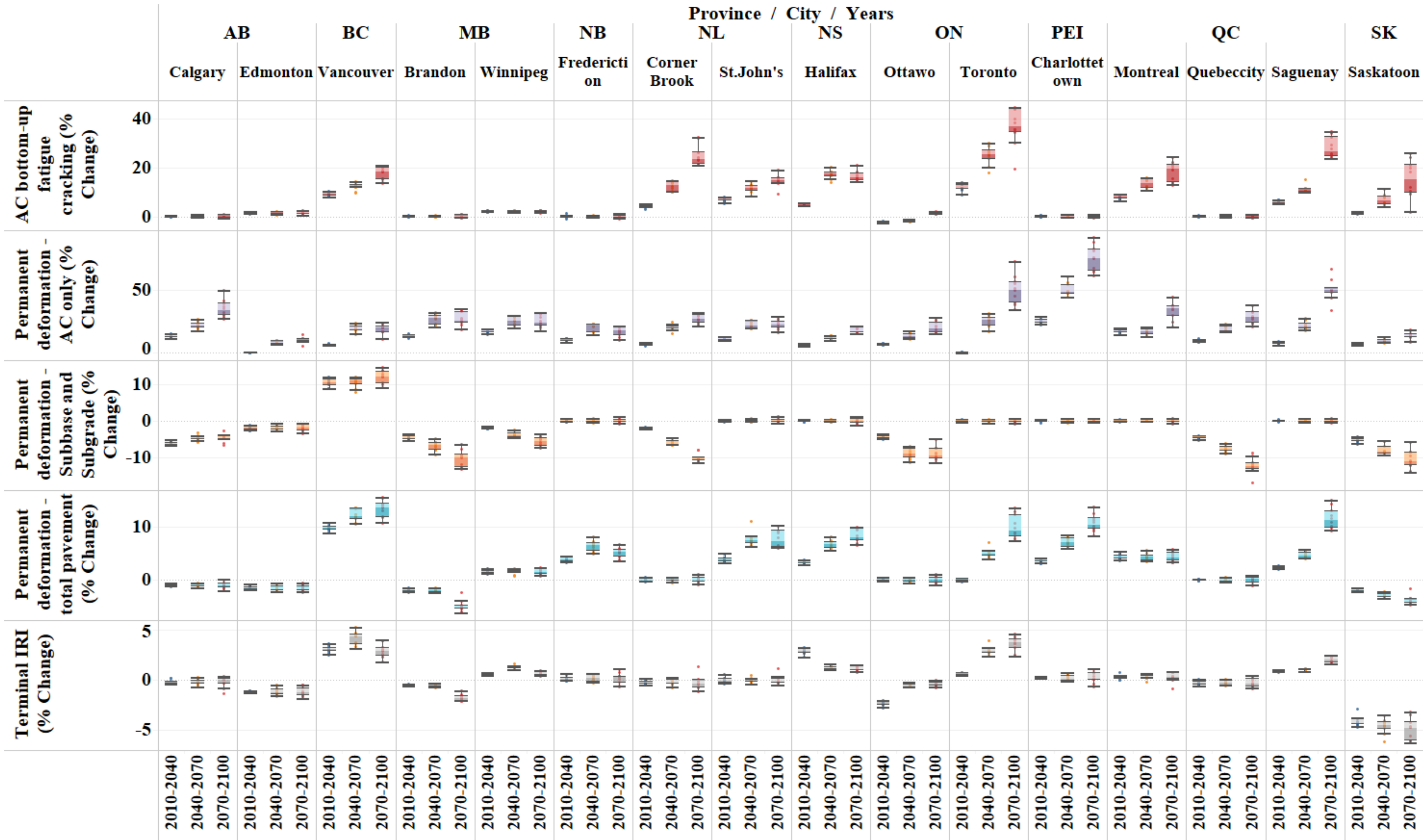

Figure 7-4: Percentage change in pavement performance parameters for various climate change models compared to baseline climate (1980-2010)

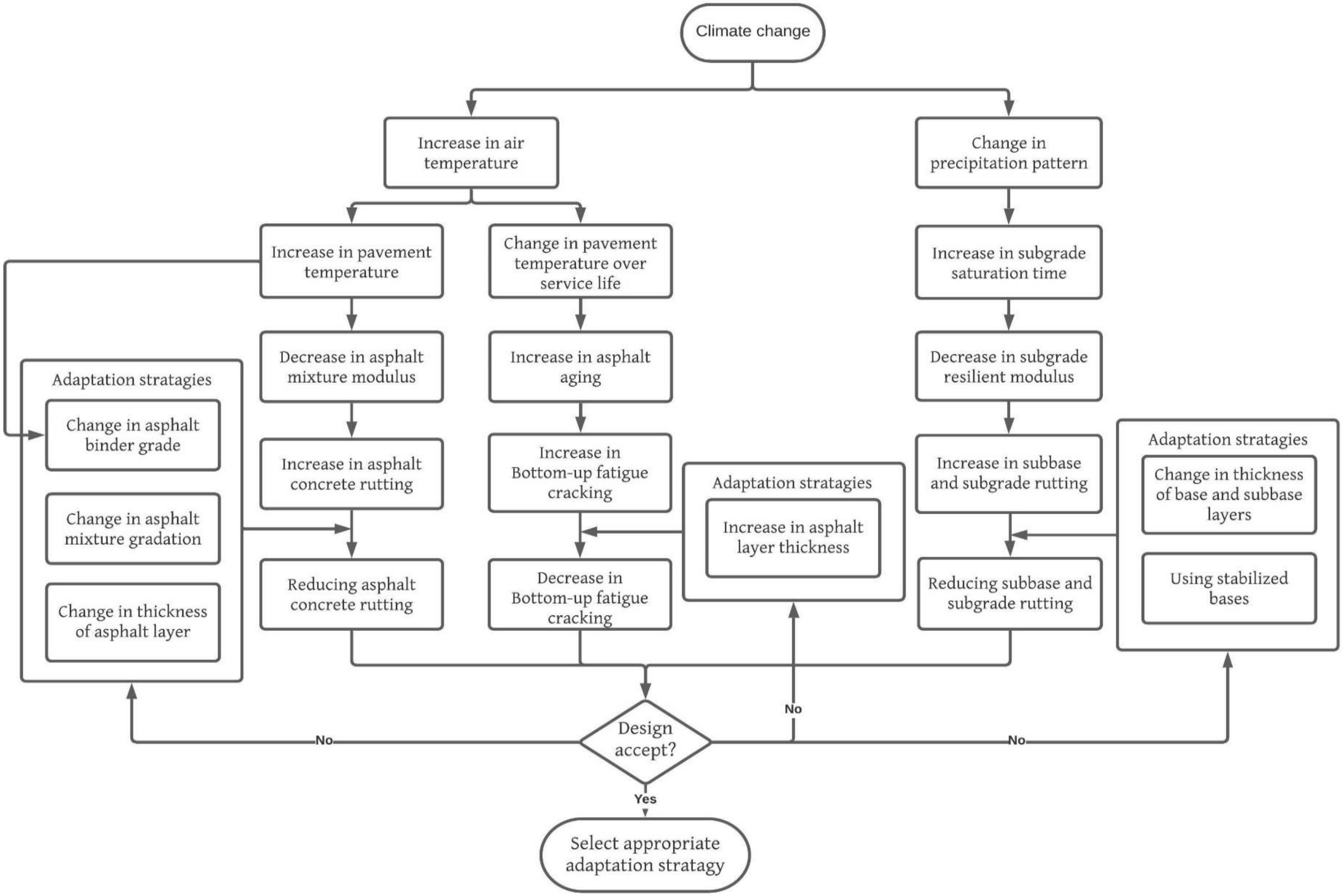

1

2 Figure 7-5: Use of various adaptation strategies based on the cause of pavement distress

It is well known that climate change leads to an increase in air temperature and precipitation. This increase in air temperature leads to an increase in pavement temperature, which decreases the elastic modulus of the asphalt concrete layer. This decrease in elastic modulus makes the asphalt mixture soft, leading to an increase in AC rutting. To mitigate this increase in AC rutting, three different adaptation strategies are considered to stiffen the mixture by increasing the elastic modulus of the AC layer. The adaptation strategies considered are (a) change in binder grade (determined using EICM pavement temperatures), (b) change in asphalt mixture gradation (using stone matrix asphalt mixture gradation) and (c) increase in the thickness of the AC layer. These adaptation strategies are attempted and found to be an appropriate strategy depending on the field condition and climatic region. However, an increase in stiffening of the layer could lead to an increase in AC BU fatigue cracking. Therefore, all other distresses were predicted and verified to select the appropriate strategy.

It is also noted that the increase in pavement temperature could increase the aging of the asphalt binder. This increase in aging stiffens the asphalt mixture, especially for thin pavements, which further increases bottom-up fatigue cracking. Therefore, an increase in AC layer thickness was considered as an adaptation strategy. This increase in thickness can decrease the tensile strains occurring at the bottom of the AC layer, reducing the AC BU fatigue cracking.

In addition to the air temperature, increase precipitation also has a significant influence on pavement performance. An increase in precipitation could increase the infiltration of water into the subgrade. This infiltration could increase the saturation of subbase and subgrade layers, which leads to a decrease in the resilient modulus of subgrade. This could be the reason for an increase in subbase and subgrade rutting. To mitigate this, two adaptation strategies are considered. The adaptation strategies considered are (a) increase in base layer thickness and (b) change in the base type. These adaptation strategies can increase the horizontal permeability of the base layer, resulting in high runoff and giving a solid foundation to the AC layer. The outline of all these adaptation strategies is illustrated in Figure 7-2 and Figure 7-5.

Table 7-1: Change in asphalt binder grade for the selected location in Canada for future climate

Province	**City**	**Base Binder**	**Upgraded Binder Grade**		
		1980 - 2010	**2010 - 2040**	**2040 - 2070**	**2070 - 2100**
BC	Vancouver	PG 52-16	PG 58-16	PG 58-16	PG 64-10
AB	Calgary	PG 52-40	PG 58-40	PG 64-34	PG 64-34
AB	Edmonton	PG 52-46	PG 58-40	PG 58-40	PG 58-34
SK	Saskatoon	PG 52-52	PG 58-40	PG 58-34	PG 64-34
MB	Brandon	PG 52-46	PG 58-34	PG 58-34	PG 58-28
MB	Winnipeg	PG 58-40	PG 58-40	PG 58-34	PG 58-34
ON	Toronto	PG 58-28	PG 58-28	PG 64-28	PG 64-22
ON	Ottawa	PG 58-34	PG 64-34	PG 64-34	PG 64-28
QC	Montreal	PG 58-34	PG 58-34	PG 58-28	PG 64-28
QC	Quebec City	PG 58-34	PG 58-34	PG 58-28	PG 64-28
QC	Saguenay	PG 58-34	PG 52-34	PG 58-34	PG 58-28
NB	Fredericton	PG 58-34	PG 58-34	PG 58-28	PG 58-22
PEI	Charlottetown	PG 52-34	PG 52-28	PG 52-22	PG 52-22
NS	Halifax	PG 52-28	PG 64-22	PG 64-22	PG 64-22
NL	Corner Brook	PG 52-28	PG 52-28	PG 52-28	PG 52-22
NL	St. John's	PG 52-28	PG 58-22	PG 58-22	PG 58-16

Note: AB = Alberta, BC = British Columbia, MB = Manitoba, NB = New Brunswick, NL = Newfoundland and Labrador, NS = Nova Scotia, ON = Ontario, PG =Performance grade, PEI = Prince Edward Island, QC = Quebec, SK = Saskatchewan.

Table 7-1 details the recommended upgraded binder grades for 16 locations across Canada.

The upgraded binders were obtained by inputting climate change weather trends into EICM and determining the corresponding predicted pavement temperatures. Superpave binder selection procedures were followed to determine which binder grade is suitable for each predicted maximum and minimum pavement temperature.

Only 6 of the 16 locations are presently employing the correct asphalt binder grade. The rest all require an upgrade. However, all locations will require a binder grade review by 2040. An even more significant review will be required by 2070.

As explained in Methodology Phase 5, various adaptation strategies are utilized to determine the optimum strategy to mitigate the climate change impact on pavements. Pavement performance indices for four different locations are presented in Figure 7-6. For the first location (Edmonton), an upgrade in asphalt binder grade alone is enough to quell the climate change impact. However, in other locations presented in this figure, the upgrade in asphalt binder alone is not enough to mitigate climate change. Therefore, for the second location (Toronto), a change in mixture gradation is implemented along with an upgrade in binder grade. This adaptation mitigated the climate change influence.

Similarly, the same practice is attempted for the third location (St. John's), but this adaptation leads to an increase in total and AC rutting. Therefore, after upgrading the asphalt binder grade, the increase in the thickness of the asphalt layer is considered to adapt to climate change. Unlike the adaptation strategy for Toronto, the adaptation strategy for St. John’s is upgrading the asphalt binder grade and increasing the thickness of the AC layer. For the fourth location (Vancouver), as AC and subbase and subgrade rutting are high, an upgrade in asphalt binder grade and change in case type are considered. However, this leads to an increase in BU fatigue cracking in the pavement. Therefore, the AC layer thickness is increased to reduce the AC

BU fatigue cracking. Finally, for the fourth location, three changes are considered in the design, (1) upgrade in binder grade, (2) change in the base type, and (3) increase in asphalt layer thickness. A similar procedure is followed for all the selected locations in Canada to determine the appropriate adaptation strategy.

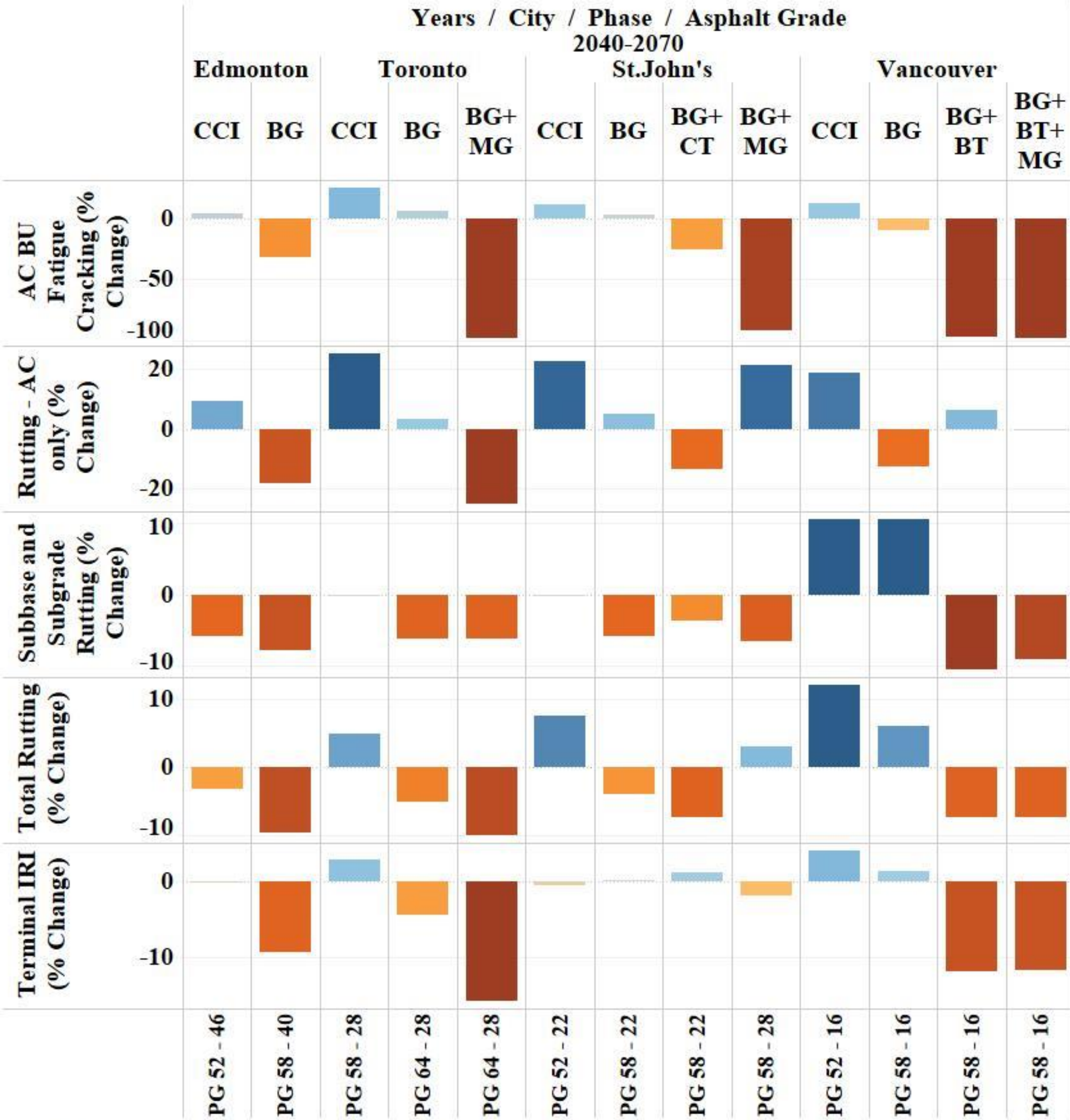

This plot represents the influence of various adaptation stratagies on pavement performance for future climate
The bars presented in this plot are the percentage change in performance parameters for various adaptation stratagies with respect to performance for baseline climate . For example, in Edmonton, the AC rutting is decreasing by 18.18% with an upgraded in asphalt binder (PG 58-40). Similarly, in Toronto, the AC rutting is reducting from 25.21% to 3.03% with the change in asphalt binder grade (PG 64-28), futher with the change in gradation, the AC rutting is reduced to -6.25%.

Figure 7-6: Adaptation strategies for various locations with distress parameters

Note: AC = Asphalt Concrete, BU = Bottom-Up, CCI = Climate change impact, BG = Change in asphalt binder grade, BT = Change in the base type, CT = Change in asphalt layer thickness, IRI

= International Roughness Index, MG = Change in asphalt mixture gradation.

Table 7-2: Appropriate adaptation strategies for selected locations

City ID	Province	City	Adaptation Strategy		
			2010-2040	**2040-2070**	**2070-2100**
BC_00	BC	Vancouver	BG+BT	BG+MG+BT	BG+BT
AB_01	AB	Calgary	BG	BG	BG
AB_02	AB	Edmonton	BG	BG	BG
SK_03	SK	Saskatoon	BG	BG	BG
MB_04	MB	Brandon	BG	BG	BG
MB_05	MB	Winnipeg	MG	BG+MG	BG
ON_06	ON	Toronto	MG	BG+MG	BG+MG
ON_07	ON	Ottawa	BG	BG	BG+MG
QC_08	QC	Montreal	MG	MG	BG
QC_09	QC	Quebec City	MG	BG	BG+MG
QC_10	QC	Saguenay	MG	MG	BG+MG
NB_11	NB	Fredericton	BG	BG	BG
PEI_12	PEI	Charlottetown	BG+MG	BG+MG	BG+MG+CT
NS_13	NS	Halifax	BG	BG	BG
NL_14	NL	Corner Brook	MG	MG	BG+MG
NL_15	NL	St. John's	BG	BG+CT	BG+MG

Note: AB = Alberta, BC = British Columbia, BG = Change in asphalt binder grade, BT = Change in the base type, CT = Change in asphalt layer thickness, MB = Manitoba, MG = Change in asphalt mixture gradation, NB = New Brunswick, NL = Newfoundland and Labrador, NS = Nova Scotia, ON = Ontario, PEI = Prince Edward Island, QC = Quebec, SK = Saskatchewan.

For the selected sixteen locations, the appropriate adaptation strategies were determined and illustrated in Table 7-2. From Table 7-2, it was noted that most of the locations need an upgrade in asphalt binder grade. In the 2010-2040 time period, it was found that the change in binder grade and change in mixture gradation are the only adaptation strategies needed to reduce the climate change impact in all locations except for Vancouver. As Vancouver falls under the high precipitation region, there is a need to change the base type to control the subbase and subgrade rutting. Similarly, for 2040-2070, a change in asphalt binder grade and change in mixture gradation are sufficient for most of the selected locations except the easternmost and westernmost locations in Canada (St. John's and Vancouver). However, in the 2070-2100 time period, all the locations need a change in binder grade, and most of the locations need a change in mixture gradation to compensate for the increased distresses due to climate change.

In the Atlantic Provinces, most of the locations need a change in binder grade and mixture gradations. However, some of the locations need an increase in the thickness of the surface AC layer. Similarly, in Central Canada (Ontario and Quebec), asphalt binder grade and mixture gradation changes are more than enough to mitigate climate change. In the Prairie Provinces (Manitoba, Saskatchewan, and Alberta), a change in asphalt binder grade alone can adapt to climate change. However, unlike all other locations, a change in asphalt binder grade and the base type is needed to mitigate climate change impact in the West Coast region.

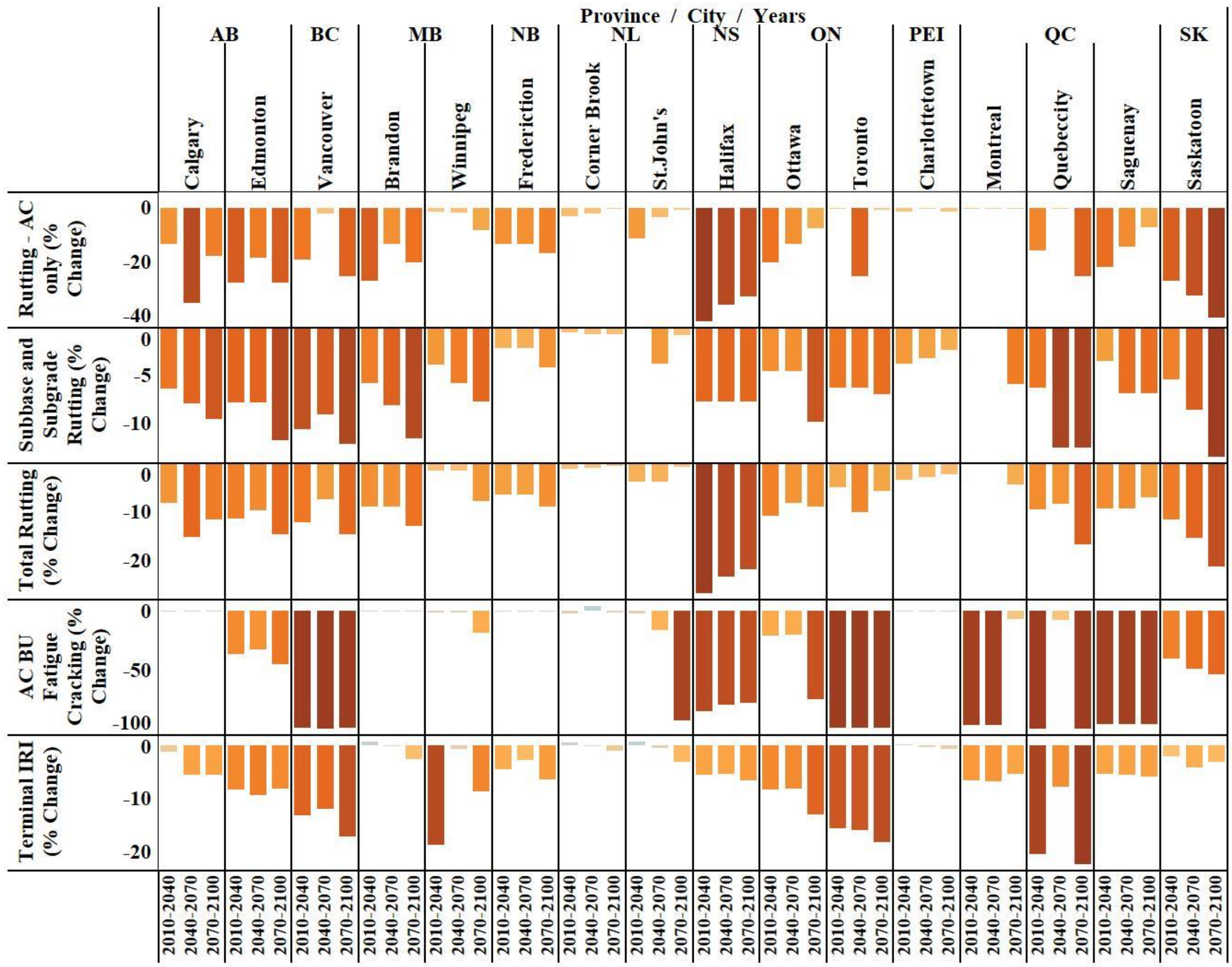

This plot represents the influence of various adaptation stratagies on pavement performance for future climate
The bars presented in this plot are the percentage change in performance parameters for various adaptation stratagies with respect to baseline climate. For example, in Calary, the AC rutting is decreasing by 13.04% for 2010-2040 with an appropriate adaptation stratagy. Similarly, the AC rutting is decreasing by 34.78% and 17.39% for 2040-2070 and 2070-2100, respectively, with the appropriate adaptation stratagy.

Figure 7-7: Percentage change in pavement performance with various adaptation strategies compared to baseline climate

Note: AC = Asphalt Concrete, BU = Bottom-Up, IRI = International Roughness Index

With the appropriate adaptation strategies, the pavement performance was predicted again, and a percentage change in performance was determined with respect to baseline climate, as presented in Figure 7-7. The outcomes from Figure 7-7 are as follows:

- With the use of appropriate adaptation strategies, all the pavement distresses could be reduced for all selected locations.
- Asphalt concrete rutting decreased by an average of 18.67% with the use of an appropriate adaptation strategy. In addition, the AC rutting decreased by a maximum of 39.92% for Saskatoon sections with a change in binder grade and reduced by a minimum of 0.28% for the Corner Brook section with a change in asphalt binder grade and mixture gradation.
- Subbase and subgrade rutting decreased with climate change for all the locations except for Vancouver. Therefore, for the Vancouver section, an emulsion stabilized base is used to restrict the increase in subbase and subgrade rutting. This adaptation led to an average of 9.21% reduction in subbase and subgrade rutting. The subbase and subgrade rutting are further reduced with a change in binder grade and mixture gradation in other sections.
- With an appropriate adaptation strategy, the total rutting is also decreased by an average of 10.54%.
- As one of the major adaptation strategies is upgrading binder grade, the BU fatigue cracking is expected to increase. However, the BU fatigue cracking decreased with the use of a stiff binder. This reduction could be because of increased temperatures due to climate change, where the stiffer binder is no longer stiff at temperature. In addition, with the change in mixture gradation, the BU fatigue cracking is drastically reduced.
- As expected, with appropriate adaptation strategies, the IRI was reduced by an average of 9.01%.

7.6 Conclusions and recommendations

In this current study, the severities of climate change impact on pavement distresses were computed using 10 different climate change models. Various adaptation strategies such as upgrading asphalt binder grade, increasing the thickness of asphalt concrete layer, increasing the base layer thickness, and using stabilized base layers were analyzed to reduce pavement deterioration and to extend the service life of the pavement. In addition to this, various combinations of adaptation strategies are considered to mitigate the climate change impact. Unlike the other studies, pavement temperatures were determined using EICM to evaluate the change in binder grade for the future climate in the adaptation process. A stone matrix asphalt mixture gradation is considered as another adaption strategy where the AC rutting is found to be very high. To reduce the subbase and subgrade rutting, an emulsion stabilized base is adapted for specific locations. Various conclusions drawn from this study are as follows:

- Only six of the sixteen selected locations in Canada are presently employing the correct asphalt binder grade. The rest all require an upgrade. However, all locations will require a binder grade review by 2040. An even more significant review will be required by 2070.
- For 2010-2040 climate, a change in asphalt binder grade and a change in mixture gradation are the only necessary adaptation strategies to reduce climate change impacts on all the locations apart from Vancouver.
- For 2040-2070 climate, a change in asphalt binder grade and a change in mixture gradation are still sufficient for most of the selected locations, but not in St. John's or Vancouver, which require additional measures.
- For 2070-2100 climate, all the selected locations require a change in binder grade, and the majority also need a change in mixture gradation to compensate for the increased climate change related pavement distresses.
- Most of the locations in the Atlantic provinces require a change in binder and mixture gradation. However, some of the locations require an increase in the thickness of the

surface AC layer as well. In Central Canada, upgrade in asphalt binder grade and mixture gradation change are sufficient to mitigate climate change. However, in the Prairie Provinces, a change in asphalt binder grade alone can adapt to climate change.

- A change in asphalt binder grade and the base type are needed in the West Coast region to mitigate climate change impact. This is mainly because of the significant increase in precipitation due to climate change.
- The study resulted in a framework for selecting appropriate adaptation strategy to mitigate climate change impact.
- With the use of appropriate adaptation strategies, all the pavement distresses are reducing more the threshold limits for all selected locations.
- Considering climate change in the design procedure could improve pavement performance and enhance pavement service life.

7.7 Contributions/limitations

7.7.1 Contributions:

- Ten different statically downscaled climate change models were considered to reduce the uncertainty involved with the climate change models.
- A statistically downscaled models using bias correction/constructed analogs with quantile mapping reordering (BCCAQ) downscaling technique are considered in this research to improve the accuracy of the climate data.
- Enhanced Integrated Climate Model (EICM) tool to determine the pavement temperatures accurately, which was further used to determine the change in asphalt binder grade for future climate.

- This study considered the variability in locations, pavement structures, and climatic regions to generalize the conclusions extracted from this study.
- The influence of various adaptation strategies and their combinations on pavement performance or service life was quantified in this current study.

7.7.2 Limitations:

- Conclusions drawn in this study were made exclusively with AASHTOWare analysis.
- Within each Canadian province, only one or two cities were considered to determine the climate change impact.
- The local calibration factors for the AASHTOWare Pavement ME model are available only for 5 out of 16 locations investigated in this study. The pavement performance factors were computed using global calibration factors instead, which might affect the predicted results for the remaining locations.

7.8 Reference

Barbi, P., Tavassoti, P., Tighe, S., & Baaj, H. (2021). Implications of climate variation in flexible airport pavement design and performance. *Airfield and Highway Pavements 2021: Airfield Pavement Technology - Selected Papers from the International Airfield and Highway Pavements Conference 2021*, 193–204. https://doi.org/10.1061/9780784483527.017

Belcher, S. E., Hacker, J. N., & Powell, D. S. (2005). Constructing design weather data for future climates. *Building Services Engineering Research and Technology*, *26*(1), 49–61. https://doi.org/10.1191/0143624405bt112oa

Bizjak, K. F., Dawson, A., Hoff, I., Makkonen, L., Ylhaisi, J. S., & Carrera, A. (2014). The impact of climate change on the European road network The impact of climate change on the European road network. *Proceedings of the Institution of Civil Engineers*, *167*(5), 281–295. https://doi.org/10.1680/tran.11.00072

Delgadillo, R., Arteaga, L., Wahr, C., Alcafuz, R., Delgadillo, R., Arteaga, L., Wahr, C., & Alcafuz, R. (2018). The influence of climate change in Superpave binder selection for Chile. *Road Materials and Pavement Design*, *0*(0), 1–16. https://doi.org/10.1080/14680629.2018.1509803

Fletcher, C. G., Matthews, L., Andrey, J., & Saunders, A. (2016). Projected changes in mid-twenty-first-century extreme maximum pavement temperature in Canada. *Journal of Applied Meteorology and Climatology*, *55*(4), 961–974. https://doi.org/10.1175/JAMC-D-15-0232.1

Gudipudi, P. P., Underwood, B. S., & Zalghout, A. (2017). Impact of climate change on pavement structural performance in the United States. *Transportation Research Part D: Transport and Environment*, *57*, 172–184. https://doi.org/10.1016/j.trd.2017.09.022

Gudmundsson, L., Bremnes, J. B., Haugen, J. E., & Engen-Skaugen, T. (2012). Technical Note: Downscaling RCM precipitation to the station scale using statistical transformations - A comparison of methods. *Hydrology and Earth System Sciences*, *16*(9), 3383–3390. https://doi.org/10.5194/hess-16-3383-2012

Haslett, K. E., Knott, J. F., Stoner, A. M. K., Sias, J. E., Dave, E. V., Jacobs, J. M., Mo, W., & Hayhoe, K. (2021). Climate change impacts on flexible pavement design and rehabilitation practices. *Road Materials and Pavement Design*. https://doi.org/10.1080/14680629.2021.1880468

Humphrey, N. (2008). Potential impacts of climate change on U.S. Transportation. *TR News*, *256*, 21–24. https://doi.org/10.17226/12179

Knott, J. F., Jacobs, J. M., Sias, J. E., Kirshen, P., & Dave, E. V. (2019). A Framework for Introducing Climate-Change Adaptation in Pavement Management. *Sustainability*, *11*(1). https://doi.org/http://dx.doi.org/10.3390/su11164382

Knott, J. F., Sias, J. E., Dave, E. V, & Jacobs, J. M. (2019). *Seasonal and Long-Term Changes to Pavement Life Caused by Rising Temperatures from Climate Change*. *2673*(6), 267–278. https://doi.org/10.1177/0361198119844249

Knott, J. F., Sias, J. E., Jacobs, J. M., Krishen, P., & Dave, E. V. (2020). Designing a Climate-Ready Coastal Road. *99th Annual Meeting of the Transportation Research Board (TRB) of National Academies of Science and Engineering, Washington DC*.

Mallick, R., Jacobs, J. M., Miller, B. J., & Daniel, J. S. (2016). Understanding the impact of climate change on pavements with CMIP5, system dynamics and simulation. *International Journal of Pavement Engineering*, *19*(8), 697–705. https://doi.org/10.1080/10298436.2016.1199880

Maurer, E. P., Hidalgo, H. G., Das, T., Dettinger, M. D., & Cayan, D. R. (2010). The utility of daily large-scale climate data in the assessment of climate change impacts on daily streamflow in California. *Hydrology and Earth System Sciences*, *14*(6), 1209–1241. https://doi.org/10.5194/hess-14-1125-2010

Meagher, W., Daniel, J. S., Jacobs, J., & Linder, E. (2012). *Method for Evaluating Implications of Climate Change for Design and Performance of Flexible Pavements*. *2305*, 111–120. https://doi.org/10.3141/2305-12

Meinshausen, M., Smith, S. J., Calvin, K., Daniel, J. S., Kainuma, M. L. T., Lamarque, J., Matsumoto, K., Montzka, S. A., Raper, S. C. B., Riahi, K., Thomson, A., Velders, G. J. M.,

& van Vuuren, D. P. P. (2011). The RCP greenhouse gas concentrations and their extensions from 1765 to 2300. *Climatic Change*, *109*(1), 213–241. https://doi.org/10.1007/s10584-011-0156-z

Mills, B., Tighe, S., Andrey, J., Smith, J., & Huen, K. (2009). Climate Change Implications for Flexible Pavement Design and Performance in Southern Canada. *Journal of Transportation Engineering*, *135*(10), 773–782. https://doi.org/10.1061/(asce)0733-947x(2009)135:10(773)

Mohseni, A. (1998). *LTPP Seasonal Asphalt Concrete Pavement Temperature Models*.

Moss, R. H., Edmonds, J. A., Hibbard, K. A., Manning, M. R., Rose, S. K., Van Vuuren, D. P., Carter, T. R., Emori, S., Kainuma, M., Kram, T., Meehl, G. A., Mitchell, J. F. B., Nakicenovic, N., Riahi, K., Smith, S. J., Stouffer, R. J., Thomson, A. M., Weyant, J. P., & Wilbanks, T. J. (2010). The next generation of scenarios for climate change research and assessment. *Nature*, *463*(7282), 747–756. https://doi.org/10.1038/nature08823

Pacific Climate. (n.d.). *Statistically Downscaled Climate Scenarios*.

Qiao, Y., Dawson, A. R., Parry, T., & Flintsch, G. W. (2015). Evaluating the effects of climate change on road maintenance intervention strategies and Life-Cycle Costs. *Transportation Research Part D: Transport and Environment*, *41*, 492–503. https://doi.org/10.1016/j.trd.2015.09.019

Qiao, Y., Flintsch, G., Dawson, A., & Parry, T. (2013). Examining Effects of Climatic Factors on Flexible Pavement Performance and Service Life. *Transportation Research Record: Journal of the Transportation Research Board*, *2349*(1), 100–107. https://doi.org/10.3141/2349-12

Sailor, D. J. (2014). Risks of summertime extreme thermal conditions in buildings as a result of climate change and exacerbation of urban heat islands. *Building and Environment*, *78*, 81–

88. https://doi.org/10.1016/j.buildenv.2014.04.012

Schweikert, A., Chinowsky, P., Espinet, X., & Tarbert, M. (2014). Climate change and infrastructure impacts: Comparing the impact on roads in ten countries through 2100. *Procedia Engineering*, *78*, 306–316. https://doi.org/10.1016/j.proeng.2014.07.072

Shao, Z., Jenkins, G., & Oh, E. (2017). Assessing the impacts of climate change on road infrastructure. *International Journal of GEOMATE*, *13*(38), 120–128.

Stocker, T. F., Qin, D., Plattner, G.-K., Tignor, M., Allen, S. K., Boschung, J., Nauels, A., Xia, Y., Bex, V., & Midgley, P. M. (2013). Climate change 2013: The physical science basis. In *Contribution of working group I to the fifth assessment report of the intergovernmental panel on climate change*. https://doi.org/10.1017/CBO9781107415324.Summary

Stoner, A. M. K., Daniel, J. S., Jacobs, J. M., Hayhoe, K., & Scott-fleming, I. (2019). *Quantifying the Impact of Climate Change on Flexible Pavement Performance and Lifetime in the United States*. https://doi.org/10.1177/0361198118821877

Swarna, S. T., Hossain, K., Pandya, H., & Mehta, Y. A. (2021). Assessing Climate Change Impact on Asphalt Binder Grade Selection and its Implications. *Transportation Research Record: Journal of the Transportation Research Board*, 1–14. https://doi.org/10.1177/03611981211013026

Taylor, K. E., Stouffer, R. J., & Meehl, G. A. (2012). An overview of CMIP5 and the experiment design. *Bulletin of the American Meteorological Society*, *93*(4), 485–498. https://doi.org/10.1175/BAMS-D-11-00094.1

Tighe, S., Mills, B., Tighe, S. L., Smith, J., Mills, B., & Andrey, J. (2008). Evaluating Climate Change Impact on Low- Volume Roads in Southern Canada on Low-Volume Roads in

Southern Canada. *Transportation Research Record: Journal of the Transportation Research Board*, *2053*(1), 9–16. https://doi.org/10.3141/2053-02

Underwood, S., Guido, Z., Gudipudi, P., & Feinberg, Y. (2017). Increased costs to US pavement infrastructure from future temperature rise. *Nature Climate Change*, *7*(10), 704–707. https://doi.org/10.1038/nclimate3390

Uzarowski, L., Moore, G., & Gamble, P. (2008). Innovative, comprehensive design and construction of perpetual pavement on the Red Hill Valley Parkway in Hamilton. *TAC/ATC 2008 - 2008 Annual Conference and Exhibition of the Transportation Association of Canada: Transportation - A Key to a Sustainable Future*.

Viola, F., & Celauro, C. (2015). Effect of climate change on asphalt binder selection for road construction in Italy. *Transportation Research Part D: Transport and Environment*, *37*, 40–47. https://doi.org/10.1016/j.trd.2015.04.012

Wigley, T. M. L., Clarke, L. E., Edmonds, J. A., Jacoby, H. D., Paltsev, S., Pitcher, H., Reilly, J. M., Richels, R., Sarofim, M. C., & Smith, S. J. (2009). Uncertainties in climate stabilization. *Climatic Change*, *97*(1), 85–121. https://doi.org/10.1007/s10584-009-9585-3

Wistuba, M. P., & Walther, A. (2013). Consideration of climate change in the mechanistic pavement design. *Road Materials and Pavement Design*, *14*(SUPPL.1), 227–241. https://doi.org/10.1080/14680629.2013.774759

Zapata, C. E., & Houston, W. N. (2008). *Calibration and Validation of the Enhanced Integrated Climatic Model for Pavement Design*. Transportation Research Board. https://doi.org/10.17226/23098

Chapter 8: LCA and LCCA of Climate Change Adaptation Strategies for Canadian Pavements

8.1 Abstract

Presently, there is a strong consensus that significant weather changes are fast approaching as a result of the onset of climate change. Pavements will be significantly affected by increased temperatures, precipitation, and flooding, and will require present design methodology to be modified accordingly. Several climate change adaptation strategies are available to agencies including upgraded asphalt binder grades, increased HMA thickness, modified mix gradations, and stabilized subgrades. The objective of this study is to conduct and investigate Life Cycle Assessment (LCA) and Life Cycle Cost Analysis (LCCA) for climate change adaptation strategies across various locations in Canada. The environmental and economic impact for three different scenarios in Canada. The investigated scenarios were (i) baseline asphalt pavement with no climate change, (ii) a baseline pavement with climate change, and (iii) an asphalt pavement adapted to withstand climate change. The study revealed that although there are initial increases in both cost and emission to administer these adaptation strategies, they are offset over the life of the pavements. Increasing the HMA thickness and using stabilized subgrades were the most expensive and the highest emitting among the investigated strategies, but they are only necessary for extreme coastal climate change regions including British Columbia and Newfoundland. Even in these locations, it was found that administering an adaptation strategy would significantly reduce use phase emissions and costs which ultimately resulted in reduced total costs and emissions across the country. Climate change adaptation strategies are highly beneficial from the standpoint of both an LCA and LCCA for all of the investigated locations.

Keywords: Climate change, Adaptation Strategies, Life Cycle Assessment (LCA), Life Cycle

Cost Analysis (LCCA), Pavement Design

8.2 Introduction

Canada has over 1.13 million kilometers of public roads, 40% of which are paved (Statistics Canada, 2018). The ongoing maintenance and upkeep of such a vast roadway network quickly accumulates high costs for all tiers of government. In addition to these high costs, the construction and maintenance of large road networks also produce high levels of carbon dioxide emissions. As the Canadian roadway network expands, the emissions associated with its upkeep continue to rise and become of more significant concern. From 2000 to 2018, the greenhouse gas (GHG) emissions related to the Canadian transportation sector increased by 27%. 84% of these emissions are a result of passenger and commercial use of roads (Natural Resources Canada, 2020). In accordance with the country's effort to produce more sustainable road construction projects, these emissions will have to be mitigated before they become too severe.

It becomes evident that an in-depth assessment of road construction's environmental and economic impact is essential. However, emissions are not limited to just the operation of paved roads. Material procurement, construction, maintenance, and removal all contribute to the emission of GHGs over the lifetime of the pavement (Santero & Horvath, 2009). A summary of considerations for the life cycle of a road is depicted in Figure 8-1. When approaching pavement design, the environmental impact over the entire life of the pavement should be considered through the form of a Life-Cycle Assessment (LCA). Similarly, the life-cycle cost of the pavement can be determined through a Life-Cycle Cost Analysis (LCCA). Completing these assessments becomes especially important when a future of climate change is considered, ensuring agencies are choosing the most environmental and economical way to adapt their pavements.

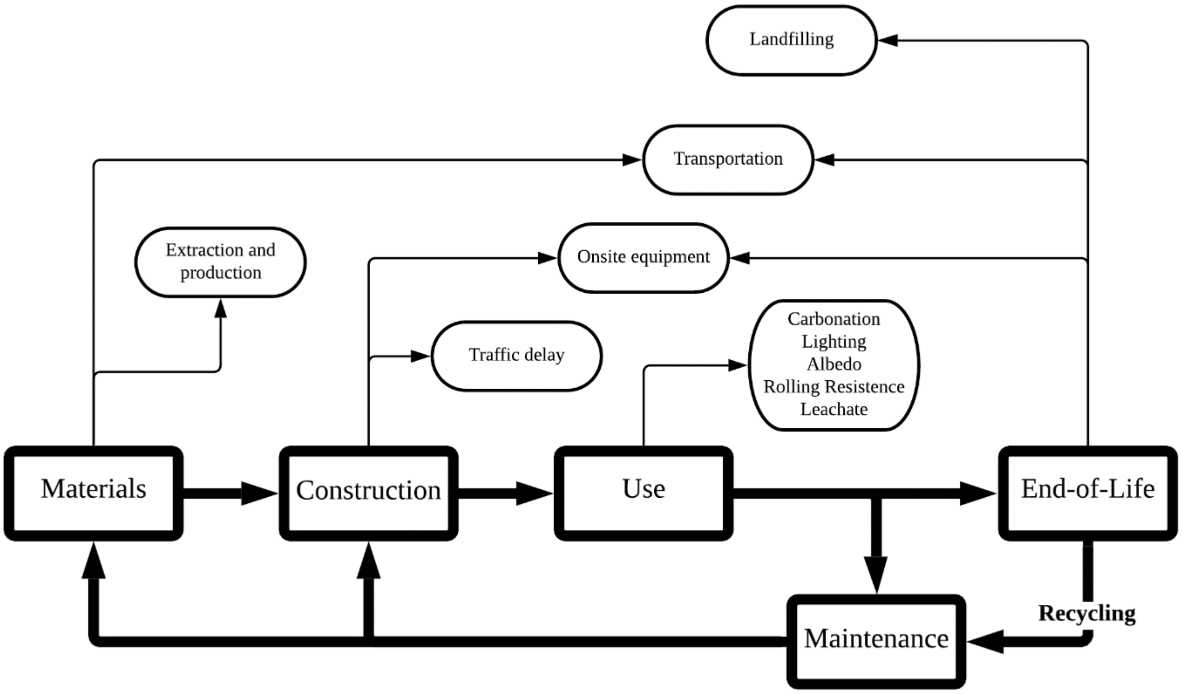

Figure 8-1: Life cycle considerations for roads (Meil & O'Connor, 2018)

8.2.1 Life-Cycle Assessment (LCA)

LCA has become a technique commonly used to investigate the environmental impact of pavements. LCA methodology allows researchers and practitioners to conduct the net environmental impact analysis over the entirety of a product's life. For pavements, this includes raw materials, construction, use, maintenance, and removal (Santero et al., 2011). Studies employing LCA methodologies to pavements have emerged in Canada as early as 1999 by Berthiaume and Bouchard (Berthiaume & Bouchard, 1999) and even earlier in the United States.

A recent Canada-wide study investigated the emissions related to asphalt construction from an LCA perspective. Due to the large quantity of data required to conduct an LCA, the study suggested that models based on collected regional data be used to approximate the emissions related to each phase of life. The study employed these models to determine emissions within each province. It was revealed that over 90% of pavement life cycle emissions were due to vehicle fuel usage. A small percentage of the fuel usage is due to pavement distresses causing excess fuel consumption. Geographically, Ontario and Quebec contributed fewer emissions than other provinces during the maintenance phase but emitted more in material production and construction (Alam et al., 2021). Studies such as this one emphasizes the importance of considering an LCA to identify which stages of the life cycle are contributing to the higher emissions.

There are many software tools available around to calculate the LCA of pavements. Some notable examples of available software are SimaPro and GaBi, Eurobitume, Pas 2050, CHANGER, and asPECT. The majority of these tools have been developed for use only within specific countries. An effective alternative to evaluate the LCA of pavements within Canada is the Athena Pavement LCA software. Athena was developed with the help of the Cement Association of Canada, Environment Canada, and several transportation engineers (Huang & Parry, 2014).

The Department of Manitoba Infrastructure recently employed Athena Pavement LCA to compare the environmental impacts of different concrete pavement mix design and construction practices. The LCA analysis allowed the Department to identify the most sustainable pavement design combination with a potential reduction of global warming potential of 5% (Ahammed et al., 2016). A Waterloo study also employed Athena Pavement LCA software to determine the life cycle environmental difference between conventional and high modulus asphalt concrete (Dhaliwal, 2019). Both of these studies determined which alternatives were best from a greenhouse gas emission standpoint using the software.

8.2.2 Climate change and LCA

The onset of climate change is predicted to impact the overall future pavement performance negatively (Barbi et al., 2021). Among other factors, variation in temperature, and rainfall have been determined to be the most critical climate change factors responsible for pavement deterioration (Mills et al., 2009; Tighe et al., 2008). Furthermore, the impact of pavement deterioration on emissions is significant. Poor pavement conditions can cause increased fuel consumption in road users, which will be amplified with climate change (Chen et al., 2021). Therefore, climate change can be expected to increase emissions and have a negative effect on the LCA of pavements. Applying the LCA methodology to pavements under future climate change conditions is vital to ensure that decisions made today remain resilient through a changing climate and that adaptation strategies do not contribute to more emissions than they would otherwise be offsetting.

A recent American study has done a case study on an eighteen-mile section of the I-95 to evaluate the LCA of construction alternatives under future climates. The study compared different pavement structures and recycled asphalt content to determine which alternative performed best at a low environmental cost (Valle et al., 2017). It is becoming more common for agencies to conduct LCA before making any new construction decisions, highlighting the potential emissions related to all of the available alternatives. Performing the LCA under future climate scenarios is important to ensure an accurate analysis is complete providing reliable results when the main concern does involve mitigating greenhouse gas emissions.

8.2.3 Life-Cycle Cost Analysis (LCCA)

LCCA is a method of applying economic principles to assess and compare design alternatives over the full life cycle of a product (Babashamsi et al., 2016). The transportation sector presents several opportunities for LCCA to be performed to make critical decisions, including timing for administrating maintenance treatments, initial construction materials, or determining the end of service life. Canadian provinces are already making significant investments into their highway networks, meaning that identifying areas of potential cost savings may prove extremely valuable to many of them. Table 8-1 presents a summary of the 2021-2022 budget for the Canadian provinces' highway maintenance and operations.

Table 8-1: 2021-2022 budget for highway maintenance and operations

Province	**2021-2022 Budget for Highways**
British Columbia	$2.39 billion (British Columbia Ministry of Finance, 2021)
Alberta	$2.40 billion (Government of Alberta, 2021)
Saskatchewan	$830 million (Saskatchewan Ministry of Finance, 2021)
Manitoba	$3.75 billion (Manitoba Finance, 2021)
Ontario	$2.41 billion (Ontario Ministry of Finance, 2021)
Quebec	$28.33 billion (over ten years) (Consil du trésor Québec, 2021)
New Brunswick	$180 million (Province of New Brunswick, 2021)
Nova Scotia	$467 million (Province of Nova Scotia, 2021)
Prince Edward Island	$66 million (Department of Finance Prince Edward Island, 2021)
Newfoundland and Labrador	$170 million (Newfoundland and Labrador, 2021)

The highest-spending provinces including Manitoba, British Columbia, and Ontario will face various climate change impacts over the next 50 years (Swarna et al., 2021). Manitoba and Ontario will see more severe fatigue cracking and rutting, which will serve to worsen the IRI. British Columbia will experience mostly subbase and subgrade damage due to the higher water table, significantly increasing overall rutting (Swarna et al., 2021). From a spending standpoint, it is critical that all provinces consider adapting their pavements to prevent the deterioration, and potentially produce significant cost savings. Performing an LCCA on these alternatives is an excellent way to determine which option is best in this situation, and which results will have the most longstanding impacts.

A recent study conducted an LCA and an LCCA to determine the most effective pavement alternative in Colorado. The LCA favored the Portland cement concrete alternative; meanwhile, the LCCA favored the asphalt alternative (Liu et al., 2015). The results of this study affirm the importance of considering both methodologies in design, for the outcome may not always be the same. It is then up to governing agencies and designers to choose if they prioritize cost savings or emission reductions, and they can then select the best alternative for them.

In Canada, all provinces, excluding Prince Edward Island, New Brunswick, and Newfoundland, already apply LCCA principles to their roadway management plans. Each province employs different discount rates, analysis periods, and computational approaches, whichever applies best to their region (Moges et al., 2017). However, the complexities of climate change are not always integrated into their analysis, which may severely skew the results. Decisions that are economical today may not withstand the onset of climate change. Understanding the life-cycle cost in a climate other than todays ensures no surprise costs occur and accumulate in the future.

8.2.4 Climate change and LCCA

Although it is understood that climate change and pavement performance are closely related, there is a limited number of studies that examine the impact of climate change on the LCCA of pavements. A recent study attempted to quantify the impact of climate variability on pavement LCCA. The authors confirmed that small climate variations will affect the LCCA, which affirms that climate change will also have an effect on LCCA (Qiao et al., 2019). Another study investigated the impact of climate change on pavement maintenance through the means of an LCCA. It was found that the timing and intensity of routine maintenance will change as a result of climate change and thus impact the LCCA (Qiao et al., 2015). In addition, the implementation of climate change adaptation strategies will change the initial costs of construction and the necessary maintenance, ultimately influencing the LCCA.

8.2.5 Climate change adaptation strategies

To prevent severe pavement deterioration related to climate change, transportation agencies may consider the administration of a climate change adaptation strategy to their new pavement constructions. In Canada, there is discourse surrounding the best adaptation strategies to employ in the face of climate change. Studies have investigated upgrading asphalt binder grades (Swarna et al., 2021), increasing hot mix asphalt (HMA) thickness (Knott, Jacobs, et al., 2019; Knott, Sias, et al., 2019), and employing stabilized subgrades (Mallick et al., 2016) as methods to adapt pavements for the onset of climate change. To properly adapt the pavements to climate change, different combinations of these strategies should be administered at different times depending on the location. Geographical factors will change the way different locations experience climate change and thus the adaptation strategies should be selected for each specific location. The efficacy of these methods has been verified in several instances, but their environmental consequences have not been thoroughly explored or compared. In addition, it is not known if the administration of these adaptation strategies will have a beneficial impact on the LCA and LCCA of the pavement.

8.2.6 Highlights of literature

With the increasing importance of environmentally conscious construction practices, LCA is becoming a prominent research topic. Several times, it has been determined that LCA can be a powerful tool in comparing material, construction, and maintenance alternatives to produce the most sustainable pavement possible. Similarly, LCCA is a thorough way of comparing the cost of these same alternatives to ensure costs are reduced over the entirety of a pavement's life. LCCA is already prominently used by most Canadian road agencies and combining it with climate change parameters will provide a unique perspective on what future pavements may cost. Throughout the literature review of combining LCA, LCCA, and climate change adaptation strategies for pavements, a few gaps were observed, which are as follows:

- Although some adaptation strategies have been investigated for efficacy, they have not been evaluated from an environmental or economic impact standpoint.
- The long-term impact of climate change adaptation strategies on greenhouse gas emissions and cost is not known. The impact of climate change on pavements in this regard has been discussed and should be compared to the adaptation strategies.
- In several studies, either LCA or LCCA has been considered. They are not always considered as a pair, which may omit important information necessary for informed decision-making.

8.3 Objective and scope

The objectives of this study include

a) Conduct an LCA and LCCA for a baseline asphalt pavement with no climate change, a baseline pavement with climate change, and an asphalt pavement adapted to withstand climate change using various strategies.
b) Determine the influence of climate change and adaptation strategies on LCA and LCCA of asphalt pavements.

The scope of this study include:

1. Select relevant climate change models and extract data to forecast future temperature and precipitation trends.
2. Obtain necessary pavement material and structural data from available databases.

3. Select required climate change adaptation strategies for each of the selected Canadian pavement sections.
4. Conduct an LCA and LCCA using Athena Pavement LCA software on a baseline pavement, a climate change pavement, and an adapted climate change pavement.
5. Determine the environmental and economic impact of administering climate change adaptation strategies.

8.4 Methodology

In a previous study, the authors of this paper quantified the impact of climate change on pavement performance using 10 different climate change models (Swarna et al., 2021). The models were obtained from the Pacific Climate Impacts Consortium database (Pacific Climate, n.d.), and the average of their predictions was extracted and used. Detailed pavement material, traffic, and structural data were obtained from the LTPP database. Pavement performance under the climate change data was computed using AASHTOWare Pavement ME Design software. A flowchart of the procedures for this study is provided in Figure 8-2.

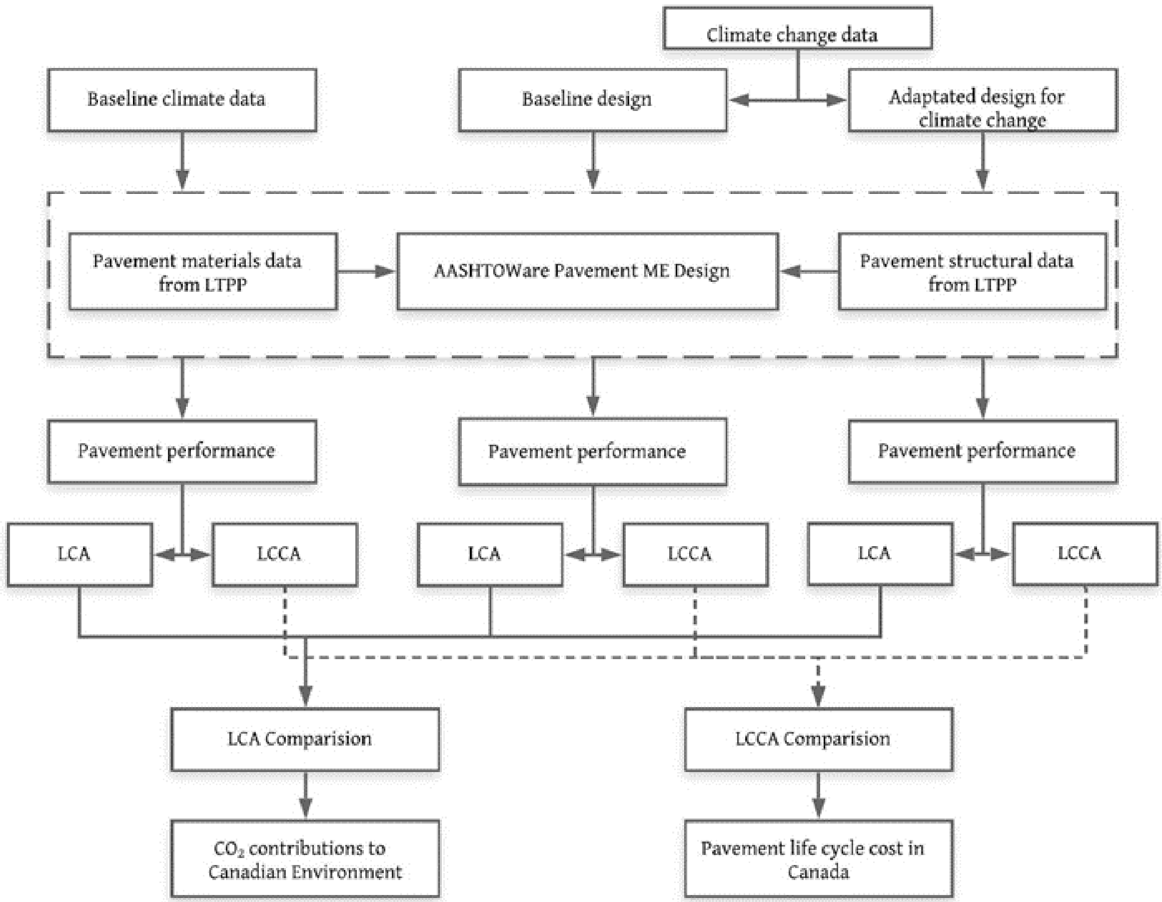

Figure 8-2: Study methodology flowchart

The previously collected data was used to assess the LCA and LCCA of each scenario. The investigated scenarios were (i) baseline asphalt pavement with no climate change, (ii) a baseline pavement with climate change, and (iii) an asphalt pavement adapted to withstand climate change. The adaptation strategies investigated were upgraded asphalt binder grade, upgraded asphalt structure, upgraded mixture gradation, and upgraded subbase/subgrade. The adaptation strategies were combined and applied only where necessary based on previous AASHTOWare provincial analysis, the recommended combinations of which are included in Table 8-2.

The LCA and LCCA were performed with all previously mentioned inputs using Athena

Pavement LCA software. The Athena Pavement LCA software divides the life cycle of pavements into four primary phases to conduct the analysis. The phases, and considerations within each phase, are as follows:

8.4.1 Site preparation and manufacturing

The first phase of the LCA and LCCA process focused on the procurement of materials and transportation to the site. Materials are considered in two categories: asphalt layers and aggregate layers. To determine emissions from the material production and manufacturing phase, equation 8-1 was followed.

$$CO_2\ emissions_{Site\ preparation+Manufacturing} = \sum_{i=material} Volume_i \times Density_i \times CO_2 emission\ rate_i \qquad \text{Equation 8-1}$$

The CO_2 emission rate was determined by equation 8-2.

$$CO_2 emission\ rate_i = CO_2 emissions/\$_i \times \frac{\$}{mass\ material\ produced_i} \qquad \text{Equation 8-2}$$

For the LCCA, the price of material and transportations were estimated based on the extensive Athena database. When adaptation strategies were applied, the excess material costs or additional transportation costs were considered in this phase.

8.4.2 Construction

The construction phase of the LCA considered equipment fuel consumption during the construction process. This phase assumes that all the transportation emissions have already been considered in the previous phase, and thus only accounts for front loaders, road graders, paving machines, and any other equipment used strictly in construction. Equation 8-3 was employed to determine the emissions.

$$CO_2\ emissions_{Construction} = \sum_{\substack{i=pavement \\ layer}} \sum_{\substack{j=construction \\ equipment}} (Volume_i \times Density_i \times Fuel\ consumption\ rate_j \times Density\ of\ fuel_j \times CO_2 emission\ rate\ per\ fuel\ mass_j)/Utility\ rate_j \quad \text{Equation 8-3}$$

Similar computations were performed for the LCCA of this phase; however, the emissions were not considered. The cost of the construction was based on the time to construct and a base hourly rate depending on the quantity of material being placed.

8.4.3 Maintenance

The maintenance phase represents all emissions and costs associated with the maintenance and upkeep of the pavements. Typical time intervals for the maintenance schedule are assumed based on the input structural information. Wastage factors for all imported materials are also considered. The LCA would focus on emissions as a result of maintenance procedures whereas the LCCA only considers the cost of the procedures.

8.4.4 Use phase

In the use phase of the LCA and LCCA, the environmental impacts of vehicles using the pavements are considered. Important considerations include vehicle fuel consumption, energy consumption for nighttime illumination, and leachates produced from the pavement (Ziyadi et al., 2017). A separate computation was performed to determine the excess fuel consumption as a result of pavement distresses. Equations 8-4 and 8-5 represent this calculation.

$$Excess\ Fuel\ Consumption_{Roughness} = (IRI_{observed} - Baseline\ IRI) \times 0.0075 \times Fuel\ consumption \qquad \text{Equation 8-4}$$

$$Excess\ Fuel\ Consumption_{Texture\ depth} = (TD_{observed} - Baseline\ TD) \times 0.0161 \times Fuel\ consumption \qquad \text{Equation 8-5}$$

The Athena Pavement LCA software does not consider demolition and disposal in any calculations. Instead, the software operates under the assumption that the long service life of the highway pavements can eliminate the need for demolition or disposal. Although many of the principles of the LCA and LCCA differ, the calculations are similar within the Athena model.

The LCA and LCCA were repeated several times to consider the different scenarios and the different time periods. An analysis was completed for four time periods, 1980-2010, 2010-2040, 2040-2070, and 2070-2100. With all of the LCA and LCCA complete, the results were compared from various standpoints to gain an in-depth understanding of the impact of implementing climate change adaptation strategies. The findings of the analysis and the comparisons are discussed in the following sections of this paper.

8.5 Results and discussions

Chapter 7 revealed that the climate change adaptation strategies would be necessary within each Canadian province. The adaptation strategies considered were upgraded asphalt binder grades, stabilized base types, increased asphalt layer thickness, and upgraded asphalt mixture gradation. Depending on local climate factors and the regional impact of climate change, different regions of the country required different combinations of adaptation strategies. A summary of the findings is presented in Table 8-2.

Table 8-2: Required adaptation strategies for selected Canadian locations

City ID	Province	City	Adaptation Strategy		
			2010-2040	**2040-2070**	**2070-2100**
BC_00	BC	Vancouver	BG+BT	BG+MG+BT	BG+BT
AB_01	AB	Calgary	BG	BG	BG
AB_02	AB	Edmonton	BG	BG	BG
SK_03	SK	Saskatoon	BG	BG	BG
MB_04	MB	Brandon	BG	BG	BG
MB_05	MB	Winnipeg	MG	BG+MG	BG
ON_06	ON	Toronto	MG	BG+MG	BG+MG
ON_07	ON	Ottawa	BG	BG	BG+MG
QC_08	QC	Montreal	MG	MG	BG
QC_09	QC	Quebec City	MG	BG	BG+MG
QC_10	QC	Saguenay	MG	MG	BG+MG
NB_11	NB	Fredericton	BG	BG	BG
PEI_12	PEI	Charlottetown	BG+MG	BG+MG	BG+MG+CT
NS_13	NS	Halifax	BG	BG	BG
NL_14	NL	Corner Brook	MG	MG	BG+MG
NL_15	NL	St. John's	BG	BG+CT	BG+MG

Note: AB = Alberta, BC = British Columbia, BG = Change in asphalt binder grade, BT = Change in the base type, CT = Change in asphalt layer thickness, MB = Manitoba, MG = Change in asphalt mixture gradation, NB = New Brunswick, NL = Newfoundland and Labrador, NS = Nova Scotia, ON = Ontario, PEI = Prince Edward Island, QC = Quebec, SK = Saskatchewan.

8.5.1 LCA and LCCA

In this study, the recommended adaptation strategies outlined in Table 8-2 were followed to complete the LCA and LCCA methodology. It is important to note that with increasing climate change impacts, some provinces will need additional adaptation measures over time, which may result in increased greenhouse gas emissions or higher costs associated. To initially compare the adaptation strategies, the results exclusively from the period of 2040-2070 were compared to a baseline scenario to evaluate their environmental and economic impact through an LCCA and an LCA. This was chosen as the primary concern as this time period represents the most significant change for most provinces and approaches quickly. Figure 8-3 presents the results of the LCA comparison while Figure 8-4 presents the results of the LCCA comparison.

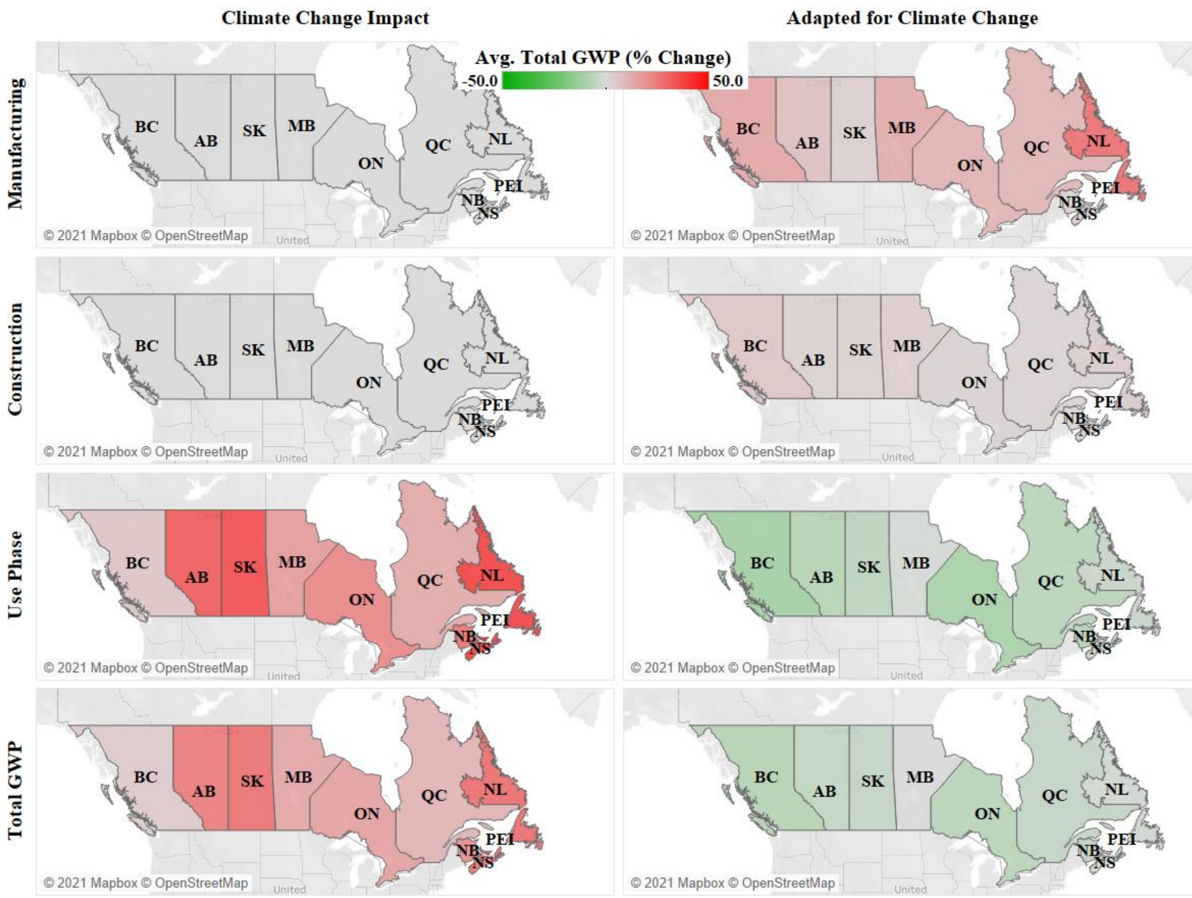

Figure 8-3: Percentage change in Emission (GWP) for climate change impact and adapted pavements compared to a baseline scenario for 2040-2070 time period

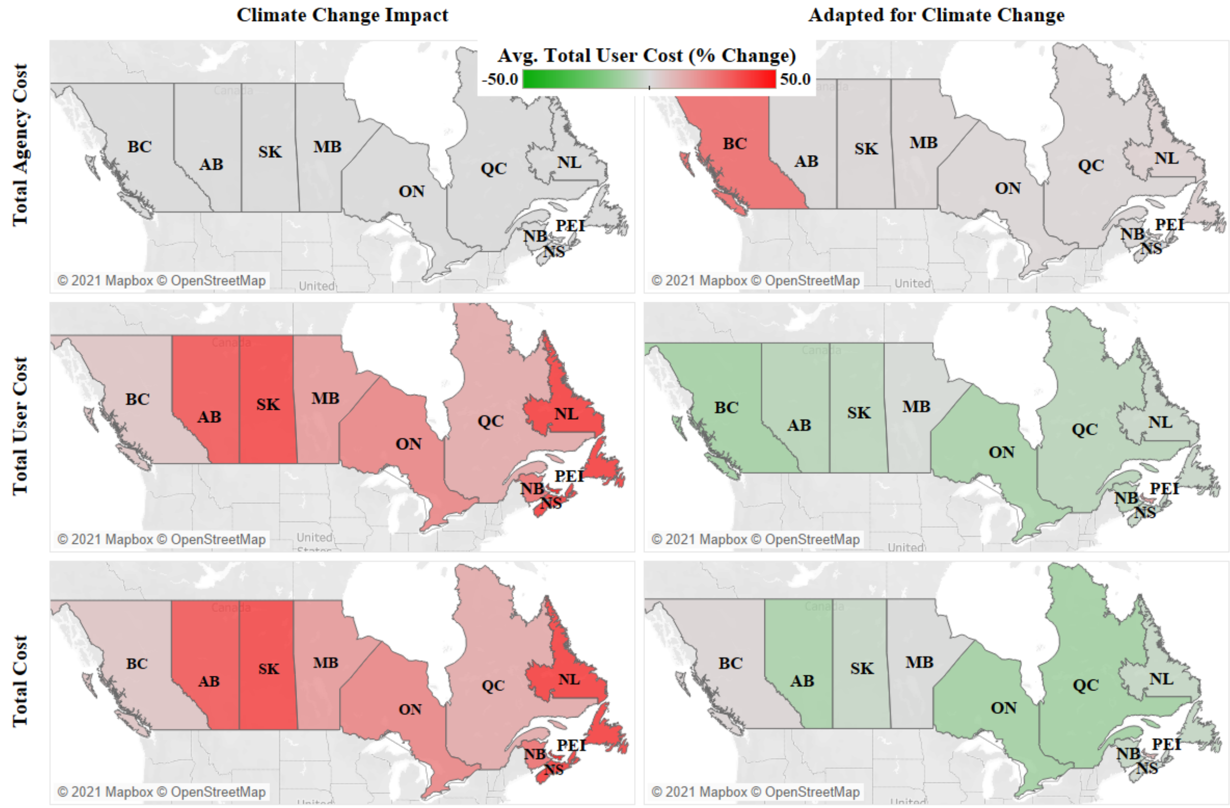

Figure 8-4: Percentage change in life cycle cost ($) for climate change impact and adapted pavement compared to a baseline pavement without climate change for 2040-2070 time period

In general, the LCA and LCCA revealed that adopting climate change adaptation strategies will benefit agencies from both a cost and an emissions perspective. The reduction of emissions is widespread across the country, while the cost emissions are focused on a few provinces. Figure 8-3 and Figure 8-4 summarized these findings, the main outcomes of which follows:

- In all of the investigated scenarios, the onset of climate change increases the total cost and the total global warming potential for all Canadian provinces.
- The onset of climate change will have a negative impact on global warming potential exclusively as a result of increased use phase emissions such as fuel consumption.

- The initial increase in agency cost for adopting an upgraded binder or mixture gradation is negligible in comparison to the cost of implementing a stabilized base or increased asphalt thickness. Therefore, the provinces of British Columbia and Newfoundland and Labrador display higher agency costs for 2040-2070.
- All provinces except for British Columbia will observe an overall reduction in total cost when they apply their respective adaptation strategies. The necessity of a stabilized base in British Columbia increases the total cost by a small percent. However, British Columbia will observe a significant reduction in global warming potential due to adaptation strategies, which should counterweigh the slight increase in total cost.
- Employing adequate climate change adaptation strategies significantly reduces the global warming potential in all provinces apart from PEI, where there is only a small increase in GWP.
- Based on the findings, applying a climate change adaptation strategy in the years 2040-2070 is beneficial for agencies, users, and the environment in the majority of Canadian provinces.

Although the benefits of the climate change adaptation strategies have been determined in 2040-2070, it remained to see if the trends continued further into the future and in the present day. In the period from 2070-2100, most provinces need to employ additional adaptation strategies, and some provinces, including PEI, will need to increase the thickness of asphalt. The thickness of asphalt has been found to increase cost and global warming potential due to the high quantity of additional material that will need to be manufactured. Other adaptation strategies, including changing the binder type and mixture gradation have been found to have little effect on the cost and global warming potential.

To further understand the impact of adaptation strategies outside of the narrow 2040-2070 time period, the environmental and economic impacts were compared over all three time periods initially mentioned in Table 8-2. The LCA conducted over time is described and compared in Figure 8-5, while the LCCA over time is described and compared in Figure 8-6.

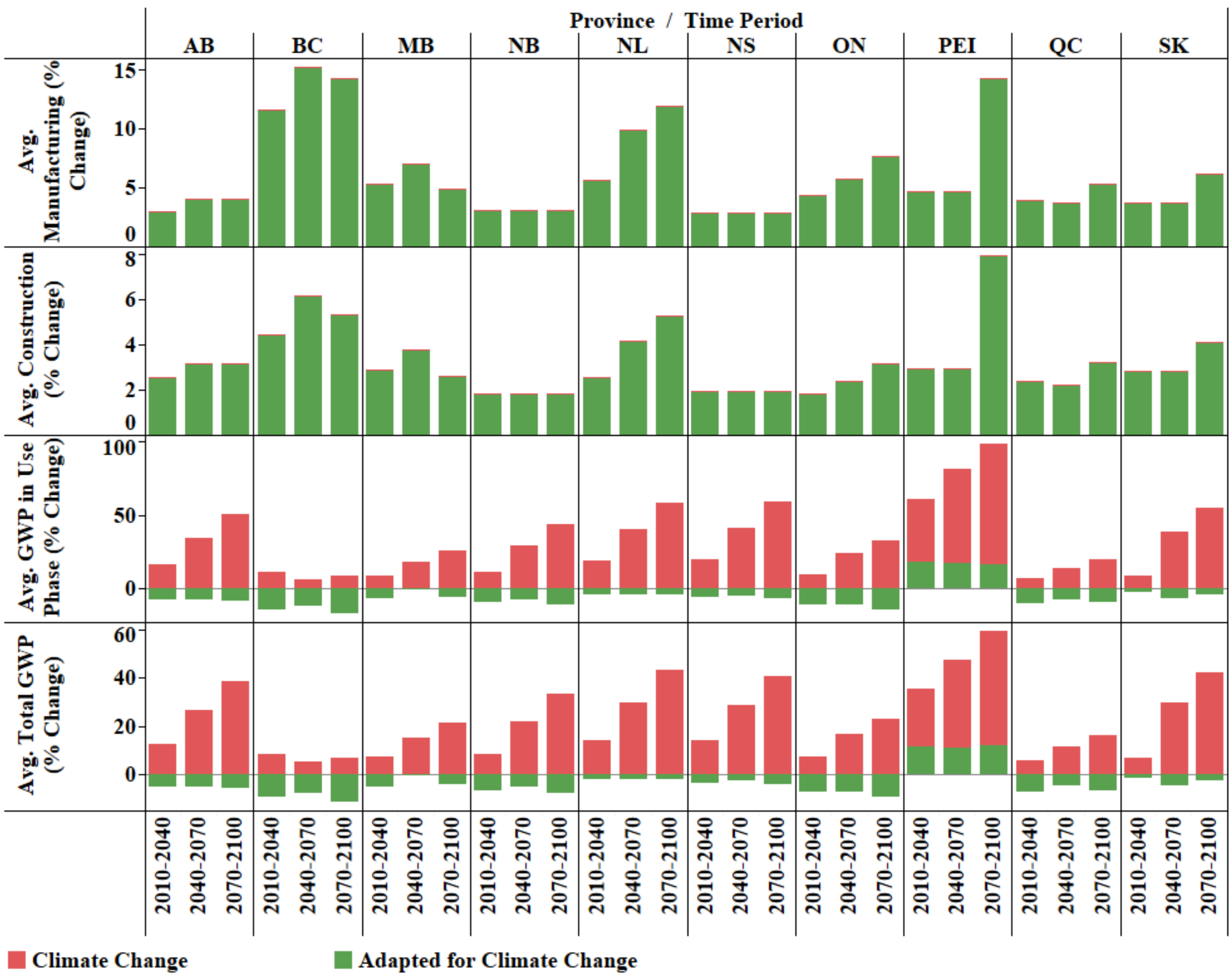

Figure 8-5: Percent change in emission (GWP) for different time periods due to climate change impact and adapted pavement

Figure 8-6: Percent change in life cycle cost ($) for different periods due to climate change impact and adapted pavement

The LCA and LCCA performed over time show that with the progression of time, emissions and cost will both increase unless adaptation strategies are employed. Climate change adaptation strategies have the potential to reduce global warming potential and reduce total costs significantly if applied at the appropriate time. The main outcomes of Figure 8-5 and Figure 8-6 are as follows:

- Emissions and costs related to climate change are consistently increasing over time for all provinces, which is due to the increase in pavement distresses.

- If no climate change adaptation measure is applied to the pavements, the excess fuel costs and the GWP in use phase will increase significantly over time, reaching a maximum of nearly a 50% and 60% increase, respectively for 2070-2100 in Prince Edward Island. This increase could be because of the strong climate impact and less traffic.
- Applying the appropriate climate change adaptation measures in each time period keeps total costs and emissions relatively consistent over time, and no significant jumps are observed in any Canadian provinces. Consistent emissions may help provinces in mitigating their carbon footprint and planning to reach international green standards.
- In conjunction with the findings reported from Figure 8-3 and Figure 8-4, Figure 8-5 and Figure 8-6 strongly support the use of climate change adaptation strategies from both LCA and LCCA perspective. The benefits of climate change adaptation strategies are only becoming more prominent over time.

8.5.2 Selecting best adaptation strategy

As each investigated location has an independent adaptation plan, the specific impacts of each adaptation strategy were considered. To illustrate the difference between the strategies, an in-depth analysis was conducted for St. John's, Newfoundland from 2040-2070. St. John's represents a unique situation as it requires more strategies than other locations, making it a good point of comparison. The results of the analysis are detailed in Figure 8-7.

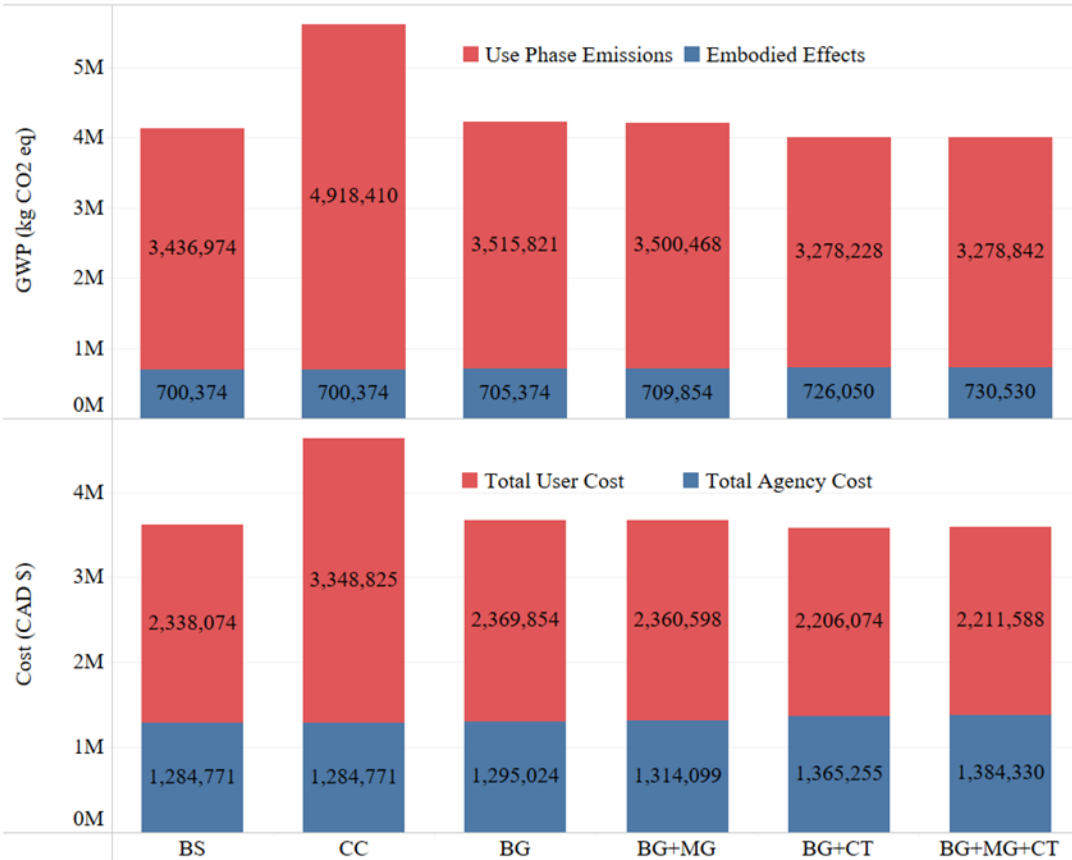

Figure 8-7: Impact of different climate change adaptation strategies in St. John's in 2040-2070 time period

Figure 8-7 compares the baseline (BS), climate change with no adaptation (CC), upgraded binder grade (BG), upgraded mixture gradation (MG), and change in asphalt thickness (CT) from a cost and GWP perspective. Since upgraded binder grade is the first strategy that should be used, it is then combined with the other two alternatives. Although it has previously been found that changing the thickness has a significant impact on costs and emissions during the construction phase, Figure 8-8 reveals that the overall difference between the strategies is not large. Because a 30-year service life was chosen for this study, the use phase dominates the overall costs and outweighs any additional construction costs and emissions. However, the application of all combination of adaptation strategies significantly reduces cost and emissions in comparison to the climate change scenario. This reinforces the importance of adapting the pavements. In addition, it has been observed that the best adaptation strategy for St. John's from both an LCA and LCCA perspective is upgrading the binder and changing the thickness of pavement. This recommendation is in accordance with the adaptation strategy that was previously selected for this location based strictly on performance. In general, the adaptation strategies proposed in Table 8-2 are again confirmed to be less costly and lower emitters in comparison with the alternatives.

8.5.3 Correlations between LCA and LCCA factors

Individually, LCA and LCCA are important factors of consideration when implementing new pavement construction. However, the relationship between the two may complicate decision-making, primarily when one needs to be prioritized over the other. To determine the correlation between LCA factor and LCCA factors, the two were analyzed statistically. Figure 8-8 highlights the correlation of the LCA factors: environmental embodied effects, use phase emissions, and total global warming potential, and the LCCA factors: agency cost, user cost, and total cost. Embodied effects represent the cumulative effects of construction, transportation, manufacturing, and material procurement.

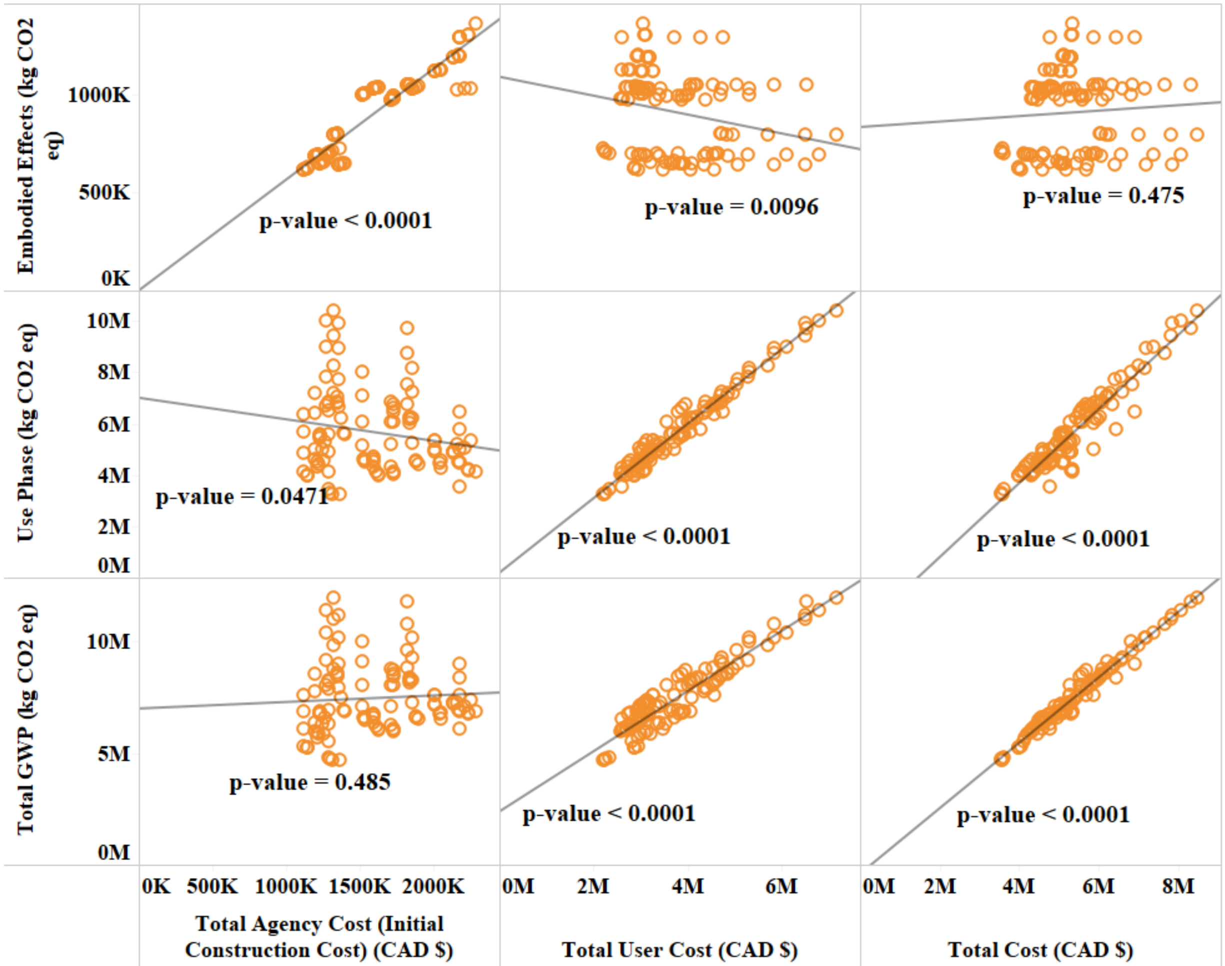

Figure 8-8: Relationship between LCA and LCCA factors

The investigation into the relationship between LCA and LCCA factors revealed that the two are closely related in several aspects. When users and agencies are spending more on their pavements, the resulting global warming potential is higher, which is a result of the increased material procurement and construction activities. The nuanced findings of Figure 8-8 follow.

- Total agency cost was found to be positively correlated to embodied effects, which emphasizes that the use of adaptation strategies will increase the embodied effects. However, as the total agency cost is negatively correlated with the emissions in use phase, these climate change adaptation strategies will negatively influence the emissions in use phase.

- Total agency cost was found to negatively correlate with use phase emissions. As agencies invest more in their pavements and adapt them to climate change, the use phase emissions will decrease. These findings are consistent with previous findings that emphasized the significant increase in emissions that high frequency pavement distresses have on the use phase.
- The total agency cost was not found to be correlated with total global warming potential, meaning that minimizing costs will not necessarily minimize emissions. Since these two are independent, decisions will have to be made to determine which is a priority for agencies.
- Total user cost is highly positively correlated to total global warming potential and use phase emissions. As users spend more on fuel costs due to the increasing pavement distresses, their emissions will also be increasing, resulting in higher GWP.

8.6 Conclusions

This study investigated the impact of climate change adaptation strategies on the life cycle cost and life cycle emissions of Canadian pavements. Appropriate adaptation strategies for the changing climate were compared to baseline scenarios throughout all phases of the pavement's life. The impact of the adaptation strategies over time was investigated to evaluate the increases in costs and emissions expected in the future. Additionally, the factors evaluated in the LCA were statistically compared with the factors in the LCCA to determine the relationship between the two. Upon completion of the research, the following main conclusions could be made:

- Investing in climate change adaptation strategies is beneficial from an LCA and LCCA standpoint for both users and agencies.
- Despite the initial increase in cost to implement some adaptation strategies, the LCCA revealed that over the lifetime of the pavement those costs will be easily offset in most locations.
- Among all of the analyzed adaptation strategies, increased thickness and stabilized bases are the most costly and highest emitters. Upgrading the asphalt binder grade and asphalt mixture type were the least expensive, the lowest emitter, and the easiest to implement. The first step to adapt to climate change for almost all investigated locations is to upgrade the binders.
- The savings incurred through the implementation of climate adaptation strategies only become more prominent over time. The savings in the years 2070-2100 are higher than those in the years 2040-2070, suggesting that with more severe climate change, adaptation strategies become more important.
- The relationship between LCA and LCCA factors is mostly positively correlated. However, total agency cost is negatively correlated with use phase emissions, emphasizes that the increased agency spending will serve to reduce the use phase emissions.
- The adaptation strategies proposed in Table 8-2 are confirmed to be the best solution from a performance perspective and also from an LCA and LCCA perspective. They will adapt the pavement to climate change and reduce costs and emissions.

8.7 Contributions and limitations

8.7.1 Contributions

- The long-term impact of climate change on greenhouse gas emissions and life cycle cost are quantified in Canada.
- Different climate change adaptation strategies are evaluated to determine the low cost and sustainable alternative to mitigate the climate change impact.
- Influence of various climate change adaptation strategies on GWP and life cycle cost are also quantified.

8.7.2 Limitations

- The pavement performance inputs are directly taken from the Pavement ME, which were computed using global calibration factors except for Ontario and Quebec provinces. This could lead to uncertainty in performance prediction, which further lead to uncertain estimations for most of the province except Ontario and Quebec.
- The GWP and life cycle cost were not computed in the maintenance phase due to data inadequacy.
- The transportation distance between the site and plant are kept constant for all the sites due to lacking of data, which might have significant effect of GWP in embodied effects and Total agency cost.
- Due to insufficient emissions and material cost data in Atlantic provinces, the Quebec emissions and life cycle cost database was used to determine the GWP and life cycle cost for the sites in Atlantic provinces.

- Emissions and life cycle cost in the manufacturing and construction phases are calculated manually due to lacking of data for different binder grades and different gradation types in the LCA model used.

8.8 References

Ahammed, M. A., Sullivan, S., Finlayson, G., Goemans, C., & Meil, J. (2016). Life cycle environmental assessment using athena pavement LCA Tool: A Manitoba case study. *2016 Transportation Association of Canada's Conference and Exhibition, TAC 2016*.

Alam, M. R., Hossain, K., & Bazan, C. (2021). Life cycle analysis for asphalt pavement in Canadian context: modelling and application. *International Journal of Pavement Engineering*, 1–15. https://doi.org/10.1080/10298436.2020.1866759

Alberta Treasury Board and Finance Communications (Government of Alberta). (2021). *Fiscal Plan: Protecting Lives and Livelihoods*.

Babashamsi, P., Md Yusoff, N. I., Ceylan, H., Md Nor, N. G., & Salarzadeh Jenatabadi, H. (2016). Evaluation of pavement life cycle cost analysis: Review and analysis. In *International Journal of Pavement Research and Technology* (Vol. 9, Issue 4). https://doi.org/10.1016/j.ijprt.2016.08.004

Barbi, P., Tavassoti, P., Tighe, S., & Baaj, H. (2021). Implications of climate variation in flexible airport pavement design and performance. *Airfield and Highway Pavements 2021: Airfield Pavement Technology - Selected Papers from the International Airfield and Highway Pavements Conference 2021*. https://doi.org/10.1061/9780784483527.017

Berthiaume, R., & Bouchard, C. (1999). Exergy analysis of the environmental impact of paving material manufacture. *Transactions of the Canadian Society for Mechanical Engineering*, *23*(1 B). https://doi.org/10.1139/tcsme-1999-0013

British Columbia Ministry of Finance. (2021). *Budget and Fiscal Plan*.

Chen, X., Wang, H., Horton, R., & DeFlorio, J. (2021). Life-cycle assessment of climate change impact on time-dependent carbon-footprint of asphalt pavement. *Transportation Research Part D: Transport and Environment*, *91*. https://doi.org/10.1016/j.trd.2021.102697

Consil du trésor Québec. (2021). *Québec Infrastructure Plan*.

Department of Finance and Treasury Board (Province of New Brunswick). (2021). *Main Estimates 2021-2022*.

Department of Finance and Treasury Board (Province of Nova Scotia). (2021). *Budget 2021 to 2022*.

Department of Finance (Newfoundland and Labrador). (2021). *Budget 2021*.

Department of Finance Prince Edward Island. (2021). *Estimates 2021-2022*.

Dhaliwal, H. S. (2019). *Incorporating GHG Mitigation into Ontario Highway Pavement Engineering Practices*. University of Waterloo.

Huang, Y., & Parry, T. (2014). Pavement life cycle assessment. *Green Energy and Technology*, *204*. https://doi.org/10.1007/978-3-662-44719-2_1

Knott, J. F., Jacobs, J. M., Sias, J. E., Kirshen, P., & Dave, E. V. (2019). A Framework for Introducing Climate-Change Adaptation in Pavement Management. *Sustainability*, *11*(1). https://doi.org/http://dx.doi.org/10.3390/su11164382

Knott, J. F., Sias, J. E., Dave, E. V, & Jacobs, J. M. (2019). *Seasonal and Long-Term Changes to Pavement Life Caused by Rising Temperatures from Climate Change*. *2673*(6), 267–278. https://doi.org/10.1177/0361198119844249

Liu, R., Smartz, B. W., & Descheneaux, B. (2015). LCCA and environmental LCA for highway pavement selection in Colorado. *International Journal of Sustainable Engineering*, *8*(2).

https://doi.org/10.1080/19397038.2014.958602

Mallick, R., Jacobs, J. M., Miller, B. J., & Daniel, J. S. (2016). Understanding the impact of climate change on pavements with CMIP5, system dynamics and simulation. *International Journal of Pavement Engineering*, *19*(8), 697–705. https://doi.org/10.1080/10298436.2016.1199880

Manitoba Finance. (2021). *Estimates of Expenditure For the Fiscal Year Ending MArch 31, 2022*.

Meil, J., & O'Connor, J. (2018). *LCA for Roadways and Bridges*.

Mills, B., Tighe, S., Andrey, J., Smith, J., & Huen, K. (2009). Climate Change Implications for Flexible Pavement Design and Performance in Southern Canada. *Journal of Transportation Engineering*, *135*(10), 773–782. https://doi.org/10.1061/(asce)0733-947x(2009)135:10(773)

Moges, M., Ayed, A., Viecili, G., & el Halim, A. A. (2017). A review and recommendations for Canadian LCCA guidelines. *2017 Transportation Association of Canada Conference and Exhibition, TAC 2017*.

Natural Resources Canada. (2020). *Energy and Greenhouse Gas Emissions (GHGs)*. https://www.nrcan.gc.ca/science-and-data/data-and-analysis/energy-data-and-analysis/energy-facts/energy-and-greenhouse-gas-emissions-ghgs/20063

Ontario Ministry of Finance. (2021). *Ontario's Action Plan*. https://doi.org/ISBN 978-1-4868-5166-9

Pacific Climate. (n.d.). *Statistically Downscaled Climate Scenarios*.

Qiao, Y., Dawson, A., Parry, T., & Flintsch, G. (2019). Life cycle cost of flexible pavements and climate variability: case studies from Virginia. *Structure and Infrastructure Engineering*, *15*(12). https://doi.org/10.1080/15732479.2019.1642364

Qiao, Y., Dawson, A. R., Parry, T., & Flintsch, G. W. (2015). Evaluating the effects of climate change on road maintenance intervention strategies and Life-Cycle Costs. *Transportation Research Part D: Transport and Environment*, *41*. https://doi.org/10.1016/j.trd.2015.09.019

Santero, N. J., & Horvath, A. (2009). Global warming potential of pavements. *Environmental Research Letters*, *4*(3), 0304011. https://doi.org/10.1088/1748-9326/4/3/034011

Santero, N. J., Masanet, E., & Horvath, A. (2011). Life-cycle assessment of pavements. Part I: Critical review. In *Resources, Conservation and Recycling* (Vol. 55, Issues 9–10). https://doi.org/10.1016/j.resconrec.2011.03.010

Saskatchewan Ministry of Finance. (2021). *Saskatchewan Provincial Budget*.

Statistics Canada. (2018). *The Canadian Transportation System*. https://www144.statcan.gc.ca/tdih-cdit/cts-rtc-eng.htm

Swarna, S. T., Hossain, K., Pandya, H., & Mehta, Y. A. (2021). Assessing Climate Change Impact on Asphalt Binder Grade Selection and its Implications. *Transportation Research Record: Journal of the Transportation Research Board*, 1–14. https://doi.org/10.1177/03611981211013026

Tighe, S., Mills, B., Tighe, S. L., Smith, J., Mills, B., & Andrey, J. (2008). Evaluating Climate Change Impact on Low- Volume Roads in Southern Canada on Low-Volume Roads in Southern Canada. *Transportation Research Record: Journal of the Transportation Research Board*, *2053*(1), 9–16. https://doi.org/10.3141/2053-02

Valle, O., Qiao, Y., Dave, E., & Mo, W. (2017). Life cycle assessment of pavements under a changing climate. *Pavement Life-Cycle Assessment*, *October*, 241–250. https://doi.org/10.1201/9781315159324-25

Ziyadi, M., Ozer, H., & Al-Qadi, I. L. (2017). Functional unit choice for comparative pavement LCA involving use-stage with pavement roughness uncertainty quantification (UQ).

Pavement Life-Cycle Assessment - Proceedings of the Pavement Life-Cycle Assessment Symposium, 2017. https://doi.org/10.1201/9781315159324-15

Chapter 9: Conclusions and Discussions

9.1 Conclusions

9.1.1 Impact of climate change on pavement performance in Canada's Newfoundland Island

In the current study, the impact of climate change on pavement performance is evaluated using AASHTOWare software for both baseline climate and climate change models (PCM 01-04). Here, a new hourly temperature estimation procedure named Sine (14R-1) is considered for a reliable estimation of hourly data based on sunrise and is also continuous over the considered period. The performance of a pavement section on the Trans-Canada Highway in NL, Canada was assessed. The material, traffic, structural design, and climate data were collected from various sources such as NL Department of Transportation and Works, LTPP, MERRA climate database and Environment Canada. This pavement design was analyzed using AASHTOWare software for both baseline climate and climate change models. The predicted pavement distresses from the baseline and climate change models are compared and drawn conclusions as presented below.

- The climate change is significantly affecting the pavement performance over a design life of twenty years. Pavement distresses including total permanent deformation, BU fatigue cracking, AC layer rutting are highly affected by climate change.
- AC layer rutting is increased by 18-27%, which might be because of the constant increase in temperature throughout the design period. However, base layer and subgrade rutting is decreasing, which might be a resultant of decrease in freeze and thaw cycles.
- The proposed method 'Sine (14R-1)' exhibits approximately same distress compared to M-IOMM method. However, the major advantage of Sine (14R-1) method is computational efficiency of using this method for estimation of hourly temperature. M-IOMM requires

historical hourly temperature to estimate the hourly temperature for future climate, while Sine (14R-1) method depends only on future daily maximum and minimum temperature.

- There is no significant difference between the distress predicted for future climate using RCP 4.5 and RCP 8.5. However, in the case of AC permanent deformation, there is a significant difference in prediction for future climate using RCP 4.5 and RCP 8.5 models.

9.1.2 *Assessing climate change impact on asphalt binder grade: selection and its implications*

In this study, the impact of climate change on pavement performance was quantified using ten different climate change models. Python codes were written and executed to extract the climate change data from the statistically downscaled climate models gathered from Pacific Canada. Using the extracted climate data, pavement temperatures were computed using the LTPP model and change in binder grade was determined for the future climatic conditions. In addition, the influence of this upgraded binder on pavement performance was estimated using AASHTOWare Pavement ME Design software and compared. This research resulted in drawing the following conclusions:

- All the locations, except Quebec City, Saguenay, and Corner Brook, need a change in binder grade to adapt to the future climate. All other cities, except Saskatoon and Brandon, need one binder grade increment to adapt to future climate. Only Saskatoon and Brandon need two binder grade increments.
- The pavement performance was susceptible to climate models. Therefore, the mean of all the ten climate models was utilized to witness the impact of climate change and the influence of change in asphalt binder grade on pavement performance.

Conclusions drawn from the impact of climate change on pavement performance are as follows:

- IRI is decreasing for 9 out of 13 sections and increasing for other sections. This decrease might be occurring due to a reduction in freezing index or freeze and thaw cycles.
- Permanent deformation in subbase and subgrade is decreasing in 12 out of 16 locations, which might be occurring due to a reduction in freezing index and an increase in temperature.
- Asphalt concrete permanent deformation is increasing at all the location, which might be a resultant of increasing temperature.
- The total permanent deformation is also increasing for 11 out of 16 locations. In these 11 sections, the increase in AC rutting is higher than the subbase and subgrade rutting.
- AC bottom-up fatigue cracking is increasing in all the pavement sections, except in the pavement sections located in Quebec City and St. John's, due to climate change.

Conclusions drawn from the influence of upgraded binder on pavement performance are as follows:

- With the upgrade of asphalt binder grade, a permanent deformation in the AC layer is significantly decreasing, which results in the extended service life of the pavement.
- The bottom-up fatigue cracking is also reduced due to change in asphalt binder grade for the future climate. This reduces the porousness of rainfall water into the base layers.
- There is no potential change in the subbase and subgrade permanent deformation in most of the pavement sections. However, there is an average of 2.2% reduction for other locations, which might be a result of the reduced BU fatigue cracking.
- There is a decrease in all the distress for the future climate with the upgraded binder.

- It was noticed that the IRI is reducing due to climate change. Besides, with the upgraded binder, the IRI is further reducing, which results in the extended service life of the pavement.
- Upgrading asphalt binder is a low cost and effective climate change adaptation strategy for Canadian pavements.

9.1.3 Asphalt binder selection for future Canadian climatic conditions using various pavement temperature prediction models

This paper presents an analysis to determine the change in asphalt binder grade over 28 different locations in Canada. This analysis aimed to understand the influence of climate change and pavement temperature prediction model on the asphalt binder grade selection process. This study considered an average of 10 different bias-corrected statistically downscaled climate change models to reduce the uncertainty involved with the climate change models. The pavement temperatures models considered in this study are the SHRP pavement temperature model, the LTPP pavement temperature prediction model, and the EICM at 98% reliability. The outcomes from this study enable us to make following conclusions:

- The SHRP pavement temperature model is under-predicting the pavement temperatures when compared to LTPP and EICM models.
- Pavement temperatures estimated using LTPP model and EICM are approximately similar at most of the locations. However, for some of the locations, EICM pavement temperatures are estimated to be higher than both SHRP and LTPP models.
- Most of the location in Canada need a conventional asphalt binder grade. However, the northern part of Canada needs a modification in asphalt binder grade.

- By 2070, Canada needs about two increments in high temperature grade and four increments in low temperature grade as per SHRP and LTPP models. Meanwhile, EICM estimates a maximum of two and three increments for high and low temperatures respectively.
- Canada might need a new pavement temperature prediction model considering all geographic regions.
- Canadian future climate expects a change in asphalt binder grade either in the high temperature or low temperature grade. Therefore, it is necessary to consider future climate in finding out the asphalt binder grade.

9.1.4 Pavement temperature model for Canadian asphalt binder selection: introduction to the CPT model

A pavement temperature model has been developed to more accurately represent pavement temperatures experienced in the Canadian climate. The country was divided into three clusters, each with a model, to address the problem caused by the varied climate. Upon completion of the research, the following conclusions could be drawn:

- Canada's climate can be divided into three clusters; wet-freeze, dry-freeze, and Western wet-non-freezing, to better represent the geographical variances in temperature and precipitation.
- Pearson correlation coefficients have been used to identify which parameters are most correlated to pavement temperature. Correlated parameters varied between clusters and model types.

- The R^2-values obtained for the clusters are generally better than that of the Canada-wide model. It is thus confirmed that representing Canadian climate with the clustered approach is a more accurate way of predicting pavement temperatures.
- The developed pavement temperature models are found to be accurate for the Canadian climatic conditions.
- The models are validated using an unused data set, randomly picked from the entire data before developing the model. And these were further verified with the field measurements.
- CABS software was developed to allow users to quickly obtain the suggested base binder grade based on pavement temperatures using SHRP, LTPP, and the newly developed CPT models.

9.1.5 Climate change adaptation strategies for Canadian asphalt pavements

In this current study, the severities of climate change impact on pavement distresses were computed using 10 different climate change models. Various adaptation strategies such as upgrading asphalt binder grade, increasing the thickness of asphalt concrete layer, increasing the base layer thickness, and using stabilized base layers were analyzed to reduce pavement deterioration and to extend the service life of the pavement. In addition to this, various combinations of adaptation strategies are considered to mitigate the climate change impact. Unlike the other studies, pavement temperatures were determined using EICM to evaluate the change in binder grade for the future climate in the adaptation process. A stone matrix asphalt mixture gradation is considered as another adaption strategy where the AC rutting is found to be very high. To reduce the subbase and subgrade rutting, an emulsion stabilized base is adapted for specific locations. Various conclusions drawn from this study are as follows:

- Only six of the sixteen selected locations in Canada are presently employing the correct asphalt binder grade. The rest all require an upgrade. However, all locations will require a binder grade review by 2040. An even more significant review will be required by 2070.
- For 2010-2040 climate, a change in asphalt binder grade and a change in mixture gradation are the only necessary adaptation strategies to reduce climate change impacts on all the locations apart from Vancouver.
- For 2040-2070 climate, a change in asphalt binder grade and a change in mixture gradation are still sufficient for most of the selected locations, but not in St. John's or Vancouver, which require additional measures.
- For 2070-2100 climate, all the selected locations require a change in binder grade, and the majority also need a change in mixture gradation to compensate for the increased climate change related pavement distresses.
- Most of the locations in the Atlantic provinces require a change in binder and mixture gradation. However, some of the locations require an increase in the thickness of the surface AC layer as well. In Central Canada, upgrade in asphalt binder grade and mixture gradation change are sufficient to mitigate climate change. However, in the Prairie Provinces, a change in asphalt binder grade alone can adapt to climate change.
- A change in asphalt binder grade and the base type are needed in the West Coast region to mitigate climate change impact. This is mainly because of the significant increase in precipitation due to climate change.
- The study resulted in a framework for selecting appropriate adaptation strategy to mitigate climate change impact.

- With the use of appropriate adaptation strategies, all the pavement distresses are reducing more the threshold limits for all selected locations.
- Considering climate change in the design procedure could improve pavement performance and enhance pavement service life.

9.1.6 LCA and LCCA of climate change adaptation strategies for Canadian pavements

This study investigated the impact of climate change adaptation strategies on the life cycle cost and life cycle emissions of Canadian pavements. Appropriate adaptation strategies for the changing climate were compared to baseline scenarios throughout all phases of the pavement's life. The impact of the adaptation strategies over time was investigated to evaluate the increases in costs and emissions expected in the future. Additionally, the factors evaluated in the LCA were statistically compared with the factors in the LCCA to determine the relationship between the two. Upon completion of the research, the following main conclusions could be made:

- Investing in climate change adaptation strategies is beneficial from an LCA and LCCA standpoint for both users and agencies.
- Despite the initial increase in cost to implement some adaptation strategies, the LCCA revealed that over the lifetime of the pavement those costs will be easily offset in most locations.
- Among all of the analyzed adaptation strategies, increased thickness and stabilized bases are the most costly and highest emitters. Upgrading the asphalt binder grade and asphalt mixture type were the least expensive, the lowest emitter, and the easiest to implement. The first step to adapt to climate change for almost all investigated locations is to upgrade the binders.

- The savings incurred through the implementation of climate adaptation strategies only become more prominent over time. The savings in the years 2070-2100 are higher than those in the years 2040-2070, suggesting that with more severe climate change, adaptation strategies become more important.
- The relationship between LCA and LCCA factors is mostly positively correlated. However, total agency cost is negatively correlated with use phase emissions, emphasizes that the increased agency spending will serve to reduce the use phase emissions.
- The adaptation strategies proposed in Table 2 are confirmed to be the best solution from a performance perspective and also from an LCA and LCCA perspective. They will adapt the pavement to climate change and reduce costs and emissions.

9.2 Recommendations

Although this study quantifies the impact of climate change on pavement materials, design, performance, there is a necessity to enhance the accuracy of estimations. Similarly, the adaptation and mitigation strategies need to be optimized for climate change impact. Accordingly, some recommendations for future work are summarized below:

1. Temperature and precipitation are the two significant factors that affect pavement materials and design. Although the other climate factors are less significant, there is an indirect effect on the pavement deterioration. Therefore, it is necessary to estimate the individual contributions of all other climate variables on pavement deterioration.
2. Future traffic is another factor that significantly affects pavement infrastructure. It is also necessary to estimate the impact of the interaction effect of climate factors and future traffic on the pavement service life.

3. Temperature rise due to climate change is the primary concern for asphalt concrete pavements. Therefore, it is necessary to evaluate the influence of temperature related extreme events (heatwaves) on pavement materials and design, especially in the western part of Canada.

4. As the most of Northern Part of Canada is in freezing condition most of the time, it is necessary to investigate the climate change impact for northern part of Canada.

References

AASHTO. (2008a). *Mechanistic-Empirical Pavement Design Guide: A Manual of Practice: Interim Edition. American Association of State Highway and Transportation Officials.*

AASHTO. (2008b). *Mechanistic-empirical pavement design guide. A manual of practice. Washington, DC: American Association of State Highway Officials, Highway Research Board.*

Adwan, I., Milad, A., Memon, Z. A., Widyatmoko, I., Zanuri, N. A., Memon, N. A., & Yusoff, N. I. M. (2021). Asphalt pavement temperature prediction models: A review. In *Applied Sciences* (Vol. 11, Issue 9). https://doi.org/10.3390/app11093794

ARA Inc. (2004). *Guide for Mechanistic-Empirical Design of New and Rehabilitated Pavement Structures, Final Report. NCHRP Project 1-37A. National Cooperative Highway Research Program. Transportation Research Board, National Research Council, Washington, DC.*

Ariawan, I. M. A., Subagio, B. S., & Setiadji, B. H. (2015). Development of asphalt pavement temperature model for tropical climate conditions in West Bali region. *Procedia Engineering*, *125*. https://doi.org/10.1016/j.proeng.2015.11.126

Asadi, M., Nazarian, S., Mallick, R. B., & Tirado, C. (2020). Computational Process for Quantifying the Impact of Flooding on Remaining Life of Flexible Pavement Structures. *Journal of Transportation Engineering, Part B: Pavements*, *146*(4), 04020060. https://doi.org/10.1061/jpeodx.0000219

Asefzadeh, A., Hashemian, L., & Bayat, A. (2017). Development of statistical temperature prediction models for a test road in Edmonton, Alberta, Canada. *International Journal of Pavement Research and Technology*, *10*(5), 369–382. https://doi.org/10.1016/j.ijprt.2017.05.004

Barbi, P., Tavassoti, P., Tighe, S., & Baaj, H. (2021). Implications of climate variation in flexible airport pavement design and performance. *Airfield and Highway Pavements 2021: Airfield Pavement Technology - Selected Papers from the International Airfield and Highway Pavements Conference 2021*, 193–204. https://doi.org/10.1061/9780784483527.017

Belcher, S. E., Hacker, J. N., & Powell, D. S. (2005). Constructing design weather data for future climates. *Building Services Engineering Research and Technology*, *26*(1), 49–61. https://doi.org/10.1191/0143624405bt112oa

Benjamin, D. M., & Budescu, D. V. (2018). The Role of Type and Source of Uncertainty on the Processing of Climate Models Projections. *Front Psychol*, *9*, 403.

Bizjak, K. F., Dawson, A., Hoff, I., Makkonen, L., Ylhaisi, J. S., & Carrera, A. (2014a). The impact of climate change on the European road network The impact of climate change on the European road network. *Proceedings of the Institution of Civil Engineers*, *167*(5), 281–295. https://doi.org/10.1680/tran.11.00072

Bizjak, K. F., Dawson, A., Hoff, I., Makkonen, L., Ylhaisi, J. S., & Carrera, A. (2014b). The impact of climate change on the European road network The impact of climate change on the European road network. *Proceedings of the Institution of Civil Engineers*, *May 2014*. https://doi.org/10.1680/tran.11.00072

Bobes-Jesus, V., Pascual-Muñoz, P., Castro-Fresno, D., & Rodriguez-Hernandez, J. (2013). Asphalt solar collectors: A literature review. *Applied Energy*, *102*, 962–970. https://doi.org/10.1016/j.apenergy.2012.08.050

Bogren, J., Gustavsson, T., & Karlsson, M. (2001). Temperature differences in the air layer close to a road surface. *Meteorological Applications*, *8*(4), 385–395. https://doi.org/10.1017/S1350482701004017

Bosscher, P. J., Bahia, H. U., Thomas, S., & Russell, J. S. (1998). Relationship between pavement temperature and weather data: Wisconsin field study to verify superpave algorithm. *Transportation Research Record*, *1609*(1), 1–11. https://doi.org/10.3141/1609-01

Camici, S., Brocca, L., Melone, F., & Moramarco, T. (2014). Impact of Climate Change on Flood Frequency Using Different Climate Models and Downscaling Approaches. *Journal of Hydrologic Engineering*, *19*(8), 1–15. https://doi.org/10.1061/(ASCE)HE.1943-5584.0000959

Chai, G., & Kelly, G. (2014). *The impacts of climate change on pavement maintenance in Queensland , Australia*. *May*.

Chandrappa, A. K., & Biligiri, K. P. (2016). Development of Pavement-Surface Temperature Predictive Models: Parametric Approach. *Journal of Materials in Civil Engineering*, *28*(3). https://doi.org/10.1061/(asce)mt.1943-5533.0001415

Chen, J., Wang, H., & Xie, P. (2019). Pavement temperature prediction: Theoretical models and critical affecting factors. *Applied Thermal Engineering*, *158*, 113755. https://doi.org/10.1016/j.applthermaleng.2019.113755

Chen, X., & Wang, H. (2020). Quantification of Warming Temperature Impact on Flexible Pavement Overlay Performance in New Jersey. *99th Annual Meeting of the Transportation Research Board (TRB) of National Academies of Science and Engineering, Washington DC*.

Chow, D. H. C., & Levermore, G. J. (2007). New algorithm for generating hourly temperature values using daily maximum, minimum and average values from climate models. *Building Services Engineering Research and Technology*, *28*(3), 237–248. https://doi.org/10.1177/0143624407078642

Dash, S. K., Jenamani, R. K., Kalsi, S. R., & Panda, S. K. (2007). Some evidence of climate change in twentieth-century India. *Climatic Change*, *85*(3–4), 299–321. https://doi.org/10.1007/s10584-007-9305-9

Dawson, A. (2014). *Anticipating and Responding to Pavement Performance as Climate Changes*. *December*, 4–5. https://doi.org/10.1007/978-3-662-44719-2

Delgadillo, R., Arteaga, L., Wahr, C., & Alcafuz, R. (2020). The influence of climate change in Superpave binder selection for Chile. *Road Materials and Pavement Design*, *21*(3), 607–622. https://doi.org/10.1080/14680629.2018.1509803

Delgadillo, R., Arteaga, L., Wahr, C., Alcafuz, R., Delgadillo, R., Arteaga, L., Wahr, C., & Alcafuz, R. (2018). The influence of climate change in Superpave binder selection for Chile. *Road Materials and Pavement Design*, *0*(0), 1–16. https://doi.org/10.1080/14680629.2018.1509803

Dempsey, B. J., Herlache, W. A., & Patel, A. J. (1986). Climatic-Materials-Structural Pavement Analysis Program. *Transportation Research Record*, *1095*, 111–123.

di Piazza, A., Conti, F. Lo, Noto, L. V., Viola, F., & La Loggia, G. (2011). Comparative analysis of different techniques for spatial interpolation of rainfall data to create a serially complete monthly time series of precipitation for Sicily, Italy. *International Journal of Applied Earth Observation and Geoinformation*, *13*(3), 396–408. https://doi.org/10.1016/j.jag.2011.01.005

Diefenderfer, B. K., Al-Qadi, I. L., & Diefenderfer, S. D. (2006). Model to predict pavement temperature profile: Development and validation. *Journal of Transportation Engineering*, *132*(2), 162–167. https://doi.org/10.1061/(ASCE)0733-947X(2006)132:2(162)

Elshaer, M., Ghayoomi, M., & Daniel, J. S. (2018). Bearing capacity analysis of pavement structures for short term flooding events. *Bearing Capacity of Roads, Railways and Airfields - Proceedings of the 10th International Conference on the Bearing Capacity of Roads,* *Railways and Airfields, BCRRA 2017*, *5*(October), 2127–2133. https://doi.org/10.1201/9781315100333-301

Evans, J. P. (2009). 21st century climate change in the Middle East. *Climatic Change*, *92*(3–4), 417–432. https://doi.org/10.1007/s10584-008-9438-5

Finnis, J., & Daraio, J. (2018). *Projected Impacts of Climate Change for the Province of Newfoundland & Labrador: 2018 Update*.

Flato, G., Marotzke, J., Abiodun, B., Braconnot, P., Chou, S. C., Collins, W., Coz, P., Driouech, F., Emori, S., & Forest, C. (2013). *Evaluation of Climate Models 9*.

Fletcher, C. G., Matthews, L., Andrey, J., & Saunders, A. (2016). Projected changes in mid-twenty-first-century extreme maximum pavement temperature in Canada. *Journal of Applied Meteorology and Climatology*, *55*(4), 961–974. https://doi.org/10.1175/JAMC-D-15-0232.1

Fletcher, C. G., Matthews, L., Matthews, L., Andrey, J., & Saunders, A. (2016). *Projected changes in mid-21st century extreme maximum pavement temperature in Canada Projected changes in mid-21 st century extreme maximum pavement temperature in Canada*. *April*. https://doi.org/10.1175/JAMC-D-15-0232.1

Gasparrini, A., Guo, Y., Sera, F., Vicedo-Cabrera, A. M., Huber, V., Tong, S., de Sousa Zanotti Stagliorio Coelho, M., Nascimento Saldiva, P. H., Lavigne, E., Matus Correa, P., Valdes Ortega, N., Kan, H., Osorio, S., Kyselý, J., Urban, A., Jaakkola, J. J. K., Ryti, N. R. I., Pascal, M., Goodman, P. G., … Armstrong, B. (2017). Projections of temperature-related excess mortality under climate change scenarios. *The Lancet Planetary Health*, *1*(9), e360–e367. https://doi.org/10.1016/S2542-5196(17)30156-0

Gudipudi, P. P., Underwood, B. S., & Zalghout, A. (2017a). Impact of climate change on pavement structural performance in the United States. *Transportation Research Part D: Transport and*

Environment, *57*(October), 172–184. https://doi.org/10.1016/j.trd.2017.09.022

Gudipudi, P. P., Underwood, B. S., & Zalghout, A. (2017b). Impact of climate change on pavement structural performance in the United States. *Transportation Research Part D: Transport and Environment*, *57*, 172–184. https://doi.org/10.1016/j.trd.2017.09.022

Gudmundsson, L., Bremnes, J. B., Haugen, J. E., & Engen-Skaugen, T. (2012a). Technical Note: Downscaling RCM precipitation to the station scale using statistical transformations - A comparison of methods. *Hydrology and Earth System Sciences*, *16*(9), 3383–3390. https://doi.org/10.5194/hess-16-3383-2012

Gudmundsson, L., Bremnes, J. B., Haugen, J. E., & Engen-Skaugen, T. (2012b). Technical Note: Downscaling RCM precipitation to the station scale using statistical transformations – A comparison of methods. *Hydrology and Earth System Sciences*, *16*(9), 3383–3390. https://doi.org/10.5194/hess-16-3383-2012

Guymon, G. L., Berg, R. L., & Hromadka, T. V. (1993). *Mathematical Model of Frost Heave and Thaw Settlement in Pavements. CRREL Report 93-2.* (Issue April).

Haslett, K. E., Knott, J. F., Stoner, A. M. K., Sias, J. E., Dave, E. V., Jacobs, J. M., Mo, W., & Hayhoe, K. (2021). Climate change impacts on flexible pavement design and rehabilitation practices. *Road Materials and Pavement Design*. https://doi.org/10.1080/14680629.2021.1880468

Hassan, H. F., Al-Nuaimi, A., Al-Oraimi, S., & Jafar, T. M. A. (2008). Development of asphalt binder performance grades for Omani climate. *Construction and Building Materials*, *22*(8), 1684–1690. https://doi.org/10.1016/j.conbuildmat.2007.06.016

Herb, W., Velasquez, R., Stefan, H., Marasteanu, M. O., & Clyne, T. (2009). Simulation and characterization of asphalt pavement temperatures. *Road Materials and Pavement Design*, *10*(1), 233–247. https://doi.org/10.1080/14680629.2009.9690190

Hermansson, A. (2000). Simulation model for calculating pavement temperatures including maximum temperature. *Transportation Research Record*, *1699*(1), 134–141. https://doi.org/10.3141/1699-19

Hermansson, Å. (2004). Mathematical model for paved surface summer and winter temperature: Comparison of calculated and measured temperatures. *Cold Regions Science and Technology*, *40*(1–2), 1–17. https://doi.org/10.1016/j.coldregions.2004.03.001

Hosseini, F., Hossain, S. M. K., Fu, L., Johnson, M., & Fei, Y. (2015). Prediction of Pavement Surface Temperature Using Meteorological Data for Optimal Winter Operations in Parking Lots. *Proceedings of the International Conference on Cold Regions Engineering*, *January*, 440–451. https://doi.org/10.1061/9780784479315.039

Huber, G. A., Heiman, G. H., & Chursinoff, R. W. (1989). Prediction of Pavement Layer Temperature During Winter Months Using a Computer Model. *Canadian Technical Asphalt Association*.

Hughes, L. (2003). Climate change and Australia: Trends, projections and impacts. *Austral Ecology*, *28*(4), 423–443. https://doi.org/10.1046/j.1442-9993.2003.01300.x

Humphrey, N. (2008). Potential impacts of climate change on U.S. Transportation. *TR News*, *256*, 21–24. https://doi.org/10.17226/12179

Islam, M. R., Ahsan, S., & Tarefder, R. A. (2015). Modeling temperature profile of hot-mix asphalt in flexible pavement. *International Journal of Pavement Research and Technology*, *8*(1), 47–52. https://doi.org/10.6135/ijprt.org.tw/2015.8(1).47

Jeong, H., Kim, H., Kim, K., & Kim, H. (2017). *Prediction of Flexible Pavement Deterioration in Relation to Climate Change Using Fuzzy Logic*. *23*(4).

https://doi.org/10.1061/(ASCE)IS.1943-555X.0000363.

Jones, P. G., & Thornton, P. K. (2009). Croppers to livestock keepers: livelihood transitions to 2050 in Africa due to climate change. *Environmental Science and Policy*, *12*(4), 427–437. https://doi.org/10.1016/j.envsci.2008.08.006

Kharin, V., Zwiers, F., Zhang, X., & Gabriele, H. (2007). *Changes in Temperature and Precipitation Extremes in the IPCC Ensemble of Global*. 1419–1444. https://doi.org/10.1175/JCLI4066.1

Knott, J. F., Jacobs, J. M., Sias, J. E., Kirshen, P., & Dave, E. V. (2019a). *A Framework for Introducing Climate-Change Adaptation in Pavement Management*.

Knott, J. F., Jacobs, J. M., Sias, J. E., Kirshen, P., & Dave, E. V. (2019b). A Framework for Introducing Climate-Change Adaptation in Pavement Management. *Sustainability*, *11*(1). https://doi.org/http://dx.doi.org/10.3390/su11164382

Knott, J. F., Sias, J. E., Dave, E. V, & Jacobs, J. M. (2019). *Seasonal and Long-Term Changes to Pavement Life Caused by Rising Temperatures from Climate Change*. *2673*(6), 267–278. https://doi.org/10.1177/0361198119844249

Knott, J. F., Sias, J. E., Jacobs, J. M., Krishen, P., & Dave, E. V. (2020). Designing a Climate-Ready Coastal Road. *99th Annual Meeting of the Transportation Research Board (TRB) of National Academies of Science and Engineering, Washington DC.*

Kudo, R., Yoshida, T., & Masumoto, T. (2017). Uncertainty Analysis of Impacts of Climate Change on Snow Processes: Case Study of Interactions of GCM Uncertainty and an Impact Model. *Journal of Hydrology*, *548*, 196–207.

Kumlai, S., Jitsangiam, P., & Pichayapan, P. (2016). The implications of increasing temperature due to climate change for asphalt concrete performance and pavement design. *KSCE Journal* *of Civil Engineering*, *21*(4), 1222–1234. https://doi.org/10.1007/s12205-016-1080-6

Kundzewicz, Z. W., Krysanova, V., Benestad, R. E., Hov, Ø., Piniewski, M., & Otto, I. M. (2018). Uncertainty in Climate Change Impacts on Water Resources. *Environmental Science & Policy*, *79*, 1–8.

Li, Q. J., Mills, L., McNeil, S., & Attoh-Okine, N. O. (2013). Integrating potential climate change into the mechanistic–empirical based pavement design. *Canadian Journal of Civil Engineering*, *40*(12), 1173–1183. https://doi.org/10.1139/cjce-2012-0465

Lioubimtseva, E., & Henebry, G. M. (2009). Climate and environmental change in arid Central Asia: Impacts, vulnerability, and adaptations. *Journal of Arid Environments*, *73*(11), 963–977. https://doi.org/10.1016/j.jaridenv.2009.04.022

Liu, C., & Yuan, D. (2000). Temperature distribution in layered road structures. *Journal of Transportation Engineering*, *126*(1). https://doi.org/10.1061/(ASCE)0733-947X(2000)126:1(93)

Lu, D., Tighe, S. L., & Xie, W. (2018). Impact of flood hazards on pavement performance Impact of fl ood hazards on pavement performance. *International Journal of Pavement Engineering*, *0*(0), 1–7. https://doi.org/10.1080/10298436.2018.1508844

Lytton, R. L., Pufahl, D. E., Michalak, C. H., Liang, H. S., & Dempsey., B. J. (1993). *An Integrated Model of the Climatic Effects on Pavements. FHWA-RD-90-033.*

Mallick, R., Jacobs, J. M., Miller, B. J., & Daniel, J. S. (2016). Understanding the impact of climate change on pavements with CMIP5, system dynamics and simulation. *International Journal of Pavement Engineering*, *19*(8), 697–705. https://doi.org/10.1080/10298436.2016.1199880

Mallick, R., Jacobs, J. M., Miller, B. J., Daniel, J. S., Mallick, R. B., Jacobs, J. M., Miller, B. J., & Daniel, J. S. (2016). *Understanding the impact of climate change on pavements with*

CMIP5 , *system dynamics and simulation*. *8436*(January 2017). https://doi.org/10.1080/10298436.2016.1199880

Mallick, R., Radzicki, M., Daniel, J., & Jacobs, J. (2014). Use of System Dynamics to Understand Long- Term Impact of Climate Change on Pavement Performance and Maintenance Cost. *Transportation Research Record Journal of the Transportation Research Board*, *5*(December 2014). https://doi.org/10.3141/2455-01

Mallick, Tao, M., Daniel, J. S., Jacobs, J., & Veeraragavan, A. (2017). Development of a methodology and a tool for the assessment of vulnerability of roadways to flood-induced damage. *Journal of Flood Risk Management*, *10*(3), 301–313. https://doi.org/10.1111/jfr3.12135

Mammeri, A., Ulmet, L., Peti, C., & Mokhtari, A. M. (2015). Temperature modelling in pavements: The effect of long-and short-wave radiation. *International Journal of Pavement Engineering*, *16*(3), 198–213. https://doi.org/10.1080/10298436.2014.937809

Marengo, J. A., Chou, S. C., Kay, G., Alves, L. M., Pesquero, J. F., Soares, W. R., Santos, D. C., Lyra, A. A., Sueiro, G., Betts, R., Chagas, D. J., Gomes, J. L., Bustamante, J. F., & Tavares, P. (2012). Development of regional future climate change scenarios in South America using the Eta CPTEC/HadCM3 climate change projections: Climatology and regional analyses for the Amazon, São Francisco and the Paraná River basins. *Climate Dynamics*, *38*(9–10), 1829–1848. https://doi.org/10.1007/s00382-011-1155-5

Matić, B., Matić, D., Sremac, S., Radović, N., & Vidikant, P. (2014). A model for the pavement temperature prediction at specified depth using neural networks. *Metalurgija*, *53*(4).

Maurer, E. P., Hidalgo, H. G., Das, T., Dettinger, M. D., & Cayan, D. R. (2010a). The utility of daily large-scale climate data in the assessment of climate change impacts on daily streamflow in California. *Hydrology and Earth System Sciences*, *14*(6), 1125–1138. https://doi.org/10.5194/hess-14-1125-2010

Maurer, E. P., Hidalgo, H. G., Das, T., Dettinger, M. D., & Cayan, D. R. (2010b). The utility of daily large-scale climate data in the assessment of climate change impacts on daily streamflow in California. *Hydrology and Earth System Sciences*, *14*(6), 1209–1241. https://doi.org/10.5194/hess-14-1125-2010

Mauritzen, C., Zivkovic, T., & Veldore, V. (2017). On the Relationship Between Climate Sensitivity and Modelling Uncertainty. *Tellus A: Dynamic Meteorology and Oceanography*, *69*(1), 1–12.

Meagher, W., Daniel, J. S., Jacobs, J., & Linder, E. (2012). *Method for Evaluating Implications of Climate Change for Design and Performance of Flexible Pavements*. *2305*, 111–120. https://doi.org/10.3141/2305-12

Meinshausen, M., Smith, S. J., Calvin, K., Daniel, J. S., Kainuma, M. L. T., Lamarque, J., Matsumoto, K., Montzka, S. A., Raper, S. C. B., Riahi, K., Thomson, A., Velders, G. J. M., & van Vuuren, D. P. P. (2011). The RCP greenhouse gas concentrations and their extensions from 1765 to 2300. *Climatic Change*, *109*(1), 213–241. https://doi.org/10.1007/s10584-011-0156-z

Meleux, F., Solmon, F., & Giorgi, F. (2007). Increase in summer European ozone amounts due to climate change. *Atmospheric Environment*, *41*(35), 7577–7587. https://doi.org/10.1016/j.atmosenv.2007.05.048

Melvin, A. M., Larsen, P., Boehlert, B., Neumann, J. E., Chinowsky, P., & Espinet, X. (2016). *Climate change damages to Alaska public infrastructure and the economics of proactive adaptation*. https://doi.org/10.1073/pnas.1611056113

Milad, A., Adwan, I., Majeed, S. A., Yusoff, N. I. M., Al-Ansari, N., & Yaseen, Z. M. (2021). Emerging Technologies of Deep Learning Models Development for Pavement Temperature Prediction. *IEEE Access*, *9*(1), 23840–23849. https://doi.org/10.1109/ACCESS.2021.3056568

Mills, B., Tighe, S., Andrey, J., Huen, K., & Parm, S. (2007). Climate change and the performance of pavement infrastructure in southern Canada: Context and case study. *2006 IEEE EIC Climate Change Technology Conference, EICCCC 2006*, *June*. https://doi.org/10.1109/EICCCC.2006.277185

Mills, B., Tighe, S., Andrey, J., Smith, J., & Huen, K. (2009). Climate Change Implications for Flexible Pavement Design and Performance in Southern Canada. *Journal of Transportation Engineering*, *135*(10), 773–782. https://doi.org/10.1061/(asce)0733-947x(2009)135:10(773)

Mills, B., Tighe, S., Huen, K., & Parm, S. (2006). *Climate Change and the Performance of Pavement Infrastructure in Southern Canada : Context and Case Study Climate change and the performance of pavement infrastructure in southern Canada : Context and case study*. *June*. https://doi.org/10.1109/EICCCC.2006.277185

Minhoto, M. J. C., Pais, J. C., Pereira, P. A. A., & Picado-Santos, L. G. (2005). Predicting asphalt pavement temperature with a three-dimensional finite element method. *Transportation Research Record*, *1919*(1), 96–110. https://doi.org/10.3141/1919-11

Mndawe, M. B., Ndambuki, J. M., Kupolati, W. K., Badejo, A. A., Dunbar, R., Ndambuki, J. M., Kupolati, W. K., Badejo, A. A., & Dunbar, R. (2016). *Assessment of the effects of climate change on the performance of pavement subgrade*. *1338*(March). https://doi.org/10.1080/20421338.2015.1023649

Mohseni, A. (1998). *LTPP Seasonal Asphalt Concrete (AC) Pavement Temperature Models,* *FHWA-RD-97-103* (Vol. 7, Issue 2).

Mohseni, A. (2005). *LTPPBIND V3.1 A SUPERPAVE Binder Selection Program, Washington Pavement Systems LLC, Maiden, MD.*

Mohseni, Alaeddin. (1998a). *LTPP Seasonal Asphalt Concrete Pavement Temperature Models*.

Mohseni, Alaeddin. (1998b). *LTPP Seasonal Asphalt Concrete Pavement Temperature Models*.

Moss, R. H., Edmonds, J. A., Hibbard, K. A., Manning, M. R., Rose, S. K., Van Vuuren, D. P., Carter, T. R., Emori, S., Kainuma, M., Kram, T., Meehl, G. A., Mitchell, J. F. B., Nakicenovic, N., Riahi, K., Smith, S. J., Stouffer, R. J., Thomson, A. M., Weyant, J. P., & Wilbanks, T. J. (2010). The next generation of scenarios for climate change research and assessment. *Nature*, *463*(7282), 747–756. https://doi.org/10.1038/nature08823

Murphy, J. (1998). An Evaluation of Statistical and Dynamical Techniques for Downscaling Local Climate. *Journal of Climate*, *12*, 2256–2284.

Nakicenovic, N., J. Alcamo, G. Davis, B. de Vries, J. Fenhann, S. Gaffin, K. Gregory, A. Grubler, T. Y. Jung, T. K., E. L. La Rovere, L. Michaelis, S. Mori, T. Morita, W. Pepper, H. Pitcher, L. Price, K. Raihi, A. Roehrl, H.-H., & Rogner, A. Sankovski, M. Schlesinger, P. Shukla, S. Smith, R. Swart, S. van Rooijen, N. Victor, and Z. D. (2000). *Emissions Scenarios. A Special Report of Working Group III of the Intergovernmental Panel on Climate Change*.

Nivitha, M. R., & Krishnan, J. M. (2014). Development of Pavement Temperature Contours for India. *Journal of The Institution of Engineers (India): Series A*, *95*(2), 83–90. https://doi.org/10.1007/s40030-014-0074-y

Pacific Climate. (n.d.). *Statistically Downscaled Climate Scenarios*.

Pacificclimate. (n.d.). *Statistically Downscaled Climate Scenarios*. Https://Www.Pacificclimate.Org/Data/Statistically-Downscaled-Climate-Scenarios.

Paquin, D., De Elía, R., & Frigon, A. (2014). Change in North American atmospheric conditions associated with deep convection and severe weather using CRCM4 climate projections. *Atmosphere - Ocean*, *52*(3), 175–190. https://doi.org/10.1080/07055900.2013.877868

Piras, M., Mascaro, G., Deidda, R., & Vivoni, E. R. (2015). Science of the Total Environment Impacts of climate change on precipitation and discharge extremes through the use of statistical downscaling approaches in a Mediterranean basin. *Science of the Total Environment*. https://doi.org/10.1016/j.scitotenv.2015.06.088

Qiao, Y., Casey, D. B., Kuna, K. K., Kelly, K., & Macgregor, I. D. (2016). *Climate Resilience of Flexible Pavement Highways : Assessment of Current Practice*. *July 2017*, 1–14.

Qiao, Y., Dawson, A., Parry, T., & Flintsch, G. (2013). Quantifying the effect of climate change on the deterioration of a flexible pavement. *Proceedings of the International Conferences on the Bearing Capacity of Roads, Railways and Airfields*, *June 2013*.

Qiao, Y., Dawson, A. R., Parry, T., & Flintsch, G. W. (2015a). Evaluating the effects of climate change on road maintenance intervention strategies and Life-Cycle Costs. *Transportation Research Part D: Transport and Environment*, *41*(November 2015), 492–503. https://doi.org/10.1016/j.trd.2015.09.019

Qiao, Y., Dawson, A. R., Parry, T., & Flintsch, G. W. (2015b). Evaluating the effects of climate change on road maintenance intervention strategies and Life-Cycle Costs. *Transportation Research Part D: Transport and Environment*, *41*, 492–503. https://doi.org/10.1016/j.trd.2015.09.019

Qiao, Y., Dawson, A. R., Parry, T., Flintsch, G., & Wang, W. (2020). Flexible pavements and climate change: A comprehensive review and implicatio. *Sustainability (Switzerland)*, *12*(3), 1–21. https://doi.org/10.3390/su12031057

Qiao, Y., Flintsch, G., Dawson, A., & Parry, T. (2013). Examining Effects of Climatic Factors on Flexible Pavement Performance and Service Life. *Transportation Research Record: Journal of the Transportation Research Board*, *2349*(1), 100–107. https://doi.org/10.3141/2349-12

Qiao, Y., Santos, J., Stoner, A. M. K., & Flinstch, G. (2019). *Climate change impacts on asphalt road pavement construction and maintenance An economic life cycle assessment of adaptation measures in the State of*. *2005*(Ipcc 2014), 1–14. https://doi.org/10.1111/jiec.12936

Raad, L., Saboundjian, S., Sebaaly, P., & Epps, J. (1998). Minimum pavement temperature modeling and mapping for alaskan conditions. *Transportation Research Record*, *1643*, 86–94. https://doi.org/10.3141/1643-12

Rana, M., Swarna, S., & Hossain, K. (2020). Climate Change Impact on Pavement Performance in Newfoundland , Canada. *99th Annual Meeting of the Transportation Research Board (TRB) of National Academies of Science and Engineering, Washington DC, USA*.

Robertson, W. . (1995). Using the SHRP Specification to Select Asphalt Binders for LowTemperature Service (Unpublished). *14th Annual Canadian Technical Asphalt Association Conference, Charlottetown, PEI*.

Sailor, D. J. (2014). Risks of summertime extreme thermal conditions in buildings as a result of climate change and exacerbation of urban heat islands. *Building and Environment*, *78*, 81–88. https://doi.org/10.1016/j.buildenv.2014.04.012

Salem, H. M., Bayomy, F. M., Al-Taher, M. G., & Genc, I. H. (2004). Using long-term pavement performance data to predict seasonal variation in asphalt concrete modulus. *Transportation Research Record*, *1896*(1), 119–128. https://doi.org/10.3141/1896-12

Schweikert, A., Chinowsky, P., Espinet, X., & Tarbert, M. (2014). Climate change and infrastructure impacts: Comparing the impact on roads in ten countries through 2100. *Procedia Engineering*, *78*, 306–316. https://doi.org/10.1016/j.proeng.2014.07.072

Schweikert, A., Chinowsky, P., Kwiatkowski, K., Johnson, A., Shilling, E., Strzepek, K., & Strzepek, N. (2015). *Road Infrastructure and Climate Change : Impacts and Adaptations for South Africa*. *21*(3), 1–9. https://doi.org/10.1061/(ASCE)IS.1943-555X.0000235.

Shao, Z., Jenkins, G., & Oh, E. (2017). Assessing the impacts of climate change on road infrastructure. *International Journal of GEOMATE, 13*(38), 120–128.

Sharma, M., Inti, S., Tandon, V., & Byreddy, H. (2020). Economical and Environmental Impact of Climate Change on Texas Pavements. *99th Annual Meeting of the Transportation Research Board (TRB) of National Academies of Science and Engineering, Washington DC*.

Sherif, A., & Hassan, Y. (2004). Modelling pavement temperature for winter maintenance operations. *Canadian Journal of Civil Engineering*, *31*(2), 369–378. https://doi.org/10.1139/l03-107

Solaimanian, M., & Bolzan, P. (1993a). Analysis of the I ntegrated Model of Climatic Effects on Pavements. In *SHRP-A-637*.

Solaimanian, M., & Bolzan, P. (1993b). Analysis of the Integrated Model of Climatic Effects on Pavements. *Strategic Highway Research Program, National Research Council, A001*.

Solaimanian, M., & Kennedy, T. W. (1993). Predicting Maximum Pavement Surface Temperature Using Maximum Air Temperature and Hourly Solar Radiation. *Transportation Research Record*, *1417*.

SP-1. (1997). *Superpave: Performance Graded Asphalt Binder Specification and Testing. Asphalt Institute*.

Sreejith, G. H. (2021). Pavement Temperature Data Maps for Worldwide Locations. *International*

Journal of Pavement Research and Technology. https://doi.org/10.1007/s42947-021-00064-8

Stocker, T. F., Qin, D., Plattner, G.-K., Tignor, M., Allen, S. K., Boschung, J., Nauels, A., Xia, Y., Bex, V., & Midgley, P. M. (2013). Climate change 2013: The physical science basis. In *Contribution of working group I to the fifth assessment report of the intergovernmental panel on climate change*. https://doi.org/10.1017/CBO9781107415324.Summary

Stoner, A. M. K., Daniel, J. S., Jacobs, J. M., Hayhoe, K., & Scott-fleming, I. (2019). *Quantifying the Impact of Climate Change on Flexible Pavement Performance and Lifetime in the United States*. https://doi.org/10.1177/0361198118821877

Swarna, S., & Hossain, K. (2018). Effect of Interface Bonds on Pavement Performance. *In TAC 2018: Innovation and Technology: Evolving Transportation-2018 Conference and Exhibition of the Transportation Association of Canada.*

Swarna, S. T., Hossain, K., Pandya, H., & Mehta, Y. A. (2021a). Assessing Climate Change Impact on Asphalt Binder Grade Selection and its Implications. *Transportation Research Record*. https://doi.org/https://doi.org/10.1177/03611981211013026

Swarna, S. T., Hossain, K., Pandya, H., & Mehta, Y. A. (2021b). Assessing Climate Change Impact on Asphalt Binder Grade Selection and its Implications. *Transportation Research Record: Journal of the Transportation Research Board*, 1–14. https://doi.org/10.1177/03611981211013026

Taylor, K. E., Stouffer, R. J., & Meehl, G. A. (2012). An overview of CMIP5 and the experiment design. *Bulletin of the American Meteorological Society*, *93*(4), 485–498. https://doi.org/10.1175/BAMS-D-11-00094.1

Tighe, S. L., Smith, J., Mills, B., & Andrey, J. (2008). Evaluating Climate Change Impact on Low-

Volume Roads in Southern Canada. *Transportation Research Record: Journal of the Transportation Research Board*, *2053*(1), 9–16. https://doi.org/10.3141/2053-02

Tighe, S., Mills, B., Tighe, S. L., Smith, J., Mills, B., & Andrey, J. (2008a). *Evaluating Climate Change Impact on Low- Volume Roads in Southern Canada on Low-Volume Roads in Southern Canada*. *October 2015*. https://doi.org/10.3141/2053-02

Tighe, S., Mills, B., Tighe, S. L., Smith, J., Mills, B., & Andrey, J. (2008b). Evaluating Climate Change Impact on Low- Volume Roads in Southern Canada on Low-Volume Roads in Southern Canada. *Transportation Research Record: Journal of the Transportation Research Board*, *2053*(1), 9–16. https://doi.org/10.3141/2053-02

Underwood, S. (2019). A method to select general circulation models for pavement performance evaluation A method to select general circulation models for pavement performance evaluation. *International Journal of Pavement Engineering*, *0*(0), 1–13. https://doi.org/10.1080/10298436.2019.1580365

Underwood, S., Guido, Z., Gudipudi, P., & Feinberg, Y. (2017a). Increased costs to US pavement infrastructure from future temperature rise. *Nature Climate Change*, *7*(10), 704–707. https://doi.org/10.1038/nclimate3390

Underwood, S., Guido, Z., Gudipudi, P., & Feinberg, Y. (2017b). Increased costs to US pavement infrastructure from future temperature rise. *Nature Climate Change*, *7*(10), 704–707. https://doi.org/10.1038/nclimate3390

Underwood, S., Guido, Z., Gudipudi, P., & Feinberg, Y. (2017c). *Increased costs to US pavement infrastructure from future temperature rise Increased costs to US pavement infrastructure from future temperature rise*. *September*. https://doi.org/10.1038/nclimate3390

Uzarowski, L., Moore, G., & Gamble, P. (2008). Innovative, comprehensive design and construction of perpetual pavement on the Red Hill Valley Parkway in Hamilton. *TAC/ATC 2008 - 2008 Annual Conference and Exhibition of the Transportation Association of Canada: Transportation - A Key to a Sustainable Future*.

Valle, O., Qiao, Y., Dave, E., & Mo, W. (2017). Life cycle assessment of pavements under a changing climate. *Pavement Life-Cycle Assessment*, *October*, 241–250. https://doi.org/10.1201/9781315159324-25

Vincent, L. A., Zhang, X., Mekis, Wan, H., & Bush, E. J. (2018). Changes in Canada's Climate: Trends in Indices Based on Daily Temperature and Precipitation Data. *Atmosphere - Ocean*, *56*(5), 332–349. https://doi.org/10.1080/07055900.2018.1514579

Viola, F., & Celauro, C. (2015). Effect of climate change on asphalt binder selection for road construction in Italy. *Transportation Research Part D: Transport and Environment*, *37*, 40–47. https://doi.org/10.1016/j.trd.2015.04.012

Wang, J., Fonseca, R. M., Rutledge, K., Martín-Torres, J., & Yu, J. (2019). Weather Simulation Uncertainty Estimation Using Bayesian Hierarchical Models. *Journal of Applied Meteorology and Climatology*, *58*(3), 585–603.

Wigley, T. M.L., Clarke, L. E., Edmonds, J. A., Jacoby, H. D., Paltsev, S., Pitcher, H., Reilly, J. M., Richels, R., Sarofim, M. C., & Smith, S. J. (2009). Uncertainties in climate stabilization. *Climatic Change*, *97*(1), 85–121. https://doi.org/10.1007/s10584-009-9585-3

Wigley, Tom M L. (2008). *MAGICC / SCENGEN 5 . 3 : USER MANUAL (version 2). version 2*.

Wistuba, M. P., & Walther, A. (2013). Consideration of climate change in the mechanistic pavement design. *Road Materials and Pavement Design*, *14*(SUPPL.1), 227–241. https://doi.org/10.1080/14680629.2013.774759

Wood, A. W., Leung, L. R., Sridhar, V., & Lettenmaier, D. P. (2004). *Hydrologic implications of* *dynamical and statistical approaches to downscaling climate model outputs*. 189–216.

Zapata, C. E., Andrei, D., Witczak, M. W., & Houston, W. N. (2007). Incorporation of environmental effects in pavement design. *Road Materials and Pavement Design*, *8*(4), 667–693. https://doi.org/10.3166/rmpd.8.667-693

Zapata, C. E., & Houston, W. N. (2008a). *Calibration and Validation of the Enhanced Integrated Climatic Model for Pavement Design*. Transportation Research Board. https://doi.org/10.17226/23098

Zapata, C. E., & Houston, W. N. (2008b). *Calibration and Validation of the Enhanced Integrated Climatic Model for Pavement Design*. Transportation Research Board. https://doi.org/10.17226/23098

Zareie, A., Amin, S. R., & Amador-jiménez, L. (2016). *Thornthwaite Moisture Index Modeling to Estimate the Implication of Climate Change on Pavement Deterioration*. *142*(4), 1–11. https://doi.org/10.1061/(ASCE)TE.1943-5436.0000840.

Zhai, P., & Pan, X. (2003). Trends in temperature extremes during 1951-1999 in China. *Geophysical Research Letters*, *30*(17). https://doi.org/10.1029/2003GL018004

Appendix A. Data Extraction and Analysis

A.1. Python Coding

A.1.1. Extracting climate change data from climate change model

```
import numpy as np
import netCDF4 as nc
import math
import random
from datetime import date

B = np.genfromtxt("Analysis_Files.txt",dtype="str")
#print(B)
loops = len(B[:,1])
#print(loops)
name = B[:,0]
#print(name)
maxmin = B[:,1]
print(maxmin)
file2 = "ltpp_lat_longs.txt"
A = np.genfromtxt("ltpp_lat_longs.txt",dtype=None)
#print(A)

for w in range(0,loops):
    file = name[w]
    if maxmin[w] == '0':
        temp = "tasmax"
    else:
        temp = "tasmin"
    part_output_name = name[w]
    part_output_name = part_output_name[0:-4]
    output_name = 'output-'+part_output_name+'.txt'
    time_name = 'time-'+part_output_name+'.txt'
    file2read = nc.Dataset(file,'r')            #open nc file to read and store it into a variable
    lat = file2read.variables['lat']        #read a variable from nc file as an attribute
    lat = lat[:]                            #read the data in a variable and store it as a masked array
    lat = np.ma.filled(lat)                 #convert maskd array into np array
    long = file2read.variables['lon']
    long = long[:]
    long = np.ma.filled(long)
    longtrue = long
    time = file2read.variables['time']
    time = time[:]
    time = np.ma.filled(time)
```

```
file2read.close()
n = long.shape[0]
m = lat.shape[0]
k = time.shape[0]
z = A.shape[0]
u = 0
index = np.zeros(z)
h = 1+m*(n-1)
v = h+m-1
d= np.random.rand(v,2)
for i in range(0,n):
    f = np.ones(m)*longtrue[i]
    h = 1+m*(u)
    v = h+m-1
    d[h-1:v,0]=f
    d[h-1:v,1]=lat
    u = u+1

for r in range(0,z):
    madlatlon=abs(d[:,1] - A[r,1]) + abs(d[:,0] - A[r,0])
    closestInd = np.argmin(madlatlon)
    index[r] = closestInd
    del madlatlon

s = index.shape[0]
row = np.random.rand(s)
row[:]=np.floor((index-1)/m)+1
column = np.random.rand(s)
column[:]=index-(row-1)*m

#F = np.random.rand(:,:)
if temp == 'tasmax':
    mmax=np.random.rand(3,len(A))
    smax=np.random.rand(3,len(A))
    tpmax=np.random.rand(3,len(A))
else:
    mmin=np.random.rand(3,len(A))
    smin=np.random.rand(3,len(A))
    tpmin=np.random.rand(3,len(A))
for j in range(0,z):
    print(file)
    print('Current iteration')
    print(j)
    print(temp)
    file2read = nc.Dataset(file,'r')
    var = file2read.variables[temp]
```

```
var = var[:,int(column[j]),int(row[j])]
#var = var[:]
var = np.ma.filled(var)
g = np.squeeze(var)
file2read.close()
p = g.T
#h = [A[j,0],A[j,1],p]
#np.savetxt(output_name,p,delimiter='\t')
#F[j,:]=h
#pause(.05)
print(temp)
if temp == 'tasmax':
    year_temp = np.random.rand(len(time),2)
    year_temp[:,1] = p
    tp=np.random.rand(55151,151)
    maxpt=np.random.rand(151,len(A))
    for i in range(0,len(time)):
        l = int(711857.5+time[i])
        d = date.fromordinal(l)
        year_temp[i,0] = int(d.year)
    print("years done")
    for i in range(1950,2101):
        for l in range (0,55151):
            if int(year_temp[l,0] == i):
                tp[l,i-1950]=year_temp[l,1]
        y=0.0
        for k in range(0,55151):
            if sum(tp[k:k+7,i-1950])/7 >= y:
                y=sum(tp[k:k+7,i-1950])/7
        maxpt[i-1950,j]=y

    print('maxpt')
    mmax[0,j]=np.mean(maxpt[61:91,j])
    smax[0,j]=np.std(maxpt[61:91,j])
    mmax[1,j]=np.mean(maxpt[91:121,j])
    smax[1,j]=np.std(maxpt[91:121,j])
    mmax[2,j]=np.mean(maxpt[121:151,j])
    smax[2,j]=np.std(maxpt[121:151,j])
    print('mmax')
else:
    year_temp = np.random.rand(len(time),2)
    year_temp[:,1] = p
    tp=np.random.rand(55151,151)
    minpt=np.random.rand(151,len(A))
    for i in range(0,len(time)):
        l = int(711857.5+time[i])
```

```
            d = date.fromordinal(l)
            year_temp[i,0] = int(d.year)
        print("years done")
        for i in range(1950,2101):
            for l in range (0,55151):
                if int(year_temp[l,0] == i):
                    tp[l,i-1950]=year_temp[l,1]

            minpt[i-1950,j]=min(tp[:,i-1950])
        print('minpt')
        mmin[0,j]=np.mean(minpt[61:91,j])
        smin[0,j]=np.std(minpt[61:91,j])
        mmin[1,j]=np.mean(minpt[91:121,j])
        smin[1,j]=np.std(minpt[91:121,j])
        mmin[2,j]=np.mean(minpt[121:151,j])
        smin[2,j]=np.std(minpt[121:151,j])
        print('mmin')
np.savetxt('mmax',mmax,delimiter='\t')
np.savetxt('mmin',mmin,delimiter='\t')
np.savetxt('smax',smax,delimiter='\t')
np.savetxt('smin',smin,delimiter='\t')
np.savetxt('tpmax',tpmax,delimiter='\t')
np.savetxt('tpmin',tpmin,delimiter='\t')
```

A.1.2. Hourly Temperature Code

```
import numpy as np
import math
import random
from datetime import date

B = np.genfromtxt("ltppdata.txt",dtype="str")
#print(B)
loops = len(B[:,1])
#print(loops)
name = B[:,0]
#print(name)

for z in range(0,loops):
    year_temp_max=np.genfromtxt("tasmaxoutput_name."+str(z)+".txt",dtype="float")
    year_temp_min=np.genfromtxt("tasminoutput_name."+str(z)+".txt",dtype="float")
    year_pr=np.genfromtxt("proutput_name."+str(z)+".txt",dtype="float")
    hist_temp_pr=np.genfromtxt("hist_temp_pr."+str(z)+".txt",dtype="str")
    A=np.genfromtxt("ex.txt",dtype="str")

    #year_temp_max[year,month,day,tasmax] - extracted tasmax from climate change model
    #year_temp_min[year,month,day,tasmin] - extracted tasmin from climate change model
    #year_pr[year,month,day,pr] - extracted pr from climate change model
    #hist_temp_pr[YYYYMMDDTT, temp, precip, other factors]

    #hist_temp_sort[year,month,day,time,hourly temperature] - Sorted historical temperatures
    hist_temp_sort=np.random.rand(len(hist_temp_pr),5)
    for i in range(0,len(hist_temp_pr)):
        histtemp=hist_temp_pr[i,0]
        hist_temp_sort[i,0]=int(histtemp[0:4])
        hist_temp_sort[i,1]=int(histtemp[4:6])
        hist_temp_sort[i,2]=int(histtemp[6:8])
        hist_temp_sort[i,3]=int(histtemp[8:10])
        hist_temp_sort[i,4]=float(hist_temp_pr[i,1])

    #hist_pr_sort[year,month,day,time,avg precipitation] - Sorted historical precipitation
    hist_pr_sort=np.random.rand(len(hist_temp_pr),5)
    for i in range(0,len(hist_temp_pr)):
        histtemp=hist_temp_pr[i,0]
        hist_pr_sort[i,0:4]=hist_temp_sort[i,0:4]
        hist_pr_sort[i,4]=float(hist_temp_pr[i,2])

    #year_temp_hist[year,month,day,tasmax,tasmin]-Computed max and mins for historial
temperatures
    year_temp_hist=np.random.rand(int(len(hist_temp_pr)/24)-1,5)
```

```
    tempmax=hist_temp_sort[0,4]
    tempmin=hist_temp_sort[0,4]
    for i in range(0,len(hist_temp_sort)-1):
        if hist_temp_sort[i,2] == hist_temp_sort[i+1,2]:
            if tempmax <= hist_temp_sort[i+1,4]:
                tempmax = hist_temp_sort[i+1,4]
            if tempmin >= hist_temp_sort[i+1,4]:
                tempmin = hist_temp_sort[i+1,4]
        if hist_temp_sort[i,2] != hist_temp_sort[i+1,2]:
            year_temp_hist[int(i/24),0]=hist_temp_sort[i,0]
            year_temp_hist[int(i/24),1]=hist_temp_sort[i,1]
            year_temp_hist[int(i/24),2]=hist_temp_sort[i,2]
            year_temp_hist[int(i/24),3]=tempmax
            year_temp_hist[int(i/24),4]=tempmin
            tempmax = hist_temp_sort[i+1,4]
            tempmin = hist_temp_sort[i+1,4]

    #year_pr_hist[year,month,day,pr]-Computed pr avges for historial temperatures
    year_pr_hist=np.random.rand(int(len(hist_temp_pr)/24)-1,4)
    pravg=hist_pr_sort[0,4]
    for i in range(0,len(hist_pr_sort)-1):
        if hist_pr_sort[i,2] == hist_pr_sort[i+1,2]:
            pravg = pravg+hist_pr_sort[i+1,4]
        if hist_pr_sort[i,2] != hist_pr_sort[i+1,2]:
            year_pr_hist[int(i/24),0]=hist_pr_sort[i,0]
            year_pr_hist[int(i/24),1]=hist_pr_sort[i,1]
            year_pr_hist[int(i/24),2]=hist_pr_sort[i,2]
            year_pr_hist[int(i/24),3]=pravg/24
            pravg = hist_pr_sort[i+1,4]
    #Hourly temperatues for 2010-2044
    #hourly_temp[year,month,day,time,hourly temperature] - computed for future climate
    hourly_temp10=np.random.rand(len(hist_temp_sort)-24,2)
    for i in range(0,len(hist_temp_sort)-24):
        a=("{:04d}".format(int(year_temp_max[int(i/24)+21915,0])))
        b=("{:02d}".format(int(year_temp_max[int(i/24)+21915,1])))
        c=("{:02d}".format(int(year_temp_max[int(i/24)+21915,2])))
        d=("{:02d}".format(int(hist_temp_sort[i,3])))
        hourly_temp10[i,0]=a+b+c+d

hourly_temp10[i,1]=year_temp_min[int(i/24)+21915,3]+((year_temp_max[int(i/24)+21915,3]-
year_temp_min[int(i/24)+21915,3])/(year_temp_hist[int(i/24),3]-
year_temp_hist[int(i/24),4])*(hist_temp_sort[i,4]-year_temp_hist[int(i/24),4]))
    #np.savetxt("hourly_temp_2010.txt",hourly_temp10,delimiter='\t')

    #Hourly temperatues for 2040-2074
    #hourly_temp[year,month,day,time,hourly temperature] - computed for future climate
```

```
    hourly_temp40=np.random.rand(len(hist_temp_sort)-24,2)
    for i in range(0,len(hist_temp_sort)-24):
        a=("{:04d}".format(int(year_temp_max[int(i/24)+32872,0])))
        b=("{:02d}".format(int(year_temp_max[int(i/24)+32872,1])))
        c=("{:02d}".format(int(year_temp_max[int(i/24)+32872,2])))
        d=("{:02d}".format(int(hist_temp_sort[i,3])))
        hourly_temp40[i,0]=a+b+c+d

hourly_temp40[i,1]=year_temp_min[int(i/24)+32872,3]+((year_temp_max[int(i/24)+32872,3]-
year_temp_min[int(i/24)+32872,3])/(year_temp_hist[int(i/24),3]-
year_temp_hist[int(i/24),4])*(hist_temp_sort[i,4]-year_temp_hist[int(i/24),4]))
    #np.savetxt("hourly_temp_2040.txt",hourly_temp40,delimiter='\t')

    #Hourly temperatues for 2070-2100
    #hourly_temp[year,month,day,time,hourly temperature] - computed for future climate
    hourly_temp70=np.random.rand(271728,2)
    for i in range(0,271728):
        hourly_temp70[i,0]=A[i,0]

hourly_temp70[i,1]=year_temp_min[int(i/24)+43792,3]+((year_temp_max[int(i/24)+43792,3]-
year_temp_min[int(i/24)+43792,3])/(year_temp_hist[int(i/24),3]-
year_temp_hist[int(i/24),4])*(hist_temp_sort[i,4]-year_temp_hist[int(i/24),4]))
    #np.savetxt("hourly_temp_2070.txt",hourly_temp70,delimiter='\t')

    #21915=2010-1950
    #32872=2040-1950
    #43830=2070-1950

    #Hourly precipitations for 2010-2044
    #hourly_precip[year,month,day,time,hourly precipitation] - computed for future climate
    hourly_pr10=np.random.rand(len(hist_pr_sort)-24,2)
    for i in range(0,len(hist_pr_sort)-24):
        a=("{:04d}".format(int(year_pr[int(i/24)+21915,0])))
        b=("{:02d}".format(int(year_pr[int(i/24)+21915,1])))
        c=("{:02d}".format(int(year_pr[int(i/24)+21915,2])))
        d=("{:02d}".format(int(hist_pr_sort[i,3])))
        hourly_pr10[i,0]=a+b+c+d
        hourly_pr10[i,1]=hist_pr_sort[i,4]+(hist_pr_sort[i,4]*(year_pr[int(i/24)+21915,3]-
year_pr_hist[int(i/24),3])/year_pr_hist[int(i/24),3])
    #np.savetxt("hourly_pr_2010.txt",hourly_pr10,delimiter='\t')

    #Hourly precipitations for 2040-2074
    #hourly_precip[year,month,day,time,hourly precipitation] - computed for future climate
    hourly_pr40=np.random.rand(len(hist_pr_sort)-24,2)
    for i in range(0,len(hist_pr_sort)-24):
        a=("{:04d}".format(int(year_pr[int(i/24)+32872,0])))
```

```
        b=("{:02d}".format(int(year_pr[int(i/24)+32872,1])))
        c=("{:02d}".format(int(year_pr[int(i/24)+32872,2])))
        d=("{:02d}".format(int(hist_pr_sort[i,3])))
        hourly_pr40[i,0]=a+b+c+d
        hourly_pr40[i,1]=hist_pr_sort[i,4]+(hist_pr_sort[i,4]*(year_pr[int(i/24)+32872,3]-
year_pr_hist[int(i/24),3])/year_pr_hist[int(i/24),3])
    #np.savetxt("hourly_pr_2040.txt",hourly_pr40,delimiter='\t')

    #Hourly precipitations for 12070-2100
    #hourly_precip[year,month,day,time,hourly precipitation] - computed for future climate
    hourly_pr70=np.random.rand(271728,2)
    for i in range(0,271728):
        hourly_pr70[i,0]=A[i,0]
        hourly_pr70[i,1]=hist_pr_sort[i,4]+(hist_pr_sort[i,4]*(year_pr[int(i/24)+43792,3]-
year_pr_hist[int(i/24),3])/year_pr_hist[int(i/24),3])
    #np.savetxt("hourly_pr_2070.txt",hourly_pr70,delimiter='\t')

    final_hourly_2010=np.random.rand(len(hourly_temp10),3)
    #for i in range(0,len(hourly_temp10)):
    final_hourly_2010[:,0:2]=hourly_temp10[:,0:2]
    final_hourly_2010[:,2]=hourly_pr10[:,1]
    np.savetxt(name[z]+"_"+str(z)+"_final_hourly_2010.txt",final_hourly_2010,delimiter='\t')

    final_hourly_2040=np.random.rand(len(hourly_temp40),3)
    #for i in range(0,len(hourly_temp40)):
    final_hourly_2040[:,0:2]=hourly_temp40[:,0:2]
    final_hourly_2040[:,2]=hourly_pr40[:,1]
    np.savetxt(name[z]+"_"+str(z)+"_final_hourly_2040.txt",final_hourly_2040,delimiter='\t')

    final_hourly_2070=np.random.rand(len(hourly_temp70),3)
    #for i in range(0,len(hourly_temp70)):
    final_hourly_2070[:,0:2]=hourly_temp70[:,0:2]
    final_hourly_2070[:,2]=hourly_pr70[:,1]
    np.savetxt(name[z]+"_"+str(z)+"_final_hourly_2070.txt",final_hourly_2070,delimiter='\t')
```

A.1.3. Extracting Pavement Temperatures

```
import numpy as np
import math
import random
from datetime import date

B = np.genfromtxt("LTPP_codes.txt",dtype="str",usecols=np.arange(0,4))
#print(B)
loops = len(B[:,1])
#print(loops)
st = B[:,0]
#print(st)
lc = B[:,1]
#print(lc)

mmax_ltpp=np.random.rand(loops,3)
smax_ltpp=np.random.rand(loops,3)
mmin_ltpp=np.random.rand(loops,3)
smin_ltpp=np.random.rand(loops,3)

mmax_eicm=np.random.rand(loops,3)
smax_eicm=np.random.rand(loops,3)
mmin_eicm=np.random.rand(loops,3)
smin_eicm=np.random.rand(loops,3)

foutput_max_20_1=np.random.rand(loops,5)
foutput_max_30_1=np.random.rand(loops,5)
foutput_max_20_2=np.random.rand(loops,5)

foutput_min_20_1=np.random.rand(loops,5)
foutput_min_30_1=np.random.rand(loops,5)
foutput_min_20_2=np.random.rand(loops,5)

for z in range(0,loops):
    eicm=np.genfromtxt(str(z+1)+".tmp",dtype="str",skip_footer=1)
    ltpp=np.genfromtxt(str(lc[z])+".hcd",delimiter=',',dtype="str")
    print(str(z)+"_Reading - Done")

    ltpp_temp=np.random.rand(len(ltpp),5)
    k=ltpp[0,0]
    ltpp[0,0]=k[3:13]
    for i in range(0,len(ltpp)):
        ltpptemp=ltpp[i,0]
        ltpp_temp[i,0]=int(ltpptemp[0:4])
```

```
    ltpp_temp[i,1]=int(ltpptemp[4:6])
    ltpp_temp[i,2]=int(ltpptemp[6:8])
    ltpp_temp[i,3]=int(ltpptemp[8:10])
    ltpp_temp[i,4]=(float(ltpp[i,1])-32)*5/9

#ltpp_temp_m[year,month,day,tasmax,tasmin]-Computed max and mins for temperatures
ltpp_temp_m=np.random.rand(int(len(ltpp)/24)-1,5)
tempmax=ltpp_temp[0,4]
tempmin=ltpp_temp[0,4]
for i in range(0,len(ltpp_temp)-1):
    if ltpp_temp[i,2] == ltpp_temp[i+1,2]:
        if tempmax <= ltpp_temp[i+1,4]:
            tempmax = ltpp_temp[i+1,4]
        if tempmin >= ltpp_temp[i+1,4]:
            tempmin = ltpp_temp[i+1,4]
    if ltpp_temp[i,2] != ltpp_temp[i+1,2]:
        ltpp_temp_m[int(i/24),0]=ltpp_temp[i,0]
        ltpp_temp_m[int(i/24),1]=ltpp_temp[i,1]
        ltpp_temp_m[int(i/24),2]=ltpp_temp[i,2]
        ltpp_temp_m[int(i/24),3]=tempmax
        ltpp_temp_m[int(i/24),4]=tempmin
        tempmax = ltpp_temp[i+1,4]
        tempmin = ltpp_temp[i+1,4]
print(str(z)+"_LTPP_Max and Mins - Done")


eicm_temp=np.random.rand(len(eicm),5)
for i in range(0,len(eicm)):
    eicmtemp=eicm[i,0]
    eicm_temp[i,0]=int(eicmtemp[0:4])
    eicm_temp[i,1]=int(eicmtemp[4:6])
    eicm_temp[i,2]=int(eicmtemp[6:8])
    eicm_temp[i,3]=int(eicmtemp[8:10])
    eicm_temp[i,4]=(float(eicm[i,1])-32)*5/9

#eicm_temp_m[year,month,day,tasmax,tasmin]-Computed max and mins for temperatures
eicm_temp_m=np.random.rand(int(len(eicm)/24),5)
tempmax=eicm_temp[0,4]
tempmin=eicm_temp[0,4]
for i in range(0,len(eicm_temp)-1):
    if eicm_temp[i,2] == eicm_temp[i+1,2]:
        if tempmax <= eicm_temp[i+1,4]:
            tempmax = eicm_temp[i+1,4]
        if tempmin >= eicm_temp[i+1,4]:
            tempmin = eicm_temp[i+1,4]
    if eicm_temp[i,2] != eicm_temp[i+1,2]:
```

```
        eicm_temp_m[int(i/24),0]=eicm_temp[i,0]
        eicm_temp_m[int(i/24),1]=eicm_temp[i,1]
        eicm_temp_m[int(i/24),2]=eicm_temp[i,2]
        eicm_temp_m[int(i/24),3]=tempmax
        eicm_temp_m[int(i/24),4]=tempmin
        tempmax = eicm_temp[i+1,4]
        tempmin = eicm_temp[i+1,4]

print(str(z)+"_EICM_Max and Mins - Done")

time_ltpp=int(ltpp_temp[len(ltpp)-1,0]-ltpp_temp[0,0])
maxpt_ltpp=np.random.rand(time_ltpp,loops)
minpt_ltpp=np.random.rand(time_ltpp,loops)
tp_ltpp=np.random.rand(len(ltpp),time_ltpp)

for i in range(0,time_ltpp):
    for l in range (0,len(ltpp_temp_m)):
        if int(ltpp_temp_m[l,0] == i+1985):
            tp_ltpp[l,i]=ltpp_temp_m[l,3]
    y=0.0
    for k in range(0,len(ltpp_temp_m)):
        if sum(tp_ltpp[k:k+7,i])/7 >= y:
            y=sum(tp_ltpp[k:k+7,i])/7
    maxpt_ltpp[i,z]=y


for i in range(0,time_ltpp):
    for l in range (0,len(ltpp_temp_m)):
        if int(ltpp_temp_m[l,0] == i+1985):
            tp_ltpp[l,i]=ltpp_temp_m[l,4]
    minpt_ltpp[i,z]=min(tp_ltpp[:,i])

print(str(z)+'_maxpt_ltpp - Done')

mmax_ltpp[z,0]=np.mean(maxpt_ltpp[0:20,z])
smax_ltpp[z,0]=np.std(maxpt_ltpp[0:20,z])
mmax_ltpp[z,1]=np.mean(maxpt_ltpp[0:30,z])
smax_ltpp[z,1]=np.std(maxpt_ltpp[0:30,z])
mmax_ltpp[z,2]=np.mean(maxpt_ltpp[14:34,z])
smax_ltpp[z,2]=np.std(maxpt_ltpp[14:34,z])
mmin_ltpp[z,0]=np.mean(minpt_ltpp[0:20,z])
smin_ltpp[z,0]=np.std(minpt_ltpp[0:20,z])
mmin_ltpp[z,1]=np.mean(minpt_ltpp[0:30,z])
smin_ltpp[z,1]=np.std(minpt_ltpp[0:30,z])
mmin_ltpp[z,2]=np.mean(minpt_ltpp[14:34,z])
smin_ltpp[z,2]=np.std(minpt_ltpp[14:34,z])
```

```
print(str(z)+'_mmax_ltpp - Done')

time_eicm=int(eicm_temp[len(eicm)-1,0]-eicm_temp[0,0])
maxpt_eicm=np.random.rand(time_eicm,loops)
minpt_eicm=np.random.rand(time_eicm,loops)
tp_eicm=np.random.rand(len(eicm),time_eicm)

for i in range(0,time_eicm):
    for l in range (0,len(eicm_temp_m)):
        if int(eicm_temp_m[l,0] == i+1985):
            tp_eicm[l,i]=eicm_temp_m[l,3]
    y=0.0
    for k in range(0,len(eicm_temp_m)):
        if sum(tp_eicm[k:k+7,i])/7 >= y:
            y=sum(tp_eicm[k:k+7,i])/7
    maxpt_eicm[i,z]=y

for i in range(0,time_eicm):
    for l in range (0,len(eicm_temp_m)):
        if int(eicm_temp_m[l,0] == i+1985):
            tp_eicm[l,i]=eicm_temp_m[l,4]
    minpt_eicm[i,z]=min(tp_eicm[:,i])

print(str(z)+'_maxpt_eicm - Done')

mmax_eicm[z,0]=np.mean(maxpt_eicm[0:20,z])
smax_eicm[z,0]=np.std(maxpt_eicm[0:20,z])
mmax_eicm[z,1]=np.mean(maxpt_eicm[0:30,z])
smax_eicm[z,1]=np.std(maxpt_eicm[0:30,z])
mmax_eicm[z,2]=np.mean(maxpt_eicm[14:34,z])
smax_eicm[z,2]=np.std(maxpt_eicm[14:34,z])
mmin_eicm[z,0]=np.mean(minpt_eicm[0:20,z])
smin_eicm[z,0]=np.std(minpt_eicm[0:20,z])
mmin_eicm[z,1]=np.mean(minpt_eicm[0:30,z])
smin_eicm[z,1]=np.std(minpt_eicm[0:30,z])
mmin_eicm[z,2]=np.mean(minpt_eicm[14:34,z])
smin_eicm[z,2]=np.std(minpt_eicm[14:34,z])

print(str(z)+'_mmax_eicm - Done')

foutput_max_20_1[z,0]=int(z+1)
foutput_max_20_1[z,1]=mmax_ltpp[z,0]
foutput_max_20_1[z,2]=smax_ltpp[z,0]
foutput_max_20_1[z,3]=mmax_eicm[z,0]
foutput_max_20_1[z,4]=smax_eicm[z,0]
```

```
    foutput_max_30_1[z,0]=int(z+1)
    foutput_max_30_1[z,1]=mmax_ltpp[z,1]
    foutput_max_30_1[z,2]=smax_ltpp[z,1]
    foutput_max_30_1[z,3]=mmax_eicm[z,1]
    foutput_max_30_1[z,4]=smax_eicm[z,1]

    foutput_max_20_2[z,0]=int(z+1)
    foutput_max_20_2[z,1]=mmax_ltpp[z,2]
    foutput_max_20_2[z,2]=smax_ltpp[z,2]
    foutput_max_20_2[z,3]=mmax_eicm[z,2]
    foutput_max_20_2[z,4]=smax_eicm[z,2]

    foutput_min_20_1[z,0]=int(z+1)
    foutput_min_20_1[z,1]=mmin_ltpp[z,0]
    foutput_min_20_1[z,2]=smin_ltpp[z,0]
    foutput_min_20_1[z,3]=mmin_eicm[z,0]
    foutput_min_20_1[z,4]=smin_eicm[z,0]

    foutput_min_30_1[z,0]=int(z+1)
    foutput_min_30_1[z,1]=mmin_ltpp[z,1]
    foutput_min_30_1[z,2]=smin_ltpp[z,1]
    foutput_min_30_1[z,3]=mmin_eicm[z,1]
    foutput_min_30_1[z,4]=smin_eicm[z,1]

    foutput_min_20_2[z,0]=int(z+1)
    foutput_min_20_2[z,1]=mmin_ltpp[z,2]
    foutput_min_20_2[z,2]=smin_ltpp[z,2]
    foutput_min_20_2[z,3]=mmin_eicm[z,2]
    foutput_min_20_2[z,4]=smin_eicm[z,2]

    print(str(z)+'_Copying - Done')

np.savetxt('foutput_max_20_1',foutput_max_20_1,delimiter='\t')
np.savetxt('foutput_max_30_1',foutput_max_30_1,delimiter='\t')
np.savetxt('foutput_max_20_2',foutput_max_20_2,delimiter='\t')
np.savetxt('foutput_min_20_1',foutput_min_20_1,delimiter='\t')
np.savetxt('foutput_min_30_1',foutput_min_30_1,delimiter='\t')
np.savetxt('foutput_min_20_2',foutput_min_20_2,delimiter='\t')

print('Task Completed')
```

A.1.4. Data Sorting for Cluster Analysis

```
import numpy as np
import math
import random
from datetime import date

B = np.genfromtxt("LTPP_codes.txt",dtype="str",usecols=np.arange(0,4))
#print(B)
loops = len(B[:,1])
#print(loops)
st = B[:,0]
#print(st)
lc = B[:,1]
#print(lc)

foutput=np.random.rand(loops,4)

for z in range(0,loops):
    ltpp=np.genfromtxt(str(lc[z])+".hcd",delimiter=',',dtype="str")
    print(str(z)+"_Reading - Done")

    ltpp_data=np.random.rand(len(ltpp),7)
    k=ltpp[0,0]
    ltpp[0,0]=k[3:13]
    for i in range(0,len(ltpp)):
        ltppdata=ltpp[i,0]
        ltpp_data[i,0]=int(ltppdata[0:4])
        ltpp_data[i,1]=int(ltppdata[4:6])
        ltpp_data[i,2]=int(ltppdata[6:8])
        ltpp_data[i,3]=int(ltppdata[8:10])
        ltpp_data[i,4]=((float(ltpp[i,1]))-32)*5/9
        ltpp_data[i,5]=float(ltpp[i,4])*25.4
        if float(ltpp_data[i,4]) < 0:
            ltpp_data[i,6] = -1*float(ltpp_data[i,4])
        else:
            ltpp_data[i,6] = 0

    ltpp_data_m=np.random.rand(int(len(ltpp)/24)-1,6)
    tempavg=ltpp_data[0,4]
    pravg=ltpp_data[0,5]
    fiavg=ltpp_data[0,6]
    for i in range(0,len(ltpp_data)-1):
        if ltpp_data[i,0] == ltpp_data[i+1,0]:
            tempavg = tempavg+ltpp_data[i+1,4]
            pravg = pravg+ltpp_data[i+1,5]
```

```
            fiavg = fiavg+ltpp_data[i+1,6]
        if ltpp_data[i,2] != ltpp_data[i+1,2]:
            ltpp_data_m[int(i/24),0]=ltpp_data[i,0]
            ltpp_data_m[int(i/24),1]=ltpp_data[i,1]
            ltpp_data_m[int(i/24),2]=ltpp_data[i,2]
            ltpp_data_m[int(i/24),3]=tempavg/24
            ltpp_data_m[int(i/24),4]=pravg
            ltpp_data_m[int(i/24),5]=fiavg/24
            tempavg = ltpp_data[i+1,4]
            pravg = ltpp_data[i+1,5]
            fiavg = ltpp_data[i+1,6]
    print(str(z)+"_LTPP_avgs - Done")


    time_ltpp=int(ltpp_data[len(ltpp)-1,0]-ltpp_data[0,0])
    ltpp_data_aa=np.random.rand(time_ltpp,4)
    tempavg=ltpp_data[0,3]
    pravg=ltpp_data[0,4]
    fiavg=ltpp_data[0,5]
    p=0
    k=0
    t=0
    for i in range(0,len(ltpp_data_m)-1):
        if ltpp_data_m[i,0] == ltpp_data_m[i+1,0]:
            tempavg = tempavg+ltpp_data_m[i+1,3]
            pravg = pravg+ltpp_data_m[i+1,4]
            fiavg = fiavg+ltpp_data_m[i+1,5]
            p=p+1
        if ltpp_data_m[i,0] != ltpp_data_m[i+1,0]:
            ltpp_data_aa[int((i-k)/p)-1+t,0]=ltpp_data_m[i,0]
            ltpp_data_aa[int((i-k)/p)-1+t,1]=tempavg/p
            ltpp_data_aa[int((i-k)/p)-1+t,2]=pravg
            ltpp_data_aa[int((i-k)/p)-1+t,3]=fiavg
            tempavg = ltpp_data_m[i+1,3]
            pravg = ltpp_data_m[i+1,4]
            fiavg = ltpp_data_m[i+1,5]
            p = 0
            k=i
            t=t+1
    print(str(z)+"_LTPP_Annual avgs - Done")
    foutput[z,0]=int(z+1)
    foutput[z,1]=np.mean(ltpp_data_aa[:,1])
    foutput[z,2]=np.mean(ltpp_data_aa[:,2])
    foutput[z,3]=np.mean(ltpp_data_aa[:,3])
np.savetxt('foutput_Cluster',foutput,delimiter='\t')
print('Task Completed')
```

A.1.5. Co-relation coefficients

```
import numpy as np
import seaborn as sns
import pandas as pd
from scipy import stats
import matplotlib.pyplot as plt
columns = ["Tpavem", "Tairm", "Lat",  "H","Lat2", "Tairm*Lat", "Tairm*H", "Log(Lat)", 
"Log(H+25)",
          "Z", "Tairs","H2",  "Z*Tairs"]
min_data = pd.read_csv("Tmin_SI Units_Clusters_H.csv", usecols=columns)
min_data = min_data[columns]
coeff_mat_min = min_data.corr()
plt.subplots(figsize=(15,10))
coeff_mat_min=round(coeff_mat_min, 2)
print(round(coeff_mat_min, 2))
sns.set(font_scale=1.5)
sns.heatmap(coeff_mat_min, cmap="Blues", fmt=".2f", annot=True, annot_kws={'size':16})
plt.show()
np.savetxt('PCorrelations_TMin',coeff_mat_min,delimiter='\t')
```

A.1.6. Regression Model

```
import numpy as np
import pandas as pd
from sklearn.model_selection import train_test_split, cross_val_predict
from sklearn.linear_model import LinearRegression
from sklearn.metrics import mean_squared_error, r2_score, max_error, mean_absolute_error,
explained_variance_score, mean_absolute_percentage_error
import statsmodels.api as sm
import matplotlib.pyplot as plt
columns = ["TairM", "Lat", "Log(H+25)", "Z*TairS"]

max_data = pd.read_csv("Tmax_SI Units_Clusters_H.csv", usecols=columns)
X = max_data[columns]
dataset = pd.read_csv('Tmax_SI Units_Clusters_H.csv')
y = dataset['TpaveM']
linear_regression = LinearRegression()
X_train, X_test, y_train, y_test = train_test_split(X, y, test_size = 0.2, random_state=9)
fit = linear_regression.fit(X_train,y_train)
y_pred = linear_regression.predict(X_test)

test_set_rmse = (np.sqrt(mean_squared_error(y_test, y_pred)))
test_set_r2 = r2_score(y_test, y_pred)
X2 = sm.add_constant(X) # Uncomment to add intercept
est = sm.OLS(y, X2) # Uncomment to add intercept
#est = sm.OLS(y, X)
est2 = est.fit()
print(est2.summary())
print(test_set_rmse)
# print(test_set_r2)
max_err = max_error(y_test, y_pred)
print(max_err)
mae = mean_absolute_error(y_test, y_pred)
print(mae)
expl = explained_variance_score(y_test, y_pred)
print(expl)
mape = mean_absolute_percentage_error(y_test, y_pred)
print(mape)
g = plt.scatter(y_test, y_pred)
np.savetxt('y_test',y_test)
np.savetxt('y_pred',y_pred)
columns = ["Tairm", "Lat", "H", "Z*Tairs"]
max_data = pd.read_csv("Tmin_SI Units_Clusters_H.csv", usecols=columns)
X = max_data[columns]
dataset = pd.read_csv('Tmin_SI Units_Clusters_H.csv')
y = dataset['Tpavem']
```

```
linear_regression = LinearRegression()
X_train, X_test, y_train, y_test = train_test_split(X, y, test_size = 0.2, random_state=9)
fit = linear_regression.fit(X_train,y_train)
y_pred = linear_regression.predict(X_test)
test_set_rmse = (np.sqrt(mean_squared_error(y_test, y_pred)))
test_set_r2 = r2_score(y_test, y_pred)
X2 = sm.add_constant(X) # Uncomment to add intercept
est = sm.OLS(y, X2) # Uncomment to add intercept
#est = sm.OLS(y, X)
est2 = est.fit()
print(est2.summary())
print(test_set_rmse)
# print(test_set_r2)
max_err = max_error(y_test, y_pred)
print(max_err)
mae = mean_absolute_error(y_test, y_pred)
print(mae)
expl = explained_variance_score(y_test, y_pred)
print(expl)
mape = mean_absolute_percentage_error(y_test, y_pred)
print(mape)
g = plt.scatter(y_test, y_pred)
```

A.2. R-Programming

A.2.1. K-Means Clustering

```
library(factoextra)

df <- read.csv(file = "Cluster Data_Filtered.csv")[, c('Province','S.No','City', 'Temperature',
'Precipitation', 'Freezing.Index')]
z1 <- df[, -c(1,2,3)]
m <- apply(z1, 2, mean)
s <- apply(z1, 2, sd)
z2 <- scale(z1, m, s)
distance <- dist(z2)
cluster <- hclust(distance)
set.seed(123)

km.res <- kmeans(z2, 3, nstart = 25)
z4 <- cbind(df, cluster=km.res$cluster)
print(km.res)

write.csv(z4,"Clusters_export_3.csv")
fviz_cluster(km.res, data = z2, ellipse.type = "norm")
```

Appendix B. Climate Change Uncertainty

Note: The units for all the parameters represented in Appendix B are as follows: Precipitation - mm and Temperature - °C.

Table **B**-1: Uncertainty for Precipitation projections, climate change model: MRI- CGCM3

Time period	**1980-2010**	**2010-2040**		**2040-2070**		**2070-2100**	
City	**Precipitation (mm)**	**Precipitation (mm)**	**Uncertainty (%)**	**Precipitation (mm)**	**Uncertainty (%)**	**Precipitation (mm)**	**Uncertainty (%)**
Vancouver	11.39	11.40	0.11	11.35	0.32	11.54	1.29
Calgary	4.38	4.41	0.56	4.46	1.67	4.49	2.51
Edmonton	3.57	3.67	3.01	3.74	4.72	3.83	7.46
Saskatoon	2.73	2.76	0.89	2.83	3.57	2.91	6.25
Brandon	3.78	3.83	1.29	3.94	4.19	4.04	6.77
Winnipeg	4.65	4.69	0.89	4.82	3.67	4.92	5.77
Toronto	7.23	7.26	0.51	7.46	3.21	7.58	4.90
Ottawa	7.15	7.25	1.37	7.43	3.92	7.64	6.83
Montreal	8.64	8.68	0.42	8.86	2.54	9.00	4.10
Quebec City	9.74	9.84	1.00	10.07	3.38	10.33	6.02
Saguenay	8.02	8.12	1.22	8.29	3.35	8.53	6.39
Fredericton	9.86	9.88	0.12	10.13	2.72	10.39	5.32
Charlottetown	9.42	9.45	0.26	9.64	2.33	9.91	5.18
Halifax	12.39	12.49	0.77	12.59	1.56	12.89	4.02
Corner Brook	9.64	9.91	2.78	10.07	4.41	10.30	6.84
St. John’s	12.34	12.60	2.12	12.82	3.86	13.18	6.83

Table B-2: Uncertainty for Precipitation projections, climate change model: CanESM2

Time period	1980-2010	2010-2040	2040-2070	2070-2100	1980-2010	2010-2040	2040-2070
City	**Precipitation (mm)**	**Precipitation (mm)**	**Uncertainty (%)**	**Precipitation (mm)**	**Uncertainty (%)**	**Precipitation (mm)**	**Uncertainty (%)**
Vancouver	11.40	11.46	0.54	11.56	1.39	11.62	1.93
Calgary	4.39	4.49	2.22	4.69	6.67	4.90	11.39
Edmonton	3.54	3.63	2.41	3.81	7.59	3.96	11.72
Saskatoon	2.75	2.89	5.33	3.02	9.78	3.10	12.89
Brandon	3.75	3.89	3.91	3.97	5.86	4.00	6.84
Winnipeg	4.61	4.69	1.59	4.85	5.03	4.91	6.35
Toronto	7.16	7.14	0.22	7.34	2.51	7.43	3.87
Ottawa	7.09	7.13	0.52	7.20	1.55	7.28	2.58
Montreal	8.57	8.67	1.14	8.92	4.13	9.00	4.99
Quebec City	9.64	9.78	1.44	10.00	3.67	10.22	5.95
Saguenay	7.92	7.92	0.00	8.23	3.85	8.37	5.70
Fredericton	9.86	9.95	0.87	10.27	4.08	10.42	5.69
Charlottetown	9.29	9.50	2.29	9.81	5.65	9.85	6.04
Halifax	12.26	12.41	1.29	12.68	3.49	12.70	3.59
Corner Brook	9.57	9.66	0.98	9.95	3.95	10.23	6.89
St. John’s	12.33	12.59	2.08	12.88	4.45	13.06	5.92

Table B-3: Uncertainty for Precipitation projections, climate change model: inmcm4

Time period	1980-2010	2010-2040		2040-2070		2070-2100	
City	Precipitation (mm)	Precipitation (mm)	Uncertainty (%)	Precipitation (mm)	Uncertainty (%)	Precipitation (mm)	Uncertainty (%)
Vancouver	11.41	11.46	0.36	11.45	0.32	11.56	1.28
Calgary	4.39	4.43	0.83	4.42	0.56	4.48	1.94
Edmonton	3.59	3.67	2.38	3.74	4.08	3.88	8.16
Saskatoon	2.75	2.81	2.22	2.83	3.11	2.91	5.78
Brandon	3.76	3.75	0.32	3.78	0.65	3.88	3.25
Winnipeg	4.60	4.55	1.06	4.65	1.06	4.75	3.18
Toronto	7.09	7.12	0.34	7.13	0.52	7.25	2.24
Ottawa	7.14	7.17	0.34	7.17	0.34	7.31	2.39
Montreal	8.65	8.65	0.00	8.66	0.10	8.75	1.16
Quebec City	9.71	9.72	0.15	9.71	0.06	9.84	1.36
Saguenay	8.04	8.06	0.15	8.09	0.61	8.29	3.03
Fredericton	9.84	9.85	0.12	9.92	0.87	10.00	1.61
Charlottetown	9.41	9.44	0.26	9.47	0.65	9.51	1.00
Halifax	12.38	12.34	0.32	12.41	0.28	12.45	0.57
Corner Brook	9.63	9.63	0.00	9.72	0.89	9.79	1.65
St. John's	12.39	12.39	0.00	12.46	0.58	12.54	1.18

Table B-4: Uncertainty for Precipitation projections, climate change model: ACCESS1-0

Time period	1980-2010	2010-2040	2040-2070	2070-2100	Time period	1980-2010	2010-2040
City	Precipitation (mm)	Precipitation (mm)	Uncertainty (%)	Precipitation (mm)	Uncertainty (%)	Precipitation (mm)	Precipitation (mm)
Vancouver	11.25	11.43	1.52	11.57	2.82	11.63	3.36
Calgary	4.35	4.38	0.84	4.38	0.84	4.37	0.56
Edmonton	3.53	3.58	1.52	3.63	2.70	3.60	2.01
Saskatoon	2.69	2.76	2.91	2.80	4.09	2.78	3.64
Brandon	3.74	3.86	3.20	3.85	2.87	3.81	1.89
Winnipeg	4.58	4.63	1.07	4.57	0.27	4.54	0.80
Toronto	7.14	7.16	0.24	7.32	2.51	7.34	2.74
Ottawa	7.21	7.21	0.00	7.39	2.37	7.48	3.74
Montreal	8.73	8.95	2.52	9.21	5.55	9.29	6.43
Quebec City	9.80	10.01	2.12	10.38	5.85	10.50	7.10
Saguenay	8.01	8.20	2.44	8.46	5.64	8.59	7.32
Fredericton	9.90	9.95	0.49	10.33	4.32	10.51	6.17
Charlottetown	9.50	9.61	1.13	9.80	3.15	9.95	4.73
Halifax	12.44	12.66	1.77	12.85	3.34	13.15	5.69
Corner Brook	9.61	9.92	3.30	10.19	6.10	10.55	9.78
St. John's	12.37	12.65	2.32	12.76	3.16	13.06	5.63

Table B-5: Uncertainty for Precipitation projections, climate change model: MICROC5

Time period	1980-2010	2010-2040	2040-2070	2070-2100	Time period	1980-2010	2010-2040
City	**Precipitation (mm)**	**Precipitation (mm)**	**Uncertainty (%)**	**Precipitation (mm)**	**Uncertainty (%)**	**Precipitation (mm)**	**Uncertainty (%)**
Vancouver	11.30	11.35	0.43	11.54	2.05	11.89	5.18
Calgary	4.36	4.38	0.56	4.42	1.40	4.47	2.52
Edmonton	3.56	3.63	1.71	3.65	2.40	3.65	2.40
Saskatoon	2.75	2.84	3.33	2.84	3.56	2.86	4.00
Brandon	3.78	3.85	1.61	3.85	1.61	3.86	1.94
Winnipeg	4.65	4.71	1.31	4.69	0.79	4.67	0.45
Toronto	7.15	7.29	1.88	7.37	3.07	7.53	5.29
Ottawa	7.21	7.39	2.37	7.47	3.55	7.56	4.74
Montreal	8.69	8.91	2.53	9.09	4.61	9.22	6.14
Quebec City	9.90	10.01	1.16	10.25	3.58	10.50	6.04
Saguenay	8.11	8.18	0.90	8.35	3.01	8.56	5.57
Fredericton	9.91	10.24	3.33	10.46	5.54	10.66	7.51
Charlottetown	9.48	9.69	2.31	9.90	4.48	10.06	6.16
Halifax	12.33	12.57	1.98	12.95	5.03	13.16	6.73
Corner Brook	9.67	9.92	2.68	10.10	4.45	10.38	7.35
St. John's	12.38	12.62	1.97	12.78	3.25	12.94	4.56

Table B-6: Uncertainty for Precipitation projections, climate change model: CCSM4

Time period	1980-2010	2010-2040	2040-2070	2070-2100	Time period	1980-2010	2010-2040
City	Precipitation (mm)	Precipitation (mm)	Uncertainty (%)	Precipitation (mm)	Uncertainty (%)	Precipitation (mm)	Uncertainty (%)
Vancouver	11.44	11.19	2.13	11.20	2.05	11.19	2.13
Calgary	4.43	4.41	0.55	4.44	0.28	4.52	1.93
Edmonton	3.58	3.58	0.00	3.58	0.00	3.60	0.68
Saskatoon	2.76	2.77	0.44	2.77	0.44	2.78	0.88
Brandon	3.75	3.80	1.30	3.85	2.61	3.83	2.28
Winnipeg	4.55	4.59	0.80	4.60	0.99	4.58	0.54
Toronto	7.19	7.26	0.98	7.35	2.17	7.45	3.53
Ottawa	7.19	7.21	0.31	7.23	0.48	7.28	1.15
Montreal	8.73	8.79	0.70	8.81	0.98	8.91	2.10
Quebec City	9.76	9.95	1.98	10.06	3.10	10.22	4.73
Saguenay	8.00	8.11	1.37	8.19	2.44	8.33	4.12
Fredericton	9.88	9.96	0.84	10.19	3.19	10.27	3.93
Charlottetown	9.42	9.51	0.96	9.72	3.16	9.89	4.98
Halifax	12.37	12.62	2.07	12.81	3.55	12.90	4.34
Corner Brook	9.62	9.76	1.50	9.95	3.43	10.06	4.57
St. John’s	12.50	12.52	0.20	12.65	1.17	12.68	1.46

Table B-7: Uncertainty for Precipitation projections, climate change model: MPI-ESM-LR

Time period	1980-2010	2010-2040	2040-2070	2070-2100	Time period	1980-2010	2010-2040
City	**Precipitation (mm)**	**Precipitation (mm)**	**Uncertainty (%)**	**Precipitation (mm)**	**Uncertainty (%)**	**Precipitation (mm)**	**Uncertainty (%)**
Vancouver	11.49	11.67	1.59	11.73	2.13	11.90	3.61
Calgary	4.35	4.30	1.12	4.30	1.12	4.39	1.12
Edmonton	3.54	3.54	0.00	3.53	0.34	3.56	0.69
Saskatoon	2.75	2.66	3.11	2.66	3.11	2.67	2.67
Brandon	3.78	3.76	0.65	3.83	1.29	3.92	3.55
Winnipeg	4.63	4.63	0.00	4.68	1.06	4.80	3.69
Toronto	7.12	7.19	1.03	7.35	3.26	7.50	5.32
Ottawa	7.12	7.17	0.69	7.37	3.60	7.57	6.35
Montreal	8.59	8.80	2.52	8.94	4.05	9.12	6.18
Quebec City	9.66	9.78	1.26	9.92	2.78	10.17	5.31
Saguenay	7.93	8.02	1.08	8.17	2.92	8.45	6.46
Fredericton	9.73	9.92	2.01	10.12	4.02	10.32	6.02
Charlottetown	9.27	9.36	1.05	9.56	3.15	9.68	4.48
Halifax	12.24	12.34	0.80	12.55	2.49	12.79	4.49
Corner Brook	9.58	9.62	0.37	9.92	3.55	10.16	5.97
St. John's	12.37	12.51	1.14	12.63	2.13	12.93	4.50

Table B-8: Uncertainty for Precipitation projections, climate change model: CSIRO-Mk3-6-0

Time period	1980-2010	2010-2040	2040-2070	2070-2100	Time period	1980-2010	2010-2040
City	Precipitation (mm)	Precipitation (mm)	Uncertainty (%)	Precipitation (mm)	Uncertainty (%)	Precipitation (mm)	Uncertainty (%)
Vancouver	11.35	11.36	0.11	11.30	0.43	11.62	2.37
Calgary	4.32	4.32	0.00	4.28	0.85	4.26	1.41
Edmonton	3.55	3.55	0.00	3.58	0.69	3.59	1.03
Saskatoon	2.76	2.76	0.00	2.77	0.44	2.80	1.33
Brandon	3.75	3.69	1.63	3.76	0.33	3.79	1.24
Winnipeg	4.63	4.57	1.32	4.68	1.06	4.78	3.35
Toronto	7.15	7.32	2.39	7.39	3.24	7.67	7.17
Ottawa	7.23	7.30	1.01	7.50	3.72	7.75	7.26
Montreal	8.72	8.88	1.88	9.19	5.46	9.52	9.24
Quebec City	9.73	10.00	2.81	10.29	5.77	10.71	10.04
Saguenay	8.03	8.20	2.13	8.40	4.56	8.64	7.60
Fredericton	9.84	10.23	3.97	10.46	6.33	10.86	10.42
Charlottetown	9.40	9.79	4.16	9.89	5.19	10.21	8.57
Halifax	12.37	12.70	2.67	12.87	4.05	13.27	7.28
Corner Brook	9.59	10.14	5.82	10.30	7.47	10.55	10.02
St. John’s	12.37	12.82	3.65	13.01	5.23	13.38	8.19

Table B-9: Uncertainty for Precipitation projections, climate change model: GFDL-ESM2G

Time period	1980-2010	2010-2040		2040-2070		2070-2100	
City	Precipitation (mm)	Precipitation (mm)	Uncertainty (%)	Precipitation (mm)	Uncertainty (%)	Precipitation (mm)	Uncertainty (%)
Vancouver	11.33	11.55	1.91	11.65	2.77	11.90	5.03
Calgary	4.36	4.48	2.80	4.59	5.32	4.61	5.88
Edmonton	3.60	3.60	0.00	3.70	2.71	3.76	4.31
Saskatoon	2.73	2.76	0.89	2.89	5.80	2.93	7.14
Brandon	3.81	3.97	4.10	4.13	8.26	4.22	10.83
Winnipeg	4.67	4.87	4.34	5.08	8.84	5.26	12.77
Toronto	7.17	7.35	2.50	7.57	5.62	7.70	7.50
Ottawa	7.20	7.35	2.09	7.64	6.16	7.79	8.19
Montreal	8.70	8.81	1.26	9.11	4.63	9.29	6.73
Quebec City	9.70	9.88	1.76	10.19	5.03	10.40	7.17
Saguenay	8.06	8.20	1.82	8.42	4.55	8.62	6.97
Fredericton	9.83	9.97	1.49	10.28	4.60	10.46	6.46
Charlottetown	9.36	9.62	2.74	9.86	5.35	10.03	7.17
Halifax	12.34	12.62	2.25	12.99	5.22	13.12	6.31
Corner Brook	9.57	9.89	3.36	10.07	5.24	10.25	7.18
St. John’s	12.28	12.54	2.06	12.81	4.24	12.98	5.63

Table B-10: Uncertainty for Precipitation projections, climate change model: CNRM-CM5

Time period	1980-2010	2010-2040		2040-2070		2070-2100	
City	Precipitation (mm)	Precipitation (mm)	Uncertainty (%)	Precipitation (mm)	Uncertainty (%)	Precipitation (mm)	Uncertainty (%)
Vancouver	11.35	11.28	0.65	11.46	0.97	11.58	2.04
Calgary	4.35	4.43	1.91	4.48	3.03	4.58	5.28
Edmonton	3.60	3.55	1.36	3.61	0.34	3.67	2.03
Saskatoon	2.76	2.72	1.33	2.75	0.44	2.82	2.21
Brandon	3.75	3.71	0.98	3.78	0.98	3.82	1.95
Winnipeg	4.61	4.50	2.38	4.57	1.06	4.59	0.53
Toronto	7.15	7.23	1.02	7.36	2.90	7.51	4.95
Ottawa	7.15	7.18	0.34	7.32	2.39	7.45	4.10
Montreal	8.58	8.65	0.85	8.86	3.27	9.11	6.12
Quebec City	9.69	9.64	0.50	9.88	1.89	10.08	4.03
Saguenay	8.03	8.06	0.38	8.29	3.19	8.53	6.23
Fredericton	9.81	9.95	1.43	10.12	3.11	10.29	4.89
Charlottetown	9.40	9.43	0.34	9.57	1.82	9.68	2.99
Halifax	12.37	12.37	0.00	12.48	0.89	12.63	2.17
Corner Brook	9.62	9.84	2.28	10.05	4.44	10.29	6.98
St. John's	12.33	12.41	0.69	12.56	1.88	12.73	3.27

Table B-11: Uncertainty for High Temperature projections, climate change model: MRI- CGCM3

Time period	1980-2010		2010-2040			2040-2070			2070-2100		
Type	10th Percentile	90th Percentile	10th Percentile	90th Percentile	Uncertainty	10th Percentile	90th Percentile	Uncertainty	10th Percentile	90th Percentile	Uncertainty
Vancouver	5.92	23.68	6.30	23.91	0.06	6.63	24.33	0.09	7.01	24.95	0.13
Calgary	-4.14	22.94	-3.76	23.20	0.10	-3.51	23.53	0.18	-3.18	24.13	0.28
Edmonton	-10.28	24.08	-9.84	24.31	0.05	-9.21	24.75	0.13	-8.85	25.33	0.19
Saskatoon	-12.98	26.39	-12.39	26.64	0.06	-12.04	26.97	0.09	-11.43	27.51	0.16
Brandon	-12.68	26.75	-12.34	27.12	0.04	-12.08	27.59	0.08	-11.27	28.17	0.16
Winnipeg	-12.39	26.19	-12.04	26.56	0.04	-11.68	26.99	0.09	-10.96	27.61	0.17
Toronto	-4.10	26.39	-4.03	26.65	0.03	-3.38	27.14	0.20	-2.71	27.73	0.39
Ottawa	-6.69	26.92	-6.55	27.19	0.03	-5.82	27.59	0.16	-5.06	28.21	0.29
Montreal	-6.08	26.69	-6.01	26.83	0.02	-5.33	27.14	0.14	-4.55	27.69	0.29
Quebec City	-7.30	25.48	-7.10	25.75	0.04	-6.37	26.14	0.15	-5.53	26.75	0.29
Saguenay	-10.46	24.83	-10.28	25.02	0.02	-9.53	25.45	0.11	-8.54	26.09	0.23
Fredericton	-4.16	26.08	-3.90	26.38	0.07	-3.00	26.84	0.31	-2.14	27.51	0.54
Charlottetown	-3.97	23.69	-3.51	24.02	0.13	-2.60	24.54	0.38	-1.58	25.22	0.67
Halifax	-1.77	23.99	-1.47	24.35	0.18	-0.58	24.90	0.71	0.19	25.55	1.17
Corner Brook	-5.05	20.17	-4.55	20.49	0.12	-3.48	20.96	0.35	-2.44	21.68	0.59
St. John’s	-1.41	21.05	-0.78	21.36	0.46	0.09	21.91	1.11	0.75	22.51	1.60

Table **B-**12: Uncertainty for High Temperature projections, climate change model: CanESM2

Time period	1980-2010		2010-2040			2040-2070			2070-2100		
Type	**10th Percentile**	**90th Percentile**	**10th Percentile**	**90th Percentile**	**Uncertainty**	**10th Percentile**	**90th Percentile**	**Uncertainty**	**10th Percentile**	**90th Percentile**	**Uncertainty**
Vancouver	5.98	23.78	6.62	24.52	0.08	7.22	25.83	0.12	7.75	0.28	0.14
Calgary	-3.92	23.11	-3.23	24.04	0.22	-2.53	25.10	0.44	-1.84	0.27	0.69
Edmonton	-10.18	24.37	-9.11	25.22	0.14	-8.24	26.22	0.27	-7.30	0.28	0.42
Saskatoon	-12.76	26.64	-11.79	27.61	0.11	-10.87	28.68	0.23	-9.68	0.30	0.38
Brandon	-12.54	26.99	-11.57	27.90	0.11	-10.62	28.93	0.22	-9.31	0.30	0.38
Winnipeg	-12.26	26.34	-11.29	27.20	0.11	-10.39	28.28	0.23	-9.16	0.30	0.38
Toronto	-3.95	26.55	-3.35	27.44	0.18	-2.69	28.63	0.40	-1.89	0.30	0.65
Ottawa	-6.54	27.04	-5.81	27.94	0.14	-5.02	29.16	0.31	-4.08	0.31	0.51
Montreal	-5.98	26.83	-5.26	27.64	0.15	-4.42	28.91	0.34	-3.51	0.30	0.55
Quebec City	-7.06	25.61	-6.27	26.41	0.14	-5.48	27.64	0.30	-4.53	0.29	0.50
Saguenay	-10.30	24.93	-9.42	25.77	0.12	-8.54	26.98	0.25	-7.46	0.29	0.43
Fredericton	-4.08	26.18	-3.36	26.96	0.21	-2.53	28.22	0.46	-1.59	0.30	0.75
Charlottetown	-3.86	23.81	-3.19	24.59	0.21	-2.52	25.71	0.43	-1.67	0.27	0.71
Halifax	-1.74	24.09	-1.11	24.85	0.39	-0.42	25.88	0.83	0.26	0.27	1.28
Corner Brook	-4.95	20.29	-4.22	21.00	0.18	-3.51	22.05	0.38	-2.70	0.23	0.60
St. John’s	-1.35	21.21	-0.87	21.82	0.39	-0.28	22.69	0.87	0.32	0.24	1.36

Table B-13: Uncertainty for High Temperature projections, climate change model: inmcm4

Time period	1980-2010		2010-2040			2040-2070			2070-2100		
Type	10th Percentile	90th Percentile	10th Percentile	90th Percentile	Uncertainty	10th Percentile	90th Percentile	Uncertainty	10th Percentile	90th Percentile	Uncertainty
Vancouver	5.85	23.60	6.31	24.01	0.06	6.65	24.51	0.10	7.04	25.17	0.14
Calgary	-4.13	23.02	-3.56	23.23	0.15	-2.92	23.58	0.32	-2.32	24.04	0.48
Edmonton	-10.47	24.10	-9.61	24.03	0.08	-8.88	24.10	0.15	-8.28	24.33	0.22
Saskatoon	-13.14	26.51	-12.04	26.64	0.09	-11.22	27.02	0.17	-10.55	27.58	0.24
Brandon	-12.83	26.83	-11.89	27.16	0.09	-11.04	27.59	0.17	-10.36	27.98	0.24
Winnipeg	-12.43	26.22	-11.51	26.51	0.08	-10.53	26.85	0.18	-9.75	27.24	0.25
Toronto	-4.01	26.42	-3.38	26.59	0.16	-2.92	26.92	0.29	-2.36	27.33	0.45
Ottawa	-6.50	26.92	-5.65	27.08	0.14	-4.91	27.34	0.26	-4.26	27.70	0.37
Montreal	-5.96	26.71	-5.15	26.85	0.14	-4.58	27.14	0.25	-4.00	27.49	0.36
Quebec City	-7.10	25.48	-6.29	25.62	0.12	-5.66	25.95	0.22	-4.96	26.32	0.33
Saguenay	-10.34	24.75	-9.40	24.98	0.10	-8.61	25.31	0.19	-7.74	25.67	0.29
Fredericton	-4.05	26.03	-3.50	26.12	0.14	-3.14	26.40	0.24	-2.62	26.76	0.38
Charlottetown	-3.97	23.63	-3.41	23.84	0.15	-3.03	24.19	0.26	-2.49	24.68	0.42
Halifax	-1.70	23.94	-1.22	24.10	0.29	-0.90	24.41	0.49	-0.51	24.85	0.73
Corner Brook	-5.01	20.10	-4.64	20.35	0.09	-4.30	20.68	0.17	-3.76	21.13	0.30
St. John's	-1.44	21.09	-1.19	21.33	0.19	-0.89	21.68	0.41	-0.50	22.24	0.71

Table B-14: Uncertainty for High Temperature projections, climate change model: ACCESS1-0

Time period	**1980-2010**		**2010-2040**			**2040-2070**			**2070-2100**		
Type	**10th Percentile**	**90th Percentile**	**10th Percentile**	**90th Percentile**	**Uncertainty**	**10th Percentile**	**90th Percentile**	**Uncertainty**	**10th Percentile**	**90th Percentile**	**Uncertainty**
Vancouver	5.94	0.24	6.35	24.55	0.03	6.73	25.77	0.04	7.20	27.38	0.05
Calgary	-4.05	0.23	-3.26	23.75	0.23	-2.76	24.94	0.40	-2.18	26.48	0.61
Edmonton	-10.33	0.24	-9.34	24.80	0.12	-8.46	25.85	0.25	-7.30	27.34	0.42
Saskatoon	-12.93	0.27	-11.89	27.31	0.10	-10.94	28.45	0.22	-9.68	29.94	0.37
Brandon	-12.69	0.27	-11.84	27.46	0.09	-10.54	28.62	0.23	-9.31	30.08	0.38
Winnipeg	-12.24	0.26	-11.36	26.91	0.09	-10.29	28.09	0.23	-8.97	29.52	0.39
Toronto	-3.85	0.26	-3.36	27.04	0.15	-2.30	28.03	0.47	-1.25	29.39	0.79
Ottawa	-6.49	0.27	-5.88	27.57	0.12	-4.64	28.63	0.35	-3.51	29.97	0.57
Montreal	-6.02	0.27	-5.34	27.32	0.13	-4.21	28.29	0.36	-3.12	29.54	0.58
Quebec City	-7.14	0.26	-6.42	26.11	0.12	-5.24	27.12	0.33	-4.15	28.41	0.53
Saguenay	-10.35	0.25	-9.54	25.48	0.10	-8.28	26.47	0.26	-6.95	27.86	0.45
Fredericton	-4.00	0.26	-3.52	26.83	0.15	-2.51	27.78	0.44	-1.46	29.05	0.75
Charlottetown	-3.88	0.24	-3.39	24.48	0.16	-2.55	25.47	0.41	-1.76	26.70	0.67
Halifax	-1.75	0.24	-1.34	24.72	0.27	-0.61	25.53	0.72	0.11	26.74	1.18
Corner Brook	-4.88	0.20	-4.29	20.96	0.16	-3.36	21.92	0.40	-2.57	23.08	0.61
St. John’s	-1.34	0.21	-0.80	21.78	0.43	-0.18	22.67	0.94	0.43	23.70	1.44

Table **B-**15: Uncertainty for High Temperature projections, climate change model: MICROC5

Time period	**1980-2010**		**2010-2040**			**2040-2070**			**2070-2100**		
Type	**10th Percentile**	**90th Percentile**	**10th Percentile**	**90th Percentile**	**Uncertainty**	**10th Percentile**	**90th Percentile**	**Uncertainty**	**10th Percentile**	**90th Percentile**	**Uncertainty**
Vancouver	5.98	23.64	6.38	24.16	0.04	6.82	0.25	0.09	7.17	25.71	0.11
Calgary	-3.98	22.99	-3.46	23.67	0.16	-2.84	0.24	0.35	-2.27	25.47	0.54
Edmonton	-10.13	24.12	-9.64	24.79	0.08	-8.95	0.26	0.18	-8.25	26.64	0.29
Saskatoon	-12.81	26.45	-12.14	27.04	0.07	-11.37	0.28	0.17	-10.45	29.10	0.28
Brandon	-12.65	26.84	-11.90	27.57	0.09	-11.02	0.29	0.19	-9.86	29.78	0.33
Winnipeg	-12.32	26.27	-11.60	27.10	0.09	-10.71	0.28	0.20	-9.58	29.22	0.33
Toronto	-4.04	26.47	-3.28	27.17	0.22	-2.57	0.28	0.42	-1.73	29.04	0.67
Ottawa	-6.53	26.99	-5.67	27.81	0.16	-4.76	0.29	0.33	-3.66	29.84	0.54
Montreal	-5.96	26.81	-5.05	27.55	0.18	-4.23	0.28	0.35	-3.14	29.46	0.57
Quebec City	-7.09	25.60	-6.22	26.29	0.15	-5.35	0.27	0.31	-4.31	28.24	0.50
Saguenay	-10.24	24.95	-9.39	25.71	0.11	-8.39	0.27	0.25	-7.17	27.75	0.41
Fredericton	-4.00	26.14	-3.21	26.82	0.22	-2.45	0.28	0.45	-1.50	28.58	0.72
Charlottetown	-3.89	23.75	-3.12	24.42	0.22	-2.44	0.25	0.43	-1.62	26.12	0.68
Halifax	-1.58	24.09	-1.02	24.72	0.38	-0.45	0.25	0.77	0.33	26.30	1.30
Corner Brook	-4.82	20.24	-4.27	20.81	0.14	-3.58	0.22	0.32	-2.79	22.45	0.53
St. John's	-1.35	21.14	-1.03	21.61	0.26	-0.60	0.22	0.61	-0.08	23.05	1.03

Table **B**-16: Uncertainty for High Temperature projections, climate change model: CCSM4

Time period	**1980-2010**		**2010-2040**			**2040-2070**			**2070-2100**		
Type	**10th Percentile**	**90th Percentile**	**10th Percentile**	**90th Percentile**	**Uncertainty**	**10th Percentile**	**90th Percentile**	**Uncertainty**	**10th Percentile**	**90th Percentile**	**Uncertainty**
Vancouver	5.91	23.61	6.27	24.45	0.02	6.70	25.27	0.06	7.09	26.31	0.09
Calgary	-3.88	22.99	-3.58	23.81	0.11	-3.21	24.73	0.25	-2.69	25.84	0.43
Edmonton	-10.27	24.12	-9.54	24.84	0.10	-8.76	25.73	0.21	-7.80	26.79	0.35
Saskatoon	-12.92	26.45	-12.18	27.23	0.09	-11.24	28.07	0.19	-10.16	29.15	0.32
Brandon	-12.69	26.83	-11.68	27.48	0.10	-10.76	28.29	0.21	-9.77	29.35	0.32
Winnipeg	-12.23	26.31	-11.36	26.88	0.09	-10.57	27.69	0.19	-9.55	28.79	0.31
Toronto	-3.99	26.53	-3.45	27.10	0.16	-2.86	27.93	0.34	-2.17	28.97	0.55
Ottawa	-6.50	27.07	-6.04	27.66	0.09	-5.47	28.49	0.21	-4.70	29.57	0.37
Montreal	-5.98	26.83	-5.51	27.46	0.10	-4.89	28.29	0.24	-4.22	29.29	0.39
Quebec City	-7.15	25.60	-6.77	26.25	0.08	-6.02	27.13	0.22	-5.23	28.09	0.37
Saguenay	-10.33	24.90	-9.89	25.60	0.07	-9.25	26.43	0.17	-8.31	27.48	0.30
Fredericton	-4.12	26.10	-3.76	26.72	0.11	-3.18	27.46	0.28	-2.42	28.33	0.50
Charlottetown	-3.98	23.75	-3.64	24.28	0.11	-3.07	24.93	0.28	-2.45	25.71	0.47
Halifax	-1.83	24.03	-1.49	24.47	0.20	-1.04	25.04	0.48	-0.56	25.68	0.76
Corner Brook	-5.01	20.25	-4.52	20.75	0.12	-3.98	21.36	0.26	-3.32	22.17	0.43
St. John’s	-1.45	21.11	-1.12	21.41	0.24	-0.78	21.84	0.50	-0.34	22.42	0.83

Table **B**-17: Uncertainty for High Temperature projections, climate change model: MPI-ESM-LR

Time period	**1980-2010**		**2010-2040**			**2040-2070**			**2070-2100**		
Type	**10th Percentile**	**90th Percentile**	**10th Percentile**	**90th Percentile**	**Uncertainty**	**10th Percentile**	**90th Percentile**	**Uncertainty**	**10th Percentile**	**90th Percentile**	**Uncertainty**
Vancouver	5.92	23.59	6.26	24.00	0.04	6.68	24.73	0.08	7.15	25.67	0.12
Calgary	-4.01	23.00	-3.29	23.46	0.20	-2.59	24.16	0.40	-1.90	24.96	0.61
Edmonton	-10.32	24.04	-9.10	24.51	0.14	-8.03	25.21	0.27	-6.89	26.09	0.42
Saskatoon	-12.80	26.43	-11.88	27.04	0.09	-10.78	27.91	0.21	-9.64	28.86	0.34
Brandon	-12.46	26.85	-11.51	27.57	0.10	-10.47	28.42	0.22	-9.38	29.47	0.34
Winnipeg	-12.07	26.25	-11.25	26.93	0.09	-10.37	27.78	0.20	-9.29	28.77	0.33
Toronto	-3.88	26.38	-3.13	27.17	0.22	-2.49	28.08	0.42	-1.74	29.37	0.66
Ottawa	-6.46	26.94	-5.71	27.64	0.14	-5.06	28.50	0.28	-4.16	29.71	0.46
Montreal	-5.90	26.72	-5.08	27.35	0.16	-4.49	28.21	0.29	-3.70	29.41	0.47
Quebec City	-7.08	25.48	-6.32	26.14	0.13	-5.53	26.97	0.28	-4.77	28.07	0.43
Saguenay	-10.24	24.86	-9.47	25.47	0.10	-8.54	26.22	0.22	-7.62	27.31	0.35
Fredericton	-3.94	26.09	-3.32	26.75	0.18	-2.65	27.56	0.38	-1.82	28.63	0.63
Charlottetown	-3.78	23.70	-3.13	24.31	0.20	-2.43	25.10	0.42	-1.70	26.07	0.65
Halifax	-1.60	23.99	-1.02	24.67	0.39	-0.33	25.41	0.85	0.26	26.45	1.26
Corner Brook	-4.82	20.20	-4.31	20.70	0.13	-3.50	21.36	0.33	-2.82	22.19	0.51
St. John’s	-1.31	21.13	-0.94	21.61	0.30	-0.46	22.14	0.69	0.00	22.86	1.08

Table **B**-18: Uncertainty for High Temperature projections, climate change model: CSIRO-Mk3-6-0

Time period	**1980-2010**		**2010-2040**			**2040-2070**			**2070-2100**		
Type	**10th Percentile**	**90th Percentile**	**10th Percentile**	**90th Percentile**	**Uncertainty**	**10th Percentile**	**90th Percentile**	**Uncertainty**	**10th Percentile**	**90th Percentile**	**Uncertainty**
Vancouver	5.97	23.69	6.29	0.24	0.03	6.66	25.49	0.04	7.19	26.82	0.07
Calgary	-4.00	23.11	-3.51	0.24	0.15	-3.14	25.01	0.30	-2.34	26.34	0.55
Edmonton	-10.07	24.15	-9.51	0.25	0.08	-8.80	25.68	0.19	-7.61	26.87	0.36
Saskatoon	-12.65	26.50	-12.05	0.27	0.07	-11.21	28.10	0.17	-9.96	29.34	0.32
Brandon	-12.55	26.88	-12.04	0.27	0.06	-11.13	28.36	0.17	-9.74	29.56	0.32
Winnipeg	-12.18	26.26	-11.67	0.27	0.06	-10.90	27.80	0.16	-9.58	28.95	0.32
Toronto	-4.05	26.51	-3.80	0.27	0.08	-3.27	27.96	0.25	-2.55	29.10	0.47
Ottawa	-6.57	26.91	-6.33	0.27	0.06	-5.62	28.41	0.20	-4.68	29.52	0.39
Montreal	-6.04	26.74	-5.73	0.27	0.07	-5.04	28.07	0.21	-4.02	29.23	0.43
Quebec City	-7.21	25.46	-6.94	0.26	0.05	-6.23	26.85	0.19	-5.24	27.98	0.37
Saguenay	-10.45	24.76	-10.20	0.25	0.04	-9.51	26.17	0.15	-8.54	27.24	0.28
Fredericton	-4.16	26.10	-3.90	0.27	0.08	-3.25	27.26	0.26	-2.47	28.15	0.49
Charlottetown	-3.98	23.71	-3.77	0.24	0.07	-3.27	24.69	0.22	-2.61	25.55	0.42
Halifax	-1.77	23.99	-1.51	0.24	0.16	-1.05	24.94	0.44	-0.44	25.72	0.82
Corner Brook	-5.11	20.13	-4.93	0.20	0.05	-4.55	20.90	0.15	-3.94	21.73	0.31
St. John's	-1.54	21.01	-1.46	0.21	0.06	-1.26	21.55	0.21	-0.85	22.16	0.51

Table **B**-19: Uncertainty for High Temperature projections, climate change model: GFDL-ESM2G

Time period	**1980-2010**		**2010-2040**			**2040-2070**			**2070-2100**		
Type	**10th Percentile**	**90th Percentile**	**10th Percentile**	**90th Percentile**	**Uncertainty**	**10th Percentile**	**90th Percentile**	**Uncertainty**	**10th Percentile**	**90th Percentile**	**Uncertainty**
Vancouver	5.92	23.75	6.37	24.37	0.05	6.77	24.94	0.09	0.07	25.64	0.13
Calgary	-4.11	23.09	-3.58	23.58	0.15	-3.08	24.17	0.30	-0.03	25.02	0.47
Edmonton	-10.17	24.10	-9.61	24.66	0.08	-9.14	25.12	0.14	-0.08	25.86	0.26
Saskatoon	-12.87	26.50	-12.14	26.83	0.07	-11.54	27.10	0.13	-0.11	27.88	0.22
Brandon	-12.60	26.85	-11.86	27.02	0.07	-11.26	27.32	0.12	-0.10	27.94	0.23
Winnipeg	-12.21	26.29	-11.54	26.42	0.06	-10.83	26.72	0.13	-0.10	27.27	0.22
Toronto	-3.92	26.44	-3.38	26.75	0.15	-2.89	27.32	0.30	-0.02	28.18	0.44
Ottawa	-6.38	26.96	-5.82	27.25	0.10	-5.26	27.79	0.21	-0.05	28.61	0.35
Montreal	-5.85	26.73	-5.19	27.08	0.13	-4.63	27.68	0.24	-0.04	28.50	0.40
Quebec City	-7.02	25.48	-6.37	25.95	0.11	-5.76	26.54	0.22	-0.05	27.33	0.36
Saguenay	-10.26	24.86	-9.63	25.22	0.07	-9.12	25.86	0.15	-0.08	26.71	0.26
Fredericton	-3.98	26.16	-3.31	26.50	0.18	-2.57	27.07	0.39	-0.02	27.92	0.61
Charlottetown	-3.84	23.70	-3.12	24.04	0.20	-2.39	24.53	0.41	-0.02	25.27	0.62
Halifax	-1.63	24.01	-1.02	24.39	0.39	-0.46	24.85	0.75	0.00	25.60	1.18
Corner Brook	-4.86	20.21	-4.08	20.49	0.18	-3.34	20.92	0.35	-0.03	21.61	0.54
St. John’s	-1.32	21.11	-0.72	21.41	0.47	-0.09	21.72	0.96	0.00	22.34	1.39

Table B-20: Uncertainty for High Temperature projections, climate change model: CNRM-CM5

Time period	1980-2010		2010-2040			2040-2070			2070-2100		
Type	**10th Percentile**	**90th Percentile**	**10th Percentile**	**90th Percentile**	**Uncertainty**	**10th Percentile**	**90th Percentile**	**Uncertainty**	**10th Percentile**	**90th Percentile**	**Uncertainty**
Vancouver	5.97	23.63	6.40	24.31	0.04	6.73	24.98	0.07	7.21	25.96	0.11
Calgary	-3.90	22.97	-3.45	23.60	0.14	-2.99	24.20	0.29	-2.31	25.04	0.50
Edmonton	-10.23	24.16	-9.77	24.88	0.07	-8.90	25.40	0.18	-7.86	26.18	0.32
Saskatoon	-12.92	26.44	-12.36	27.14	0.07	-11.47	27.79	0.16	-10.25	28.67	0.29
Brandon	-12.70	26.85	-12.35	27.36	0.05	-11.26	28.11	0.16	-9.97	29.09	0.30
Winnipeg	-12.39	26.26	-11.97	26.75	0.05	-10.91	27.39	0.16	-9.73	28.38	0.29
Toronto	-4.02	26.39	-3.50	26.68	0.14	-2.70	27.39	0.37	-1.88	28.25	0.60
Ottawa	-6.60	26.98	-5.97	27.27	0.11	-5.06	27.95	0.27	-4.21	28.80	0.43
Montreal	-5.92	26.76	-5.33	27.07	0.11	-4.46	27.68	0.28	-3.61	28.48	0.45
Quebec City	-7.13	25.55	-6.52	25.85	0.10	-5.69	26.43	0.24	-4.80	27.20	0.39
Saguenay	-10.32	24.94	-9.71	25.23	0.07	-8.77	25.78	0.18	-7.86	26.48	0.30
Fredericton	-3.98	26.13	-3.55	26.49	0.12	-2.71	27.03	0.35	-1.89	27.73	0.58
Charlottetown	-3.79	23.74	-3.30	24.12	0.15	-2.60	24.72	0.36	-1.84	25.45	0.59
Halifax	-1.67	24.03	-1.23	24.39	0.28	-0.58	24.98	0.69	0.01	25.66	1.07
Corner Brook	-4.90	20.27	-4.54	20.58	0.09	-3.94	21.22	0.24	-3.23	22.00	0.43
St. John's	-1.34	21.10	-1.03	21.39	0.25	-0.57	21.94	0.61	-0.06	22.66	1.03

Table B-21: Uncertainty for Low Temperature projections, climate change model: MRI- CGCM3

Time period	1980-2010		2010-2040			2040-2070			2070-2100		
City	10th Percentile	90th Percentile	10th Percentile	90th Percentile	Uncertainty	10th Percentile	90th Percentile	Uncertainty	10th Percentile	90th Percentile	Uncertainty
Vancouver	-0.78	12.61	-0.29	12.91	0.65	0.07	13.31	1.15	0.52	13.95	1.78
Calgary	-17.73	6.82	-17.07	7.18	0.09	-16.58	7.71	0.20	-15.95	8.42	0.33
Edmonton	-20.50	10.20	-19.65	10.47	0.07	-19.17	10.95	0.14	-18.41	11.58	0.24
Saskatoon	-23.15	11.78	-22.50	12.09	0.06	-21.93	12.59	0.12	-21.06	13.27	0.22
Brandon	-23.55	13.25	-23.23	13.64	0.04	-22.67	14.15	0.11	-21.49	14.89	0.21
Winnipeg	-25.22	12.83	-24.92	13.27	0.05	-24.35	13.75	0.11	-23.17	14.43	0.21
Toronto	-13.24	14.82	-13.04	15.12	0.04	-12.10	15.62	0.14	-11.09	16.25	0.26
Ottawa	-18.95	13.84	-18.84	14.09	0.02	-17.94	14.58	0.11	-16.77	15.19	0.21
Montreal	-16.97	15.29	-16.81	15.56	0.03	-15.76	15.99	0.12	-14.64	16.70	0.23
Quebec City	-18.39	13.81	-18.15	14.08	0.03	-17.11	14.52	0.12	-16.05	15.21	0.23
Saguenay	-23.30	12.54	-23.07	12.73	0.02	-22.00	13.13	0.10	-20.76	13.84	0.21
Fredericton	-15.35	13.58	-14.98	13.85	0.04	-13.93	14.28	0.14	-12.84	14.94	0.26
Charlottetown	-12.60	14.28	-11.99	14.57	0.07	-10.64	15.03	0.21	-9.21	15.73	0.37
Halifax	-11.17	13.58	-10.43	13.87	0.09	-9.22	14.30	0.23	-8.04	14.98	0.38
Corner Brook	-13.24	10.87	-12.58	11.18	0.08	-11.35	11.60	0.21	-10.04	12.34	0.38
St. John’s	-8.84	11.44	-8.04	11.75	0.12	-6.85	12.21	0.29	-5.69	12.93	0.49

Table B-22: Uncertainty for Low Temperature projections, climate change model: CanESM2

Time period	1980-2010		2010-2040			2040-2070			2070-2100		
City	**10th Percentile**	**90th Percentile**	**10th Percentile**	**90th Percentile**	**Uncertainty**	**10th Percentile**	**90th Percentile**	**Uncertainty**	**10th Percentile**	**90th Percentile**	**Uncertainty**
Vancouver	-0.65	12.73	0.13	13.47	1.25	0.79	14.50	2.36	1.37	0.16	3.39
Calgary	-17.47	6.94	-16.36	7.52	0.15	-15.40	8.56	0.35	-14.24	0.10	0.61
Edmonton	-20.32	10.33	-19.01	11.05	0.13	-17.99	12.03	0.28	-16.73	0.13	0.46
Saskatoon	-22.96	11.94	-21.72	12.75	0.12	-20.55	13.84	0.26	-18.92	0.15	0.45
Brandon	-23.26	13.43	-22.00	14.22	0.11	-20.63	15.14	0.24	-19.19	0.16	0.39
Winnipeg	-24.97	13.00	-23.80	13.67	0.10	-22.74	14.65	0.22	-21.13	0.16	0.38
Toronto	-13.09	14.84	-12.09	15.68	0.13	-11.10	16.73	0.28	-10.00	0.18	0.45
Ottawa	-18.76	13.92	-17.60	14.63	0.11	-16.49	15.80	0.26	-15.09	0.17	0.43
Montreal	-16.70	15.36	-15.54	16.13	0.12	-14.37	17.24	0.26	-12.93	0.19	0.44
Quebec City	-18.16	13.86	-16.97	14.70	0.13	-15.72	15.77	0.27	-14.19	0.17	0.46
Saguenay	-23.05	12.55	-21.74	13.25	0.11	-20.32	14.35	0.26	-18.74	0.16	0.44
Fredericton	-15.18	13.69	-14.11	14.49	0.13	-13.00	15.53	0.28	-11.76	0.17	0.46
Charlottetown	-12.53	14.38	-11.57	15.06	0.12	-10.58	16.14	0.28	-9.48	0.17	0.46
Halifax	-11.05	13.65	-10.19	14.31	0.13	-9.35	15.31	0.28	-8.45	0.17	0.44
Corner Brook	-13.22	10.99	-12.30	11.69	0.13	-11.41	12.68	0.29	-10.45	0.14	0.48
St. John’s	-8.73	11.58	-8.03	12.22	0.13	-7.35	13.16	0.29	-6.57	0.14	0.49

Table **B-**23: Uncertainty for Low Temperature projections, climate change model: inmcm4

Time period	**1980-2010**		**2010-2040**			**2040-2070**			**2070-2100**		
City	**10th Percentile**	**90th Percentile**	**10th Percentile**	**90th Percentile**	**Uncertainty**	**10th Percentile**	**90th Percentile**	**Uncertainty**	**10th Percentile**	**90th Percentile**	**Uncertainty**
Vancouver	-0.83	12.63	-0.31	12.79	0.64	0.02	13.01	1.05	0.44	13.51	1.60
Calgary	-18.00	6.78	-16.78	6.99	0.10	-15.62	7.25	0.20	-14.34	7.77	0.35
Edmonton	-20.75	10.18	-19.53	10.53	0.09	-18.54	11.02	0.19	-17.74	11.64	0.29
Saskatoon	-23.28	11.78	-22.01	12.16	0.09	-20.79	12.61	0.18	-19.60	13.27	0.29
Brandon	-23.51	13.25	-22.38	13.62	0.08	-21.31	14.24	0.17	-20.02	14.81	0.27
Winnipeg	-25.24	12.87	-23.86	13.24	0.08	-22.54	13.75	0.18	-21.15	14.29	0.27
Toronto	-13.06	14.80	-11.89	15.07	0.11	-10.82	15.44	0.21	-9.61	16.02	0.35
Ottawa	-18.60	13.85	-17.23	14.08	0.09	-15.84	14.42	0.19	-14.58	14.96	0.30
Montreal	-16.66	15.26	-15.47	15.52	0.09	-14.30	15.93	0.19	-13.04	16.53	0.30
Quebec City	-18.07	13.80	-16.92	14.06	0.08	-15.65	14.45	0.18	-14.28	15.04	0.30
Saguenay	-22.98	12.48	-21.97	12.72	0.06	-20.65	13.13	0.15	-19.08	13.66	0.26
Fredericton	-15.19	13.61	-14.35	13.83	0.07	-13.54	14.29	0.16	-12.37	14.83	0.28
Charlottetown	-12.57	14.25	-11.82	14.51	0.08	-11.16	15.00	0.17	-10.23	15.55	0.28
Halifax	-11.10	13.52	-10.40	13.75	0.08	-9.84	14.13	0.16	-9.13	14.61	0.26
Corner Brook	-13.33	10.94	-12.65	11.29	0.08	-11.94	11.88	0.19	-11.12	12.53	0.31
St. John’s	-8.87	11.50	-8.63	11.76	0.05	-8.27	12.16	0.13	-7.71	12.77	0.24

Table B-24: Uncertainty for Low Temperature projections, climate change model: ACCESS1-0

Time period	1980-2010		2010-2040			2040-2070			2070-2100		
City	10th Percentile	90th Percentile	10th Percentile	90th Percentile	Uncertainty	10th Percentile	90th Percentile	Uncertainty	10th Percentile	90th Percentile	Uncertainty
Vancouver	-0.72	0.13	-0.21	13.22	0.75	0.38	13.98	1.64	0.96	15.13	2.53
Calgary	-17.72	0.07	-16.71	7.42	0.14	-16.03	8.40	0.32	-15.14	9.66	0.56
Edmonton	-20.47	0.10	-19.28	10.80	0.11	-18.36	11.65	0.24	-17.07	12.83	0.42
Saskatoon	-23.14	0.12	-22.07	12.37	0.09	-20.98	13.34	0.22	-19.55	14.55	0.38
Brandon	-23.42	0.13	-22.44	13.84	0.08	-21.11	14.73	0.21	-19.51	15.83	0.36
Winnipeg	-25.10	0.13	-24.11	13.45	0.08	-22.73	14.38	0.21	-21.22	15.53	0.36
Toronto	-13.03	0.15	-12.16	15.28	0.10	-10.83	16.15	0.26	-9.40	17.30	0.44
Ottawa	-18.71	0.14	-17.86	14.31	0.08	-16.40	15.15	0.22	-14.91	16.39	0.38
Montreal	-16.72	0.15	-15.88	15.75	0.08	-14.36	16.58	0.22	-12.91	17.73	0.39
Quebec City	-18.14	0.14	-17.17	14.33	0.09	-15.76	15.18	0.23	-14.23	16.34	0.40
Saguenay	-23.04	0.13	-22.09	12.95	0.08	-20.51	13.79	0.21	-18.84	14.96	0.38
Fredericton	-15.18	0.14	-14.33	14.17	0.10	-13.09	15.06	0.24	-11.66	16.14	0.42
Charlottetown	-12.42	0.14	-11.67	14.95	0.11	-10.55	15.93	0.26	-9.37	17.07	0.44
Halifax	-10.93	0.14	-10.30	14.16	0.10	-9.14	14.98	0.27	-8.13	15.98	0.43
Corner Brook	-13.15	0.11	-12.30	11.57	0.12	-11.35	12.50	0.28	-10.32	13.65	0.47
St. John's	-8.72	0.12	-7.89	12.21	0.16	-7.03	13.19	0.34	-6.21	14.21	0.52

Table B-25: Uncertainty for Low Temperature projections, climate change model: MICROC5

Time period	1980-2010		2010-2040			2040-2070			2070-2100		
City	**10th Percentile**	**90th Percentile**	**10th Percentile**	**90th Percentile**	**Uncertainty**	**10th Percentile**	**90th Percentile**	**Uncertainty**	**10th Percentile**	**90th Percentile**	**Uncertainty**
Vancouver	-0.68	12.62	-0.32	13.12	0.57	0.19	0.14	1.36	0.52	14.44	1.91
Calgary	-17.60	6.83	-16.96	7.47	0.13	-16.17	0.08	0.27	-15.39	9.04	0.45
Edmonton	-20.36	10.27	-19.77	10.85	0.08	-18.90	0.12	0.19	-18.12	12.48	0.33
Saskatoon	-22.96	11.82	-22.36	12.40	0.08	-21.49	0.13	0.18	-20.49	14.22	0.31
Brandon	-23.31	13.27	-22.45	13.93	0.09	-21.39	0.15	0.19	-20.17	15.94	0.34
Winnipeg	-25.05	12.88	-24.23	13.65	0.09	-23.04	0.14	0.20	-21.69	15.62	0.35
Toronto	-13.03	14.81	-12.12	15.53	0.12	-11.24	0.16	0.23	-10.19	17.20	0.38
Ottawa	-18.73	13.91	-17.64	14.53	0.10	-16.50	0.15	0.22	-14.95	16.29	0.37
Montreal	-16.71	15.33	-15.56	15.95	0.11	-14.37	0.17	0.23	-12.95	17.62	0.37
Quebec City	-18.06	13.87	-16.99	14.45	0.10	-15.77	0.15	0.22	-14.31	16.13	0.37
Saguenay	-22.97	12.55	-21.86	13.13	0.09	-20.54	0.14	0.21	-18.93	14.88	0.36
Fredericton	-15.08	13.62	-14.18	14.19	0.10	-13.14	0.15	0.22	-11.72	15.75	0.38
Charlottetown	-12.42	14.32	-11.51	14.86	0.11	-10.60	0.16	0.24	-9.40	16.48	0.39
Halifax	-10.91	13.63	-10.08	14.18	0.12	-9.26	0.15	0.24	-8.25	15.62	0.39
Corner Brook	-13.12	10.95	-12.41	11.46	0.10	-11.53	0.12	0.23	-10.51	13.04	0.39
St. John’s	-8.72	11.57	-8.32	12.05	0.09	-7.79	0.13	0.20	-7.10	13.51	0.35

Table B-26: Uncertainty for Low Temperature projections, climate change model: CCSM4

Time period	1980-2010		2010-2040			2040-2070			2070-2100		
City	10th Percentile	90th Percentile	10th Percentile	90th Percentile	Uncertainty	10th Percentile	90th Percentile	Uncertainty	10th Percentile	90th Percentile	Uncertainty
Vancouver	-0.75	12.64	-0.32	13.05	0.60	0.09	13.73	1.21	0.69	14.57	2.06
Calgary	-17.65	6.83	-17.08	7.46	0.13	-16.59	8.18	0.26	-15.76	9.12	0.44
Edmonton	-20.46	10.27	-19.55	10.90	0.11	-18.77	11.66	0.22	-17.38	12.70	0.39
Saskatoon	-23.03	11.81	-22.23	12.53	0.10	-21.31	13.31	0.20	-19.87	14.33	0.35
Brandon	-23.36	13.33	-22.45	13.94	0.09	-21.48	14.66	0.18	-20.12	15.64	0.31
Winnipeg	-25.06	12.93	-24.11	13.42	0.08	-23.10	14.07	0.17	-21.62	14.94	0.29
Toronto	-12.95	14.89	-12.23	15.42	0.09	-11.35	16.08	0.20	-10.29	16.94	0.34
Ottawa	-18.62	13.93	-17.98	14.54	0.08	-17.01	15.23	0.18	-15.63	16.14	0.32
Montreal	-16.62	15.36	-15.98	16.00	0.08	-14.99	16.76	0.19	-13.78	17.74	0.33
Quebec City	-18.12	13.93	-17.45	14.61	0.09	-16.43	15.35	0.19	-15.03	16.27	0.34
Saguenay	-23.18	12.60	-22.44	13.31	0.09	-21.38	14.00	0.19	-19.88	14.87	0.32
Fredericton	-15.23	13.67	-14.61	14.40	0.09	-13.73	15.07	0.20	-12.52	15.94	0.34
Charlottetown	-12.60	14.35	-11.95	14.90	0.09	-10.94	15.55	0.21	-9.90	16.41	0.36
Halifax	-11.03	13.60	-10.51	14.12	0.09	-9.76	14.70	0.20	-8.80	15.43	0.34
Corner Brook	-13.30	10.94	-12.63	11.53	0.10	-11.88	12.11	0.21	-11.00	12.89	0.35
St. John’s	-8.87	11.53	-8.39	11.93	0.09	-7.88	12.39	0.19	-7.13	13.02	0.33

Table B-27: Uncertainty for Low Temperature projections, climate change model: MPI-ESM-LR

Time period	1980-2010		2010-2040			2040-2070			2070-2100		
City	**10th Percentile**	**90th Percentile**	**10th Percentile**	**90th Percentile**	**Uncertainty**	**10th Percentile**	**90th Percentile**	**Uncertainty**	**10th Percentile**	**90th Percentile**	**Uncertainty**
Vancouver	-0.64	12.64	-0.16	0.13	0.79	0.27	13.96	1.53	0.86	15.22	2.55
Calgary	-17.49	6.90	-16.78	0.07	0.11	-16.02	8.41	0.30	-14.94	9.64	0.54
Edmonton	-20.33	10.29	-19.33	0.11	0.09	-18.21	11.50	0.22	-16.70	12.55	0.40
Saskatoon	-22.88	11.82	-22.09	0.12	0.08	-20.96	13.22	0.20	-19.38	14.36	0.37
Brandon	-23.14	13.27	-22.36	0.14	0.07	-21.06	14.64	0.19	-19.55	15.78	0.34
Winnipeg	-24.84	12.88	-24.17	0.13	0.07	-22.97	14.25	0.18	-21.27	15.42	0.34
Toronto	-13.17	14.87	-12.65	0.15	0.07	-11.50	16.24	0.22	-10.21	17.44	0.40
Ottawa	-18.87	13.89	-18.36	0.14	0.06	-17.31	15.23	0.18	-15.75	16.34	0.34
Montreal	-16.89	15.30	-16.42	0.16	0.06	-15.32	16.59	0.18	-13.87	17.66	0.33
Quebec City	-18.26	13.85	-17.91	0.14	0.05	-16.83	15.08	0.17	-15.49	16.10	0.31
Saguenay	-23.32	12.51	-22.99	0.13	0.04	-21.89	13.63	0.15	-20.52	14.67	0.29
Fredericton	-15.32	13.57	-14.96	0.14	0.05	-14.03	14.60	0.16	-12.86	15.52	0.30
Charlottetown	-12.69	14.20	-12.40	0.15	0.05	-11.59	15.15	0.15	-10.66	15.98	0.29
Halifax	-11.17	13.51	-10.85	0.14	0.05	-10.19	14.39	0.15	-9.29	15.16	0.29
Corner Brook	-13.44	10.81	-13.21	0.11	0.04	-12.81	11.59	0.12	-12.08	12.34	0.24
St. John’s	-9.00	11.39	-8.85	0.12	0.03	-8.61	11.88	0.09	-8.09	12.48	0.20

Table B-28: Uncertainty for Low Temperature projections, climate change model: CSIRO-Mk3-6-0

Time period	1980-2010		2010-2040			2040-2070			2070-2100		
City	10th Percentile	90th Percentile	10th Percentile	90th Percentile	Uncertainty	10th Percentile	90th Percentile	Uncertainty	10th Percentile	90th Percentile	Uncertainty
Vancouver	-0.78	12.65	-0.23	13.01	0.73	0.40	13.74	1.59	1.15	14.58	2.62
Calgary	-17.70	6.80	-16.78	7.28	0.12	-15.83	8.05	0.29	-14.79	8.91	0.47
Edmonton	-20.46	10.20	-19.19	10.70	0.11	-17.90	11.40	0.24	-16.72	12.21	0.38
Saskatoon	-23.00	11.78	-22.04	12.38	0.09	-20.75	13.19	0.22	-19.40	14.11	0.35
Brandon	-23.39	13.27	-22.24	13.99	0.10	-20.89	14.81	0.22	-19.49	15.78	0.36
Winnipeg	-25.00	12.85	-23.81	13.57	0.10	-22.42	14.37	0.22	-20.98	15.31	0.35
Toronto	-12.91	14.82	-11.78	15.56	0.14	-10.78	16.47	0.28	-9.61	17.62	0.45
Ottawa	-18.51	13.87	-17.44	14.52	0.10	-16.32	15.42	0.23	-14.91	16.45	0.38
Montreal	-16.53	15.27	-15.31	15.90	0.12	-14.18	16.75	0.24	-12.93	17.86	0.39
Quebec City	-18.08	13.83	-16.84	14.48	0.12	-15.59	15.23	0.24	-14.26	16.24	0.39
Saguenay	-22.85	12.47	-21.88	13.05	0.09	-20.50	13.74	0.20	-19.00	14.71	0.35
Fredericton	-15.01	13.61	-14.10	14.25	0.11	-13.03	14.97	0.23	-11.95	15.95	0.38
Charlottetown	-12.38	14.23	-11.43	14.85	0.12	-10.40	15.56	0.25	-9.25	16.43	0.41
Halifax	-10.91	13.54	-10.04	14.18	0.13	-9.12	14.89	0.26	-8.26	15.79	0.41
Corner Brook	-13.09	10.89	-12.34	11.37	0.10	-11.21	11.98	0.24	-10.11	12.76	0.40
St. John's	-8.69	11.52	-8.16	11.99	0.10	-7.39	12.60	0.24	-6.69	13.32	0.39

Table B-29: Uncertainty for Low Temperature projections, climate change model: GFDL-ESM2G

Time period	1980-2010		2010-2040			2040-2070			2070-2100		
City	**10th Percentile**	**90th Percentile**	**10th Percentile**	**90th Percentile**	**Uncertainty**	**10th Percentile**	**90th Percentile**	**Uncertainty**	**10th Percentile**	**90th Percentile**	**Uncertainty**
Vancouver	-0.87	12.68	-0.41	13.21	0.57	0.24	13.77	1.36	0.01	14.51	2.11
Calgary	-17.72	6.85	-17.10	7.32	0.10	-16.50	7.84	0.21	-0.16	8.70	0.38
Edmonton	-20.40	10.19	-19.74	10.71	0.08	-19.14	11.04	0.15	-0.18	11.60	0.25
Saskatoon	-23.02	11.79	-22.29	12.25	0.07	-21.61	12.55	0.13	-0.21	13.21	0.22
Brandon	-23.39	13.27	-22.55	13.59	0.06	-21.82	13.94	0.12	-0.21	14.44	0.20
Winnipeg	-25.11	12.89	-24.33	13.19	0.05	-23.44	13.56	0.12	-0.22	14.09	0.20
Toronto	-12.94	14.84	-12.32	15.21	0.07	-11.71	15.78	0.16	-0.11	16.61	0.27
Ottawa	-18.57	13.86	-17.90	14.18	0.06	-17.22	14.63	0.13	-0.16	15.44	0.24
Montreal	-16.67	15.33	-15.86	15.71	0.07	-15.18	16.22	0.15	-0.14	16.96	0.25
Quebec City	-18.09	13.89	-17.39	14.25	0.06	-16.74	14.83	0.14	-0.16	15.60	0.25
Saguenay	-23.09	12.54	-22.45	12.92	0.06	-21.73	13.54	0.14	-0.21	14.40	0.25
Fredericton	-15.09	13.63	-14.27	13.98	0.08	-13.61	14.49	0.16	-0.13	15.16	0.27
Charlottetown	-12.43	14.28	-11.57	14.56	0.09	-10.79	15.00	0.18	-0.10	15.69	0.31
Halifax	-10.94	13.58	-10.12	13.89	0.10	-9.38	14.32	0.20	-0.09	14.97	0.32
Corner Brook	-13.09	10.88	-12.23	11.23	0.10	-11.44	11.61	0.19	-0.10	12.27	0.33
St. John’s	-8.67	11.53	-7.99	11.76	0.10	-7.13	12.14	0.23	-0.06	12.70	0.39

Table B-30: Uncertainty for Low Temperature projections, climate change model: CNRM-CM5

Time period	1980-2010		2010-2040			2040-2070			2070-2100		
City	10th Percentile	90th Percentile	10th Percentile	90th Percentile	Uncertainty	10th Percentile	90th Percentile	Uncertainty	10th Percentile	90th Percentile	Uncertainty
Vancouver	-0.67	12.68	-0.23	13.30	0.71	0.23	13.84	1.44	0.76	14.78	2.30
Calgary	-17.60	6.86	-17.08	7.39	0.11	-16.44	8.07	0.24	-15.50	8.94	0.42
Edmonton	-20.44	10.31	-19.78	10.89	0.09	-18.81	11.48	0.19	-17.57	12.38	0.34
Saskatoon	-23.09	11.84	-22.53	12.40	0.07	-21.44	13.12	0.18	-19.97	14.10	0.33
Brandon	-23.50	13.32	-23.06	13.75	0.05	-21.67	14.58	0.17	-20.12	15.57	0.31
Winnipeg	-25.22	12.96	-24.69	13.39	0.05	-23.36	14.13	0.16	-21.75	15.14	0.31
Toronto	-13.10	14.85	-12.39	15.19	0.08	-11.20	15.92	0.22	-10.04	16.80	0.36
Ottawa	-18.66	13.92	-18.11	14.23	0.05	-17.03	14.96	0.16	-15.77	15.83	0.29
Montreal	-16.74	15.31	-15.95	15.68	0.07	-14.71	16.31	0.19	-13.55	17.19	0.31
Quebec City	-18.13	13.94	-17.48	14.21	0.06	-16.34	14.91	0.17	-15.17	15.73	0.29
Saguenay	-23.03	12.60	-22.38	12.92	0.05	-21.17	13.58	0.16	-19.89	14.38	0.28
Fredericton	-15.13	13.66	-14.51	14.00	0.07	-13.48	14.64	0.18	-12.30	15.38	0.31
Charlottetown	-12.45	14.34	-11.83	14.66	0.07	-10.90	15.27	0.19	-9.81	16.02	0.33
Halifax	-10.95	13.60	-10.38	13.94	0.08	-9.52	14.53	0.20	-8.57	15.25	0.34
Corner Brook	-13.17	10.92	-12.86	11.33	0.06	-12.12	11.99	0.18	-11.29	12.86	0.32
St. John’s	-8.67	11.58	-8.33	11.89	0.07	-7.73	12.46	0.18	-6.98	13.24	0.34

Appendix C. Mechanistic-Empirical Pavement Design

C.1 Design Inputs

C.2 Design Inputs

C.2.1 Hierarchical Approach

Level 1

- Input parameter is measured directly
- Site- or project-specific values

Level 2

- Input parameter is estimated from correlations
- Measured regional values

Level 3

- Input parameter is based on “best-estimated” or default values

C.2.2 Climate

Hourly data

- Temperatures, precipitations, wind speed, humidity, cloud cover, …

ICM prediction

- Temperature and moisture for each layer, and more

Data source

- MERRA climate files from InfoPave website (NASA)
- Project specific virtual weather station

The data source and the climate statistics for Ottawa, ON section are presented below:

Table **Error! No text of specified style in document.**-31: Climate Data Source and Annual Statistics

Climate Station Cities:	**Location (lat lon elevation(ft))**
CA, ON	45.50000 -75.62500 243
Mean annual air temperature (ºF)	42.64
Mean annual precipitation (in)	16.58
Freezing index (ºF - days)	1822.06
Average annual number of freeze/thaw cycles:	96.45

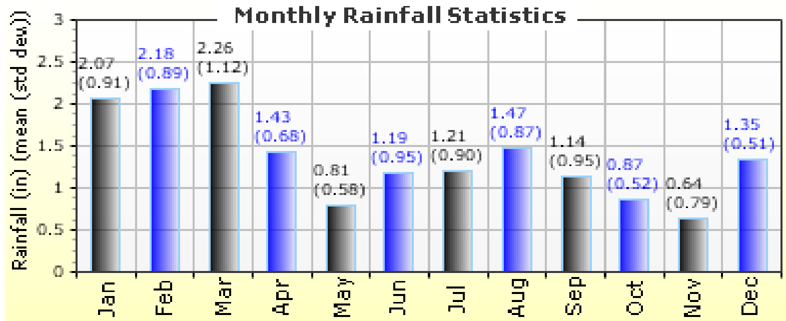

Figure 0-1: Monthly Rainfall Statistics

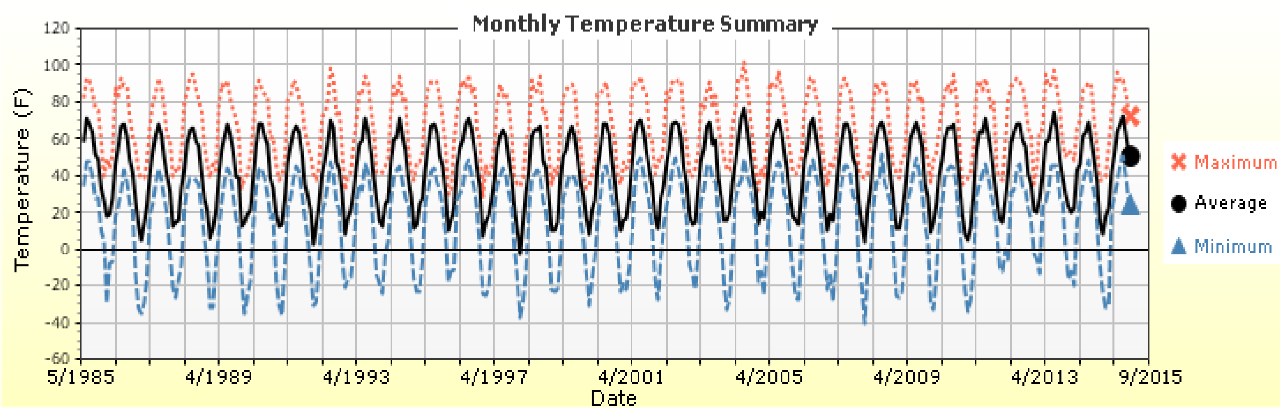

Figure 0-2: Monthly Temperature Summary

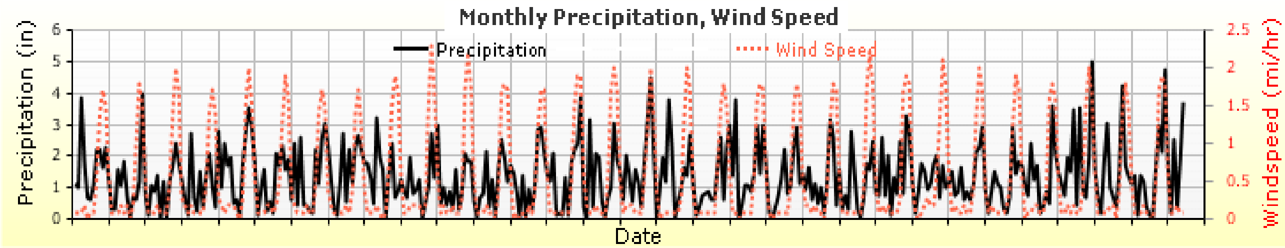

Figure 0-3: Monthly Precipitation and Windspeed

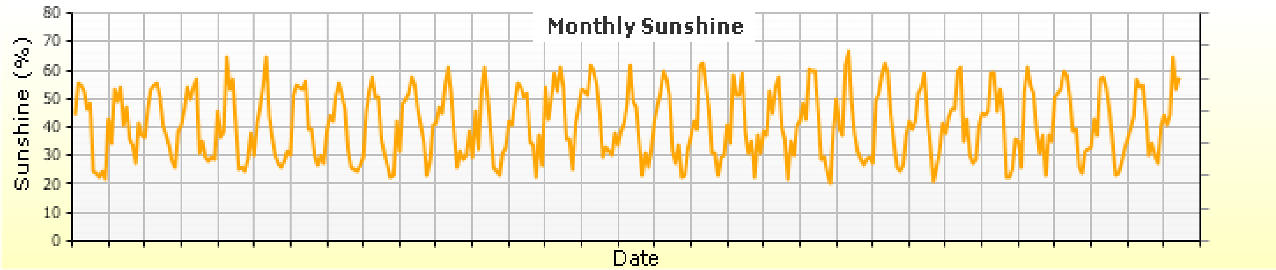

Figure 0-4: Monthly Sunshine

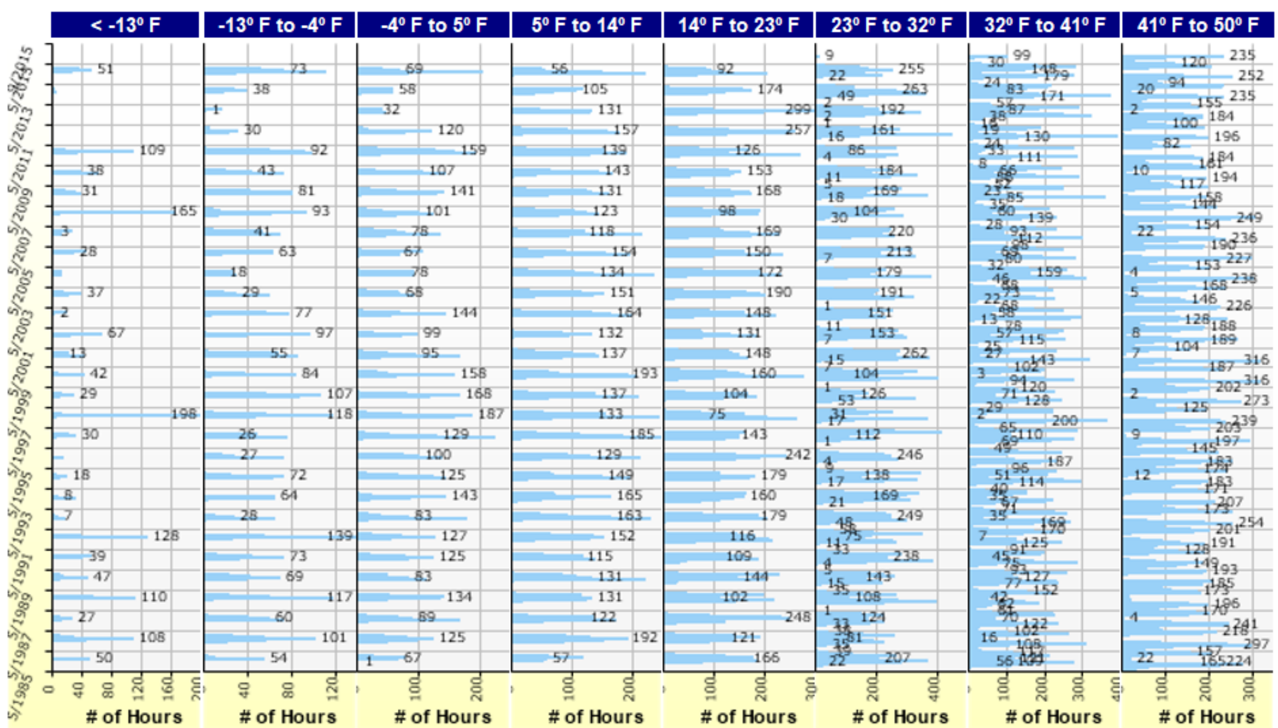

Figure 0-5: Hourly Air Temperature Distribution by Month (<-13 °F to 50 °F)

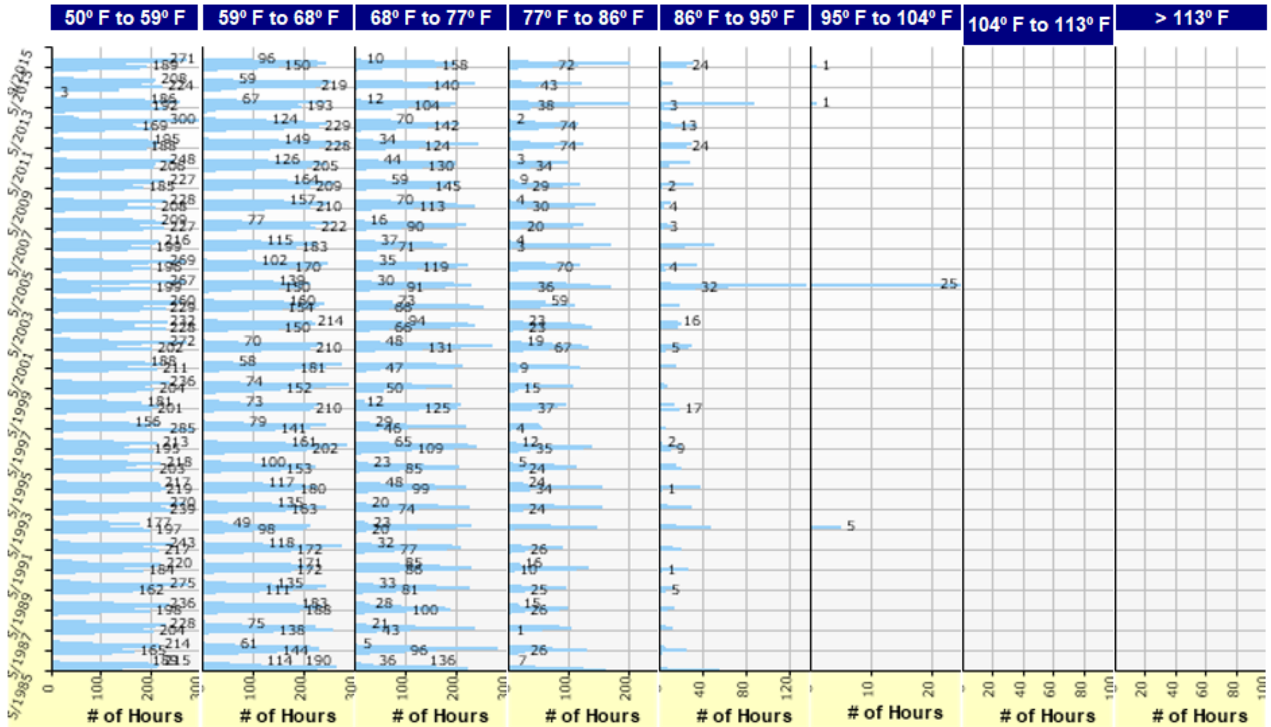

Figure 0-6: Hourly Air Temperature Distribution by Month (50 ºF to >113 ºF)

C.2.3 Traffic

Roadway-specific

- AADTT, percent of trucks, operational speed, growth of trucks

Table **Error! No text of specified style in document.**-32: Roadway specific input

Initial two-way AADTT:	1350
Number of lanes in design direction:	2
Percent of trucks in design direction (%):	50.0
Percent of trucks in design lane (%):	95.0
Operational speed (mph)	60.0

WIM data

- Axle-load distributions and configurations
- Hourly and monthly distribution factors

Table **Error! No text of specified style in document.**-33: Distributions by Vehicle Class

Vehicle Class	AADTT Distribution (%) (Level 3)	Growth Factor	
		Rate (%)	Function
Class 4	3%	5.199999809%	Compound
Class 5	46%	5.230000019%	Compound
Class 6	21%	5.21999979%	Compound
Class 7	3%	5.239999771%	Compound
Class 8	7%	5.239999771%	Linear
Class 9	4%	5.269999981%	Compound
Class 10	5%	5.269999981%	Compound
Class 11	3%	5.230000019%	Compound
Class 12	4%	5.289999962%	Compound
Class 13	4%	5.260000229%	Compound

Table **Error! No text of specified style in document.**-34: Volume Monthly Adjustment Factors

Month	Vehicle Class									
	4	5	6	7	8	9	10	11	12	13
January	0.9	0.8	0.8	0.5	0.6	0.7	0.8	0.0	0.6	0.9
February	0.8	0.9	1.0	0.5	0.8	1.0	1.1	0.0	1.1	0.7
March	0.7	1.0	0.9	0.5	0.6	0.9	1.1	0.8	0.9	0.8
April	1.0	1.2	0.8	0.5	0.8	1.0	1.0	0.8	1.1	1.0
May	1.2	1.0	1.0	0.5	0.9	1.1	1.1	0.8	1.3	1.5
June	1.5	1.2	1.0	1.3	1.3	1.1	0.9	0.8	1.0	1.2
July	1.1	1.0	1.1	1.3	1.4	1.1	0.9	0.8	1.0	1.0
August	0.9	1.0	1.0	1.6	1.4	1.1	1.1	1.6	1.0	1.1
September	0.9	1.0	1.2	1.0	1.2	1.2	1.1	3.2	1.1	1.2
October	1.1	1.0	1.5	2.1	1.3	1.1	1.1	1.6	1.6	1.2
November	1.0	1.0	0.9	1.0	1.0	0.9	1.0	0.8	0.9	0.9
December	1.0	0.9	0.8	1.0	0.8	0.8	0.8	0.8	0.6	0.7

Table **Error! No text of specified style in document.**-35: Number of Axles per Truck

Vehicle Class	Single Axle	Tandem Axle	Tridem Axle	Quad Axle
Class 4	1.51	0.49	0	0
Class 5	2.00	0.01	0	0
Class 6	1.00	1.00	0.01	0

Class 7	1.48	1.35	0.43	0.18
Class 8	2.03	0.75	0.01	0
Class 9	1.14	1.93	0.01	0
Class 10	1.37	1.23	0.72	0.04
Class 11	1.88	1.53	0.17	0.01
Class 12	2.15	1.58	0.23	0.01
Class 13	2.23	1.79	0.49	0.09

(a)

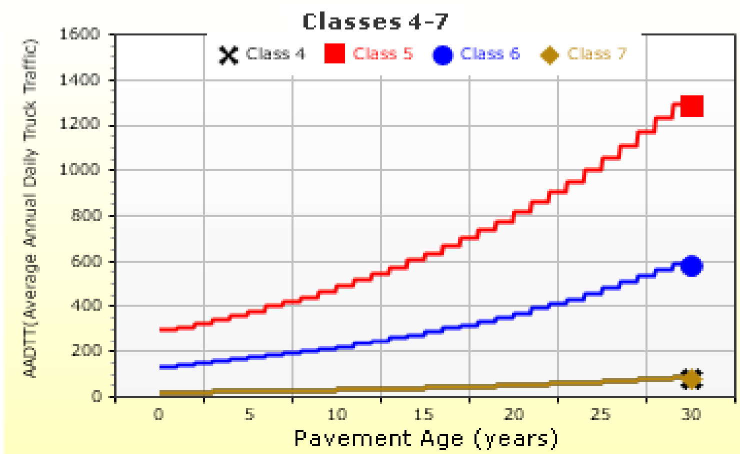

(b)

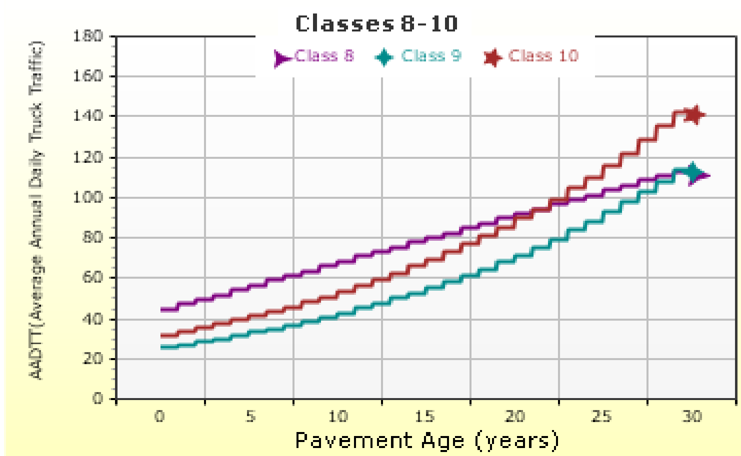

(c) 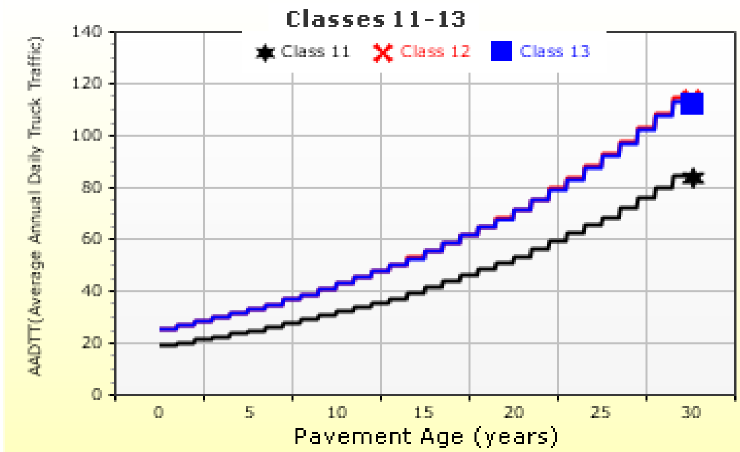

(d) 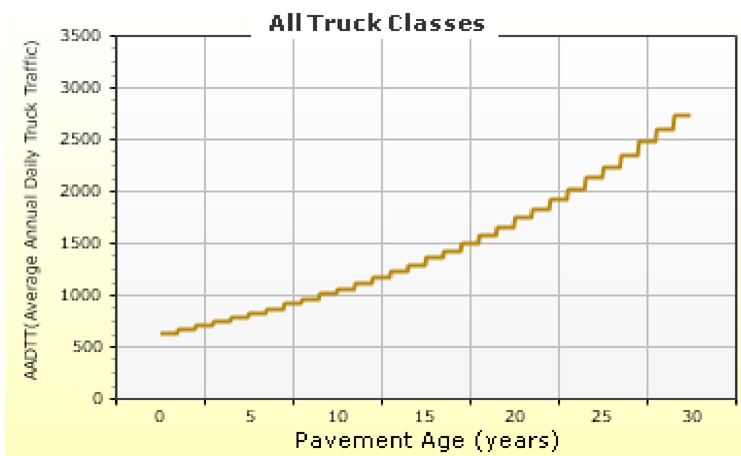

Figure 0-7: AADTT (Average Annual Daily Truck Traffic) growth over 30 years; (a)Classes 4-7, (b)Classes 8-10, (c) Classes 11-13, and (d) All Truck Classes

Others

- Dual tire spacing, tire pressure, lateral wander, truck wheelbase

C.2.4 Asphalt Mixes

Mixture Volumetrics

- Thickness
- Air voids
- Effective binder content

- Poisson's ratio
  - Constant value
  - Function of temperature
- Unit weight

Table **Error! No text of specified style in document.**-36: Design structure details

Layer type	Material Type	Thickness (in)
Flexible	Default asphalt concrete	2.8
Flexible	Default asphalt concrete	3.1
Non-Stabilized	Crushed gravel	9.0
Non-Stabilized	A-1-b	26.0
Subgrade	A-2-7	Semi-infinite

Mechanical Properties

Asphalt binder

- Level 1 & 2
  - Superpave Grade: G* and phase angle at different temperatures
  - Conventional Grade: Penetration and viscosity at diff temp
- Level 3
  - Binder Grade: Superpave, penetration or viscosity

Table **Error! No text of specified style in document.**-37: Temperature Viscosity Relationship at (Short Term Aging and/or RTFO Condition)

Ao	10.035
VTSo	-3.35
Log Temp (Rankine)	**Log(Viscosity (cp))**
2.69870935	9.87014833
2.72402997	8.11894484
2.74795531	6.7507142

2.77063113	5.66742422

Dynamic modulus

- Level 1: Values at different temperatures and frequencies
- Level 2 & 3: Gradation and asphalt binder properties

Creep compliance and indirect tensile strength

- Level 1: 3 temperatures (-20, -10 and 0ºC)
- Level 2: 1 temperature (-10ºC)
- Level 3: Default values

Table **Error! No text of specified style in document.**-38: Master curve data

Log (Reduced Time(sec))	E* (psi)	14 °F	40 °F	70 °F	100 °F	130 °F
-6.02711079	3058785.68	3058785.68				
-5.62917078	2825028.16	2825028.16				
-4.62917078	2222464.75	2222464.75				
-4.32814079	2041940.22	2041940.22				
-3.59724495	1618267.36		1618267.36			
-3.19930495	1401732.94		1401732.94			
-2.19930495	923120.664		923120.664			
-1.89827495	800837.227		800837.227			
-1.39794001	621847.212			621847.212		
-1	501131.881			501131.881		
0	276386.841			276386.841		
0.30103	228077.778			228077.778		
0.32039622	225236.276				225236.276	
0.71833623	173346.829				173346.829	
1.71833623	87441.1758				87441.158	
2.01936623	70886.7258				70886.728	
1.6808806	89749.539					89749.539
2.07882061	68004.968					68004.968
3.07882061	34029.732					34029.732
3.37985061	27767.268					27767.268

Delta	2.898769

Alpha	3.870018
Beta	-0.6501216
Gamma	0.313351
c	1.255882
SSE	0
Se/Sy	0

Table **Error! No text of specified style in document.**-39: Shift factors for the master curve

Temp (F)	Shift	14 °F	40 °F	70 °F	100 °F	130 °F
14	4.62917078	4.62917078				
40	2.19930495		2.19930495			
70	0			0		
100	-1.71833623				-1.71833623	
130	-3.07882061					-3.07882061

Table **Error! No text of specified style in document.**-40: Creep compliance input

Creep Compliance (1/psi)			
Loading time (sec)	**-4 ºF**	**14 ºF**	**32 ºF**
1	3.31e-007	5.00e-007	6.78e-007
2	3.76e-007	6.06e-007	9.41e-007
5	4.45e-007	7.82e-007	1.45e-006
10	5.06e-007	9.48e-007	2.02e-006
20	5.74e-007	1.15e-006	2.80e-006
50	6.80e-007	1.48e-006	4.31e-006
100	7.73e-007	1.80e-006	5.99e-006

Thermal Properties

- Heat capacity
- Thermal conductivity

Thermal contraction

- Constant value
- Calculated if aggregate coefficient of thermal contraction

Table **Error! No text of specified style in document.**-41: Thermal properties input

Is thermal contraction calculated?	TRUE
Mix coefficient of thermal contraction (in/in/ºF)	-
Aggregate coefficient of thermal contraction (in/in/ºF)	5.00E-06
Voids in Mineral Aggregate (%)	14

C.2.5 Unbound materials

- Coefficient of lateral earth pressure
- Layer thickness
- Poisson's ratio

Modulus

- Level 2
    - Resilient modulus
    - CBR
    - R-Value
    - Layer coefficient
    - DCP
    - PI and gradation

Sieve

- Gradation
- Other engineering properties
    - Liquid limit
    - Plasticity index
    - Compacted
    - Maximum dry unit weight
    - Saturated hydraulic conductivity

- Specific gravity of solids
- Water content
- Soil water characteristic curve

Table **Error! No text of specified style in document.**-42: Non-stabilized Base: Crushed gravel properties

Layer thickness (in)	9.0
Poisson's ratio	0.35
Coefficient of lateral earth pressure (k0)	0.5
Resilient Modulus (psi)	10000
Maximum dry unit weight (pcf)	127.2
Saturated hydraulic conductivity (ft/hr)	5.054e-02
Specific gravity of solids	2.7
Water Content (%)	7.4
Liquid Limit	6.0
Plasticity Index	1.0
Is layer compacted?	False
af	7.2555
bf	1.3328
cf	0.8242
hr	117.4000

Table **Error! No text of specified style in document.**-43: Crushed gravel gradation

Sieve Size	**% Passing**
0.001mm	
0.002mm	
0.020mm	
#200	8.7
#100	
#80	12.9
#60	
#50	
#40	20.0
#30	
#20	
#16	
#10	33.8

#8	
#4	44.7
3/8-in.	57.2
1/2-in.	63.1
3/4-in.	72.7
1-in.	78.8
1 1/2-in.	85.8
2-in.	91.6
2 1/2-in.	
3-in.	
3 1/2-in.	97.6

Analysis types

- Modify by temperature/moisture
- Monthly representative value
- Annual representative value

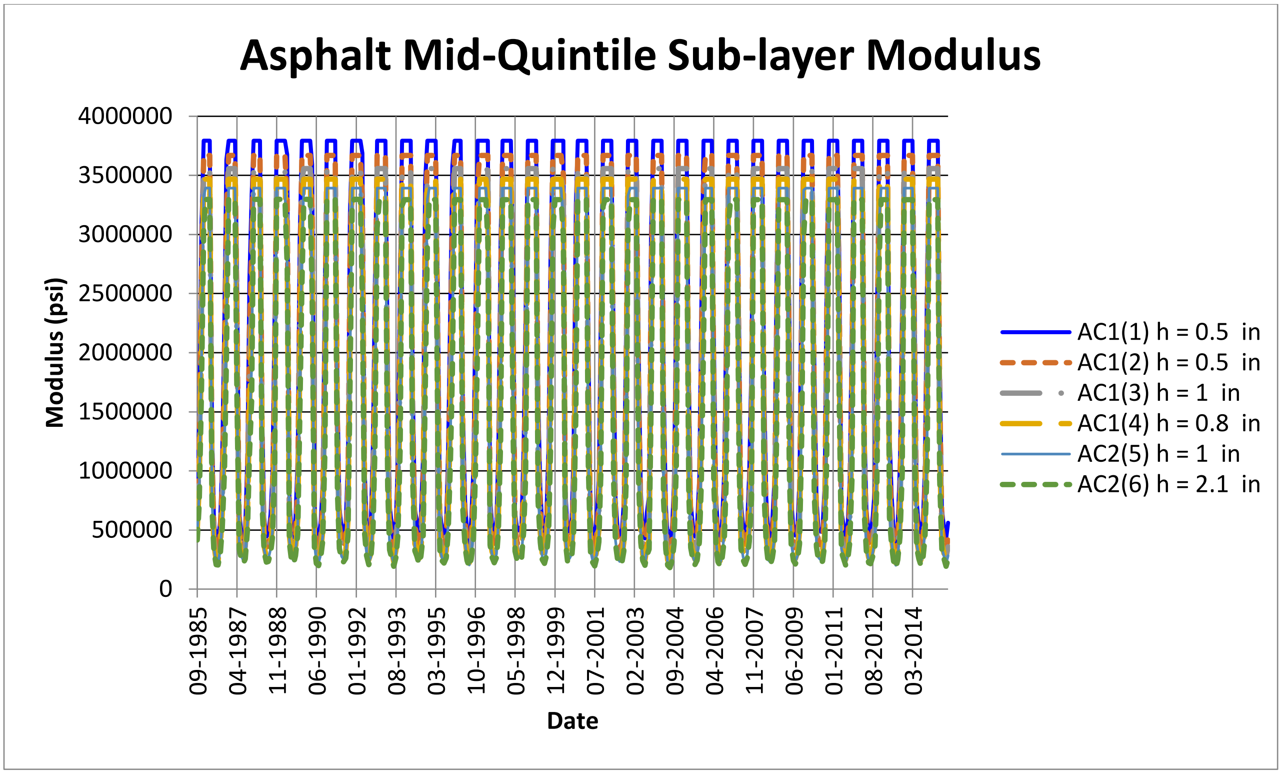

Figure 0-8: Change in asphalt sub-layer modulus over 30 years

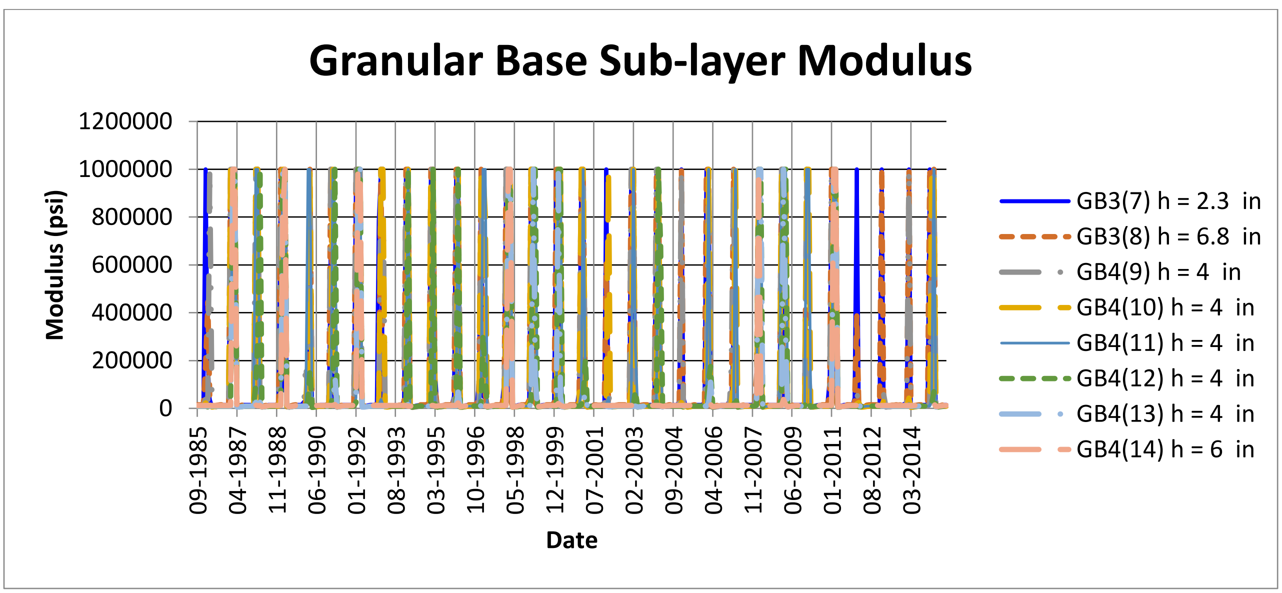

Figure 0-9: Change in granular base sub-layer modulus over 30 years

C.3 Methodology

The methodology of the Mechanistic-Empirical Pavement Design Method followed in this research is illustrated in Figure C-10.

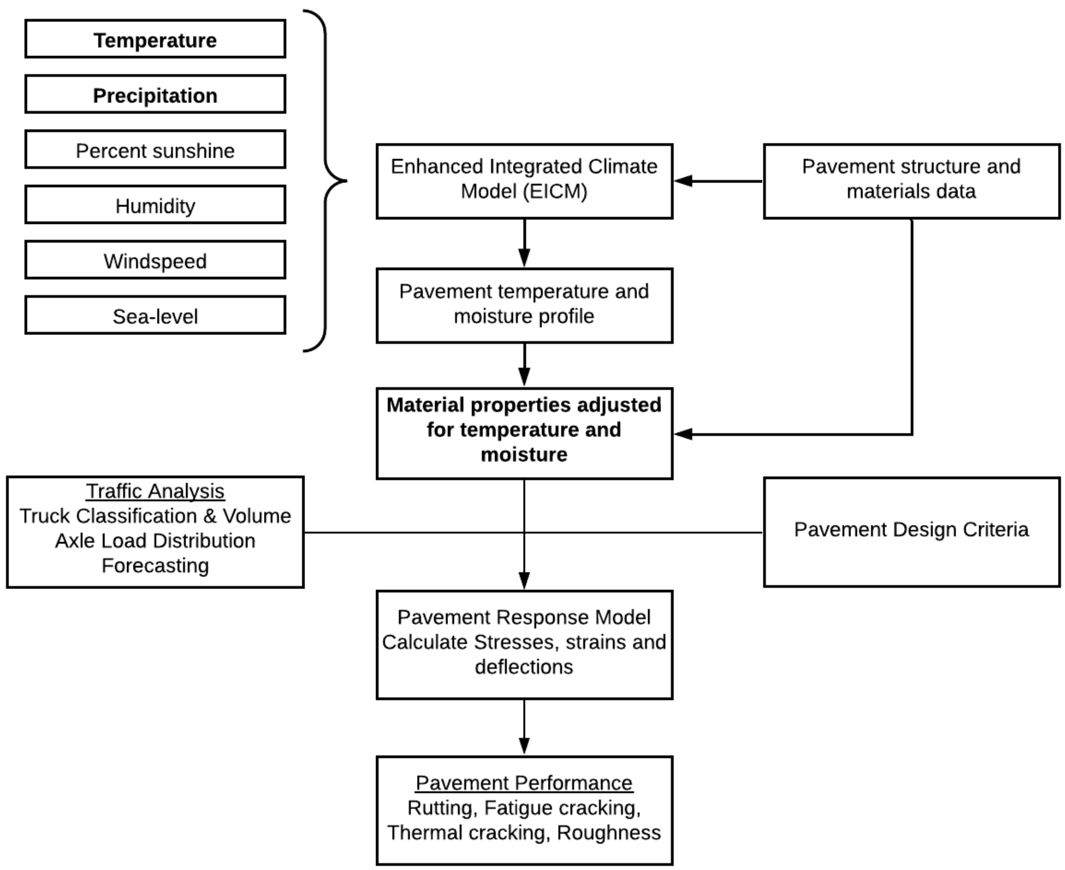

Figure 0-10: Mechanistic-Empirical Pavement Design methodology

The Integrated Climatic Model is a one-dimensional coupled heat and moisture flow program that is intended for use in analyzing pavement-soil systems. It has the capability of generating internally realistic patterns of rainfall, solar radiation, cloud cover, wind speed, and air temperature to simulate the upper boundary conditions of a pavement-soil system. It has a variety of options for specifying the moisture and temperature, or the flux of these at the lower boundary and at the interface between the subgrade and the base course. It considers the lateral and vertical drainage of the base course in determining the amount of water that enters the subgrade by infiltration through the pavement surface and drainage through the base course.

EICM is developed based on three primary components, which includes (1) Climate Materials Structural (CMS) model developed by University of Illinois Urbana-Champaign, (2) frost-heave and settlement model (CRREL model) developed at the United States Army Cold Regions Research and Engineering Laboratory, and (3) infiltration-drainage model (ID model) developed at the Texas A&M University Texas Transportation Institute.

Instrumentation packages developed by LTPP for measurement of moisture, temperature, and frost penetration in pavement sections were placed at the edge of the test lane in various pavement sections to validate the EICM predictions. The following sensors were placed at each of these locations:

- 10 TDR probes,
- 18 probes to measure pavement surface temperature, and
- 35 electrical resistivity probes to measure frost penetration.

Data from the temperature and resistivity probes were continuously recorded, while data from TDR probes were recorded at approximately 2-week intervals. Readings were monitored continuously at 0.5 in. intervals in the pavement. The TDR data was presented in NCHRP Report 455.

C.4 Design Outputs

C.4.1 Rutting

Total Permanent Vertical Deformation

- Surface rutting from incremental rutting calculations within each AC, unbound and soil sublayer
- Permanently deformations under specific conditions for the number of trucks within that condition using the “strain hardening” approach
- Measured in the laboratory with a repeated load permanent deformation triaxial test

$$\Delta_{p(HMA)} = \epsilon_{p(HMA)} h_{HMA} = \beta_{1r}\, k_z \varepsilon_{r(HMA)}\ 10^{k_{1r}} n^{k_{2r}\beta_{2r}} T^{k_{3r}\beta_{3r}}$$

Where

- $\Delta_{p(HMA)} =$ accumulated permanent or plastic vertical deformation(mm) in the HMA layer/sublayer (mm)
- $\epsilon_{p(HMA)}$ =accumulated permanent or plastic axial strain(mm) in the HMA layer/ sublayer (mm/mm)
- $\varepsilon_{r(HMA)}$ = resilient or elastic strain calculated by the structural response model at the mid-depth of each HMA sublayer (mm/mm)
- h_{HMA} = thickness of the HMA layer/sublayer, (mm)
- n = number of axle load repetitions
- T =mix or pavement temperature, (c or F)
- k_z = depth confinement factor
- k_{1r}, $k_{2r,}$ k_{3r}= global field calibration parameters (from the NCHRP I-40D recalibration)
- k_{1r} = -3.35412, k_{2r} = 0.4791, k3r = 1.5606
- β_{1r}, β_{2r} , β_{3r} = local and/or mixture field calibration constants; for the global calibration, these constants were all set to 1.0
- $k_z = (c_1 + c_2 D)\ 0.328196^D$

- $C_1 = -0.1039(H_{HMA})^2 + 2.4868H_{HMA} - 17.342$
- $C_2 = 0.01712(H_{HMA})^2 - 1.7331\ H_{HMA} + 27.428$
- D = depth below the surface, (in.)
- H_{HMA} = total HMA thickness, (in.)

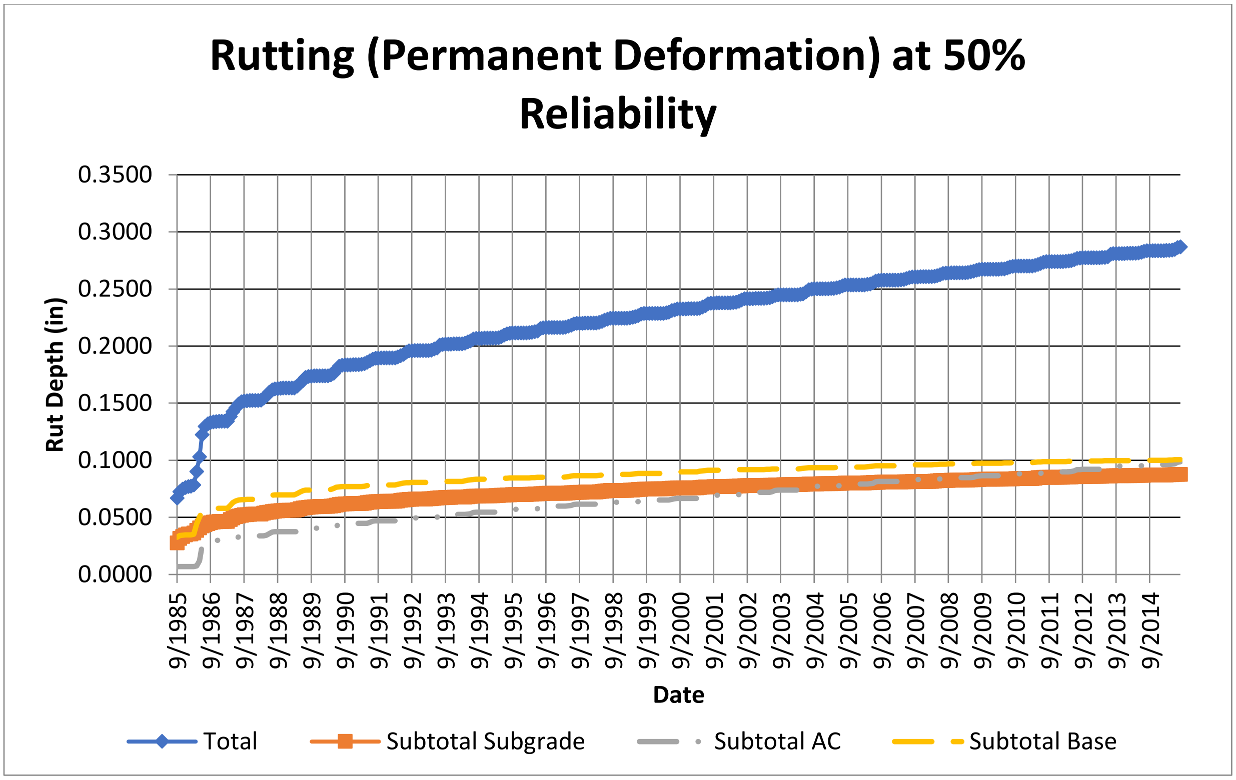

Figure 0-11: Permanent deformation over 30-year service life at 50% reliability

C.4.2 Fatigue Cracking

Alligator & Longitudinal Cracking

- Alligator cracking is assumed to initiate from the bottom of the AC layers and propagate to the surface
- Longitudinal cracking is assumed to initiate at the surface
- Incremental damages indices are calculated on a grid pattern throughout the AC Layers at

critical depths

- Endurance limit can be used but was not calibrated

$$N_{f-HMA} = k_{f1}(C)(\,C_H)\beta_{f1}(\varepsilon_t)^{k_{f2}\beta_{f2}}(\,E_{HMA})^{k_{f3}\beta_{f3}}$$

Where

- N_{f-HMA} = allowable number of axle load applications for a flexible pavement and HMA overlay
- ε_t = tensile strain at critical locations and calculated by the structural response model,(mm/mm)
- E_{HMA} = dynamic modulus of the HMA measured in compression (MPa)
- k_{f1}, k_{f2}, k_{f3} = global field-calibration parameters; k_{f1}=0.007566, k_{f2}=3.49492 and k_{f3}= -1.281
- β_{f1}, β_{f2}, β_{f3} = local or mixture specific calibration constants; these were set to 1 in the global calibration effort
- C_H = thickness correction term, dependent on the type of cracking
- C = 10^M, with M calculated as
- $M = 4.84(\frac{V_{be}}{V_a+V_{be}} - 0.69)$
- V_{be}= effective asphalt content by volume, percent
- V_a = percentage of air voids(mm) the HMA mixture

For Bottom-up or alligator cracking, the thickness correction term, C_H:

$$C_H = \frac{1}{0.000398 + \frac{0.003602}{1 + e^{(11.02-3.49H_{HMA})}}}$$

For Top-down or longitudinal cracking, the thickness correction term, C_H:

$$C_H = \frac{1}{0.01 + \frac{12.00}{1 + e^{(15.676 - 2.8186 H_{HMA})}}}$$

- H_{HMA} = total HMA thickness,(mm)

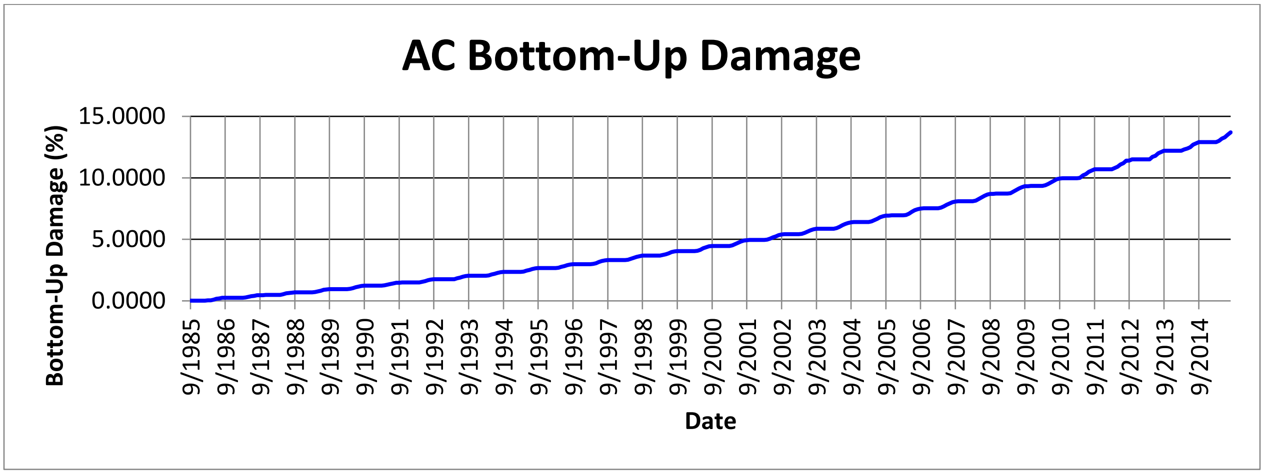

Figure 0-12: AC Bottom-Up fatigue damage over 30-year service life at 50% reliability

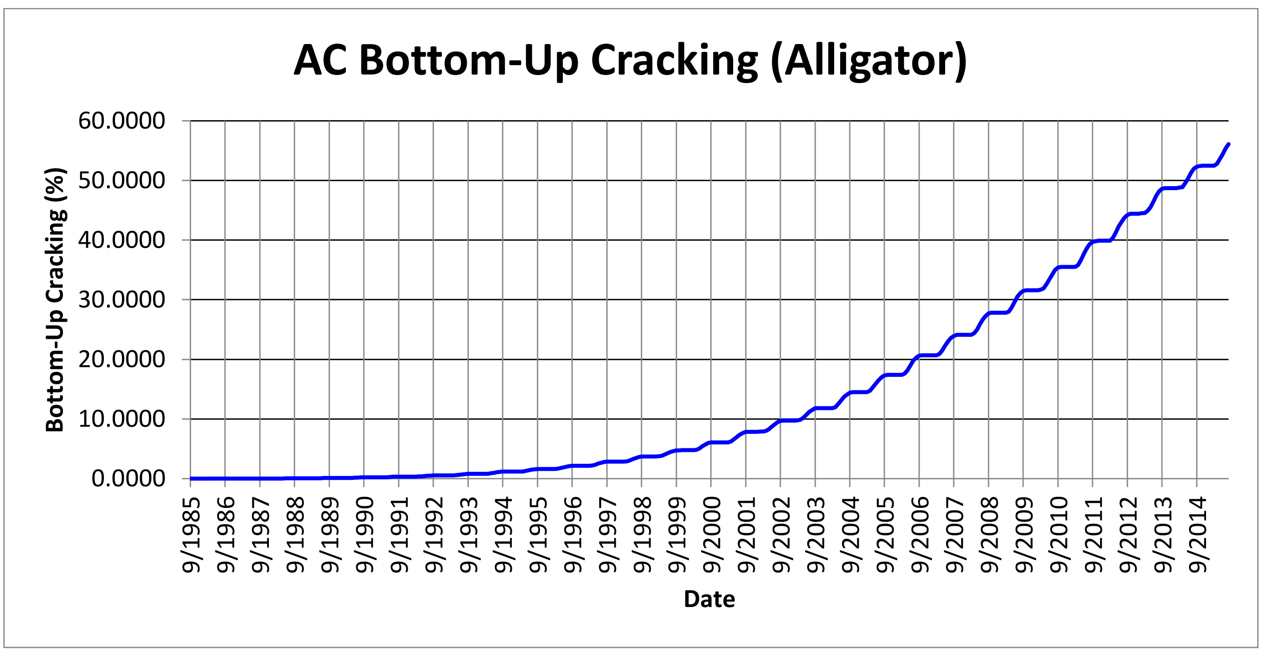

Figure 0-13: AC Bottom-Up fatigue cracking (Alligator) over 30-year service life at 50% reliability

C.4.3 Thermal Cracking

Transverse Cracking

- Prediction model is based on fracture mechanics
- Parameters (A, n) can be obtained from the indirect tensile creep- compliance and strength tests
- The stress intensity factor (ΔK) is incorporated through the use of a simplified equation developed from theoretical finite element studies

$$\Delta C = A(\Delta K)^{\eta}$$

where

- ΔC= change in crack depth due to a cooling cycle
- ΔK = change in the stress intensity factor due to a cooling cycle
- A, η = fracture parameters for the HMA mixture

Where

$$\mathrm{A} = 10^{\mathrm{k_t}\beta_\mathrm{t}(4.389-2.521\log(\mathrm{E_{HMA}}\sigma_\mathrm{m}\eta))}$$

$$\eta = 0.8\left[1+\frac{1}{\mathrm{m}}\right]$$

- k_t = coefficient determined through global calibration for each input level
- (Level 1 = 5.0; Level 2 = 1.5, and Level 3 = 3.0)
- E_{HMA} = HMA indirect tensile modulus (MPa)
- σ_m = mixture tensile strength (MPa)
- m = the m-value derived from the indirect tensile creep compliance curve measured in the laboratory
- β_t = local or mixture calibration factor

$$K = \sigma_{tip}(0.45 + 1.99\ (C_o)^{0.56})$$

Where

- K = the stress intensity factor
- σ_{tip} = far-field stress from pavement response model at depth of crack tip (MPa)
- C_o = current crack length (m)

$$TC = \beta_{t1} N_{f-HMA}[\frac{1}{\sigma_d}\log(\frac{C_d}{H_{HMA}})$$

Where

- TC = observed amount of thermal cracking (m/km)
- β_{t1} = regression coefficient determined through the global calibration (400)
- N_{f-HMA} = allowable number of axle load applications for a flexible pavement and HMA overlay
- σ_d= standard normal deviation of the log of the depth of cracks in the pavement (0.769) (mm)
- C_d= crack depth (mm)
- H_{HMA} = thickness of HMA layers (mm)

C.4.4 Smoothness

International Roughness Index

- Functional adequacy is quantified by pavement smoothness
- Smoothness degradation by the occurrence of surface distress will result in increased roughness (IRI value)
- IRI is predicted empirically as a function of pavement distresses, site factors (soils shrink/swell and frost heave capabilities) and the initial IRI

$$\mathrm{IRI} = \mathrm{IRI_o} + 0.0150(\mathrm{SF}) + 0.400(\mathrm{FC_{total}}) + 0.0080(\mathrm{TC}) + 40.0(\mathrm{RD})$$

Where

- $\mathrm{IRI_o}$ =initial IRI after construction (m/km)
- $\mathrm{FC_{total}}$= area of fatigue cracking (combined alligator, longitudinal and reflection cracking in the wheel path) percent of total area. All load-related cracks are combined on an area basis—length of cracks is multiplied by 0.3m to convert length into area basis
- TC = length of transverse cracking (m/km)
- RD = average rut depth (mm)
- SF = site factor

$$\mathrm{SF} = \mathrm{Age}\big(0.02003(\mathrm{PI} + 1) + 0.007947(\mathrm{Precip} + 1) + 0.000636(\mathrm{FI} + 1)\big)$$

Where

- Age = pavement age (yrs)
- PI = percent plasticity index
- FI = average annual freezing index, °C days
- Precip = average annual precipitation or rainfall, (mm)

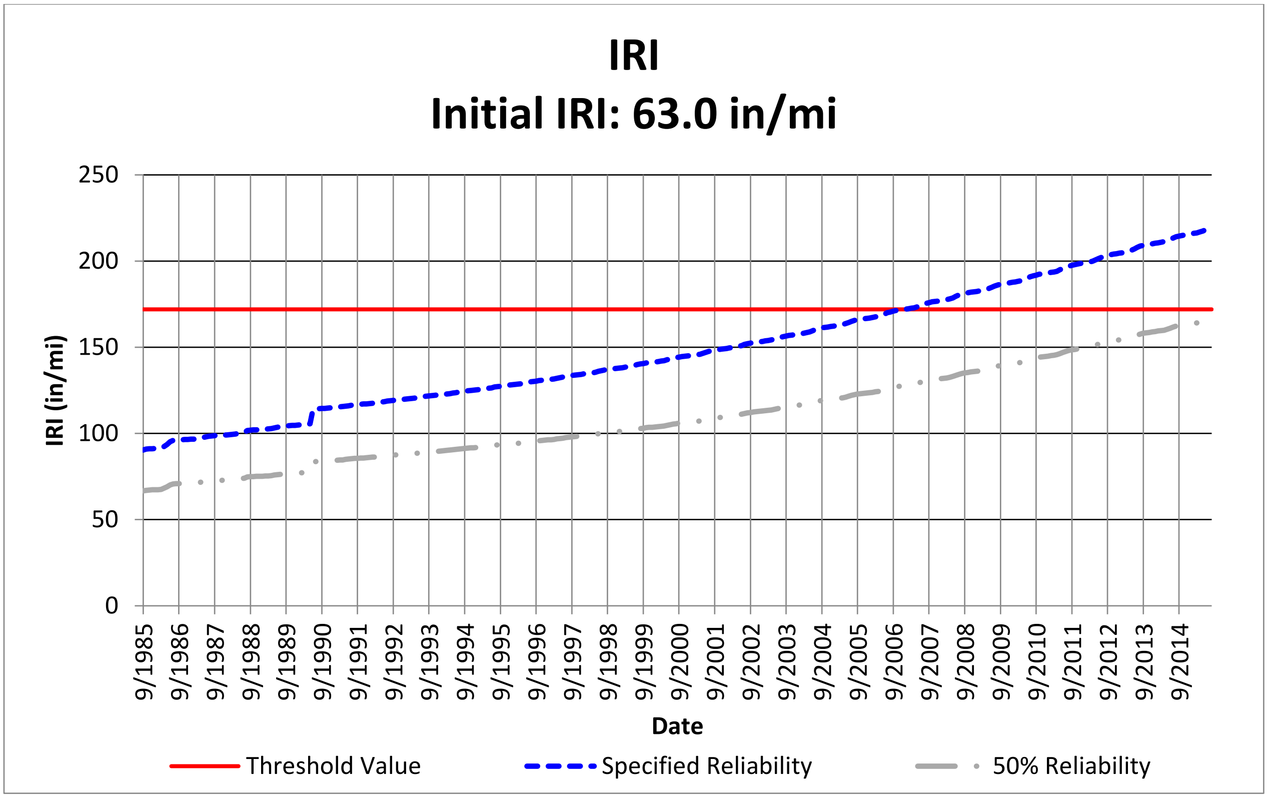

Figure 0-14: International Roughness Index (IRI) over 30-year service life

Appendix D. LCA and LCCA

D.1 Life Cycle Assessment (LCA)

D.1.1 Material Data

Table **Error! No text of specified style in document.**-44: Material report input

Material Name	Quantity	Unit	Mass Value	Mass Unit	Record Type
Emulsified Asphalt Tack Coat	5.63	m3	5.72	tonnes	Database
Emulsified Asphalt Primer Coat	41.85	m3	42.48	tonnes	Database
AB Surface HMA	1,173.48	m3	2,757.68	tonnes	Database
AB Base HMA	1,062.99	m3	2,524.60	tonnes	Database
OGDL Asphalt Treated	236.22	m3	619.23	tonnes	Database
AB Crushed Base	1,028.70	m3	2,287.83	tonnes	Database
AB Crushed Subbase	2,971.80	m3	6,650.89	tonnes	Database

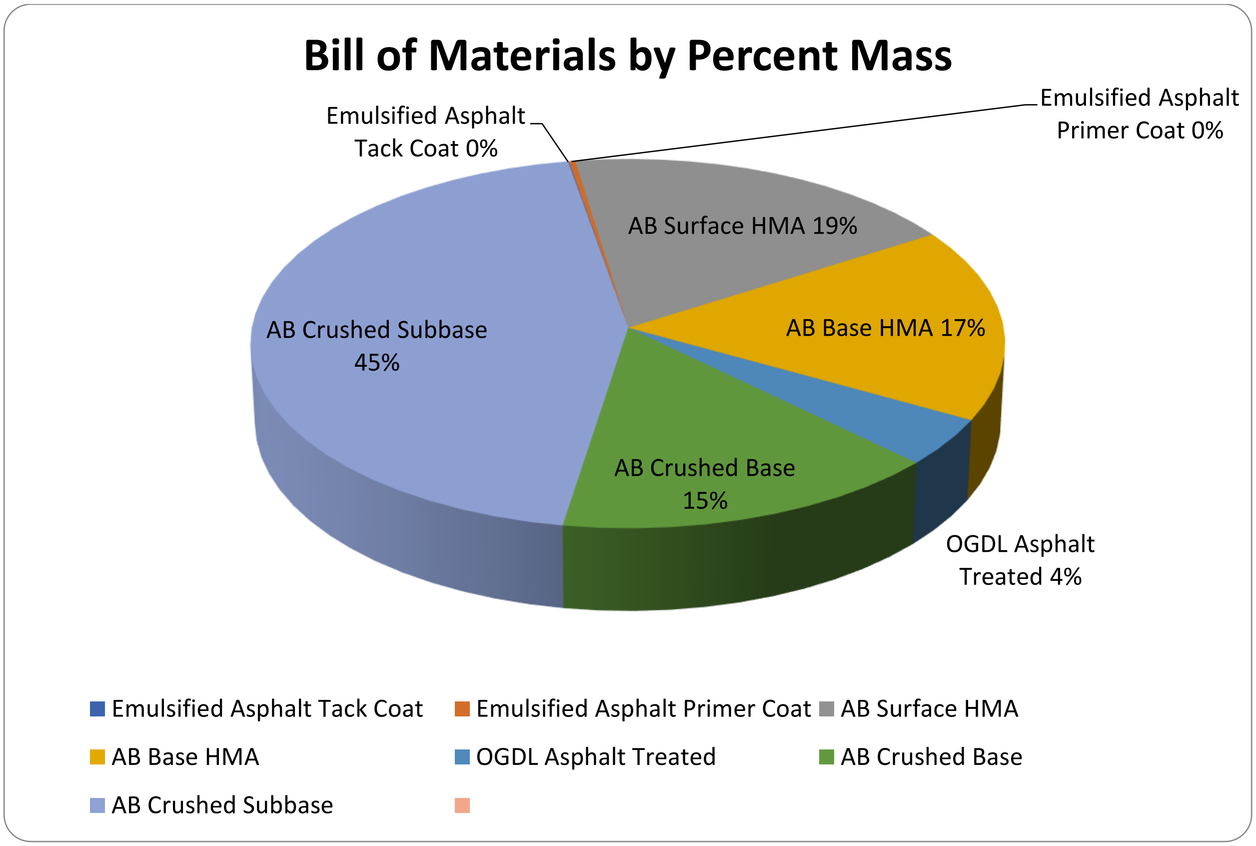

Figure 0-15: Material input by percent mass

D.1.2 Summary of LCA output

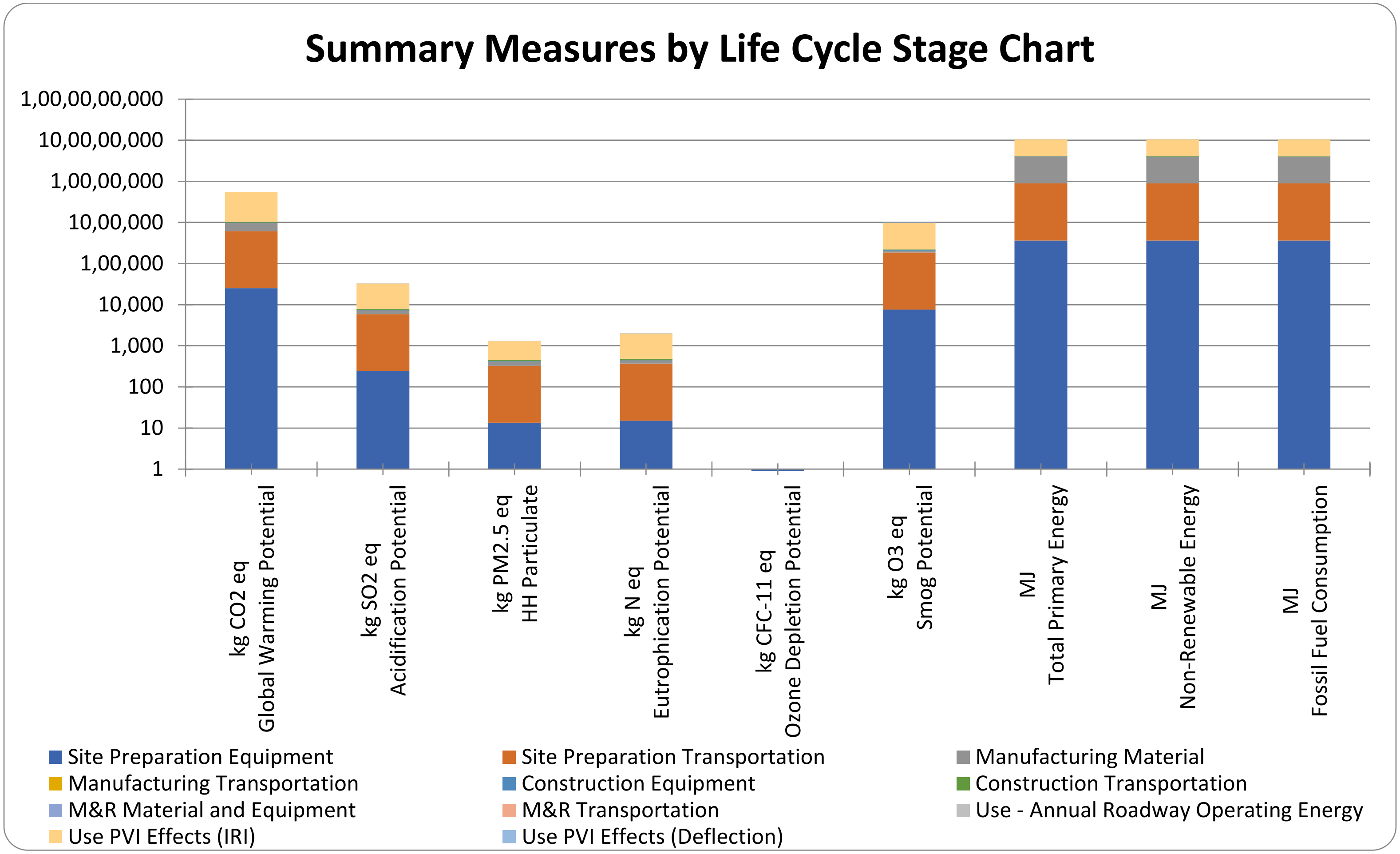

Figure 0-16: Summary measures by life cycle stage chart

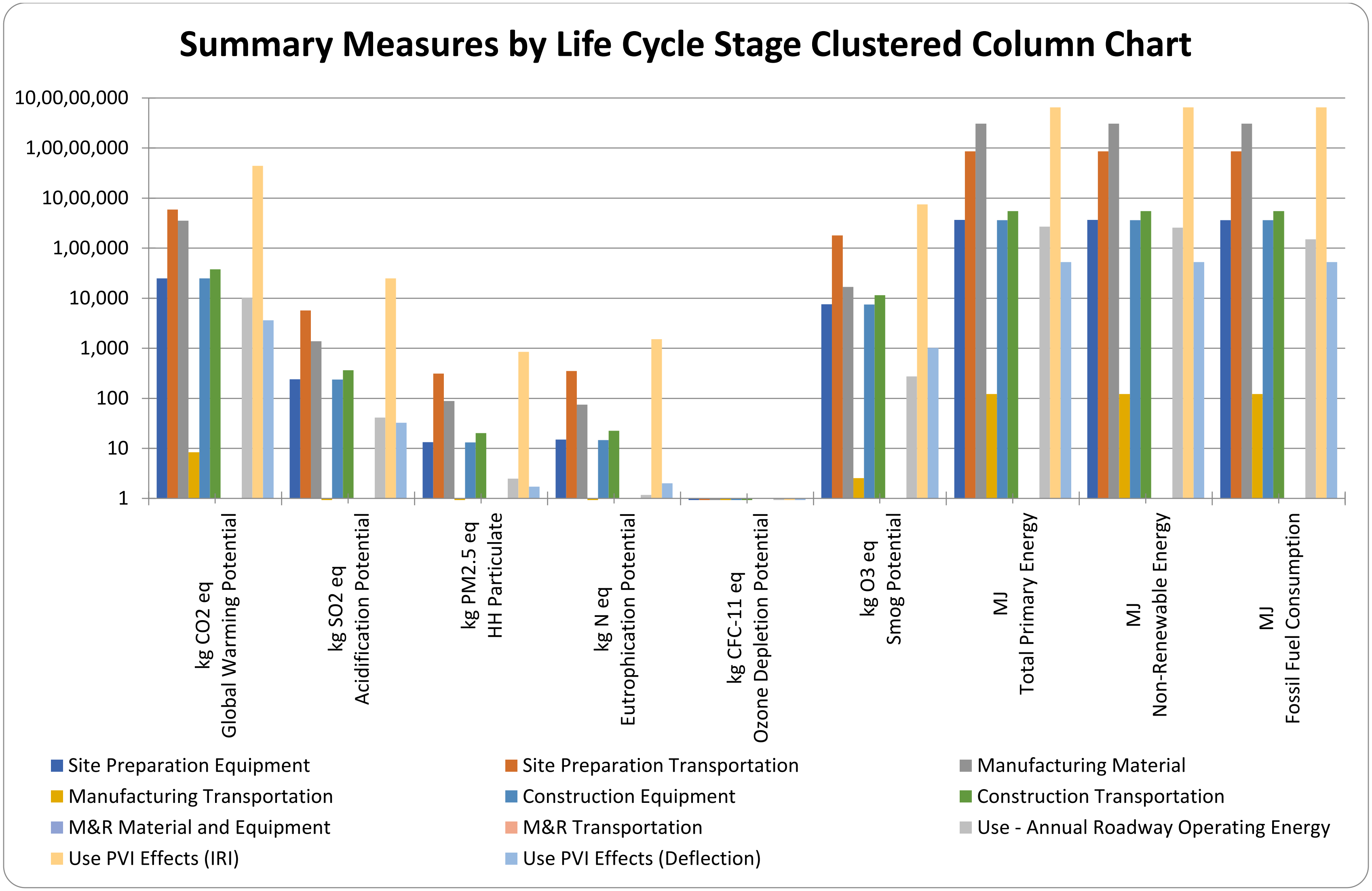

Figure 0-17: Summary measures by life cycle stage clustered column chart

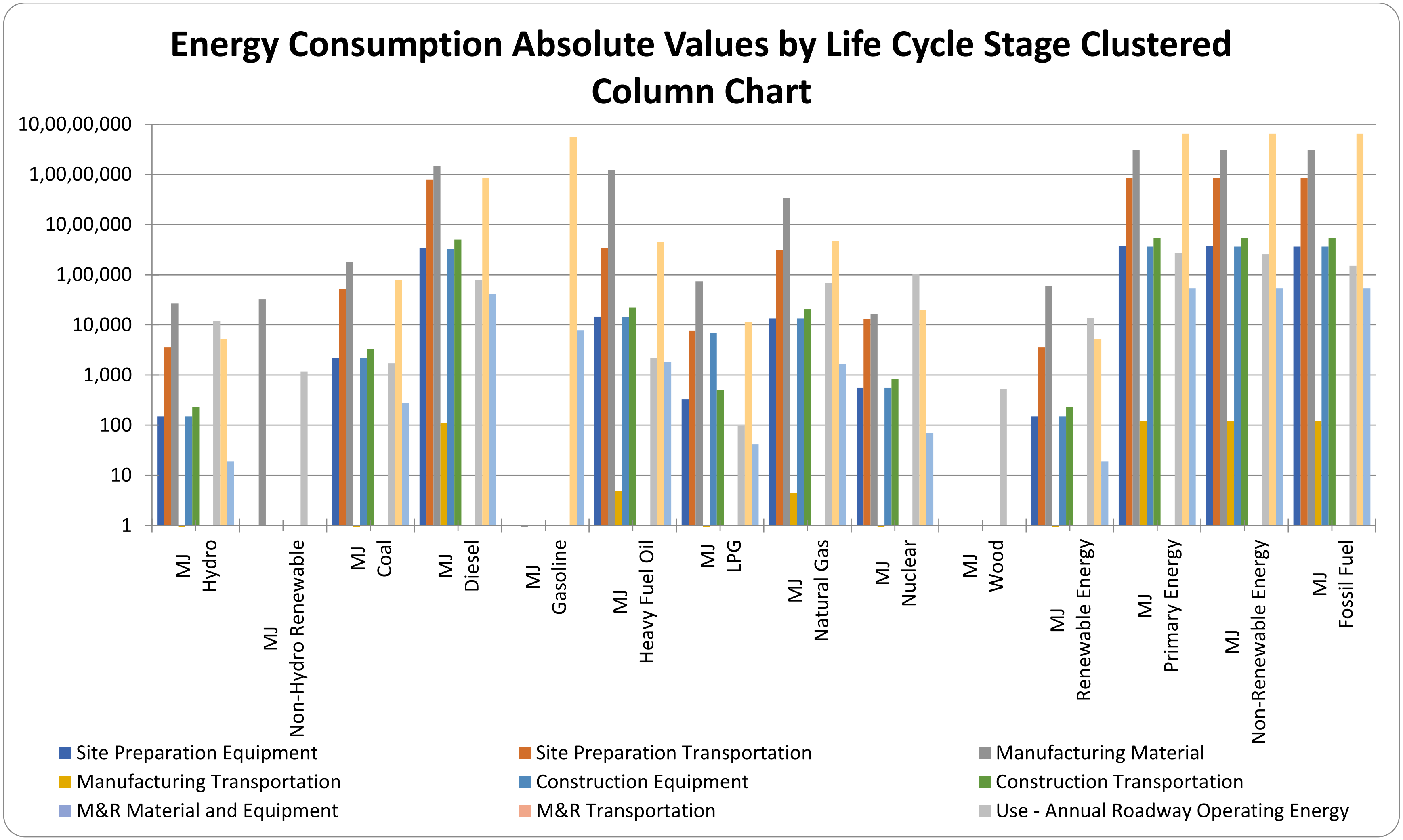

Figure 0-18: Energy consumption absolute values by life cycle stage clustered column chart

D.2 Life Cycle Cost Analysis (LCCA)

Table **Error! No text of specified style in document.**-45: Life cycle cost by various categories over 30-year design life

Year	Sequence	Category	Sub-category	Specification Description	Total Cost	Total Net Present Value
0	0	Site Preparation	Earth Moving		$56,106.00	$56,106.00
0	1	Site Preparation	Excavation		$4,20,795.00	$4,20,795.00
0	2	Site Preparation	Hauling		$28,053.00	$28,053.00
0	3	Construction	Initial Construction	ASPHALT-9	$12,55,816.20	$12,55,816.20
1	2	Operation	Operating Energy Consumption	Diesel (Industrial Boiler)	$3,470.79	$3,410.79
1	3	Operation	Gasoline	PVI IRI - Gasoline	$13,371.46	$13,140.28
1	4	Operation	Gasoline	PVI Deflection - Gasoline	$7.43	$7.30
2	2	Operation	Operating Energy Consumption	Diesel (Industrial Boiler)	$3,543.06	$3,421.61
2	3	Operation	Gasoline	PVI IRI - Gasoline	$16,185.16	$15,630.35
2	4	Operation	Gasoline	PVI Deflection - Gasoline	$7.96	$7.69
3	2	Operation	Operating Energy Consumption	Diesel (Industrial Boiler)	$3,616.83	$3,432.46
3	3	Operation	Gasoline	PVI IRI - Gasoline	$19,334.20	$18,348.64
3	4	Operation	Gasoline	PVI Deflection - Gasoline	$8.53	$8.10

4	2	Operation	Operating Energy Consumption	Diesel (Industrial Boiler)	$3,692.13	$3,443.35
4	3	Operation	Gasoline	PVI IRI - Gasoline	$22,852.26	$21,312.42
4	4	Operation	Gasoline	PVI Deflection - Gasoline	$9.15	$8.53
5	2	Operation	Operating Energy Consumption	Diesel (Industrial Boiler)	$3,769.01	$3,454.27
5	3	Operation	Gasoline	PVI IRI - Gasoline	$26,776.11	$24,540.13
5	4	Operation	Gasoline	PVI Deflection - Gasoline	$9.81	$8.99
6	2	Operation	Operating Energy Consumption	Diesel (Industrial Boiler)	$3,847.48	$3,465.23
6	3	Operation	Gasoline	PVI IRI - Gasoline	$31,145.89	$28,051.50
6	4	Operation	Gasoline	PVI Deflection - Gasoline	$8.50	$7.66
7	2	Operation	Operating Energy Consumption	Diesel (Industrial Boiler)	$3,927.59	$3,476.22
7	3	Operation	Gasoline	PVI IRI - Gasoline	$34,333.86	$30,388.12
7	4	Operation	Gasoline	PVI Deflection - Gasoline	$9.12	$8.07
8	2	Operation	Operating Energy Consumption	Diesel (Industrial Boiler)	$4,009.37	$3,487.25
8	3	Operation	Gasoline	PVI IRI - Gasoline	$37,819.17	$32,894.19
8	4	Operation	Gasoline	PVI Deflection - Gasoline	$9.77	$8.50
9	2	Operation	Operating Energy Consumption	Diesel (Industrial Boiler)	$4,092.85	$3,498.31
9	3	Operation	Gasoline	PVI IRI - Gasoline	$41,628.11	$35,581.12
9	4	Operation	Gasoline	PVI Deflection - Gasoline	$10.47	$8.95

10	2	Operation	Operating Energy Consumption	Diesel (Industrial Boiler)	$4,178.06	$3,509.41
10	3	Operation	Gasoline	PVI IRI - Gasoline	$45,789.18	$38,461.10
10	4	Operation	Gasoline	PVI Deflection - Gasoline	$11.23	$9.43
11	2	Operation	Operating Energy Consumption	Diesel (Industrial Boiler)	$4,265.06	$3,520.54
11	3	Operation	Gasoline	PVI IRI - Gasoline	$50,333.32	$41,547.06
11	4	Operation	Gasoline	PVI Deflection - Gasoline	$10.50	$8.67
12	2	Operation	Operating Energy Consumption	Diesel (Industrial Boiler)	$4,353.86	$3,531.71
12	3	Operation	Gasoline	PVI IRI - Gasoline	$56,127.20	$45,528.57
12	4	Operation	Gasoline	PVI Deflection - Gasoline	$11.25	$9.13
13	2	Operation	Operating Energy Consumption	Diesel (Industrial Boiler)	$4,444.51	$3,542.91
13	3	Operation	Gasoline	PVI IRI - Gasoline	$62,493.88	$49,816.59
13	4	Operation	Gasoline	PVI Deflection - Gasoline	$12.06	$9.61
14	2	Operation	Operating Energy Consumption	Diesel (Industrial Boiler)	$4,537.05	$3,554.15
14	3	Operation	Gasoline	PVI IRI - Gasoline	$69,485.75	$54,432.49
14	4	Operation	Gasoline	PVI Deflection - Gasoline	$12.93	$10.13
15	2	Operation	Operating Energy Consumption	Diesel (Industrial Boiler)	$4,631.52	$3,565.43
15	3	Operation	Gasoline	PVI IRI - Gasoline	$77,159.80	$59,399.03
15	4	Operation	Gasoline	PVI Deflection - Gasoline	$13.86	$10.67

16	2	Operation	Operating Energy Consumption	Diesel (Industrial Boiler)	$4,727.95	$3,576.74
16	3	Operation	Gasoline	PVI IRI - Gasoline	$85,577.95	$64,740.51
16	4	Operation	Gasoline	PVI Deflection - Gasoline	$14.94	$11.30
17	2	Operation	Operating Energy Consumption	Diesel (Industrial Boiler)	$4,826.39	$3,588.08
17	3	Operation	Gasoline	PVI IRI - Gasoline	$96,271.38	$71,571.03
17	4	Operation	Gasoline	PVI Deflection - Gasoline	$16.01	$11.90
18	2	Operation	Operating Energy Consumption	Diesel (Industrial Boiler)	$4,926.88	$3,599.47
18	3	Operation	Gasoline	PVI IRI - Gasoline	$1,08,059.77	$78,945.98
18	4	Operation	Gasoline	PVI Deflection - Gasoline	$17.16	$12.54
19	2	Operation	Operating Energy Consumption	Diesel (Industrial Boiler)	$5,029.46	$3,610.88
19	3	Operation	Gasoline	PVI IRI - Gasoline	$1,21,045.28	$86,903.99
19	4	Operation	Gasoline	PVI Deflection - Gasoline	$18.40	$13.21
20	2	Operation	Operating Energy Consumption	Diesel (Industrial Boiler)	$5,134.18	$3,622.34
20	3	Operation	Gasoline	PVI IRI - Gasoline	$1,35,339.08	$95,486.28
20	4	Operation	Gasoline	PVI Deflection - Gasoline	$19.72	$13.91
21	2	Operation	Operating Energy Consumption	Diesel (Industrial Boiler)	$5,241.08	$3,633.83
21	3	Operation	Gasoline	PVI IRI - Gasoline	$1,51,062.15	$1,04,736.80
21	4	Operation	Gasoline	PVI Deflection - Gasoline	$23.26	$16.12

22	2	Operation	Operating Energy Consumption	Diesel (Industrial Boiler)	$5,350.21	$3,645.36
22	3	Operation	Gasoline	PVI IRI - Gasoline	$1,70,121.28	$1,15,911.93
22	4	Operation	Gasoline	PVI Deflection - Gasoline	$24.93	$16.98
23	2	Operation	Operating Energy Consumption	Diesel (Industrial Boiler)	$5,461.60	$3,656.92
23	3	Operation	Gasoline	PVI IRI - Gasoline	$1,91,139.55	$1,27,981.13
23	4	Operation	Gasoline	PVI Deflection - Gasoline	$26.72	$17.89
24	2	Operation	Operating Energy Consumption	Diesel (Industrial Boiler)	$5,575.32	$3,668.52
24	3	Operation	Gasoline	PVI IRI - Gasoline	$2,14,300.12	$1,41,007.98
24	4	Operation	Gasoline	PVI Deflection - Gasoline	$28.64	$18.84
25	2	Operation	Operating Energy Consumption	Diesel (Industrial Boiler)	$5,691.40	$3,680.16
25	3	Operation	Gasoline	PVI IRI - Gasoline	$2,39,802.35	$1,55,060.29
25	4	Operation	Gasoline	PVI Deflection - Gasoline	$30.70	$19.85
26	2	Operation	Operating Energy Consumption	Diesel (Industrial Boiler)	$5,809.91	$3,691.83
26	3	Operation	Gasoline	PVI IRI - Gasoline	$2,67,863.18	$1,70,210.40
26	4	Operation	Gasoline	PVI Deflection - Gasoline	$34.21	$21.74
27	2	Operation	Operating Energy Consumption	Diesel (Industrial Boiler)	$5,930.87	$3,703.54
27	3	Operation	Gasoline	PVI IRI - Gasoline	$3,43,431.33	$2,14,456.32
27	4	Operation	Gasoline	PVI Deflection - Gasoline	$36.66	$22.89

28	2	Operation	Operating Energy Consumption	Diesel (Industrial Boiler)	$6,054.36	$3,715.29
28	3	Operation	Gasoline	PVI IRI - Gasoline	$4,28,477.16	$2,62,937.49
28	4	Operation	Gasoline	PVI Deflection - Gasoline	$39.30	$24.12
29	2	Operation	Operating Energy Consumption	Diesel (Industrial Boiler)	$6,180.42	$3,727.08
29	3	Operation	Gasoline	PVI IRI - Gasoline	$5,23,972.60	$3,15,979.78
29	4	Operation	Gasoline	PVI Deflection - Gasoline	$42.12	$25.40
30	3	Operation	Operating Energy Consumption	Diesel (Industrial Boiler)	$6,309.10	$3,738.90
30	4	Operation	Gasoline	PVI IRI - Gasoline	$6,30,980.33	$3,73,931.82
30	5	Operation	Gasoline	PVI Deflection - Gasoline	$45.15	$26.76